

## ABSTRACT

Title of Document: FIELD-SCALE OPTIMIZATION AND  
EVALUATION OF A RECYCLED-  
MATERIALS BASED STORMWATER  
TREATMENT TECHNIQUE

David Gleason, Master of Science, 2013

Directed By: Dr. Allen Davis, Civil and Environmental  
Engineering

This research project evaluates and enhances a novel stormwater control measure for heavy metals called the Biomat. The water quality effects of Biomat treatment on a field scale were examined. Dissolved Pb and Cu were major contaminants, found in roof runoff at mean values of 2.7 mg/L Pb and 0.8 mg/L Cu at the research site. Biomat treatment reduced concentrations to mean values of 30 µg/L Pb and 13 µg/L Cu. Results indicate that an approximate steady-state concentration was reached for dissolved metals. This concentration appears to result from equilibrium between native metals on the media and metals dissolved in stormwater. Water quality results from a second site where influent metals concentrations were significantly lower (mean influent Pb at 15 µg/L, Cu at 9 µg/L) supported this hypothesis. Further water quality improvement was achieved with an additional aluminum-based water treatment residual and sand media, focusing on phosphorous.

FIELD-SCALE OPTIMIZATION AND EVALUATION OF A RECYCLED-  
MATERIALS BASED STORMWATER TREATMENT TECHNIQUE

By

David Jacob Gleason

Thesis submitted to the Faculty of the Graduate School of the  
University of Maryland, College Park, in partial fulfillment  
of the requirements for the degree of  
Master of Science  
2013

Advisory Committee:  
Professor Allen P. Davis, Chair  
Professor Alba Torrents  
Dr. Rufus Chaney

© Copyright by  
David Jacob Gleason  
2013

## Acknowledgement

Sincere thanks are due to the Animal and Plant Health Inspection Service of the USDA for funding this project, and especially to Mr. Wayne Claus for extensive on-site assistance.

Credit is also due to Chris Jennings, Daniel Salgado, Connie Chen, Rosemary Myers, Julian Oliver, Jordan Koebler, Sarah Igielski, and Michael Goglia for their assistance in the laboratory and field.

## Table of Contents

Acknowledgement .....	ii
Table of Contents .....	iii
List of Tables .....	v
List of Figures .....	viii
Introduction .....	1
Materials and Methods.....	6
Field site preparation.....	6
Preparation of mat media .....	7
Sampling equipment and setup .....	12
Estimation of rational runoff coefficients .....	15
Water quality analysis of samples.....	16
Batch experiments: finishing treatment of field effluent samples using water treatment residual (WTR) .....	18
Metal speciation experiments: quality assurance protocol to establish the efficacy of DEAE Sephadex A-25 resin (chloride form) to remove anionic metal complexes .....	18
WTR finishing treatment at the wooden structure .....	20
Spatially-distributed analysis of used Biomat media lability .....	22
Data .....	26
Results and Discussion .....	29
Direct roof runoff treatment.....	29
Volume and water balance at the wooden structure .....	31
Treatment efficacy at the wooden structure.....	32
Treatment efficacy on a mass removal basis .....	42
Intra-storm variability .....	43
Equilibrium model of effluent pollutant concentrations.....	48
Variables affecting treatment efficacy at the wooden structure.....	59
Speciation experiments .....	61
Phosphorous leaching .....	65
Development of a secondary treatment for enhanced P and metals removal .....	71
Storms sampled at the swale site .....	76
Site Hydrology .....	78
Treatment efficacy at the swale .....	80
Inter-site comparison of metals removal efficiencies .....	91
Phosphorous leaching at the swale .....	97
Sequential extractions performed on treatment media from the wooden structure .....	99
Mass balance of metals removed at the wooden structure.....	111
Sequential extractions performed on treatment media from the swale.....	114
Comparison of extraction data from both sites .....	123
Conclusions and Recommendations .....	126
Recommendations for application at the APHIS site .....	130
Research Recommendations .....	135

Appendix A- Water quality and flow data listed by rainfall event .....	137
Appendix B – Raw Data from Extraction Experiments.....	172
Appendix C – Material specifications of the roof tiles at APHIS Building #580.....	181
Appendix D – Filter cloth specifications .....	187
Bibliography .....	188

## List of Tables

Table 1: Dimensions of each biomat and their drainage areas .....	10
Table 2: Ratios of drainage area : treatment area for each Biomat.....	10
Table 3: Analytical methods used in field stormwater sample laboratory tests .....	16
Table 4: Concentrations of Pb, Cu, and Zn (in $\mu\text{g/L}$ ) measured in quality control tests performed with Sephadex DEAE A-25 resin (GE Life Sciences).....	20
Table 5: Depth-duration distribution of sampled rainfall events at the wooden structure. White/lighter boxes indicate higher frequencies, and darker boxes indicate lower frequencies. ....	30
Table 6: Depth-duration distribution of all rainfall events in Maryland (Kreeb, 2003). White/lighter boxes indicate higher frequencies, and darker boxes indicate lower frequencies. ....	31
Table 7: Regulatory standards for metals of concern at the APHIS site (EPA, 2013; COMAR, 2013).....	37
Table 8: Annual pollutant mass loadings for Pb, Cu, and Zn.....	43
Table 9: Mean effluent steady-state concentrations for dissolved metals at the wooden structure. Standard deviation and range are shown as well. The values in parentheses in the Pb column indicate values which exclude the rainfall event on October 12, 2012, during which some bypass was suspected. Outflow was small enough in this event as to not affect the mean overall concentration, which is flow-weighted.....	50
Table 10: Annual pollutant mass loadings for total and dissolved P, based on Biomat data.....	70
Table 11: Dissolved P concentrations in untreated and WTR-treated samples at varying media: solution mass ratios. These data were obtained by performing batch experiments on a sample of Biomat effluent collected after a storm event on July 14, 2012. Method detection limit = 0.010 mg/L. ....	72
Table 12: Pollutant masses and flow-weighted mean concentration values observed during the 3 storms in which WTR/sand treatment was added after the Biomat to treat residual metals and leached nutrients in Biomat outflow. Standard deviations between the 3 storm event EMC values are listed below each mean concentration.....	76
Table 13: Depth-duration distribution of the 18 storms sampled at the swale site. White/lighter boxes indicate higher frequencies, and darker boxes indicate lower frequencies. ....	78
Table 14: Percent concentration reductions for each metal by site. ....	97
Table 15: Metals background levels from control media extractions. The method detection limit for these measurements (performed on flame AAS) was 0.8 mg/kg. The mean of three replicates is shown in each cell, with the standard deviation among the three replicates shown in parentheses. ....	100
Table 16: Pb concentrations in samples from the side cross-section of Biomat treatment media at the wooden structure. Data for each of the three sequential extractions are presented below. Because the cross-section was not perfectly rectangular, no sample could be taken at Layer 5, Depth A. The mean of three	

replicates is shown in each cell, with the standard deviation among the three replicates shown in parentheses. .... 104

Table 17: Pb concentrations in samples from the hotspot cross-section of Biomat treatment media at the wooden structure. Data for each of the three sequential extractions are presented below. The mean of three replicates is shown in each cell, with the standard deviation among the three replicates shown in parentheses. .... 105

Table 18: Cu concentrations in samples from the side cross-section of Biomat treatment media at the wooden structure. Data for each of the three sequential extractions are presented below. The method detection limit for these measurements (performed on flame AAS) was 0.8 mg/kg. Because the cross-section was not perfectly rectangular, no sample could be taken at Layer 5, Depth A. The mean of three replicates is shown in each cell, with the standard deviation among the three replicates shown in parentheses. .... 107

Table 19: Cu concentrations in samples from the hotspot cross-section of Biomat treatment media at the wooden structure. Data for each of the three sequential extractions are presented below. The method detection limit for these measurements (performed on flame AAS) was 0.8 mg/kg. The mean of three replicates is shown in each cell, with the standard deviation among the three replicates shown in parentheses. .... 108

Table 20: Zn concentrations in samples from the side cross-section of Biomat treatment media at the wooden structure. Data for each of the three sequential extractions are presented below. The method detection limit for these measurements (performed on flame AAS) was 0.8 mg/kg. Because the cross-section was not perfectly rectangular, no sample could be taken at Layer 5, Depth A. The mean of three replicates is shown in each cell, with the standard deviation among the three replicates shown in parentheses. .... 110

Table 21: Zn concentrations in samples from the hotspot cross-section of Biomat treatment media at the wooden structure. Data for each of the three sequential extractions are presented below. The method detection limit for these measurements (performed on flame AAS) was 0.8 mg/kg. The mean of three replicates is shown in each cell, with the standard deviation among the three replicates shown in parentheses. .... 110

Table 22: Pb concentrations in samples from the side cross-section of Biomat treatment media at the swale. Data for each of the three sequential extractions are presented below. The method detection limit for these measurements (performed on furnace AAS) was 0.04 mg/kg. The mean of three replicates is shown in each cell, with the standard deviation among the three replicates shown in parentheses. .... 116

Table 23: Pb concentrations in samples from the middle cross-section of Biomat treatment media at the swale. Data for each of the three sequential extractions are presented below. The method detection limit for these measurements (performed on furnace AAS) was 0.04 mg/kg. The mean of three replicates is shown in each cell, with the standard deviation among the three replicates shown in parentheses. .... 117



Table 24: Cu concentrations in samples from the side cross-section of Biomat treatment media at the swale. Data for each of the three sequential extractions are presented below. The method detection limit for these measurements (performed on furnace AAS) was 0.1 mg/kg. The mean of three replicates is shown in each cell, with the standard deviation among the three replicates shown in parentheses. .... 119

Table 25: Cu concentrations in samples from the middle cross-section of Biomat treatment media at the swale. Data for each of the three sequential extractions are presented below. The method detection limit for these measurements (performed on furnace AAS) was 0.1 mg/kg. The mean of three replicates is shown in each cell, with the standard deviation among the three replicates shown in parentheses. .... 120

Table 26: Zn concentrations in samples from the side cross-section of Biomat treatment media at the swale. Data for each of the three sequential extractions are presented below. The method detection limit for these measurements (performed on flame AAS) was 0.8 mg/kg. The mean of three replicates is shown in each cell, with the standard deviation among the three replicates shown in parentheses. .... 122

Table 27: Zn concentrations in samples from the middle cross-section of Biomat treatment media at the swale. Data for each of the three sequential extractions are presented below. The method detection limit for these measurements (performed on flame AAS) was 0.8 mg/kg. The mean of three replicates is shown in each cell, with the standard deviation among the three replicates shown in parentheses. .... 123

Table 28: The cross-sectional variation of total Pb concentrations at the rear Biomat hotspot, as-is (a), and after 90<sup>0</sup> counterclockwise rotation (b) ..... 134

## List of Figures

Figure 1: Box reactor design for bench scale experiments .....	3
Figure 2: Swale and parking lot with autosamplers and mat visible .....	6
Figure 3: The roof runoff collection area.....	7
Figure 4: The Biomat placed across the swale, with influent stormwater visible on the right side.....	9
Figure 5: Biomat across the wooden structure, with plastic-wrapped cinder blocks as shape supports.....	10
Figure 6: (a) the placement of one bucket, to contain the treatment media inside another, to contain the sampling lines (b) the drainage holes at the bottom of the upper bucket to allow for flow-through (c) a diagram of flow during a storm through the WTR/sand treatment.....	21
Figure 7: Location of each media sample taken at the swale mat in the middle (a), and at the side (b).....	23
Figure 8: Swale media samples being subdivided .....	23
Figure 9: Cross-sections taken at the wooden structure in two locations, a hotspot of high flows, and a second location to the side.....	24
Figure 10: Two photographs taken during media sampling at the wooden structure: a) the rear hotspot cross-section, with only one sample (5DH) remaining in-situ b) the two rear cross-sections completely removed (side cross-section is in the foreground) .....	24
Figure 11: The variety of rainfall events sampled at the wooden structure with regard to depth, duration, and season. The extreme event at upper right represents data from from Hurricane Sandy (10/29/2012) .....	30
Figure 12: The rainfall-runoff relationship determined from rainfall events measured at the wooden structure. ....	<b>Error! Bookmark not defined.</b>
Figure 13: Intra-storm pollutograph for Pb and Cu, taken from data collected in a rainfall event on December 22, 2011. Note the log y-axis, used so that variation in both influent and effluent concentrations is visible.....	35
Figure 14: Exceedance probabilities for Pb and Cu in direct roof runoff influent and effluent at the APHIS building. Each data point represents an event mean concentration. Hollow triangles represent the 10 rainfall events in which no outflow was produced, and th .....	38
Figure 15: Exceedance probabilities for Zn in direct roof runoff influent and effluent at the APHIS building. Each data point represents an event mean concentration. Hollow triangles represent the 10 rainfall events in which no outflow was produced, and therefore no metal was released. ....	41
Figure 16: Intra-storm variation of Pb and Cu in effluent samples taken on September 23, 2011.....	46
Figure 17: Intra-storm variation of Pb and Cu in effluent samples taken on December 22, 2011.....	46
Figure 18: Intra-storm variation of Pb and Cu in effluent samples taken on February 29, 2012.....	47
Figure 19: Intra-storm variation of Pb and Cu in effluent samples taken on October 29, 2012.....	47

Figure 20: Pb pollutant duration curve. Data from all 17 storms in which discrete sampling was used are included. Concentration data were ranked and assigned a representative sample time based on the sampling program used (see methods). The dashed lines labeled “MC In/Out” show the mean concentrations observed. ....	55
Figure 21: Cu pollutant duration curves. Data from all 17 storms in which discrete sampling was used are included. Concentration data were ranked and assigned a representative sample time based on the sampling program used (see methods). The dashed lines labeled “MC In/Out” show the mean concentrations observed. ....	56
Figure 22: Zn pollutant duration curve. Data from all 17 storms in which discrete sampling was used are included. Concentration data were sorted high-to-low and assigned a representative sample time based on the sampling program used (see methods). The dashed lines labeled “MC In/Out” show the mean concentrations observed. The dashed lines labeled “MC In/Out” show the mean concentrations observed. ....	57
Figure 23: A zoomed-in version of Figure 20, showing concentrations of Pb near the steady-state mean value. ....	58
Figure 24: A zoomed-in version of Figure 21, showing concentrations of Cu near the steady-state mean value. ....	58
Figure 25: EMC effluent dissolved metals concentrations as a function of effluent pH. ....	59
Figure 26: Effluent Pb concentrations as a function of pH. Each data point represents a single discrete measurement from storm events at the wooden structure which produced outflow and were sampled using the discrete (as opposed to composite) sampling regimen. ....	60
Figure 27: Effluent Cu concentrations as a function of pH. Each data point represents a single discrete measurement from storm events at the wooden structure which produced outflow and were sampled using the discrete (as opposed to composite) sampling regimen. ....	60
Figure 28: Proportions of anionic vis-a-vis cationic/neutral Cu anions and complexes present in Biomat influent and effluent. Proportions are calculated from mean flow-weighted concentrations measured in discrete samples taken on January 30, 2013, and February 26, 2013. ....	62
Figure 29: Flow-weighted mean concentrations of anionic vis-vis cationic/neutral Cu present in Biomat influent and effluent. From discrete data taken on January 30, 2013 and February 26, 2013. ....	63
Figure 30: Proportions of anionic vis-a-vis cationic/neutral Pb anions and complexes present in Biomat influent and effluent. From discrete data taken on January 30, 2013 and February 26, 2013. Flow-weighted mean concentration values for each species are shown in mg/L on the data bars. ....	64
Figure 31: An inflow sample, left, opposite a Biomat outflow sample, right. These samples were taken in August, 2011, shortly after the mat was constructed. ....	65
Figure 32: Intra-storm variation of phosphorous concentrations during the storm of 12/22/11 at the wooden structure. Each data point represents a single discrete sample. Total storm depth: 0.64 cm. ....	67

Figure 33: Exceedance probabilities for P based on event mean concentrations from 24 storms. Hollow triangles denote those storms in which no effluent was discharged. ....	68
Figure 34: Concentrations of effluent total phosphorous measured over the course of 14 storms. Each data point represents one discrete measurement. ....	69
Figure 35: P concentrations in inflow, Biomat outflow, and WTR-treated outflow from a rainfall event sampled on 2/26/13. ....	73
Figure 36: Forms of P present in Biomat effluent during the storm event sampled on 2/26/13. ....	74
Figure 37: Phosphorous species concentrations in influent, Biomat effluent, and WTR-treated effluent in samples taken on January 30, 2013. The values shown are EMCs. ....	75
Figure 38: Depth-duration distribution of the 18 storms sampled at the swale site. ..	77
Figure 39: Rainfall-discharge relationship at the swale. Each point represents a data point measured at the swale during a single storm. ....	79
Figure 40: Rainfall-runoff relationship during large storms at the swale site with the Biomat in place (squares), and with no Biomat in place (diamonds). ....	80
Figure 41: Adsorption curves for Pb, Cu, and Zn onto amorphous Fe hydroxides, from Benjamin and Leckie (1981). ....	81
Figure 42: Probability plot for Pb and Cu concentrations at the swale site. Each data point represents an EMC value recorded in one of 18 storm events sampled ...	82
Figure 43: Probability plot for Zn concentrations at the swale site. Each data point represents an EMC value recorded in one of 18 storm events sampled. ....	83
Figure 44: Dissolved and total Pb concentrations measured at the swale on June 12, 2012. The dashed line indicates the method detection limit. ....	84
Figure 45: Dissolved and total Cu concentrations measured at the swale on June 12, 2012. The dashed line indicates the method detection limit. ....	85
Figure 46: Dissolved and total Pb concentrations measured at the swale on May 29, 2012. The dashed line indicates the method detection limit. ....	86
Figure 47: Dissolved and total Cu concentrations measured at the swale on May 29, 2012. The dashed line indicates the method detection limit. ....	87
Figure 48: Effluent dissolved metals concentrations at the swale as a function of effluent pH value. ....	88
Figure 49: Pb Pollutant duration curve for swale data, showing both influent and effluent concentrations of total and dissolved Pb. ....	89
Figure 50: Cu pollutant duration curve for swale data, showing both influent and effluent concentrations of total and dissolved Cu. ....	90
Figure 51: Zn pollutant duration curve for concentrations measured at the swale. Influent and effluent concentrations are both shown, in their total and dissolved forms. ....	91
Figure 52: Pb dissolved pollutant duration curve showing effluent data from both sites. ....	93
Figure 53: Cu dissolved pollutant duration curve showing effluent data from both sites. ....	94
Figure 54: Zn dissolved pollutant duration curve showing effluent data from both sites. ....	96

Figure 55: Exceedance plot characterizing P concentrations at the swale site. ....	98
Figure 56: The two sections of the Biomat, used to estimate the typical concentrations of metals in the mat media .....	114
Figure 57: The two roofs of environmental concern at the APHIS complex .....	131
Figure 58: Proposed full-scale deployment for Biomat media at the APHIS building to treat direct roof runoff.....	133
Figure 59: Plants growing across the length of the Biomat on March 11, 2013.....	133

## Introduction

Metals, second only to pathogens, are the most problematic pollutant in the 303(d) list of impaired and threatened waters in the United States, according to the USEPA. Among all metals causing impairment of natural waters, lead (Pb), copper (Cu), and zinc (Zn) are all among the top six. In the United States, Pb alone was found to be the main cause of impairment in 851 natural water bodies, with Cu and Zn causing 764 and 388 impairments, respectively (USEPA, 2013). Pb, Zn, and Cu are each associated with nonpoint source pollution. Stormwater is the primary vector of nonpoint source metals to natural water bodies, and stormwater control measures therefore present a unique opportunity to treat diffuse sources of metals. But in order to apply stormwater control measures on a scale large enough to control nonpoint source pollution, research and development to identify inexpensive treatment media are necessary. In light of these pressing problems, this research project field tests and optimizes the design of a novel, byproduct-based treatment to remove heavy metals from stormwater.

The research described in this thesis is the continuation of lab and bench-scale research conducted by Hunho Kim under the supervision of Dr. Allen Davis and Dr. Rufus Chaney from 2007 – 2010. During this time, Kim performed experiments to characterize roof runoff and soil in the immediate surroundings of the USDA Animal and Plant Health Inspection Service (APHIS) building #580 in Beltsville, MD. As had been previously suspected at this building, Pb and Cu concentrations in roof runoff were found to be extremely high. Once metals concentrations in stormwater runoff were quantified and the extent of metals migration had been assessed, side-by-side

column experiments were performed to assess the potential of a variety of media mixtures to act as metal adsorbents. Different mixtures of sand, steel slag, hubcutter heavies (an amorphous Fe rich byproduct of train wheel manufacturing), grass and food waste compost, and manure compost were all examined during this period. Media mixtures were evaluated based on their ability to remove metals, specifically lead (Pb), copper (Cu), and Zinc (Zn), from synthetic stormwater, and on expected treatment lifetimes (as quantified by breakthrough time). The most promising media tested consisted of 5% by weight steel slag, 25% grass/food waste compost, and 70% sand.

Kim then tested this mixed media on a bench scale, using a plastic box with two stainless steel screens inside to hold the media in a mat formation (Figure 1). Kim called this treatment the Biomat.

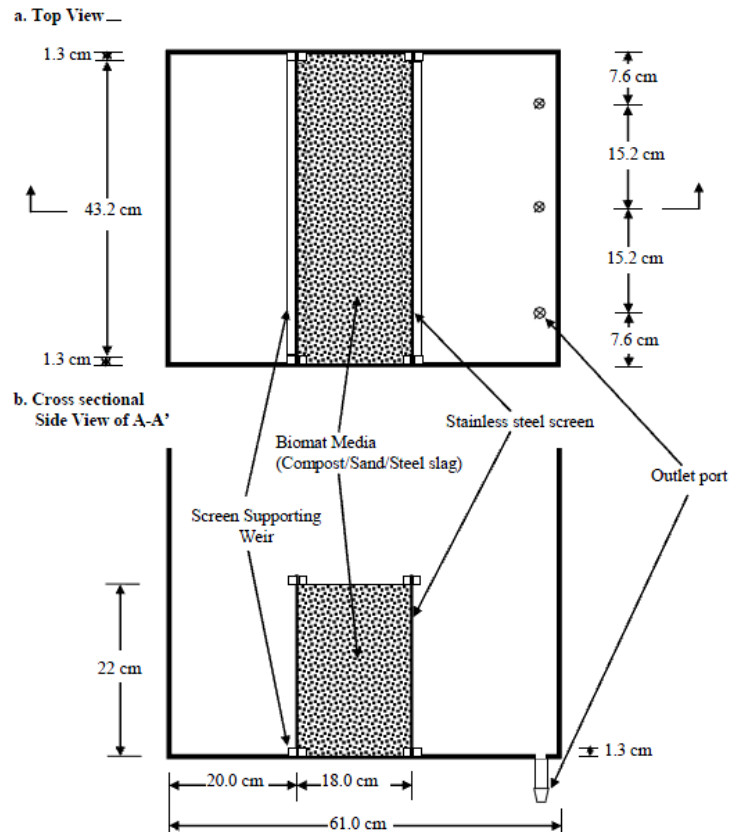


Figure 1: Box reactor design for bench scale experiments.

The experiments performed at this stage were conducted to assess treatment efficiency at lower metals loadings, to determine the hydraulic characteristics of the mat, and to test metals removal performance at a variety of hydraulic loadings. Finally, after all bench scale experiments had been executed, the lability of metals retained within the mat was assessed by performing sequential extractions on the treatment media. The results of these experiments suggest that metals, especially Pb and Cu removed onto the mat media were tightly held to inner surfaces of the treatment media. These experiments suggested that metal leaching from the mats was not expected to occur to a significant extent. Although an increase of metal mobility with increased pH (Bradl, 2004) was expected, the bench scale results suggested that



not enough soluble organic matter was present for this effect to become noticeable (Kim, 2010).

The current research project adapts Biomat treatment for field implementation at two sites in Beltsville, MD: one receiving direct roof runoff from the APHIS building, where lead (Pb) and copper (Cu) are both major contaminants, and a second site, a swale adjacent to a parking lot receiving stormwater with metals concentrations largely below regulatory limits. Research goals are to (1) evaluate the effectiveness of treatment on site (2) identify likely treatment mechanisms by monitoring and analyzing water quality parameters and performing sequential extractions on media, (3) improve effluent water quality from a metals and nutrient perspective, and (4) determine the potential for broader scale applicability of this treatment, if any.

Research consisted of three phases. In the preparatory phase, treatment mats (consisting of media wrapped in filter cloth) and sampling equipment were set up on site. In the water quality monitoring phase, influent and effluent to the treatments were sampled during storm events, and water quality parameters were measured in these samples and used to assess treatment efficiency. In the media extraction phase, sequential extractions were performed on treatment media to assess the lability of sequestered metals.

During the water quality monitoring phase, two treatments were evaluated. The first treatment was the previously described Biomat, which was designed under laboratory conditions to remove heavy metals at a wide range of concentrations (200 µg/L Pb – 10 mg/L) and water heads. A second layer of treatment, consisting of 50% sand, 50% water treatment residual (WTR) was added after the Biomat to adsorb

leached phosphorous, which was observed at high levels in Biomat effluent throughout the water quality monitoring phase. Phosphorous leaching associated with the use of compost in water treatment has been widely reported (Zhou & Hanes, 2009), and Kim had observed such a problem during bench scale experimentation. Previous researchers (Babatunde & Zhao, 2007; O'Neill & Davis, 2011) have found WTR to effectively remove phosphorous from stormwater and waste water in certain situations, with treatment efficacy depending on the speciation of phosphorous. Selection of WTR treatment in this case was supported by lab experiments in which batch adsorption studies were conducted using biomat effluent to assess the potential efficacy of water treatment residual to remove phosphorous.

Three media extractions were performed on Biomat treatment media at both sites following the water quality monitoring phase. These experiments characterized the stability of metals held on the mat after an extended period of use. In addition, the extraction experiments assessed the degree to which heavy metals had penetrated treatment media and therefore helped to estimate treatment lifetime, and to identify likely treatment mechanisms by assessing the relative binding strength of each metal. Finally, results are compared to comparable research carried out by fellow researchers, and implementation and design recommendations for future Biomat applications are suggested.

## Materials and Methods

### Field site preparation

To collect runoff from the front of the APHIS building and the adjacent parking lot, a polypropylene-lined, trapezoidal swale was built, designated the swale site. Curbs direct nearly all flow from the parking lot to the swale. A 120 degree v-notch weir was installed on the downstream end of the swale to allow for effluent flow measurement. A picture of this swale and the parking lot is shown in Figure 2.



Figure 2: Swale and parking lot with autosamplers and mat visible

On the backside of the building, a polypropylene-lined wooden structure was built directly parallel to the building back wall to collect direct roof runoff, known as the wooden structure. The structure slopes downward away from the building in order to facilitate flow through the mat, which was placed across the length of the wooden structure. This site is shown in Figure 3. At the bottom of the structure, rainwater collects in a gutter and flows through a 15.25 cm pipe with a Thel-mar<sup>TM</sup> insert weir to allow for effluent flow measurement.



Figure 3: The roof runoff collection area

#### Preparation of mat media

Compost was obtained from the USDA BARC campus in Beltsville, MD with assistance from the Environmental Management and Byproducts Utilization Laboratory. Two varieties of compost, leaf compost and compost made from manure and a small amount of food waste were mixed together in approximately equal proportions estimated by eye. The two composts were mixed together several times with a bulldozer. This mixture was initially used at both sites, but because of problems with insufficient hydraulic conductivity at the swale site, discussed below, the swale treatment mat was rebuilt using sieved manure compost only. Steel slag was obtained from Phoenix Services, a slag vendor in Sparrows Point, MD. Washed concrete sand was purchased from The Stone Store in Harmans, MD.

Following the results of column studies, the optimal media mixture for lead removal had been predetermined to be 70% sand : 25% compost : 5% slag by mass. The dry bulk density of the mixed compost was determined according to ASTM

D2216 with one modification: compost samples were dried for 2 hours instead of 24 hours, and due to this change in drying time they were estimated to be 90% dry instead of 100%. This shortening of the drying period allowed the media to be mixed together the same day as the compost moisture tests were performed, while the moisture content of the compost in the field was still similar to the moisture content measured in the laboratory (55.3% water by mass).

Using dry bulk densities of the compost, sand, and slag, the mass ratio above was converted to a volumetric ratio of 14 units sand to 29 units compost to 1 unit slag. The constituents were then mixed on site according to this volumetric ratio, using 5 gallon buckets to measure approximate volumes. Media were mixed together thoroughly with shovels, well past the point that the mixture appeared homogenous to the naked eye.

A 1.2 m (4 ft.) wide roll of black filter cloth (NO35 nonwoven needle-punched geotextile, see Appendix C for full specifications) was used to hold in the media and allow water to penetrate the mat and receive treatment. At the swale site, a section of cloth approximately 0.6 m (2 ft.) longer than the width of the swale was cut from this roll and placed across the width of the swale before being partially filled with media, which had been pre-mixed as described above. The filter cloth was then folded over the media and fastened shut with UV-resistant cable ties. The mat was filled with sufficient material (approximately 344 L, or 91 gal.) to ensure that it was taller than swale height at all points. In this way runoff could not overtop the mat during intense storms. Additionally, in order to prevent the mat from washing away in intense storms (an early problem at the swale,) two 1.2 m (4 ft.) pieces of iron rebar

were hammered into the ground on either side and a rope was run across, tied to each piece of rebar, and fastened to the mat itself with zip ties. The installed swale mat is shown in Figure 4.



Figure 4: The Biommat placed across the swale, with influent stormwater visible on the right side

This same mixing and installation procedure was followed at the wooden structure on the back side of the building. The incoming water head at this site was low enough that securing the mat with rope and rebar was unnecessary. The mat installed on the wooden structure held approximately 530 L (140 gal.) of media. To ensure that no overtopping occurred, cinder blocks, which supported the mat and helped it to retain its shape were used as shape supports, preventing the mat from settling. These cinder blocks were wrapped with 6-mm thick plastic and sealed with duct tape to prevent the concrete from affecting the pH of the incoming rainwater. The mat on the wooden structure is shown in Figure 5.



Figure 5: Biommat across the wooden structure, with plastic-wrapped cinder blocks as shape supports

The two treatment sites varied in the amount of treatment media used, the dimensions of treatment mats, and the ratio of drainage area : treatment media. These differences are quantified in Tables 1 and 2.

Table 1: Dimensions of each biommat and their drainage areas

	Drainage Area	Length of mat	Height of mat
Swale site	1390 m <sup>2</sup> (15,000 ft. <sup>2</sup> )	1.5 m (5 ft.)	0.3 m (1 ft.)
Wooden structure	23.1 m <sup>2</sup> (248 ft. <sup>2</sup> )	6.7 m (22 ft.)	20 cm (8 in.)

Table 2: Ratios of drainage area : treatment area for each Biommat.

	$\frac{m^2 \text{ drainage area}}{\text{linear meter of mat}}$	$\frac{ft.^2 \text{ drainage area}}{\text{linear foot of mat}}$	$\frac{\text{unit drainage area}}{\text{unit mat } \times \text{ sectional area}}$
Swale site	914	3000	3000
Wooden structure	4.9	11	24

The differences in ratios between the two sites, as calculated in Table 6, indicate that the swale receives a much higher hydraulic loading relative to the wooden structure. The higher loading is a practical necessity of using swale treatment; a drainage area as large as that of an entire parking lot would require an impractically wide treatment mat to provide the same ratio of drainage area : mat length as that at the wooden structure.

After approximately three months of attempting to test at the swale site, it became clear that rainwater was overtopping the treatment mat in nearly all storms above 0.4 cm. Laboratory infiltration tests were performed on the mixed media and separately on the sand and compost, the two materials suspected of decreasing flow rates. The infiltration tests were performed by filling two plastic columns separately, one with sand and one with compost. Water ran through the sand column at a rapid drip, but took days to flow through the column filled with compost. Once sieved to sizes above ASTM #10 (>2 mm), the compost was again placed in a plastic column of the same dimensions. The sieved compost media allowed for visibly faster infiltration, similar to the rate of sand infiltration. Although previous research (Seelsaen et al., 2007; Gibert et al., 2005) has indicated that smaller compost particles are more effective adsorbents due to their higher specific surface area relative to larger particles, these same fine particles are known to be responsible for decreased hydraulic conductivity through a porous media.

In November 2011, the swale treatment mat was rebuilt using manure compost sieved to >2 mm. The compost was separated by retaining the fraction which did not pass through an ASTM #10 sieve when placed on top of the sieve and hosed



with water. After rebuilding the treatment mat, overtopping occurred much less frequently, generally only in storms great than 1.27 cm (0.5 in.).

#### Sampling equipment and setup

ISCO 6712 Fullsize Portable Samplers were placed upstream and downstream of the mats at each site to collect influent and effluent stormwater samples, respectively. One ISCO 674 tipping bucket rain gauge was connected to the influent sampler at the swale site. The four samplers were synchronized to the minute and because of this and their close proximity to one another (all within 100 m of one another,) one rain gauge was used to record timed rainfall data that could be matched to the timed stormwater samples taken by all four samplers. Each sampler was additionally equipped with an ISCO 730 Bubbler Flow Module to measure effluent flows by constantly measuring the height of water in the channel. The bubbler tubes to detect water on the influent side were placed directly in front of each mat. But without weirs or flumes upstream of each mat, these bubblers served only to determine when rainfall was occurring by detecting water in the channel. Sampler tubes on the inflow side were placed far enough upstream of the mat that the samplers would not take in water ponded just in front of the mats during storms. On the wooden structure the inflow sampler was placed about 0.3 m (1 ft.) upstream of the mat, and at the swale site the inflow sampler was placed roughly 2.4 m (8 ft.) upstream of the mat. Downstream of the mats, the bubbler tubes were placed just upstream of each weir, so that flows could be accurately calculated from level readings. Sampler tubes on the effluent side were placed just upstream from each weir as well.

Before sampling runoff from a storm, one of two sampling regimes was selected. In order to obtain data from which it would be possible to analyze intra-storm variations of pollutants, discrete samples were taken in roughly half of the storms sampled. Each sampler was first outfitted with 12 plastic 1-L bottles, and then programmed to fill the bottles one at a time with 900 mL of stormwater each at discrete time intervals, which were set according to the predicted duration of the storm. The first sample was programmed to be taken once water at the inflow and outflow channels of each site surpassed a critical level (3.05 cm at the swale, and 2.13 cm at the wooden structure). As an example, the sampling program for a six-hour storm was set as follows:

- 1 sample at the start point
- 8 samples thereafter with 20 minutes between samples
- 2 samples thereafter with 60 minutes between samples
- 1 sample thereafter with 80 minutes between samples

Storm durations ranging from 0.4 hours to 23 hours were sampled. Before each storm, to obtain multiple samples during periods of flow, the discrete time intervals were adjusted. During storms predicted to last fewer than 2 hours, for example, the program was adjusted to:

- 1 sample at the start point
- 11 samples thereafter, each taken after a 15 minute period of flow.

For storms predicted to last 24 hours, programmed sample intervals were as follows:

- 1 sample at the start point
- 2 samples thereafter with 40 minutes between samples

- 2 samples thereafter with 60 minutes between samples
- 3 samples thereafter with 90 minutes between samples
- 3 samples thereafter with 180 minutes between samples
- 1 sample thereafter with 430 minutes between samples

Flow was defined at the wooden structure as periods in which water was measured in the channel at a depth of at least 1.5 cm (0.05 ft.) at the inflow and 3 cm (0.1 ft.), or the height of the weir opening, at the outflow. Flow was defined at the swale as periods in which water was measured at the inflow or outflow at a depth of 1.5 cm (0.05 ft.) or more.

As described above, one bottle was filled per sample during a storm, so that up to 12 distinct samples were taken in total. These 12 samples were used to analyze the variation of different water quality parameters over time during each storm. Not all twelve bottles were always filled, depending on how well actual rainfall agreed with predictions. Discrete data were accepted as valid when samples were deemed to have been taken at enough points during the storm such that they were adequately representative of the hydrograph.

In the other half of the storms sampled, a composite sample was taken. Under this second sampling regimen, all samples were pumped into the same 10-liter glass bottle. These samples were flow weighted by the sampler, so that the concentrations of pollutants within the bottle represent an estimation of event mean concentrations (EMC). Effluent samples were taken after a specific amount of flow had passed (e.g., 100 mL of sample per 50 L of stormwater flow). The volume of sample taken per volume of flow varied with the amount of rainfall predicted. A formula was used

based on the drainage area of each site with the goal of taking a total of 5 L per composite sample, with each composite consisting of roughly 100 individual samples, as shown in Equation 1.

$$\frac{5 \text{ L composite}}{W \text{ m}^2 \text{ area} * X \text{ cm rain}} * \frac{\frac{1000 \text{ mL} * 100 \text{ samples}}{1 \text{ L} * \text{ composite}}}{\frac{1 \text{ m}}{100 \text{ cm}} * \frac{1000 \text{ L}}{\text{m}^3}} = \frac{Y \text{ mL sample}}{Z \text{ L flow}} \quad (1)$$

Where W is the drainage area of the site in square meters, X is the predicted rainfall depth in cm, and Y and Z are the values entered into the autosampler.

Upstream of the treatment mat no weir was present to measure flow.

Therefore, a tipping bucket rain gauge was connected to the influent sampler under the composite sampling method; the inflow sampler was programmed to sample once every 0.01 inches of rain, and the volume of sample to be taken was changed given the amount of rainfall predicted, according to Equation 2.

$$\frac{5000 \text{ mL sample}}{X \text{ in. rain predicted} * \frac{100 \text{ rain gauge tips}}{\text{in. rain}}} = \frac{Y \text{ mL sample}}{\text{rain gauge tip}} \quad (2)$$

Where X is the predicted rainfall depth in inches, and Y is the value entered into the autosampler. Typically at least 50 of these smaller samples made up a single composite sample taken during a given storm. These composite samples were thus rainfall-weighted.

Estimation of rational runoff coefficients

During 4 storms at each site, inflow was measured with no Biomat present.

These data were used to estimate a rational runoff coefficient, as shown in Equation 3.

$$c = \frac{Q}{i * A} \quad (3)$$

Where  $c$  is the rational coefficient,  $Q$  is the measured flow,  $i$  is storm depth and  $A$  is the measured drainage area. The  $c$  value estimation was optimized by least squares, regressing  $iA$  against  $Q$  and estimating  $c$  to be the slope of this regression. For a given watershed, the value of the rational runoff coefficient is assumed to be a constant, independent of  $Q$ ,  $i$ , and  $A$ . With the  $c$  value estimate, inflow volumes were then calculated from rainfall depths for the storms in which water quality samples were taken, again according to the rational method.

#### Water quality analysis of samples

Stormwater samples were analyzed for the constituents and methods listed in

Table 3.

Table 3: Analytical methods used in field stormwater sample laboratory tests

<b>Water Quality Parameter</b>	<b>Method</b>	<b>Reference</b>	<b>Detection Limit</b>	<b>Operational Range</b>
Pb (total and dissolved)	Standard Method 3111, 3113	APHA (1998)	2 µg/L	2 µg/L – 14 mg/L
Zn (total and dissolved)	Standard Method 3111	APHA (1998)	40 µg/L	40 µg/L – 1 mg/L
Cu (total and dissolved)	Standard Method 3111, 3113	APHA (1998)	5 µg/L	5 µg/L – 10 mg/L
Total and dissolved P	Standard Method 4500 P	APHA (1998)	0.01 mg/L	0.01 mg/L – 0.5 mg/L (5 cm path length) 0.05 mg/L – 2.5 mg/L (1 cm path length)
Total Suspended Solids	Standard Method 2540 D	APHA (1998)	1 mg/L	1 mg/L or more
pH	Standard Method 4500 H+	APHA (1998)		

After every monitored storm, samples were analyzed for total and dissolved Pb, Cu, and Zn, total P, TSS, and pH. Dissolved P measurements were taken every other storm.

Both influent and effluent levels of Zn, as well as influent levels of Cu and Pb in samples from the wooden structure were measured on the flame module of a 5100 Perkin Elmer atomic absorption spectrophotometer. All other metals measurements were made on the graphite furnace module.

Samples were collected within 24 hours of the end of each monitored rainfall event. Within 24 hours of sample collection, pH was measured, filtration for TSS was performed, and filtrations in preparation for dissolved phosphorous measurement, and dissolved metals measurements were performed. Samples to be tested for metals were preserved at 4 degrees C after being acidified with trace metal grade HCl (Fisher Scientific). Samples to be tested for phosphorous were preserved with H<sub>2</sub>SO<sub>4</sub> (Reagent Grade, Fisher Scientific). TSS filtrations were performed with 0.45 μm glass fiber filters (Pall). Filtrations to separate dissolved metals and dissolved phosphorous were performed with 0.22 μm membrane filters (Millipore Express). Sample bottles, made of polypropylene, and other laboratory equipment contaminated during analyses were cleaned by first soaking in a tap water and Alconox solution, scrubbing, and then rinsing with deionized water before soaking at least 12 hours in a 0.5 M HNO<sub>3</sub> or HCl acid bath. Acid was rinsed from sample bottles with three successive washes in deionized water baths, which were replaced with fresh water at least once every four months.

Batch experiments: finishing treatment of field effluent samples using water treatment residual (WTR)

In May 2012, aluminum-based water treatment residual (WTR) was obtained from the Washington Suburban Sanitary Commission Potomac Water Filtration Plant in Potomac, MD. WTR for all experiments was obtained from a single filter pressing. Before batch experiments, WTR was air dried for one week, crushed, and sieved to <2 mm (ASTM #10).

Effluent storm samples were taken at the wooden structure on June 22, 2012 and July 14, 2012. After running each sample through a 0.22  $\mu\text{m}$  filter, duplicate mixtures of WTR and stormwater effluent were prepared at three separate effluent:WTR mass ratios: 15:1, 25:1, and 30:1. These samples were spun at 29 rpm on an Appropriate Technical Resources tumbler in 50 mL centrifuge tubes for 24 hrs. . Mixing began within 48 hours of runoff sample collection. After mixing, particulate matter was again removed by 0.22  $\mu\text{m}$  filters. Both WTR-treated and untreated effluent samples were tested for pH, DP, Pb, Cu, and Zn.

Metal speciation experiments: quality assurance protocol to establish the efficacy of DEAE Sephadex A-25 resin (chloride form) to remove anionic metal complexes

The chloride form of DEAE Sephadex A-25 resin (GE Healthcare life sciences) was used to separate anions in several samples, with the intent of distinguishing anionic metal complexes from positively-charged and/or neutral metal complexes in stormwater effluent sampled at the wooden structure. This resin was successfully used for the same purpose by Jensen et al. (1999) in experiments on

landfill leachate. To confirm that the resin effectively and selectively removes anionic complexes from solution, the following procedure was carried out.

Anionic metal complexes were synthetically created using the chelating agent EDTA (Fisher Scientific) to determine if the Sephadex resin would effectively remove these complexes. Above pH 6 and in the presence of excess EDTA, it was hypothesized that nearly all Pb, Cu, and Zn would be present as Pb-EDTA<sup>2-</sup>, Cu-EDTA<sup>2-</sup>, and Zn-EDTA<sup>2-</sup>. By using quantities of resin, EDTA, and metal such that resin binding sites were in excess relative to moles of EDTA, and EDTA was present in excess relative to metal, the experiment was conducted so that all metal would be present as anionic complexes and therefore captured by the resin. Relying on this assumption, 50 mL of a solution containing 200 µg/L PbNO<sub>3</sub> and 200 µg/L CuNO<sub>3</sub> with 1% HNO<sub>3</sub> (VWR atomic absorption standards) and 240 µg/L ZnCl (Fisher Chemical - ACS grade) were mixed with 50 mL 2\*10<sup>-5</sup> mol/L EDTA in a 120 mL borosilicate beaker using a magnetic stir bar. After 10 minutes of stirring, pH was adjusted to 6 < sample pH < 8. At this point 50 mL of sample was reserved for Pb, Cu, and Zn measurement. After 20 minutes additional stirring, 0.15 g resin was added and stirring continued for an additional 20 minutes before samples were filtered through 0.22 µm membrane filters into 50 mL centrifuge tubes to be reserved for Pb and Cu measurement. This process was repeated the next day using the same stock solutions of EDTA and metals in order to have duplicate samples. Recovery of Pb and Cu in samples treated with resin was below 10% of the mean Pb and Cu concentrations measured in the portions of each sample which had been reserved before resin addition. Recovery of Zn was slightly above 10% for one of two replicates. Table 4



shows the concentrations of Pb, Cu, and Zn in each group. These results demonstrate that the Sephadex resin effectively and selectively removed anionic metal complexes from solution.

Table 4: Concentrations of Pb, Cu, and Zn (in  $\mu\text{g/L}$ ) measured in quality control tests performed with Sephadex DEAE A-25 resin (GE Life Sciences).

concentrations, in $\mu\text{g/L}$	replicate 1	replicate 2
<b>Pb</b>		
<i>control</i>	101	81
<i>with resin</i>	<10	<10
<b>Cu</b>		
<i>control</i>	85	87
<i>with resin</i>	<10	<10
<b>Zn</b>		
<i>control</i>	120	122
<i>with resin</i>	15	<10

WTR finishing treatment at the wooden structure

To capture and further treat effluent from the Biomat, a second treatment technique was added during 3 final storms. Several holes were drilled into a 5 gallon plastic bucket at its base to allow flow through its bottom. This drilled bucket was placed inside of another 5-gallon bucket, which was cut with a 2 cm high by 5 cm wide rectangular hole, 2.5 cm above its base. Both buckets were acid-washed overnight. A circle of filter cloth was then cut and sealed to cover the bottom of the drilled 5 gal bucket, which was subsequently filled to a height of 10 cm with a mixture of 50% sand, 50% WTR (by dry weight). A piece of cinder block was placed on top of the sand/WTR mixture to prevent falling water from carving into the layer of treatment media. The drilled bucket was then placed inside of the second bucket, and these were placed beneath the outlet pipe to capture Biomat effluent (Figure 6).

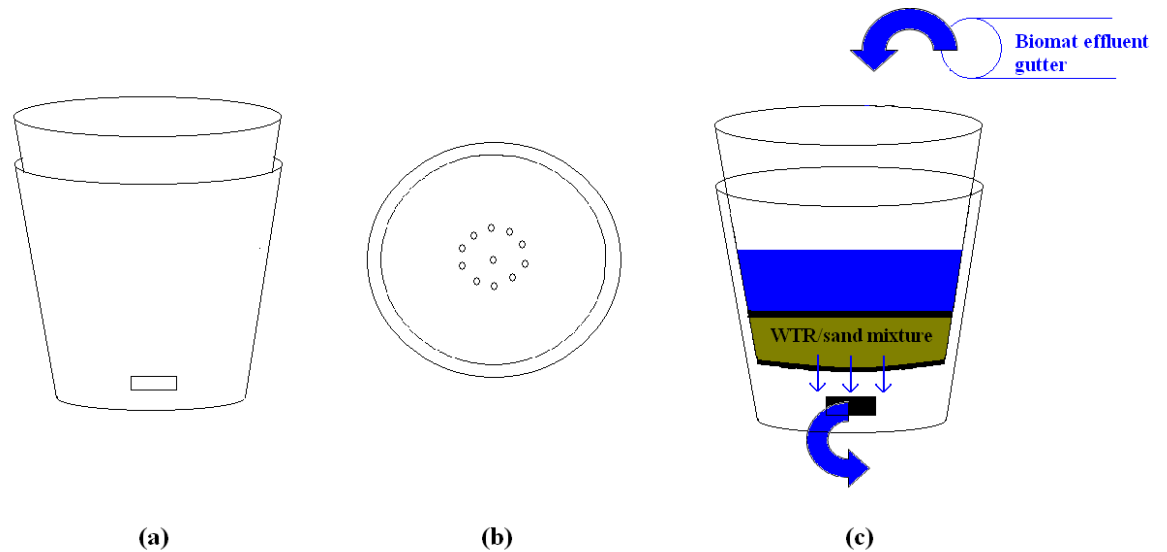


Figure 6: (a) the placement of one bucket, to contain the treatment media inside another, to contain the sampling lines (b) the drainage holes at the bottom of the upper bucket to allow for flow-through (c) a diagram of flow during a storm through the WTR/sand treatment

In this way, effluent from the Biomat at the wooden structure flowed into the WTR/sand mixture, through the drilled holes, and down into the second bucket, where an ISCO sampling line was placed to capture storm samples. Samples were taken in 3 storms to obtain preliminary data on the efficacy of this secondary treatment to remove metals and phosphorous. All normal water quality data were taken for effluent from the sand/WTR mix during these 3 storms. Speciation experiments were also performed using DEAE Sephadex A-25 resin as follows.

DEAE Sephadex A-25 resin was prepared by shaking in 3 M NaCl for 24 hours on a horizontal shake table. After filtering and washing 3 times with deionized water, the resin was air-dried for at least one week and then left in a desiccator until use. 0.25 g of resin were weighed and added to filtered samples of influent, Biomat effluent, and sand/WTR effluent. These samples were individually stirred for 20

minutes before filtration through 0.22  $\mu\text{m}$  membrane filters to remove the spent resin. A portion of each sample was immediately measured for pH and TOC, and the remainder was preserved in plastic centrifuge tubes and refrigerated at 4° C for analysis of P, Zn, Cu, and Pb. Samples to which no resin was added were also analyzed for all water quality parameters.

#### Spatially-distributed analysis of used Biomat media lability

In order to characterize the metals captured by each Biomat, and to characterize the stability of those metals, sequential extractions were performed on samples of used Biomat media. Media samples were taken at discrete locations in each mat. These samples were taken in January, 2013 at the swale and March, 2013 at the wooden structure, after all water quality data had been compiled. At the swale, samples were taken in two cross-sections parallel to flow: one in the middle, and one on the side of the swale, halfway up the slope of the trapezoidal leg. Within each cross-section, samples were divided along two axes, as show in Figure 7. Figure 8 shows the media samples being taken:

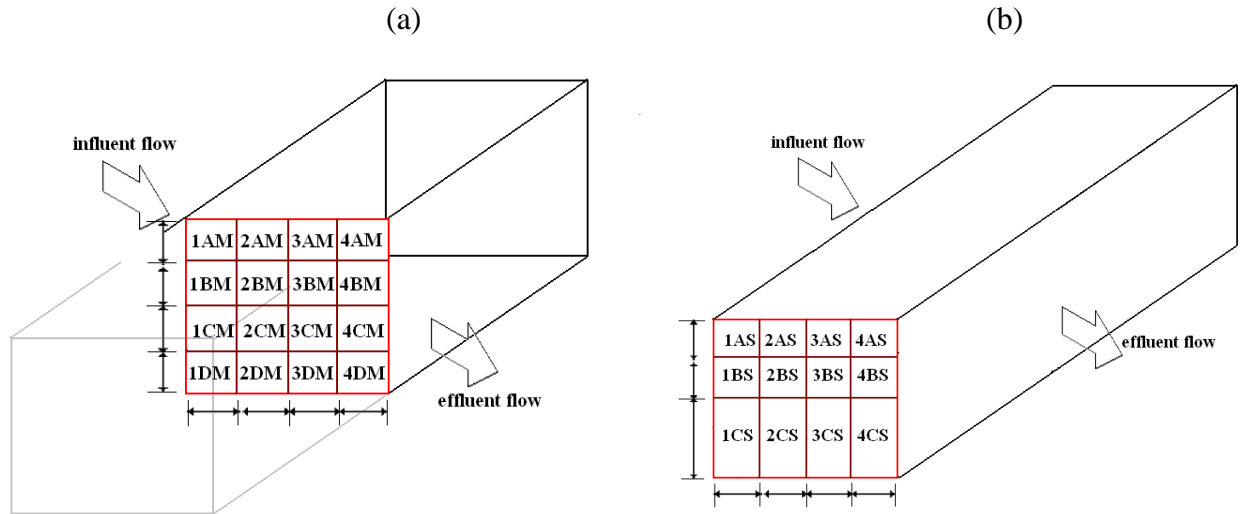


Figure 7: Location of each media sample taken at the swale mat in the middle (a), and at the side (b).



Figure 8: Swale media samples being subdivided

Figures 9 and 10 show the cross-sections taken at the rear mat, and the media sampling process

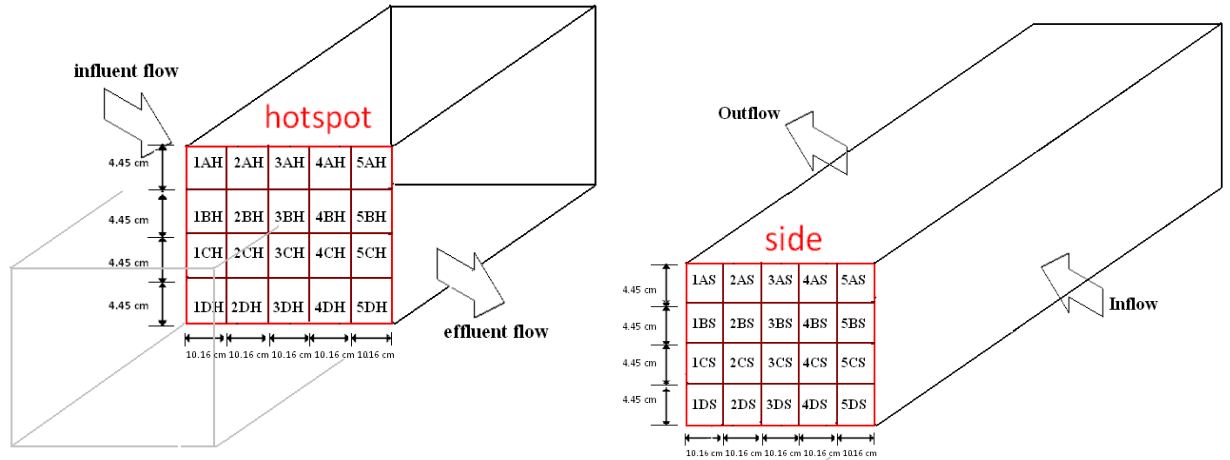


Figure 9: Cross-sections taken at the wooden structure in two locations, a hotspot of high flows, and a second location to the side



Figure 10: Two photographs taken during media sampling at the wooden structure: a) the rear hotspot cross-section, with only one sample (5DH) remaining in-situ b) the two rear cross-sections completely removed (side cross-section is in the foreground)

Samples were air-dried for 1-2 weeks, crushed to  $<4.75$  mm, and then stored in covered plastic weighing dishes. The ASTM #4 (4.75 mm) sieve was used in place of ASTM #10 (2.0 mm) so as to retain the steel slag pebbles, which were not crushable with a handheld mortar and pestle, in media samples.

In order to characterize the strength with which metals are held by this treatment, 3 sequential extractions were performed on the spent Biomat media from both sites. For each sample and each extraction step, procedures were carried out in triplicate. Phytoavailable metals were removed in the first extraction. This was

performed according to the method outlined by Madden (1988), shaking 20 g of used Biomat media sample in 40 mL of 0.01 M  $\text{Sr}(\text{NO}_3)_2$  extraction solution for 1 hr on a horizontal shake table. The extracted solution was filtered using an Ahlstrom #513 fluted filter paper inside of a #40 Whatman filter paper. A portion of the unfiltered slurry was used to measure the pH. The filtered solution was stored and refrigerated at 4° C for subsequent metals measurement by GFAAS/FAAS.

Secondly, acid ammonium oxalate extraction in darkness was performed according to an adaptation of the methods of Loeppert and Inskeep (1996). To synthesize this extracting solution, 0.2 M  $(\text{NH}_4)_2\text{C}_2\text{O}_4$  and 0.2 M  $\text{H}_2\text{C}_2\text{O}_4$  were combined to reach a pH of 3.0. 40 mL of extracting solution and 1g of Biomat media were combined in a 50 mL centrifuge tube and mixed for 2 hrs in darkness on an Applied Technical Resources tumbler at 29 rpm. The extracted samples were centrifuged for 10 min at 4000 rpm on an Allegra X-22 centrifuge and filtered with 0.22  $\mu\text{m}$  membrane filters, after which they were refrigerated at 4° C and stored until metals analysis by GFAAS/FAAS.

The third extraction was an aqua regia method adapted from McGrath and Cunliffe (1985). Several modifications to this method were implemented. Hot plates were used in this procedure in place of batch digesters, and 25 mL Ehrlenmeyer flasks were used in place of batch digester-fitted test tubes. Additionally, 5 mL of 30%  $\text{H}_2\text{O}_2$  were added to each sample prior to the addition of acids, so as to reduce the foaming associated with high organic matter in samples. Additional nitric acid (4 mL) was also added to each sample prior to the addition of the volumes described by McGrath and Cunliffe (8 mL HCl and 2 mL  $\text{HNO}_3$ ). In describing this method,

however, the authors do allow for additional nitric acid addition prior to aqua regia digestion. Apart from these modifications, the method was performed as-written. Triplicate samples of 0.5 g were used, and samples were allowed to digest overnight prior to heating.

#### Data

Data from the autosamplers were analyzed using Flowlink 4.16. All data were compiled and analyzed in Microsoft Excel. Flowlink data, including timed rainfall, water level, and flow data were imported to Excel in .csv format. From the concentration values measured for total and dissolved metals, total and dissolved P, and TSS, values for mass in, mass out, and EMC were calculated.

When composite samples were analyzed, EMC values were estimated as the concentrations measured in each composite sample. When discrete samples were analyzed, EMC values were flow-weighted using the trapezoidal linear multistep method as shown in Equation 4.

$$EMC = \frac{1}{2} * (C_1 * F_1 + 2C_2 * F_2 + 2C_3 * F_3 + \dots + 2C_{n-1} * F_{n-1} + C_n * F_n) \quad (4)$$

Where  $C_1, C_2, C_3, \dots, C_n$  are the concentrations (in mg/L) measured from each discrete sample and  $F_1, F_2, F_3, \dots, F_n$  are the volumes of flow (in L) associated with each sample, integrated from rainfall data at the influent and level data at the effluent, shown Equation 5.

$$F_{j \text{ influent}} = r * \text{Drainage Area} * \frac{1}{2} * \Sigma (\text{depth of rain deposited between } t_{j-1} \text{ and } t_{j+1}) \quad (5)$$

Where  $t_{j-1}$  represents the times at which the sample before sample  $j$  was taken,  $t_{j+1}$  is the time when the sample after sample  $j$  was taken, and  $r$  represents the calculated

rational coefficient for each site. The drainage area is measured in meters and the depth of rain is in millimeters.

Mass in and mass out were calculated for each pollutant as the product of the the EMC (in mg/L) multiplied by volume (in L) integrated across the entire storm duration:

$$\text{mass in} = EMC * r * \text{rainfall depth} * \text{drainage area} \quad (6)$$

$$\text{mass out} = EMC * \text{total volume measured at weir} \quad (7)$$

Equation 6 is the rational equation, with r based on hydrologic data from several storms measured at each site. Total flow measured at the weir was calculated internally by the ISCO autosamplers using measurements of the level of water above each weir. These measurements were taken every two minutes.

Based on the EMC values calculated for metals, probability plots were created to estimate the likelihood that influent and effluent concentrations would exceed regulatory limits in any given storm. To create these plots, EMC values were ranked from highest to lowest for each category, and assigned a rank number (highest value, 1; second highest value 2, ..., lowest value n). Nonexceedance probabilities were then calculated based on rank and sample size (n), according Equation 8 (Li and Davis, 2009). A value of  $\alpha=3/8$  in equation 8 is used for the normal distribution (Cunnane, 1978; Harter, 1984).

$$\text{exceedance probability} = \left[ \frac{\text{rank} - \frac{3}{8}}{n + \frac{1}{4}} \right] \quad (8)$$

Each exceedance value was plotted on the X-axis, paired with the corresponding metal concentration on the Y-axis. The X-scale is a probability scale and the Y-scale



is logarithmic. Straight lines on these charts would therefore suggest that the log-normal distribution is a good fit for the data.

Pollutant duration curves were established to quantify intra-storm variation of pollutants. Utilizing the trapezoidal method of integration, each discrete sample had already been assigned a representative incremental time duration [ $\frac{1}{2} * (t_{j-1} \text{ and } t_{j+1})$ ] based on the sampling frequency. Discrete concentration data from the wooden structure were ranked from largest to smallest. Concentrations were then plotted on the Y-axis and cumulative representative sample times were plotted on the X-axis.

Annual pollutant mass loadings were also calculated. Total masses in and out were calculated by summing the individual masses in and out from each storm, as calculated in Equations 6 and 7. These masses were then normalized based on drainage area and annual average rainfall in Maryland (101.6 cm), as shown in Equation 9.

$$\frac{\text{mass in (kg)}}{\text{drainage area (ha)}} * \frac{101.6 \frac{\text{cm rain}}{\text{yr}}}{\text{total depth of rainfall sampled (cm)}} = \text{mass loading} \frac{\text{kg}}{\text{ha*yr}} \quad (9)$$

## Results and Discussion

### Direct roof runoff treatment

From September, 2011 until February, 2013, twenty-six storms were sampled at the wooden structure. A wide variety of storm depths and durations were included in these samples, which were taken in all seasons (Figure 11). In order to compare the distribution of rainfall events sampled at the wooden structure to the typical climatic distribution of Maryland, rainfall events were classified according to the depth of rainfall measured and the duration of each storm (Table 5). The characteristic distribution of storms in Maryland, was previously compiled by Kreeb (2003), and is shown in Table 6. Storms ranged in duration from 24 minutes to 48 hours, and in depth from 0.08 cm to 15.6 cm. Four storms were sampled in fall, nine in winter, eight in spring, and five in summer. Mean daily temperature during sampled rainfall events ranged from a minimum of 3°C to a maximum of 27.2°C. This variety of storm events, shown in Figure 11 and Table 5, was deemed representative of the distribution of rainfall events in Maryland. At least one storm was sampled at every discrete duration category (shown in Table 100 and 101), except for the 2-3 hour rainfall duration category. Every discrete depth category was sampled as well, such that samples were taken at both the smallest and largest, shortest and longest, and warmest and coldest rainfall events. Visually comparing the distributions of Tables 5 and 6, no obvious deviation or skew from the typical distribution is visible in the distribution of rainfall events which were sampled.

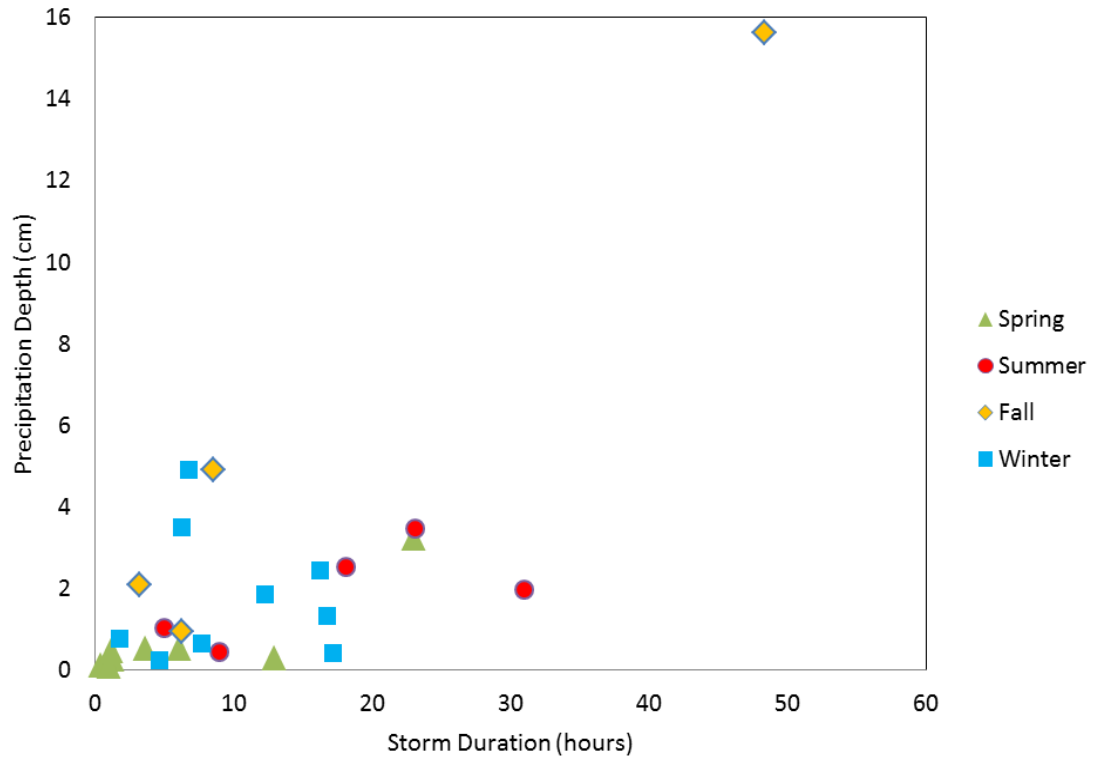


Figure 11: The variety of rainfall events sampled at the wooden structure with regard to depth, duration, and season. The extreme event at upper right represents data from from Hurricane Sandy (10/29/2012)

Table 5: Depth-duration distribution of sampled rainfall events at the wooden structure. White/lighter boxes indicate higher frequencies, and darker boxes indicate lower frequencies.

Event	Rainfall Depth (cm)					Sum
	0.0254-0.254	0.255-0.635	0.636-1.27	1.28-2.54	> 2.54	
0-2 hr	0.12	0.04	0.04	0	0	0.200
2-3 hr	0	0	0	0	0	0.000
3-4 hr	0	0.04	0	0.04	0	0.080
4-7 hr	0.04	0.04	0.08	0	0.08	0.240
7-13 hr	0	0.08	0	0.04	0.04	0.160
13-24 hr	0	0.08	0	0.08	0.08	0.240
>24 hr	0	0	0	0.04	0.04	0.080
Sum	0.160	0.280	0.120	0.200	0.240	1

Table 6: Depth-duration distribution of all rainfall events in Maryland (Kreeb, 2003). White/lighter boxes indicate higher frequencies, and darker boxes indicate lower frequencies.

Event Duration	Rainfall Depth (cm)					Sum
	0.0254-0.254	0.255-0.635	0.636-1.27	1.28-2.54	> 2.54	
0-2 hr	0.29	0.02	0.02	0.00	0.00	0.33
2-3 hr	0.02	0.03	0.02	0.01	0.00	0.08
3-4 hr	0.01	0.02	0.02	0.01	0.00	0.06
4-7 hr	0.01	0.04	0.05	0.02	0.01	0.12
7-13 hr	0.01	0.03	0.06	0.05	0.03	0.18
13-24 hr	0.00	0.01	0.04	0.06	0.05	0.16
>24 hr	0.00	0.00	0.00	0.02	0.04	0.07
Sum	0.33	0.15	0.21	0.17	0.14	1.00

#### Volume and water balance at the wooden structure

After water quality monitoring had been completed in March, 2013, and the treatment mat at the wooden structure removed, hydrologic monitoring continued until May 2, 2013, through six additional rainfall events. This allowed for the estimation of a rational coefficient. The rainfall-runoff volume relationship is shown in Figure 12.

The slope calculated in Figure 12, 0.70, was used as the rational runoff coefficient to estimate inflow volume in the storms where water quality parameters were measured. An extremely small initial abstraction volume (9.8 L), shown as the x-intercept on Figure 12, was calculated, consistent with typical findings for roof

runoff. The calculated rational coefficient is slightly smaller than comparable findings from roof runoff (>0.9). It is possible that some roof runoff was not collected due to an imperfect seal between the wooden structure and the side of the APHIS building.

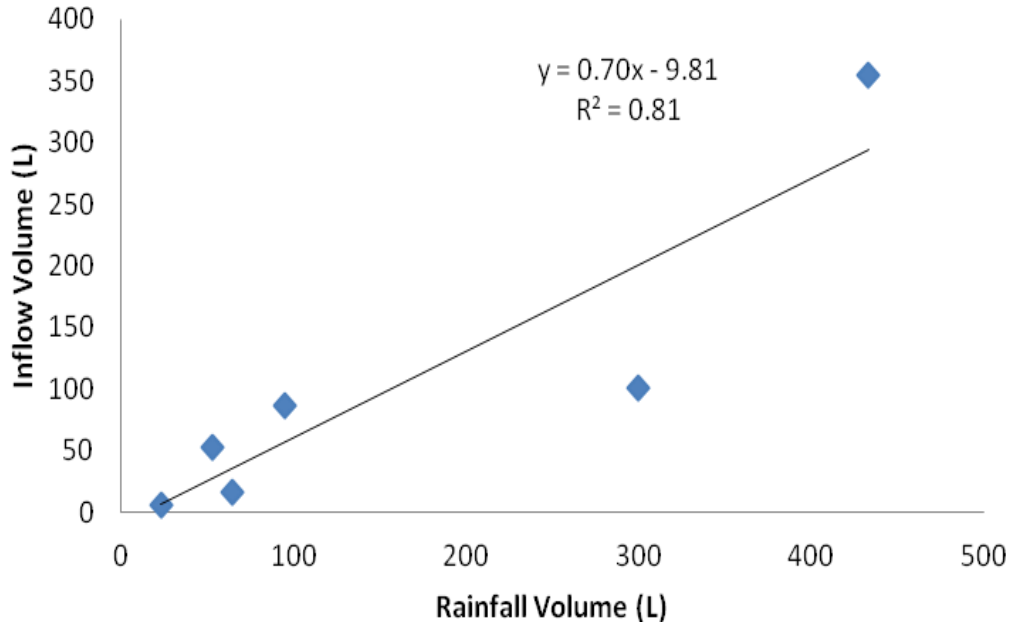


Figure 12: The rainfall-runoff relationship determined from rainfall events measured at the wooden structure. Drainage area = 23.0 m<sup>2</sup> (248 ft<sup>2</sup>.)

#### Treatment efficacy at the wooden structure

Treatment efficacy was measured mainly by reductions in the mass loading of pollutants in the effluent. Pollutant concentration reductions are also of concern however, especially for heavy metals. Figure 14 shows a typical pollutograph characterizing intra-storm variation of Pb and Cu concentrations. The concentrations shown in Figure 14 are representative of the inflow and outflow values of Pb and Cu regularly measured at the wooden structure.

Metals reductions by the mat were excellent; on the log scale in Figure 14, nearly 2-log removals are visible for each metal. Across all storms sampled, influent total Pb and Cu concentrations were observed to vary from around 1-10 mg/L and 0.2-4 mg/L, respectively. Effluent total Pb and Cu concentrations were observed to vary from around 15-200 µg/L and 5-60 µg/L, respectively. Mean concentration percent reductions were 99% for total Pb and 98% for total Cu. Total Zn was observed to vary from 20-400 µg/L as influent, and 9-90 µg/L as effluent. The mean concentration of total Zn was reduced by 41%.

Influent Pb and Cu concentrations at the APHIS building were far higher than those typically observed in urban runoff, where concentrations are typically between 5-200 µg/L for Pb and Cu (Davis et al., 2001). The concentrations of discharged Pb, however, are typical of normal urban runoff, and discharged Cu concentrations are somewhat lower. Davis et al. (2001) also reported typical Zn concentrations in urban stormwater of 20-5000 µg/L. Influent concentrations in APHIS roof runoff were therefore already on the lower end of concentrations observed in typical urban runoff, and effluent Zn concentrations were significantly lower than typical urban levels. In their review of experiments measuring roof runoff characteristics, Mason et al. (2009) found typical metal concentrations in roof runoff ranging from 20 to 324 µg/L Cu, 8 to 63 µg/L Zn, and 2.6 to 20 µg/L Pb. Boller (1997) reported average roof runoff concentrations of 90 µg/L Pb, 200 µg/L Cu, and 400 µg/L Zn. Influent Pb and Cu levels in roof runoff at the APHIS building are therefore significantly higher than typical concentrations, but Zn influent concentrations appear normal relative to these previously reported values.

Levels of Pb and Cu are so elevated in roof runoff due to the interaction of several factors. Firstly, the composition of the roof tiles, which are made of ASTM B370 lead-coated copper (materials specifications for the roof tiles are shown in Appendix C). Secondly, the pH of rainfall in the state of Maryland is generally below 5 (National Atmospheric Deposition Program, 2011), a level acidic enough to dissolve significant levels of the lead and copper oxides and carbonates which have likely formed on the roof through oxidation, a phenomenon which was observed from physical appearance of the roof tiles shown in Figure 3. Given that phosphorous concentrations were low in the influent (complete influent/effluent P concentration data is shown below in Figures 31-33) and that no obvious sources of organic carbon were present in the roof drainage area, it is likely that inorganic ligands such as  $\text{CO}_3^{2-}$  dominated the roof runoff influent. At a pH values below 5, most carbonate would be present as carbonic acid (first acid dissociation constant for carbonic acid,  $\text{pK}_{a1} = 5.6$ ) (Stumm and Morgan, 1996). At this pH, the hydroxide ion is also present at levels far exceed by the concentrations of Pb and Cu on the order of 1 mg/L observed in influent (Figure 13) and therefore much of the Pb and Cu in solution would be likely to exist as free ions,  $\text{Pb}^{2+}$  and  $\text{Cu}^{2+}$ . Upon penetrating the mat media however, solution pH likely rose due to the CaO present in steel slag, and humic matter in the compost provided a host of additional organic ligands which were available to bind with the metals present in the influent.

Because, as Figure 13 shows, Pb and Cu concentrations were reduced to such a significant degree, the environmental risk posed by the metal roof tiles coating the APHIS building was dramatically reduced, to levels that are typical of any roadway in

American cities. Given that the metals in Biomat effluent are typical to urban runoff, it is likely that bioretention or other typical SCMs could effectively treat the effluent for residual metals. Jones and Davis (2013) and Li and Davis (2009) both demonstrated that bioretention was able to effect significant removals of Pb, Cu, and Zn at metals concentrations similar to those observed in Biomat effluent. This suggests that the Biomat may be an effective pre-treatment for dissolved metals hotspots, where the risk of quickly overloading the top layers of media in swales, detention basins, or bioretention cells would demand an unreasonable frequency of maintenance.

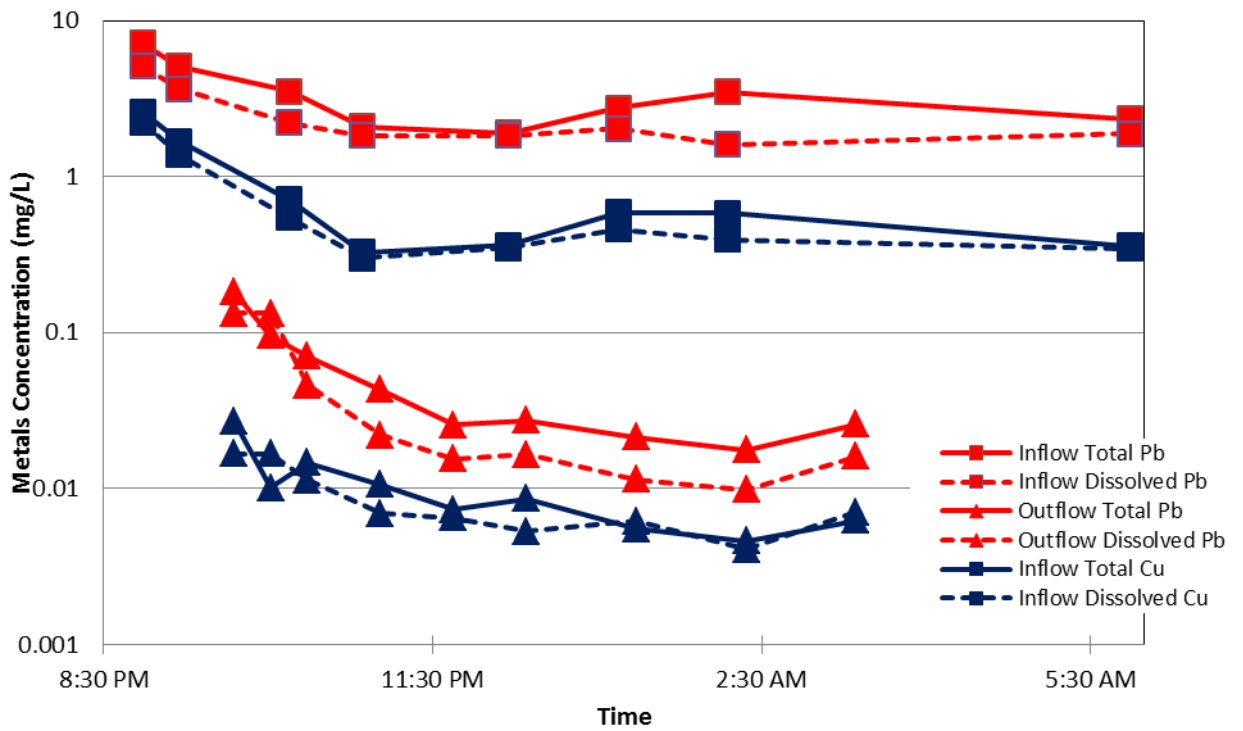


Figure 13: Intra-storm pollutograph for Pb and Cu, taken from data collected in a rainfall event on December 22, 2011. Note the log y-axis, used so that variation in both influent and effluent concentrations is visible.



The dissolved fraction accounted for a large portion of total Pb, Cu, and Zn in both the influent and effluent at the wooden structure. Approximately 55% of total influent Pb was present as dissolved species, relative to 66% of total influent Cu and 73% of total influent Zn. Karlen et al. (2002) found that nearly all Cu in direct runoff water from a copper roof was dissolved; the data here show that a majority of Cu was present in the dissolved fraction, but that significant particulate Cu was also present. As effluent, dissolved Pb accounted for 36% of total Pb, relative to 58% dissolved for Cu and 57% for Zn. The reduction in the fraction of dissolved in the effluent indicates that the Biomat removed dissolved species more effectively than particulates. Kim et al. (2013) designed the Biomat specifically to remove dissolved metals species. In previous experiments on Biomat media (Kim et al., 2013), it was hypothesized that some particulates in the effluent were freshly formed amorphous solids, which may have been too fine to be filtered out by the Biomat media.

Because Pb and Cu (and, to a lesser extent, Zn) have the potential to harm aquatic freshwater flora and fauna even at extremely low concentrations, it is important to quantify expected effluent concentrations of these metals in order to assess the likelihood of persisting negative environmental impacts after treatment. Numerous water quality standards have been established for Pb, Cu, and Zn; this study compared effluent concentrations to the most stringent of these regulations, which are listed in Table 7.

Table 7: Regulatory standards for metals of concern at the APHIS site (EPA, 2013; COMAR, 2013)

<b>Pollutant</b>	<b>Standard</b>	<b>Issuing body</b>	<b>Regulation</b>
Lead (Pb)	65 µg/L	MD Dept. of the Environment	Acute freshwater toxicity limit for aquatic life
Lead (Pb)	2.5 µg/L	MD Dept. of the Environment	Chronic freshwater toxicity limit for aquatic life
Copper (Cu)	9 µg/L	MD Dept. of the Environment	Acute freshwater toxicity limit for aquatic life
Copper (Cu)	13 µg/L	MD Dept. of the Environment	Chronic freshwater toxicity limit for aquatic life
Zinc (Zn)	120 µg/L	MD Dept. of the Environment	Freshwater toxicity limit for aquatic life

Over the course of 10 smaller storms at the wooden structure, 100% of runoff was captured by the treatment mat. Because all runoff was captured and stored, no pollutants were released to the surrounding environment during such storm events. In larger storms which did produce outflow from the Biomat, the likelihood of regulatory compliance was assessed using probability plots (Figures 15 and 16).

Figures 14 and 15 demonstrate that the Biomat effectively and consistently removed Pb, Cu, and Zn to concentrations at or relatively near to regulatory standards. Regulatory compliance (i.e., Biomat effluent concentrations at or below regulatory standards) is expected to be achieved in 81% of storms with regard to acute Pb and in 65% of storms with regard to acute Cu standards. With respect to aquatic toxicity standards, the Pb level of 2.5 µg/L is only complied with in zero-outflow events, but in 56% of storms Cu concentrations are expected to fall below the chronic freshwater aquatic toxicity limit of 9 µg/L. Given the inflow data, regulatory

compliance is never expected in untreated direct roof runoff (influent), and Pb and Cu concentrations are frequently 100 or more times higher than their regulatory standards. Treatment using the Biomat therefore greatly reduces the risk of Pb and Cu causing harm to animals in the surrounding environment on both a long term (chronic) and individual storm (acute) basis, although further reductions are desirable in some storms.

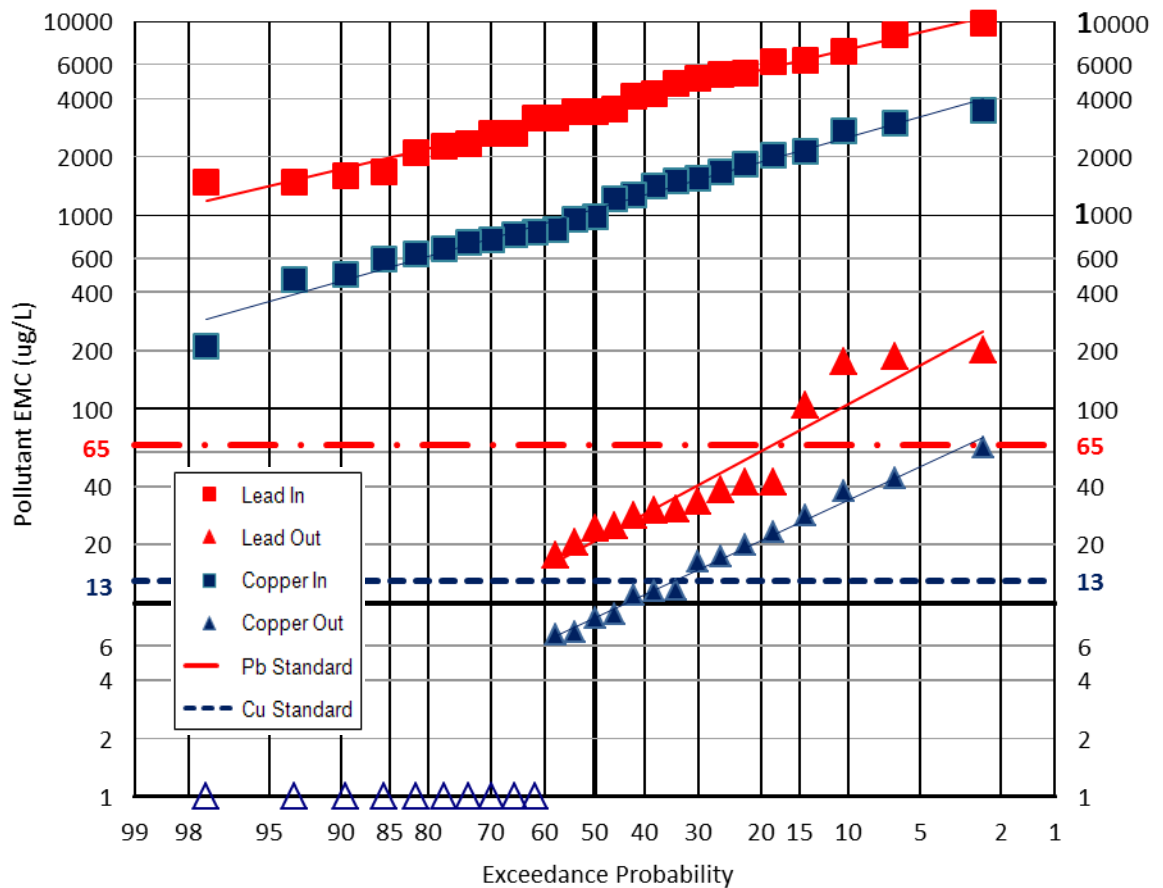


Figure 14: Exceedance probabilities for Pb and Cu in direct roof runoff influent and effluent at the APHIS building. Each data point represents an event mean concentration. Hollow triangles represent the 10 rainfall events in which no outflow was produced, and th

Figure 14 demonstrates dramatic concentration reductions for both Pb and Cu. Inflow and outflow Pb and Cu appear to be sampled from log-normal populations, as

indicated by the high degree of linearity (Davis, 2007). The parallel lines between inflow Pb and Cu and between outflow Pb and Cu indicate that a similar degree of inter-storm variation in EMCs is expected for Pb as for Cu. Figures 13 and 14 show that Biomat treatment for Pb effects the same removals as treatment for Cu, both in the amount by which metals are removed and the variation of metals removals across multiple storms in which samples were taken. These observations suggest that treatment mechanisms in the Biomat are not specific to either Pb or Cu but may operate similarly for both metals. Evans (1989) noted that the retention of metals in soil solutions depends on concentrations of metals in the solution, the metal itself (e.g., its Lewis-acid hardness, its charge, its tendency to form (hydr)oxy complexes), and the characteristics of ligands present (e.g. inorganic vis-a-vis organic, the Lewis-base hardness, surface charge). Influent concentrations of Pb and Cu are typically on the same order of magnitude, and by virtue of entering the same treatment media, the characteristics of the ligands to which both metals are exposed can be assumed to be the same. As transition Lewis acids,  $\text{Cu}^+$ ,  $\text{Cu}^{2+}$ , and  $\text{Pb}^{2+}$  all also possess a similar electron-attracting propensities (Nieboer and Richardson, 1980; Stumm and Morgan, 1996). It should not therefore be surprising that Pb and Cu removals are so similar.

Kim (2010) found weaker binding of Zn based on column and bench-scale evaluation of Biomat media. Sorption order preference was found to follow the order  $\text{Cu}^{2+} > \text{Pb}^{2+} \gg \text{Zn}^{2+}$ . Breakthrough for Zn was expected more rapidly relative to Pb and Cu because of this. Seelsaen et al. (2007) reported the order of metal removal affinity by compost as  $\text{Pb}^{2+} > \text{Cu}^{2+} > \text{Zn}^{2+}$ , based on batch studies with a plant-waste based compost. Jang et al. (2005) found the same removal affinity order based on batch

adsorption studies with hardwood bark mulch as the adsorbent. Irving and Williams (1948) found the above results to fit within their findings as well, with the complete order for the stability of bivalent metal complexes with organic ligands listed as Pb>Cu>Ni>Co>Zn>Cd>Fe>Mn>Mg.

Considering the factors proposed by Evans (1989), the removal of Zn by the Biomat is predicted to be different from that of Pb and Cu.  $Zn^{2+}$  is a less electronegative ion relative to  $Cu^+$ ,  $Cu^{2+}$ , and  $Pb^{2+}$  based on the  $X_{mr}^2$  index (Nieboer and Richardson, 1980; Stumm and Morgan, 1996). Zn concentrations observed in the effluent were typically at least a full order of magnitude lower than Pb and Cu concentrations.

Nonetheless, Figure 15 demonstrates excellent removal of Zn, resulting in consistent (>95%) compliance with the regulatory limit for effluent from the Biomat. Concentration percent reductions of Zn were clearly lower than those observed for Pb and Cu, but regulatory compliance was achieved with greater consistency for Zn relative to other metals. The fact that Zn entered the Biomat at significantly lower concentrations relative to Pb and Cu is important to consider. Given that regulatory compliance was achieved in 80% of storms as influent with regard to total Zn, 95%+ concentration reductions should not be expected or even necessarily desired from an aquatic toxicity and/or environmental risk standpoint.

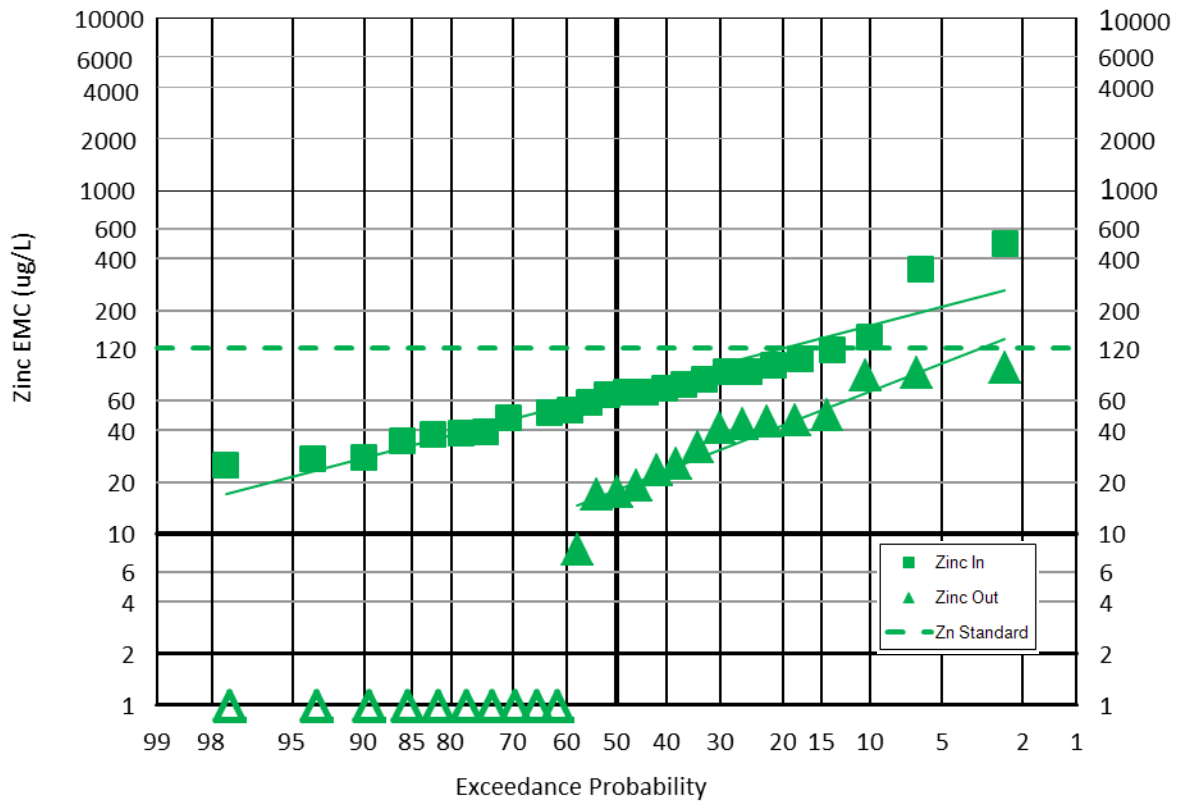


Figure 15: Exceedance probabilities for Zn in direct roof runoff influent and effluent at the APHIS building. Each data point represents an event mean concentration. Hollow triangles represent the 10 rainfall events in which no outflow was produced, and therefore no metal was released.

The metal concentration data presented here demonstrate that concentration percent reductions are a weak measure of treatment efficacy when considered alone. The parameters of primary environmental concern are the concentration of pollutants in the effluent and the total mass of each pollutant released (i.e., the acute severity and the amount of pollution released). By definition, concentration percent reduction depends on the concentration of pollutants in the influent. Because of this, the effectiveness of treatments is not adequately measured by percent concentration removals, particularly for those treatment mechanisms which rely on a concentration gradient to remove pollutants.

## Treatment efficacy on a mass removal basis

Total mass inputs and outputs from sampled events for each metal were calculated by summing the values of Equation 6 (mass in) and Equation 7 (mass out) from each storm. Over the course of the 26 storms sampled, for example, 22.2 g of Pb entered the Biomat at the wooden structure and 62 mg Pb were discharged. Extrapolating these Pb data and the Cu and Zn data, annual pollutant mass loadings (Table 8) were calculated for each metal at the influent and effluent, based on Equation 9.

The influent loadings for Pb, Cu, and Zn, reflect the clear environmental risk posed by buildings such as APHIS 580, a risk that comes to light once all architectural zinc, copper, and lead is taken into account. Although the concentration of Pb measured in the roof runoff at the APHIS building is likely exceptional, architectural Cu and Zn are common design elements throughout the country. Table 8 quantifies the amount of toxic compounds leached to stormwater runoff on an annual basis and demonstrates that metal roofing may be a significant source of nonpoint source metals. The effluent mass loadings are dramatically lower for all metals, and underscore the potential for widespread application of this treatment to reduce the risk of toxic effects in natural waters resulting from stormwater metals. These effluent mass loadings also demonstrate that Biomat treatment would reduce Pb, Cu, and Zn mass loadings at hotspots with severe contamination issues to loadings more typical to urban runoff. Li and Davis (2009) measuring Pb, Cu, and Zn loads at two parking lots in urban areas of Maryland, found pollutant loads for Pb ranging from 0.03-0.09 kg/ha-yr and 0.12-0.26 kg/ha-yr for Cu. The Zn loadings measured by Li and Davis,

however, ranged from 0.36-1.0 kg/ha-yr, a finding not significantly different from the influent loading at the APHIS building.

Table 8: Annual pollutant mass loadings for Pb, Cu, and Zn

Annual Pollutant Mass Loadings (kg/ha/yr)			
<i>Pollutant:</i>	<b>Pb</b>	<b>Cu</b>	<b>Zn</b>
Influent Loading:	19.0	5.8	0.6
Effluent Loading:	0.05	0.02	0.06

#### Intra-storm variability

Several trends within individual storms were observed based on discrete storm sample water quality data such as Figure 13. No outflow, and therefore no metals release, occurred during 10 storms at the wooden structure. However, a first flush behavior in the effluent was observed in most outflow-producing storms, especially for Pb. This could suggest that prior to these outflow-producing storm events, a small fraction of the metals held within the mat were weakly bound, and therefore easily released once effluent began to flow. A similar trend for Zn and Cu in the runoff from green roofs was observed by Berndtsson et al. (2010), who interpreted the results as a first flush from the green roof media, suggesting that loosely-bound metals had built up prior to the storm. Two other trends are visible in Figure 13. Firstly, an initial release of elevated amounts of metal is visible in the influent as well as the effluent. Influent first flushes are considered characteristic of stormwater for metallic pollutants, which do not volatilize during dry periods and therefore accumulate until storm events wash deposited metals off of surfaces in the watershed. For this reason,



previous studies (Gupta and Saul, 1996; Hewitt and Rashed, 1991) have found the antecedent dry period to be a major factor controlling pollutant concentrations observed in urban stormwater runoff.

The second phenomenon visible from the data in Figure 13 is a steady state or equilibrium concentration for metals in the effluent. After the first flush, effluent metals are present at significantly lower concentrations, and can be accurately described by an equilibrium model (Equation 10), with  $c^*$  approximately equal to  $c_{out}$ . This is evidenced by the small amount of variation in dissolved metals concentrations that was observed in storms where discrete sampling was used (e.g., Figures 13 and 16-19). As the storm progresses, initially high metals concentrations (largely particulate) level off, and do not appear to continue decreasing. This trend was observed in most storms, and several additional pollutographs (Figures 16-19) from other sampled storm events were compiled to demonstrate the persisting trend. Although the speed of equilibration varies, the pattern of reduction to a constant, nonzero concentration for both Pb and Cu appears to indicate that an equilibrium pollutant level between the treatment media (which are not completely free of metals) and the influent runoff is eventually reached.

Effluent metals concentrations were reasonably constant from storm to storm following the first flush, which varied considerably in duration and consisted overwhelmingly of particulate metals. Data from the 10 storms where discrete data was taken and effluent was produced at the wooden structure were compiled. Hydrologic data and water quality data from samples taken in the rising limb of the hydrograph, as shown beneath the blue line in Figure 16 for example, were

discounted in order to calculate a steady-state event mean concentration from the remaining hydrologic and water quality data for each of the 10 storms, according to Equation 4. An example of this steady-state period is shown under the green line in Figure 16. The rising limb of each hydrograph was specifically removed because it was presumed that no new flushing of previously-stored metals would occur after hydraulic head began decreasing. This technique is also easily transferable to storms of differing durations and depths.

Comparing water quality data post-rising limb to discrete data sets from entire rainfall events quantified the flushing of particulate metals. Examining the data for Pb and Cu, dissolved concentrations post-rising limb were present at concentrations constituting 65% and 91% of total Pb and Cu, respectively. When including the rising limb of each effluent hydrograph however, dissolved Pb and Cu account for only 34% and 58% of total Pb and Cu, respectively. This difference can be attributed to the qualitative observation in Figures 18 and 19 that the first flush often was characterized by high particulate metals concentrations, while dissolved concentrations often remained comparable to those observed later in storm events. The post-rising limb mean concentration of total effluent Pb over the 10 discretely-sampled storms was 30  $\mu\text{g/L}$ , somewhat lower than the mean total effluent Pb concentration of 38  $\mu\text{g/L}$  which included water quality data taken during the rising limb of each of the ten outflow producing, discretely measured storm events. This also suggests that greater amounts of particulate Pb were released during the beginning of storm events.

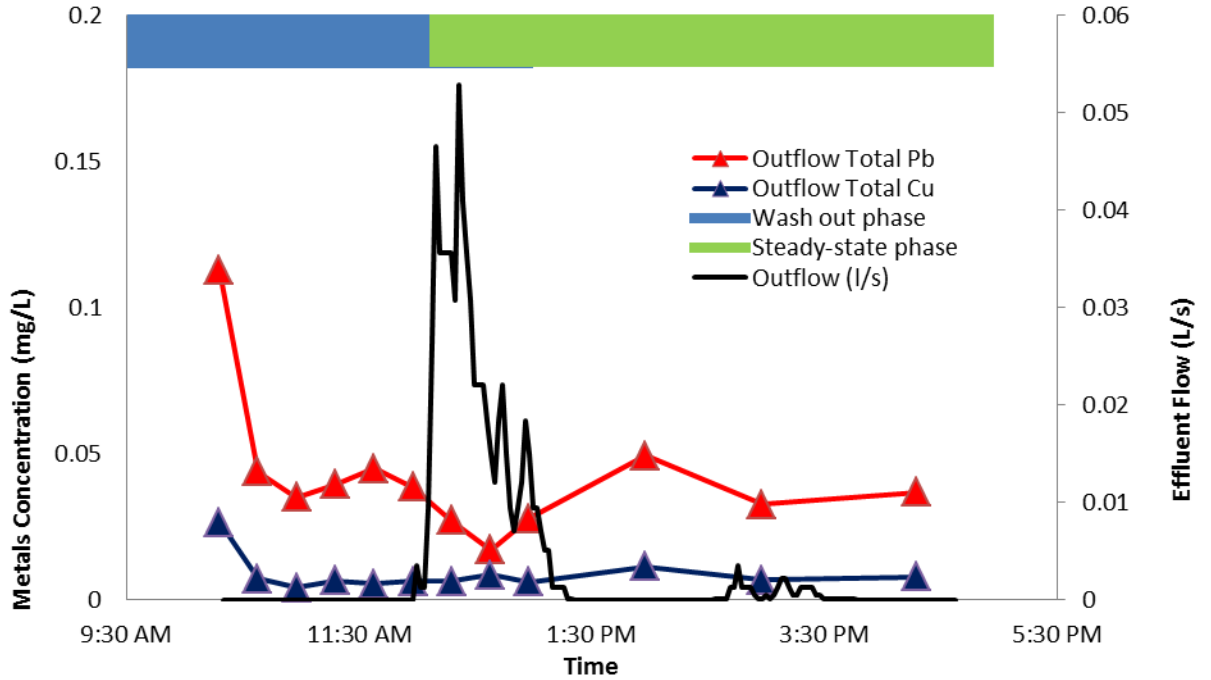


Figure 16: Intra-storm variation of Pb and Cu in effluent samples taken on September 23, 2011.

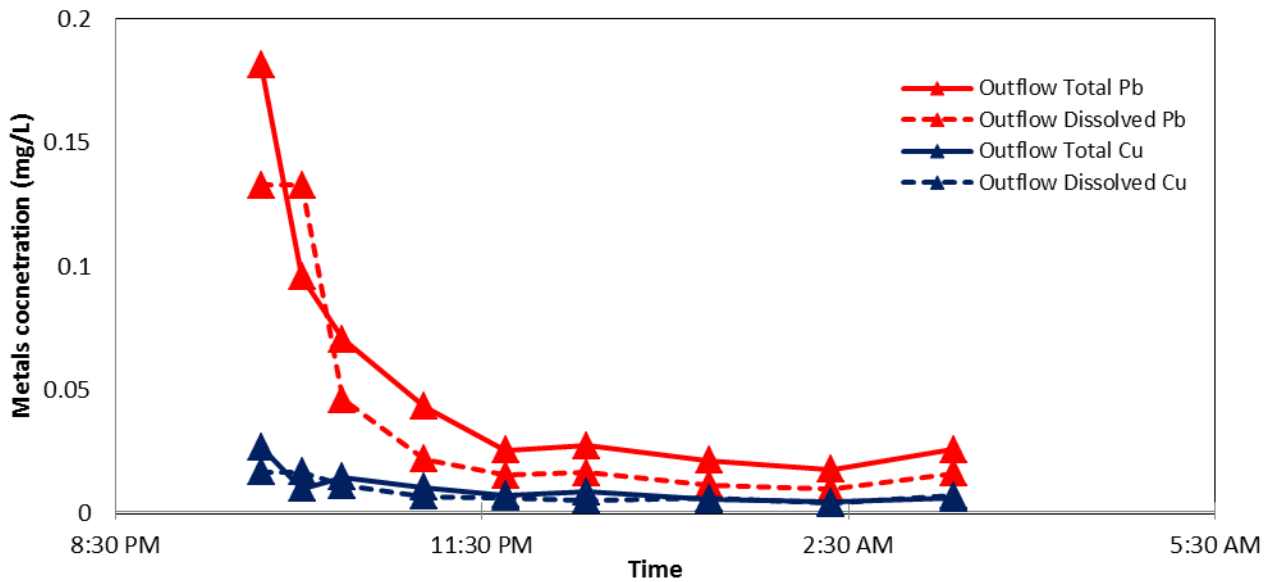


Figure 17: Intra-storm variation of Pb and Cu in effluent samples taken on December 22, 2011.

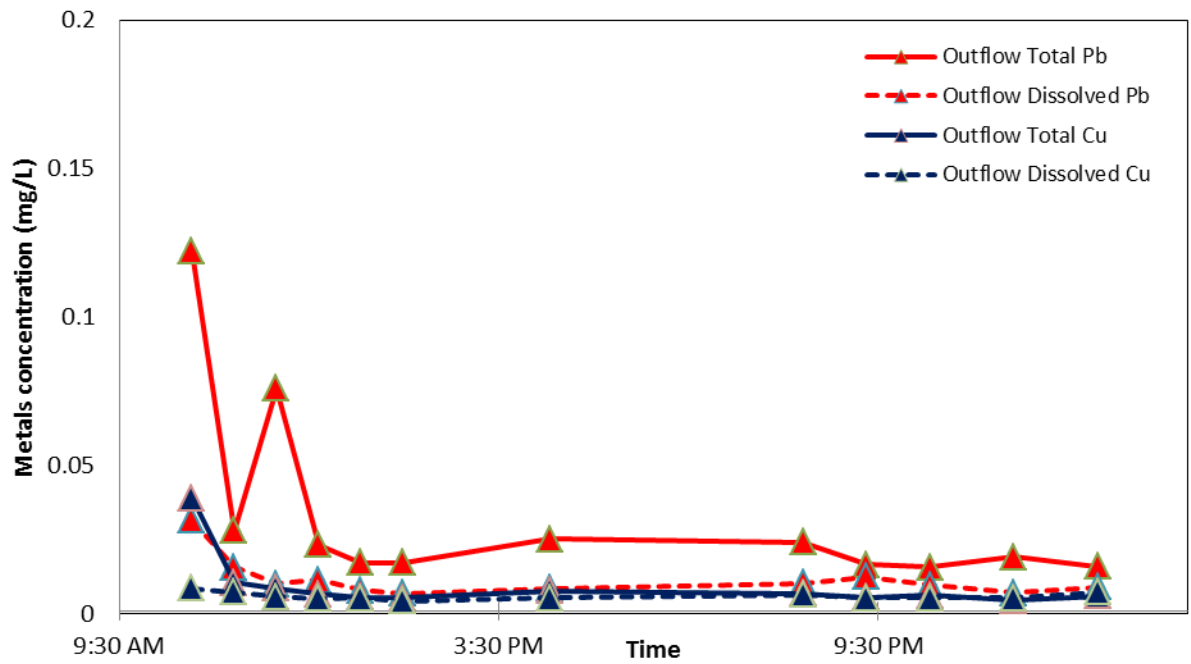


Figure 18: Intra-storm variation of Pb and Cu in effluent samples taken on February 29, 2012.

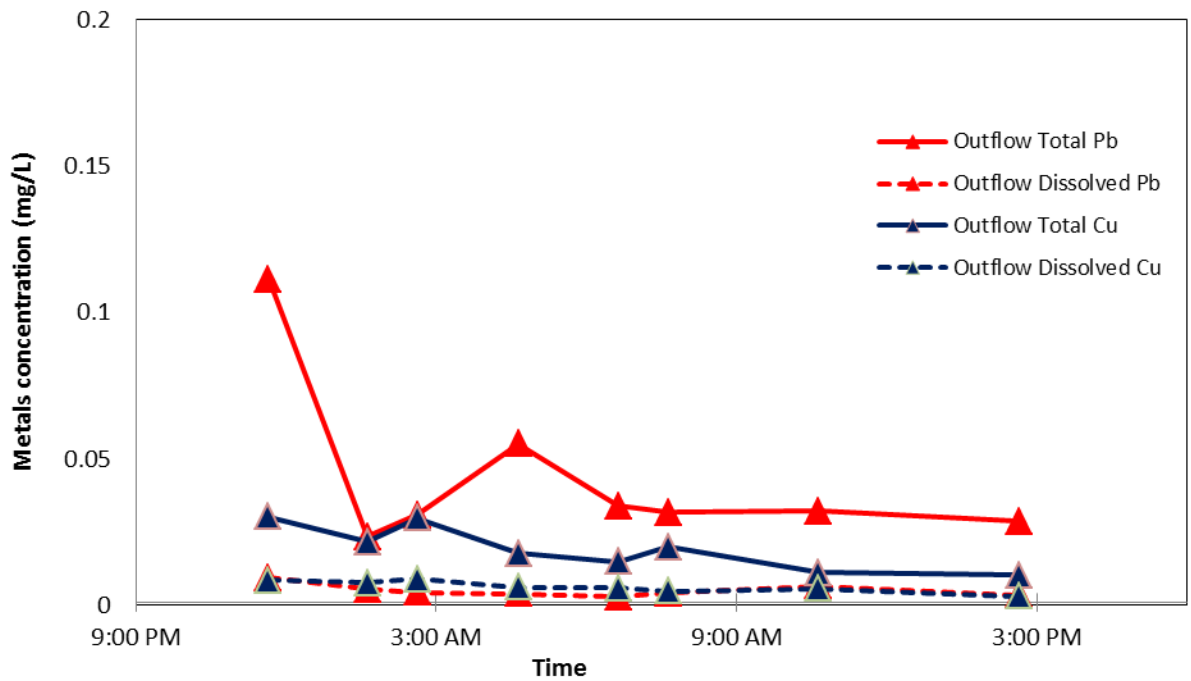


Figure 19: Intra-storm variation of Pb and Cu in effluent samples taken on October 29, 2012

As mentioned, Figures 13 and 16-19 all indicate that stormwater runoff entering the Biomat is treated to a specific steady-state level which can be modeled as an equilibrium relationship between the liquid runoff and the solid treatment media. Kim (2010) analyzed the chemical characteristics of steel slag and two composts similar to those used in the APHIS Biomats, one manure-based and the other grass/food waste-based. The reported ranges of total metals concentrations were 13-36 mg/kg Pb, 24-35 mg/kg Cu, and 113-172 mg/kg Zn. Although these values do not speak directly to the lability of the metals present in each material, they demonstrate that the Biomat media are not a purified treatment media and suggest that metals removals will not be 100% efficient. As will be directly demonstrated by the sequential extraction data performed on media samples, a small fraction of the metal that is present on the outer and inner surfaces of the treatment media does release into solution. A simple model will therefore be introduced to explain the equilibrium relationship that exists between incoming dissolved metals in stormwater runoff and the treatment media.

#### Equilibrium model of effluent pollutant concentrations

Erickson et al. (2007), in their study to increase dissolved P removal in stormwater sand filtration systems, proposed Equation 10 as a simplified model to explain the mass balance of P between incoming synthetic stormwater and their treatment media. This same model can be used to explain the individual mass balances of dissolved Pb, Cu, and Zn between incoming roof runoff and the Biomat media.

$$c_{in} - c_{out} = (c_{in} - c^*)(1 - e^{-kat_c}) \quad (10)$$

The variables in Equation 10 quantify properties related to the incoming stormwater, reactor design, and treatment media.  $c_{in}$  refers to the dissolved pollutant concentration in influent stormwater runoff, and  $c_{out}$  denotes the dissolved pollutant concentration in effluent stormwater runoff. The variables in the exponent describe the extent of the reaction:  $t_c$  is the contact time,  $a$  is the volume specific surface area, and  $k$  is the rate constant, with units of length/time.  $c^*$  describes a steady-state concentration, which  $c_{out}$  approaches as the contact time increases. For this study,  $c^*$  was assumed to be constant because metals breakthrough did not occur. The data collected here, including the water quality data described by Figures 13 and 16-19, as well as the extraction data which will be presented later in this thesis, suggest that a steady-state concentration is reached in every storm, i.e., that  $c^* \approx c_{out}$ .

Separate from the observed steady-state behavior, the leaching of effluent metals at the beginning of most storms is explained by the accumulation of weakly bound metals from previous storms, where a fraction of influent roof runoff was stored in the pores and subsequently evaporated, leaving a small amount of unbound or weakly-bound metals behind. This explains the flushing behavior, most easily distinguishable in Figures 18 and 19, where effluent particulate metals represent a dominant fraction of total metals in the first sample from each storm. The extent of the effluent first flush likely depends on the antecedent dry period, a variable which was not included in this study.

Table 9 shows the overall mean concentration values for each dissolved metal as well as characterizing the variation of these values across all sampled storms. The low concentrations for each metal in Table 9 suggest that the Biomat is likely to be an

effective treatment media for achieving metals reductions at hotspots. The entire range of mean concentrations is shown in the bottom two rows of Table 9. The small range in observed effluent dissolved metals concentrations indicates that similar effluent dissolved Pb and Cu concentrations were observed in each storm, with little overall variation. This suggests that equilibrium is being reached between the media and the stormwater runoff, and that consistent reductions below these values are not possible with this treatment media. The observed consistency in effluent dissolved metals concentrations occurs despite wide ranges of influent metals EMCs, storm depths, durations, and ambient temperatures. Whatever the reaction rates of dissolved Pb and Cu removals within the mat, kinetics does not appear to limit treatment performance for these two metals at the wooden structure. The findings in Table 9 therefore show that the Biomat is likely to be effective as a dissolved metals removal technique in a wide variety of environmental conditions: in large and small storms, hot and cold temperatures, and at a wide variety of metals loadings.

Table 9: Mean effluent steady-state concentrations for dissolved metals at the wooden structure. Standard deviation and range are shown as well. The values in parentheses in the Pb column indicate values which exclude the rainfall event on October 12, 2012, during which some bypass was suspected. Outflow was small enough in this event as to not affect the mean overall concentration, which is flow-weighted.

	Dissolved Pb	Dissolved Cu	Dissolved Zn
Mean overall concentration (mg/L)	0.012	0.008	0.066
Standard deviation (mg/L)	0.046 (0.019)	0.015	0.064
Maximum EMC (mg/L)	0.18 (0.068)	0.028	0.249
Minimum EMC (mg/L)	0.004	0.004	0.015

The observations of such consistent effluent dissolved metals concentrations and the data in Figures 13 and 16-19 all suggest that at some point prior to discharge

from the mat, Pb, Cu, and Zn dissolved in solution had equilibrated with Pb, Cu, and Zn on the treatment media. The observed steady-state effluent concentrations of Pb, Cu, and Zn appear to indicate that metals removal in the mat occurred quickly relative to overall retention time of water during storm events. Given that the wide variety of storm depths and durations exerted a wide range of hydraulic heads on the Biomat media and yet effluent concentrations remained relatively constant, it is evident that within the range of treatment times observed (on the order of minutes) effluent dissolved metals concentrations were independent of treatment time. The chemical reactions governing the efficacy of treatment appear to occur much more quickly relative to the time required for influent water to pass through the porous treatment mat despite the wide ranges of treatment times and influent concentrations.

However, it is important to note that the kinetically-controlled equilibrium levels of Pb, Cu, and Zn (estimated in Table 9) could change due to a variety of factors inherent to Biomat treatment. If treatment time were extended from minutes to weeks (e.g., if the mat were designed with insufficient slope to fully drain water following rainfall events), another set of slower reactions could alter the steady-state level of effluent dissolved metals. As the product of the biological breakdown of organic matter, compost is a dynamic material which is expected to continue to mature while in use as Biomat treatment media. Warm temperatures and reducing conditions immediately following rainfall events would be expected to accelerate the breakdown process, freeing more organic matter and, potentially, metals which had previously bound to these organic ligands. Similarly, steel slag is also expected to continue breaking down as time passes, and if left in solution for weeks or months



could push the pH of effluent solution increasingly higher, altering the chemistry of Biomat effluent greatly. The steady-state levels estimated in Table 9 do not therefore represent the concentrations of Pb, Cu, and Zn expected at thermodynamic equilibrium, when all reactions have proceeded to their final steady-state.

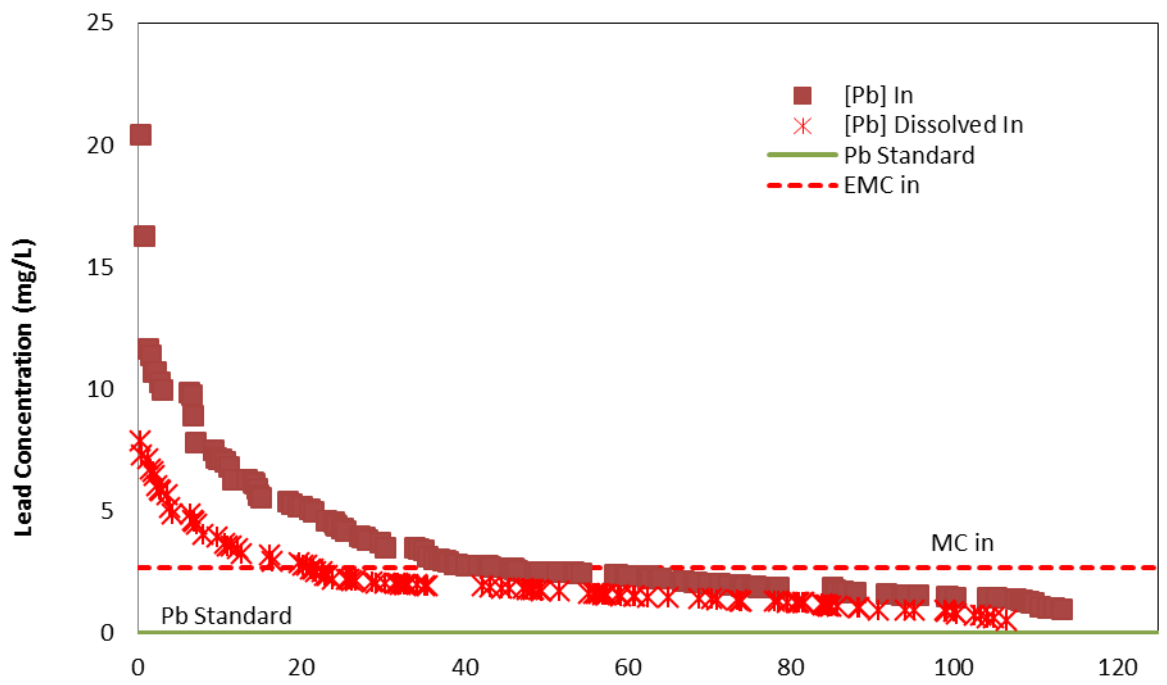
The high degree of intra-storm variation in both influent and effluent pollutant concentrations also suggests that from an aquatic toxicity perspective, conditions in receiving environments would often deviate from the values predicted by EMC estimates. Pollutant duration curves (Figures 20-22) were therefore prepared to provide perspective on the typical concentrations of metals released.

Effluent Pb and Cu are both present at levels at or below water quality standards approximately 75% of the time (Figures 20 and 21). Influent Zn concentrations are below the aquatic toxicity limit over 85% of the time (Figure 22), and effluent Zn concentrations are below this standard over 95% of the time.

Similar to the pollutographs in Figures 17-20, the pollutant duration curves for Pb and Cu (Figures 20-21) suggest that equilibria may exist between metals in the effluent and trace amounts of each of these metals (Pb, Cu, and Zn) in the treatment media. If an equilibrium does exist between stormwater discharge and the treatment media, then consistent reductions below an equilibrated metals concentration are not possible with this media. Figures 23-24 provide a closer look at lower concentrations of Pb and Cu. In order to show these data more clearly, the range on Figures 20-21 was adjusted to show only values at or below one standard deviation above the maximum event mean concentration for each metal, thereby excluding a small portion

of the data. A second figure was not created for Zn, because this range was already adequately shown in Figure 22.

Figure 23 shows that among the lowest Pb concentrations measured in discrete data, no threshold value distinguishes itself as an asymptote, i.e., concentration data do not flatten out at a discrete, non-zero value. The lower end of the curve is instead fairly linear in an apparent approach to zero, or to some value below the method detection limit (2 µg/L). The data in Figure 24 show that Cu was removed to levels near the overall mean concentration with great consistency. Over 90% of all discrete effluent data for dissolved Cu is included in Figure 24, and all Cu concentration measurements in Figure 24 are within a 35 µg/L range. This consistency is best explained by a steady-state relationship, where several factors are driving the incoming roof runoff towards equilibrium (e.g., concentration gradient, availability of sites, and contact time) before water is discharged from the mat as effluent. The data for Cu do appear to asymptotically approach a nonzero value, which appears to be at or just below the method detection limit for Cu, 5 µg/L. A clear flattening of the curve is visible in Figure 24, indicating that Cu concentrations may be approaching an equilibrium threshold that cannot be crossed using the existing Biomat media.



## Lead OF steady state PDC

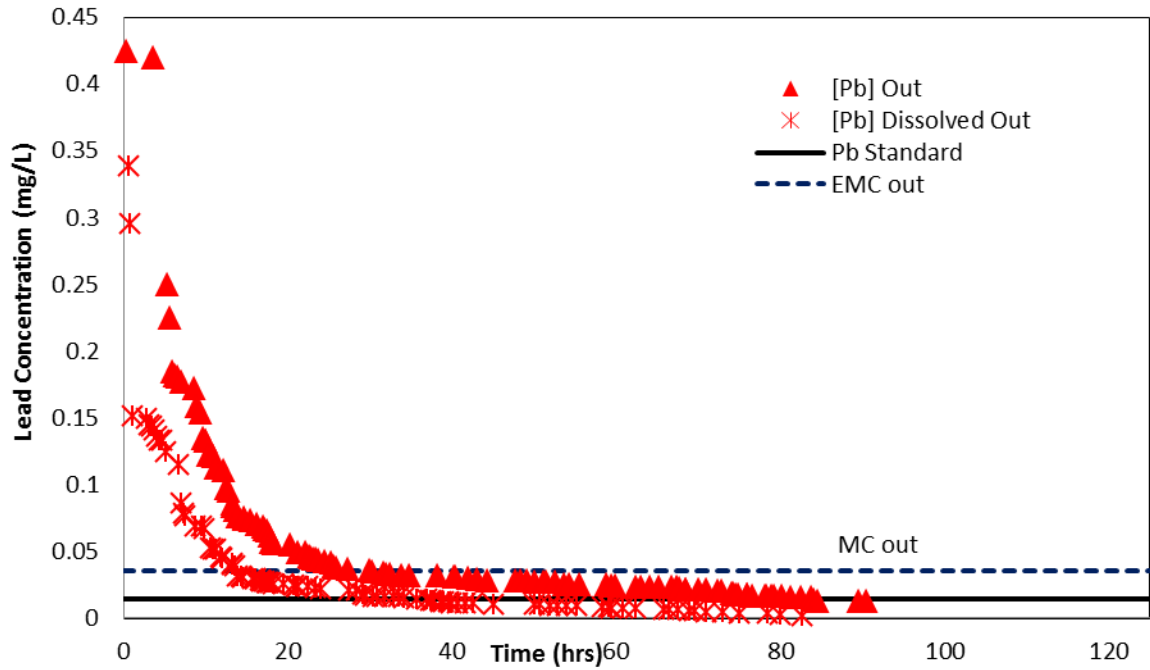


Figure 20: Pb pollutant duration curve. Data from all 17 storms in which discrete sampling was used are included. Concentration data were ranked and assigned a representative sample time based on the sampling program used (see methods). The dashed lines labeled "MC In/Out" show the mean concentrations observed.

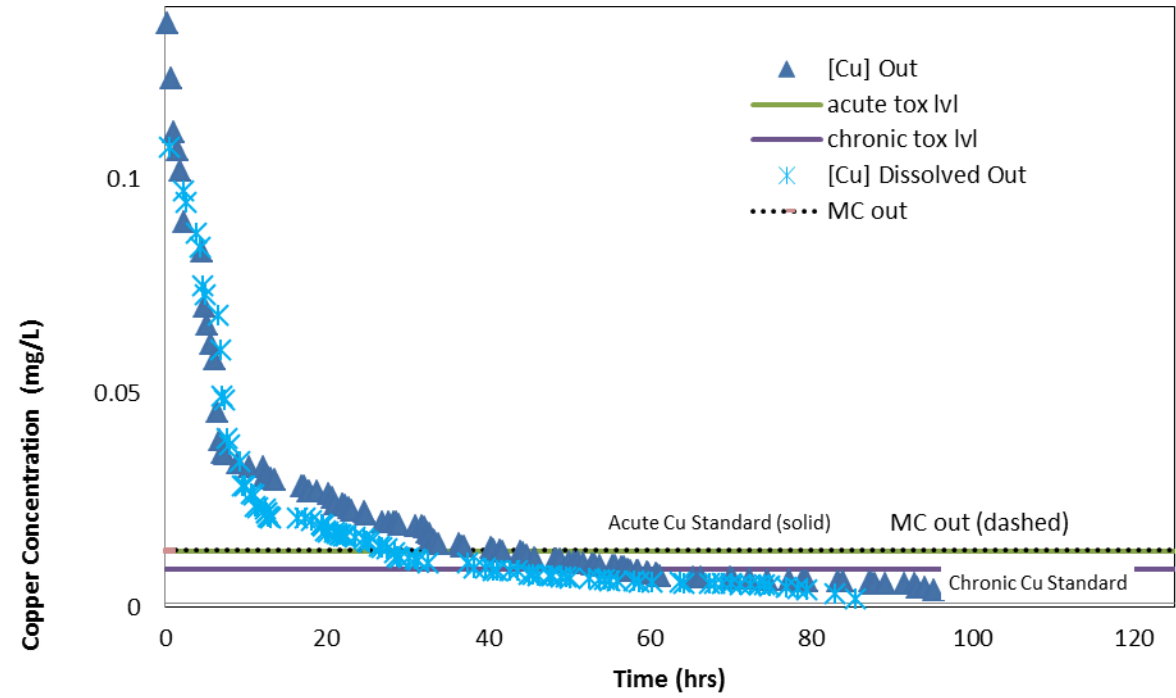
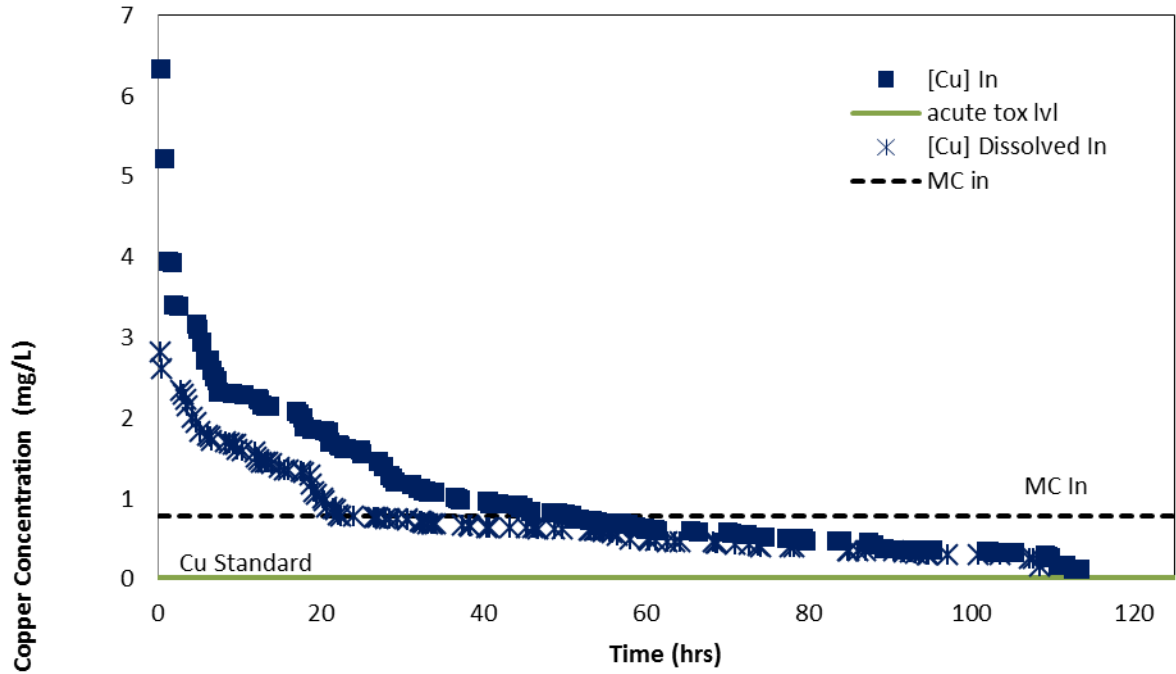


Figure 21: Cu pollutant duration curves. Data from all 17 storms in which discrete sampling was used are included. Concentration data were ranked and assigned a representative sample time based on the sampling program used (see methods). The dashed lines labeled “MC In/Out” show the mean concentrations observed.

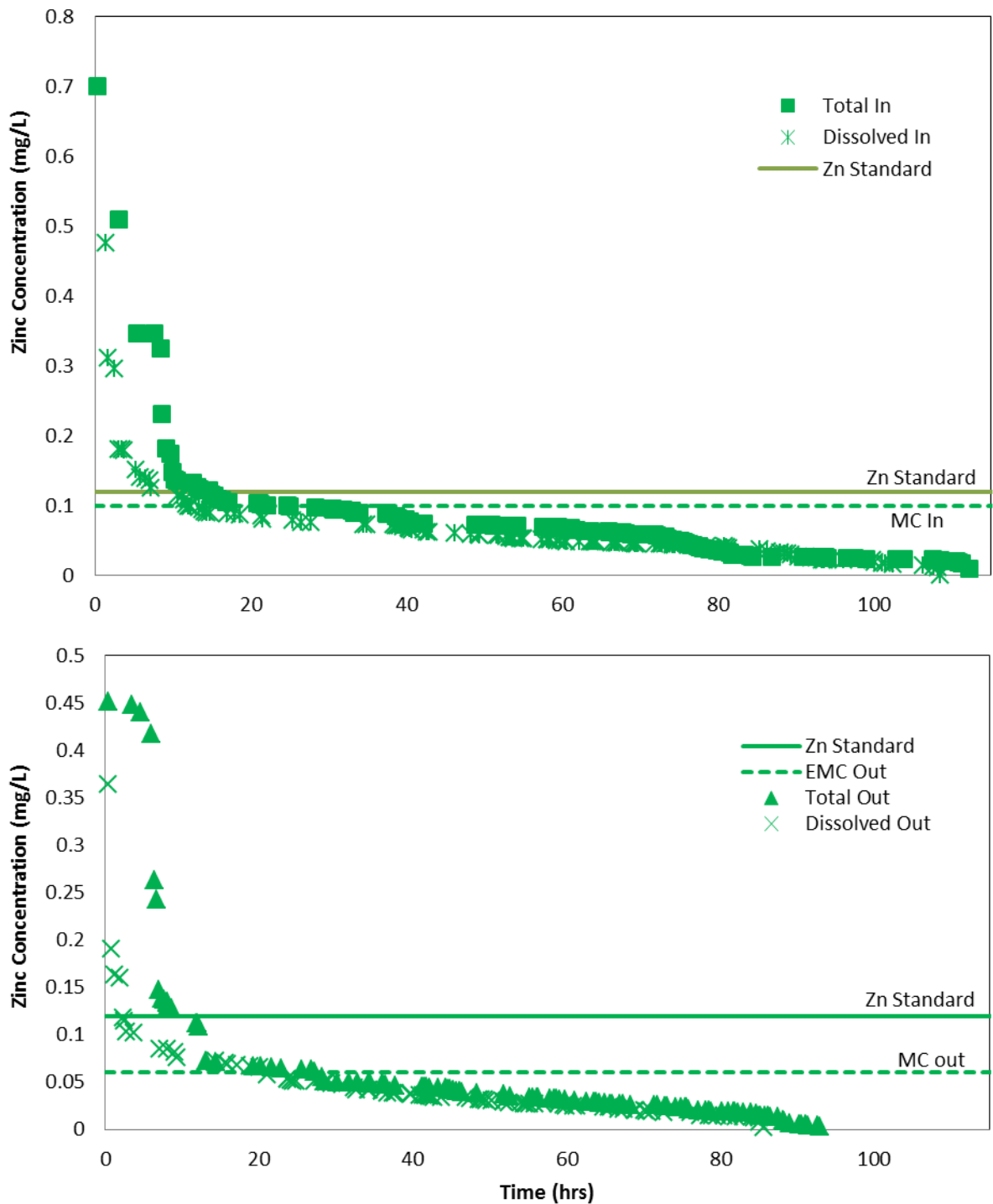


Figure 22: Zn pollutant duration curve. Data from all 17 storms in which discrete sampling was used are included. Concentration data were sorted high-to-low and assigned a representative sample time based on the sampling program used (see methods). The dashed lines labeled “MC In/Out” show the mean concentrations observed. The dashed lines labeled “MC In/Out” show the mean concentrations observed.

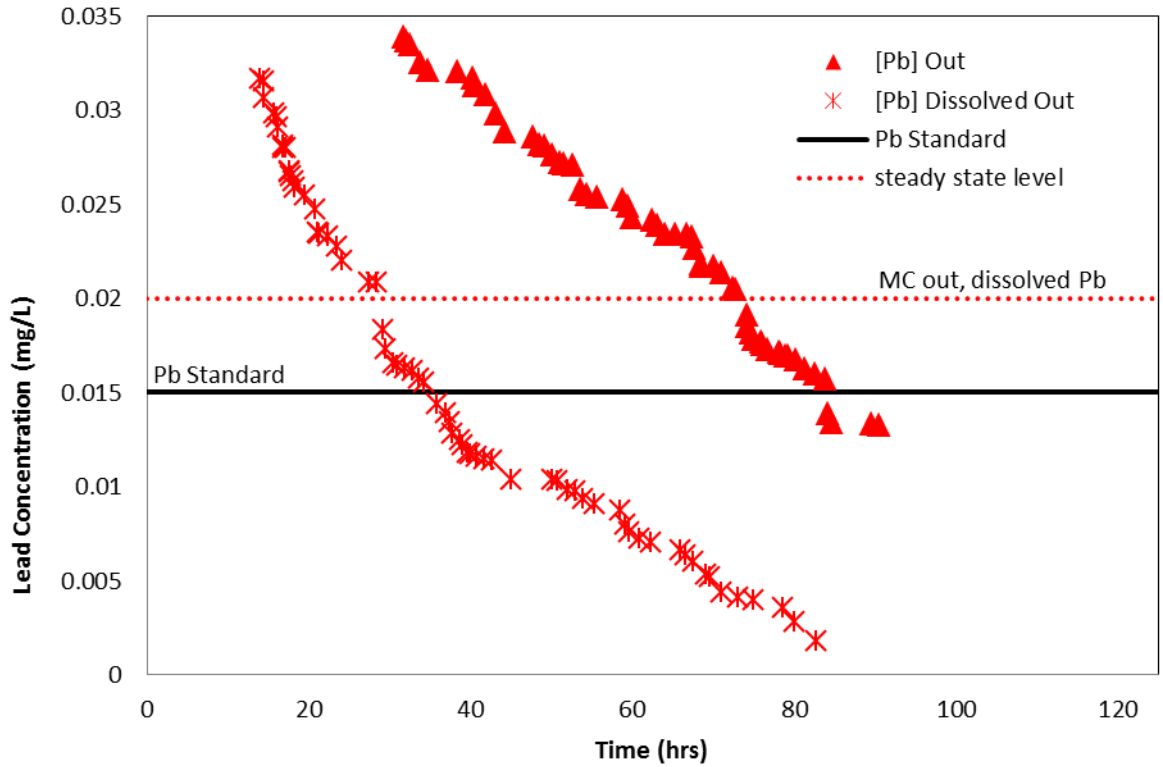


Figure 23: A zoomed-in version of Figure 20, showing concentrations of Pb near the steady-state mean value.

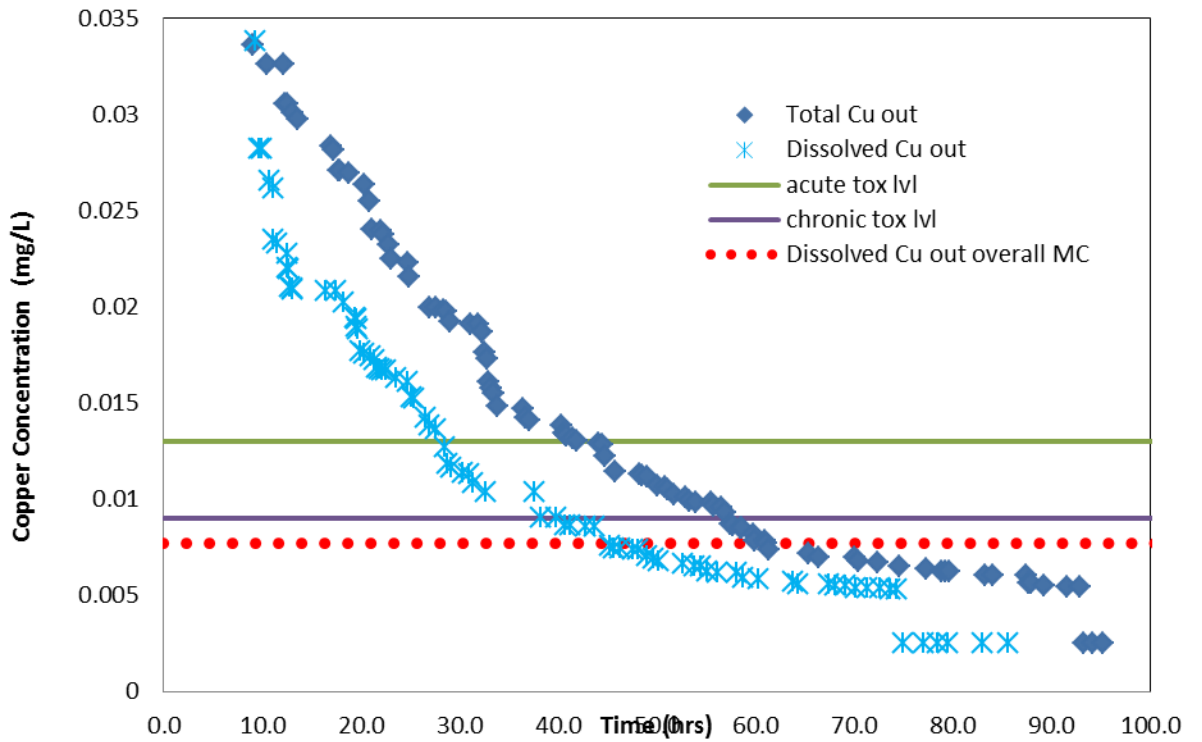


Figure 24: A zoomed-in version of Figure 21, showing concentrations of Cu near the steady-state mean value.

Variables affecting treatment efficacy at the wooden structure

Kim (2010) hypothesized that several treatment mechanisms were at work during treatment by the Biomat: specific and nonspecific adsorption, precipitation by reaction with specific anions such as sulfide, phosphate, carbonate, and hydroxide, and finally coprecipitation with iron and/or aluminum. Precipitation and adsorption are both controlled to a large extent by solution pH, and therefore the relationship between effluent pH and effluent metals concentrations is likely significant. Figures 25-27 plot observed pH levels against metals concentrations.

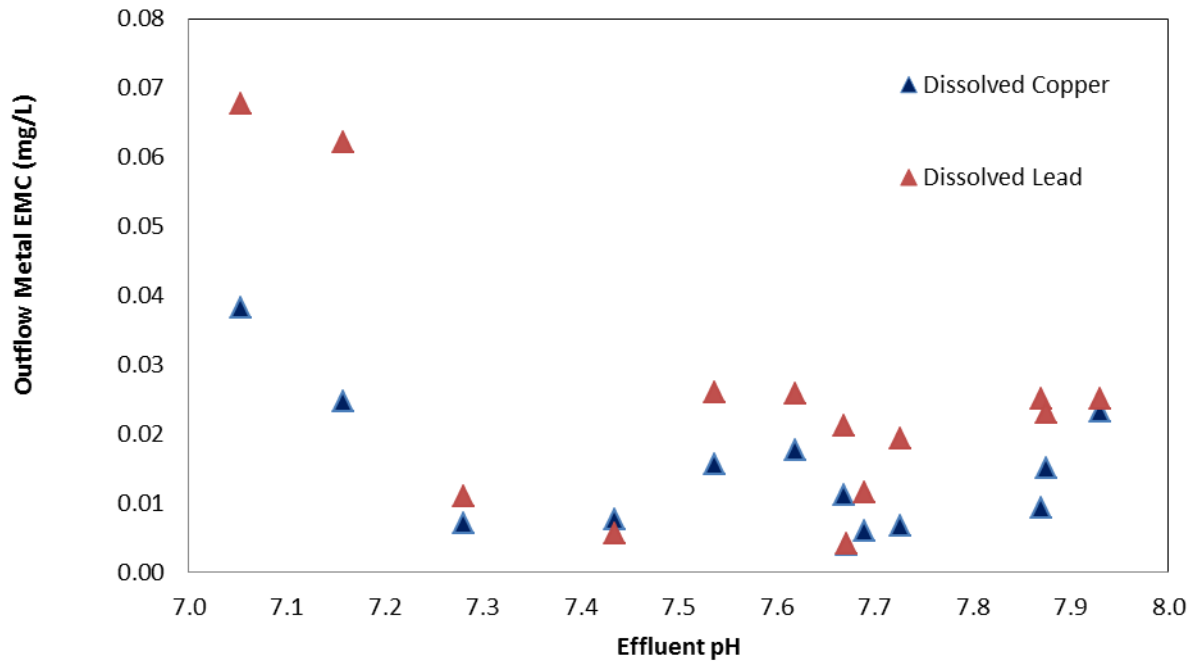


Figure 25: EMC effluent dissolved metals concentrations as a function of effluent pH.



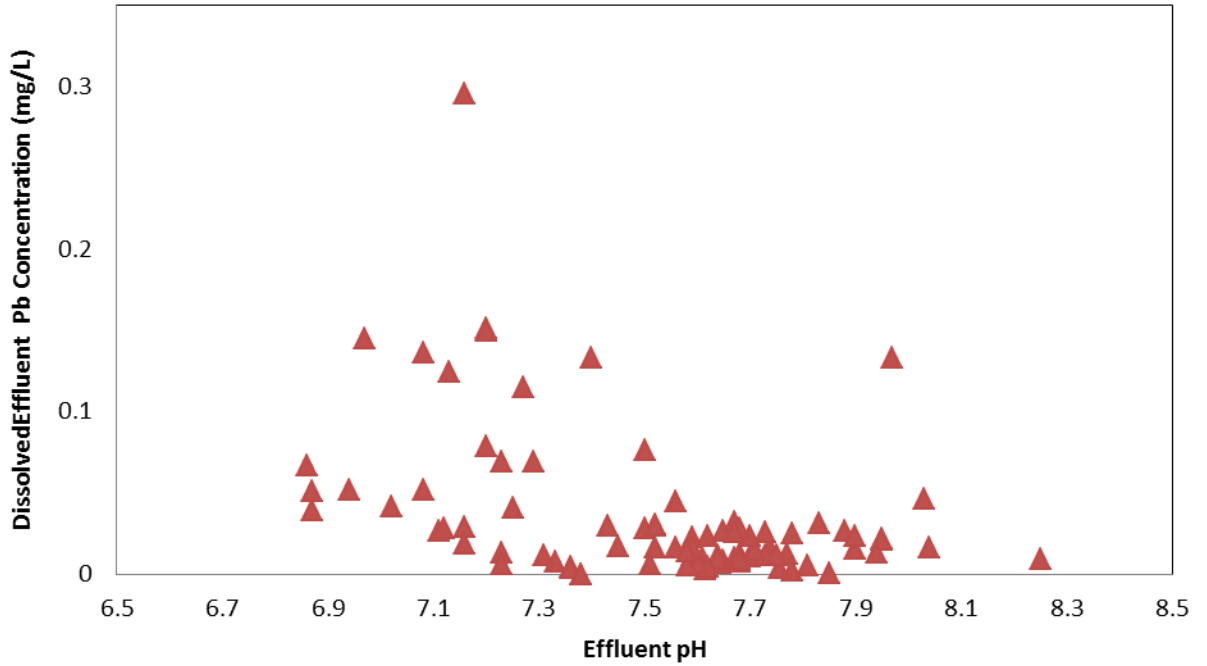


Figure 26: Effluent Pb concentrations as a function of pH. Each data point represents a single discrete measurement from storm events at the wooden structure which produced outflow and were sampled using the discrete (as opposed to composite) sampling regimen.

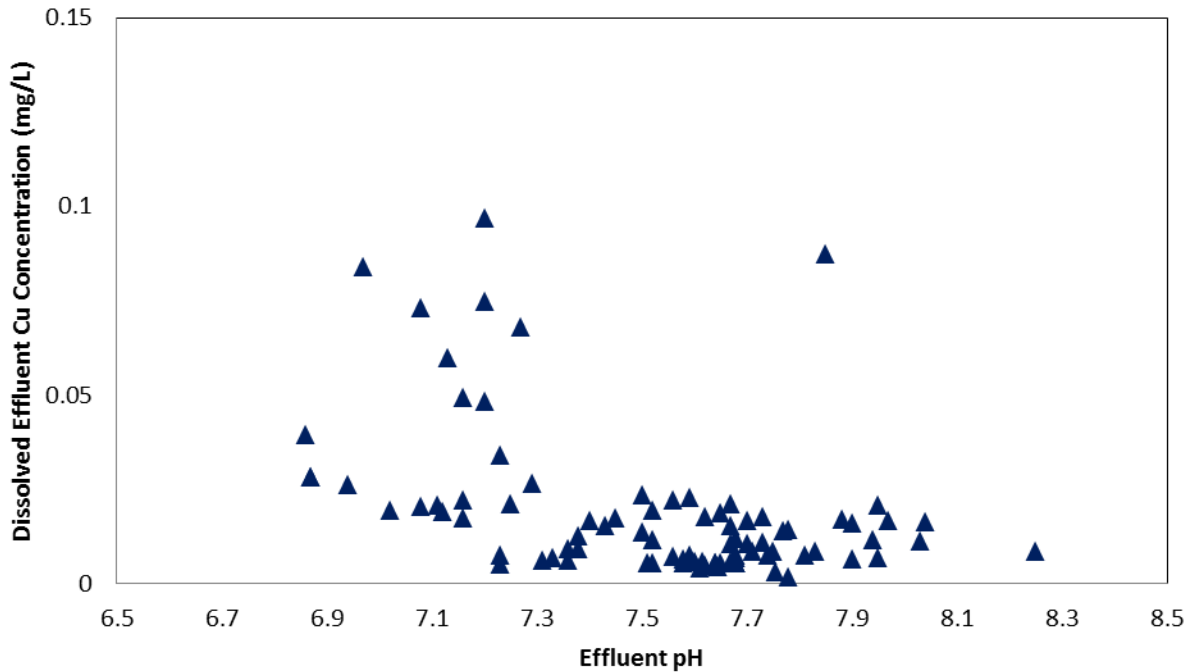


Figure 27: Effluent Cu concentrations as a function of pH. Each data point represents a single discrete measurement from storm events at the wooden structure which produced outflow and were sampled using the discrete (as opposed to composite) sampling regimen.

Previous research has shown increased metal and phosphorous removal at pH ranges elevated by steel slag addition (Drizo et al., 2006; Okochi and McMartin, 2011). However, when organic matter is also present, increased metal mobility has also been observed to occur at alkaline pH ranges through dissolution of metals bound to fulvic and humic acids, which have a strong affinity for heavy metal cations (Zhou and Haynes, 2010). These two observations are not necessarily contradictory; it is likely that, from a metals removal perspective, an ideal pH exists, at which increased removal is effected by precipitation and sorption without significantly increasing organic matter dissolution. The data from Figures 25-27 suggest that at least up to pH 7.5, increasing pH is clearly correlated with decreased metals concentrations. Above pH 7.5, however, it appears that further increases in effluent pH have diminishing returns on metals removals. This may indicate that increased precipitation and adsorption is offset by the dissolution of organic matter, to which metals may be adsorbed.

#### Speciation experiments

Given that the Biomat was observed to lower metals concentrations to trace amounts, raise pH, and add organic matter (as discussed later in the section ‘Phosphorous leaching’), it was suspected that effluent speciation of metals would vary significantly relative to the influent. Specifically, it was hypothesized that a greater proportion of dissolved effluent metals would be associated with negatively-charged organic complexes relative to the influent. Jensen et al. (1999) and Christensen et al. (1997) successfully applied an anion-exchange technique to

estimate the fraction of anionic/organic complexes in landfill leachate, and their methods were reproduced to speciate metals in discrete samples of influent and Biomat effluent taken on January 16, 2013, January 30, 2013, and February 26, 2013.

Figure 28 shows the change in Cu speciation that accompanies Biomat treatment. In municipal wastewaters and landfill leachate, Cu has been observed to bind predominantly to organic matter (Jensen et al., 1999). The results observed in this study are in line with these previous results. In the presence of an excess of organic ligands, the small amount of dissolved Cu which passed the Biomat appears to exist in majority as anionic complexes. In the influent, pH is significantly lower (average effluent pH 1/30/13 = 7.62, relative to an average influent pH = 5.54), and fewer organic ligands are present. These two factors explain why influent Cu exists in majority cationic/neutral forms.

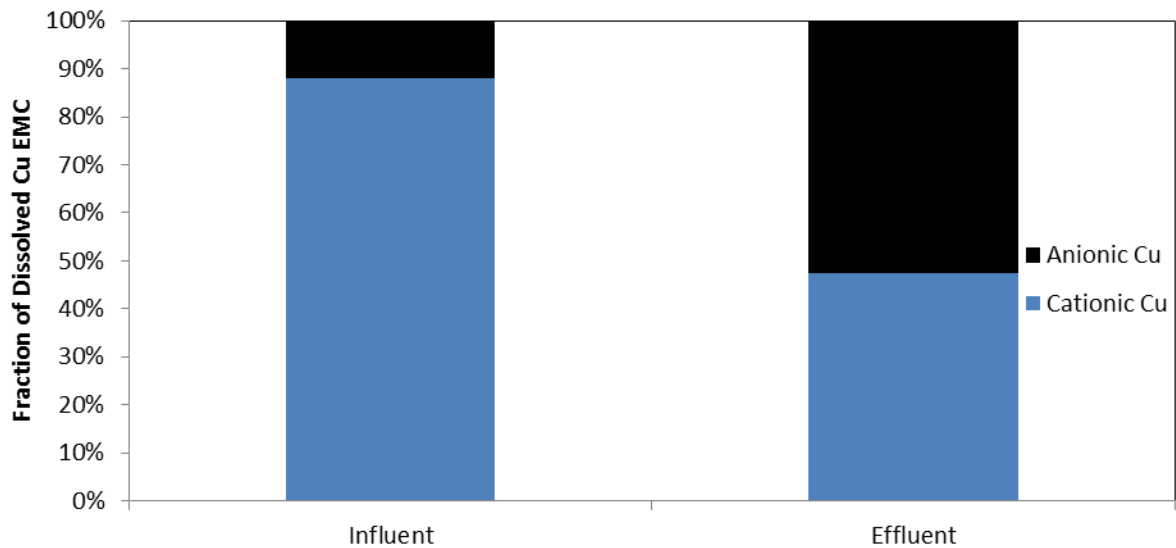


Figure 28: Proportions of anionic vis-a-vis cationic/neutral Cu anions and complexes present in Biomat influent and effluent. Proportions are calculated from mean flow-weighted concentrations measured in discrete samples taken on January 30, 2013, and February 26, 2013.

Although it is clear that conditions are more favorable to formation of anionic complexes in the effluent relative to influent at the APHIS roof runoff site, preferential wash-through of anionic Cu may also be occurring. It was not possible to distinguish between wash-through and formation/release of anionic Cu complexes, however, because effluent concentrations are so low relative to outflow levels. Figure 29 highlights this observation.

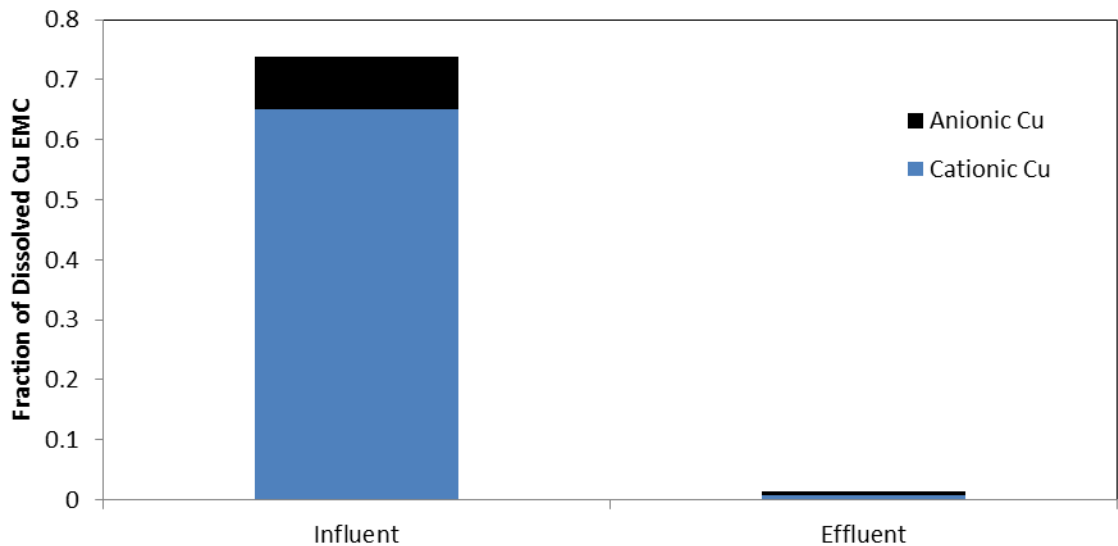


Figure 29: Flow-weighted mean concentrations of anionic vis-vis cationic/neutral Cu present in Biomat influent and effluent. From discrete data taken on January 30, 2013 and February 26, 2013.

Results for Pb from the same two storms are presented in Figures 30. The data indicate a small increase in the proportion of anionic-Pb complexes, but again effluent concentrations could be purely attributable to wash through as opposed to formation and release of anionic complexes. In both storms, effluent dissolved Pb was approximately 30% anionic, suggesting that effluent dissolved Pb was not as predominantly bound to dissolved organic matter as effluent dissolved Cu, which exhibited 50-60% anionic complexes (Figures 28 and 29). Jensen (1999), however,

found that Pb and Cu in landfill leachate bound with similar relative frequencies to negatively-charged dissolved organic matter. This discrepancy may be due to differences in the landfill leachate and Biomat effluent matrices, however more speciation data from Biomat effluent is required to make definite conclusions.

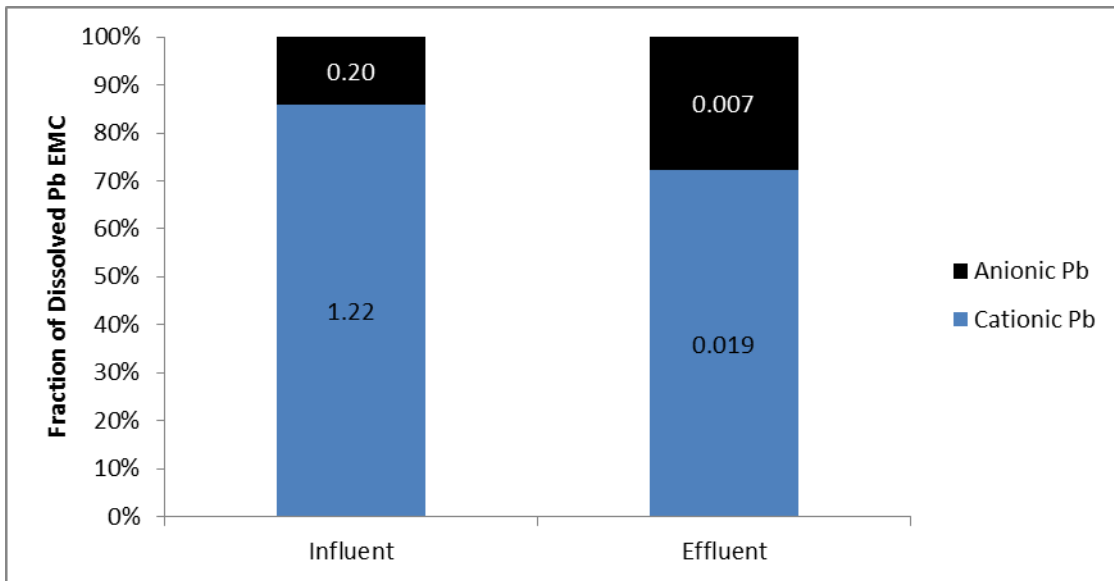


Figure 30: Proportions of anionic vis-a-vis cationic/neutral Pb anions and complexes present in Biomat influent and effluent. From discrete data taken on January 30, 2013 and February 26, 2013. Flow-weighted mean concentration values for each species are shown in mg/L on the data bars.

The speciation data presented in Figures 27-30 suggest that the Biomat does increase the fraction of metals which are bound to organic matter. This is consistent with the observations of pH increase in effluent samples, dissolved organic matter visible in effluent samples (Figure 31), and increased nutrient concentrations at the effluent. A greater fraction of effluent dissolved Cu appears to bind with organic matter relative to Pb.

## Phosphorous leaching

Compost has proven an effective treatment media for heavy metals in many previous studies (Glanville et al., 2003; Seelsaen et al., 2007; Gibert et al., 2005; Chang-Chien et al., 2007). However, as a decaying organic substance, compost is also likely to leach a certain amount of nutrients as the breakdown of organic acids continues within the Biomat. Evidence of organic leaching was visible in effluent samples, manifested as a dark yellow color. The most dramatic example of this, from one of the first effluent samples collected in August, 2011, is shown in Figure 31.



Figure 31: An inflow sample, left, opposite a Biomat outflow sample, right. These samples were taken in August, 2011, shortly after the mat was constructed.

The mean, flow-weighted concentration of total phosphorous in Biomat effluent over all storms measured at the wooden structure was 0.7 mg/L, much higher than the mean influent concentration (0.049 mg/L). Mason et al. (1999) found concentrations of total P in roof runoff of 0.004-0.018 mg/L, indicating that while the APHIS site may receive slightly more deposition of pollen and/or other P-containing compounds, the influent concentrations observed in this study are on the order of those reported in previous results. The Environmental Protection Agency recommends that for rivers and streams in the Beltsville, MD, as part of ecoregion

XIV (Eastern Coastal Plane), concentrations of phosphorous should be below 31.25 µg/L to prevent eutrophication and protect aquatic life to acceptable levels (USEPA, 2000).

Although such a nutrient addition would be undesirable if outflow from the wooden structure were draining directly to a stream or river, the lawn surrounding APHIS Building #580 should ensure that most of these nutrients are taken up by the grass and trees and not deposited into receiving waters draining to the Chesapeake Bay. However, the potential to contribute to eutrophication should be considered in other potential applications of the Biomat where effluent from treatment mats is expected to directly enter natural water bodies. Figure 32 plots typical phosphorous behavior at the wooden structure, where effluent phosphorous concentrations tend to build over the course of each storm at the effluent. Dissolved P, as shown, typically accounted for more than 80% of Total P in Biomat effluent. A more thorough analysis of the P speciation of Biomat effluent was also conducted during the 3 final storms monitored at the wooden structure.

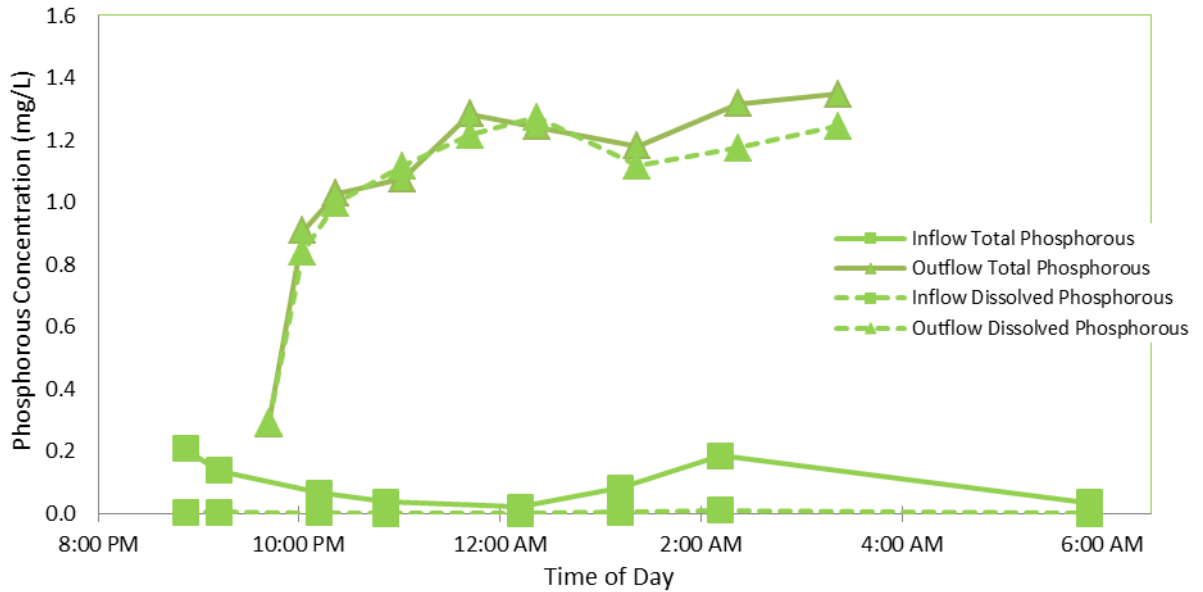


Figure 32: Intra-storm variation of phosphorous concentrations during the storm of 12/22/11 at the wooden structure. Each data point represents a single discrete sample. Total storm depth: 0.64 cm.

Given the concerns of nutrient addition, a probability plot of total P EMCs at the wooden structure was prepared (Figure 33). Influent total P ranged from 0.008-0.5 mg/L, while effluent total P ranged from 0.4-1.9 mg/L. As shown in Figure 33, effluent total P is always expected to be at least one order of magnitude above the regulatory standard of 31.25  $\mu\text{g/L}$ . Sibbesen and Sharpley (1997), in their tests on the relationship between P sorption capacity of a soil and dissolved P in surface runoff, found dissolved P concentrations of as much as 2.5 mg/L in surface runoff from a wide variety of poultry-litter amended soils where P sorption capacity exceeded 50%. In the Biomat, where the media is 25% compost by mass, it is likely that P sorption capacity is also well over 50%.



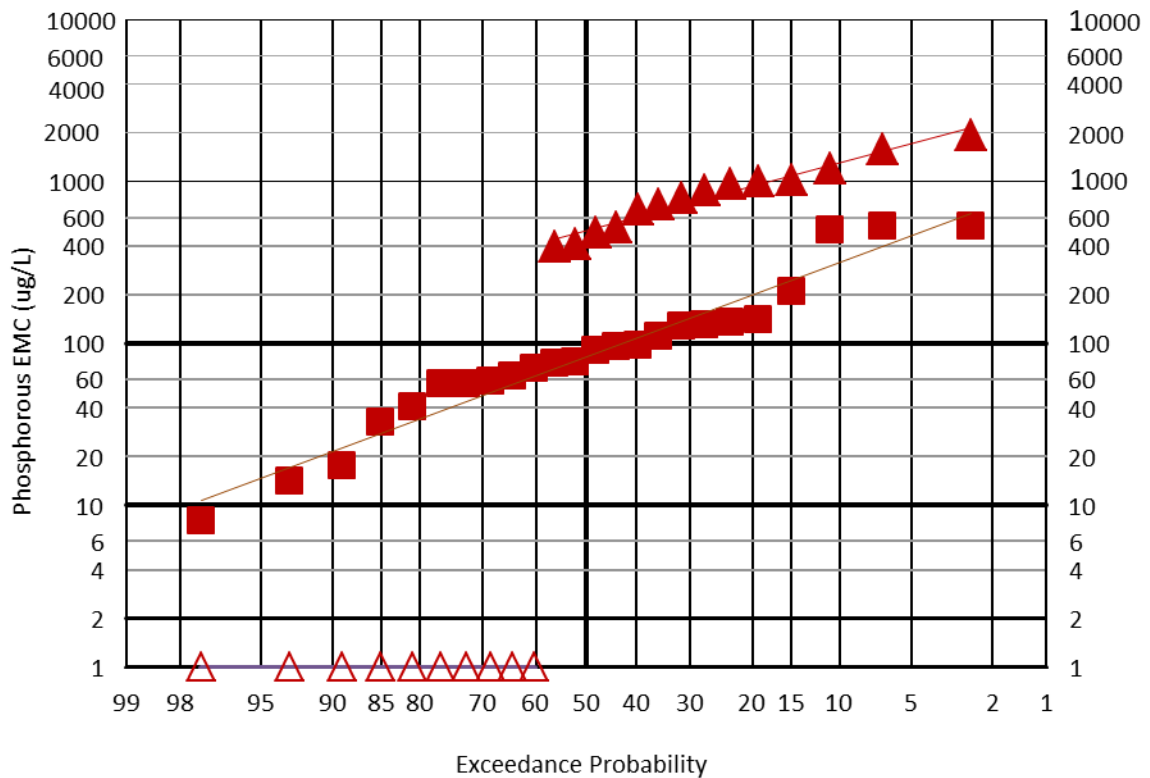


Figure 33: Exceedance probabilities for P based on event mean concentrations from 24 storms. Hollow triangles denote those storms in which no effluent was discharged.

While it is true that concentrations of effluent total P well above regulatory limits were observed in all outflow-producing storms, a trend of decreasing effluent total P concentrations was observed at the wooden structure. Figure 34 highlights this trend. The data in Figure 34 suggest that more mature, stabilized compost may be less prone to organic leaching and therefore more suitable for Biomat use. Madrid (1999) found that the processes used to mature composts significantly affected the amount of organic leaching that occurred when the composts studied were later land-applied. Zhou and Haynes (2010), in their review of compost usage for heavy metal sorption applications, found that compost with high soluble organic matter, such as manure

and biosolids-based composts, were more likely not only to leach this organic matter, but also leach metals that were sorbed to these organic constituents. This may suggest that purely plant or food-waste compost may be more effective for Biomat use, and that the use of some manure-based compost may have increased P leaching and limited the effectiveness of treatment.

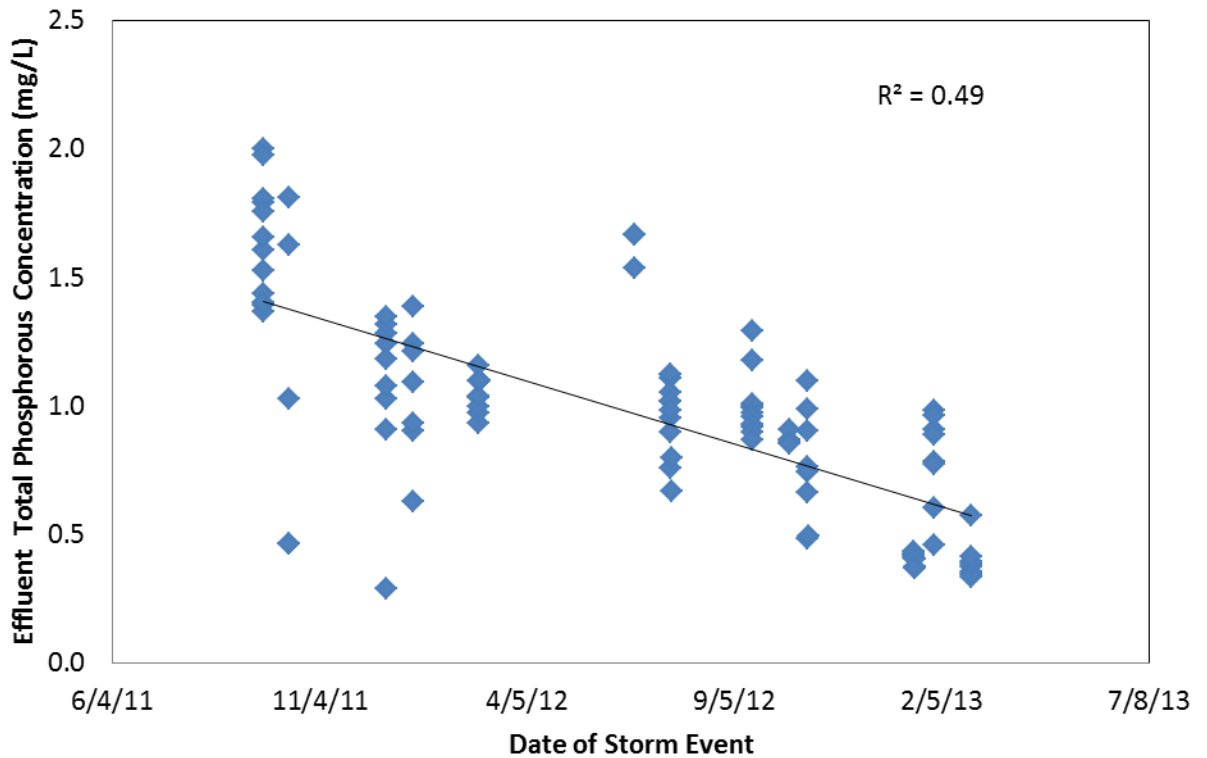


Figure 34: Concentrations of effluent total phosphorous measured over the course of 14 storms. Each data point represents one discrete measurement. The equation of the regression line is: (Effluent P Conc. = 1.43 mg/L – 0.0016 mg/L/day) where day 1 is the date of the first storm sampled event (9/23/2011).

P leaching was also considered from a loading perspective. Mass loads for total and dissolved P were calculated by summing the differences between Equation 6 (mass in) and Equation 7 (mass out) from each storm. Over the course of the 26

storms sampled, for example, 459 mg of total P entered the Biomat at the wooden structure and 1.2 g P were discharged. Extrapolating the P data based on drainage area, total rainfall depth sampled, and annual rainfall depth in MD (see Methods), annual phosphorous mass loadings were calculated at the influent and effluent (Table 10). Because the main source of effluent P is the Biomat itself, these calculations assume a constant sizing ratio of linear feet of Biomat: square feet of drainage area (in this case 1:11) in future applications. The influent loading for total P is somewhat lower than that observed by Li and Davis (2009) in their study of mass loadings at two parking lots in Maryland. The effluent loading from the Biomat is slightly higher than the effluent loadings from bioretention systems observed by Li and Davis, but on the same order as the influent mass loadings observed in this 2009 study. This suggests that despite the high concentrations of P in Biomat effluent, the water storage capability of the Biomat mitigates P mass loading to a certain extent.

Table 10: Annual pollutant mass loadings for total and dissolved P, based on Biomat data.

<i>Pollutant:</i>	<b>Total P</b>	<b>Dissolved P</b>
Influent Loading (kg/(ha*yr):	0.39	0.11
Effluent Loading (kg/ha*yr):	1.03	0.73

The data in Figures 32-34 demonstrate phosphorous leaching and suggest that, without further treatment, use of the Biomat would be best limited to situations where effluent does not reach natural waters. Another option considered was the use of a secondary treatment to remove phosphorous and residual metals from the Biomat effluent. It appears likely that those metals which do pass through the treatment media

may be attached to dissolved organic matter. Therefore, a treatment for organic matter may also be able to remove metals in Biomat effluent.

#### Development of a secondary treatment for enhanced P and metals removal

The moderately alkaline pH, high amount of organic acids, and high phosphorous concentrations which characterize Biomat effluent all suggested that an aluminum (hydr)oxide sorbent such as water treatment residual (WTR) may be able to effectively remove the phosphorous and/or residual metals from solution.

Phosphorous removal by WTR has been noted in similar waters (i.e., those with high organic matter) by Codling et al. (2000), Babatunde and Zhao (2007), and Zhou and Haynes (2010), among others. Metals removal has also been noted, for Pb by Chu (1999) and Zhou and Haynes (2011), and for Cu in wastewaters by Lee et al. (2006). Furthermore, metals sorption onto WTR in some feasibility studies has been found to increase with increasing pH (Lee et al., 2006).

Using Biomat effluent samples from two sampled rainfall events, on June 22, 2012 and July 14, 2012, duplicate batch tests were conducted to assess the ability of WTR to remove phosphorous and metals. At a mass ratio of 40 mL solution sample: 2.67 g WTR, reductions in phosphorous concentrations were greater than 99%. Post-treatment concentrations were at or below the detection limit (0.01 mg/L) for total P, relative to 1.5 mg/L total P as Biomat effluent (pre-WTR treatment). Metals reductions were also observed, with concentrations reductions above 80%, even at extremely low levels of metals. Biomat effluent concentrations of total Pb in the

samples taken were 17 µg/L and 28 µg/L. Post-WTR treatment at a mass ratio of 40 mL solution sample: 2.67 g WTR, mean concentrations of total Pb were 5.7 µg/L and <2 µg/L (the method detection limit for Pb), respectively. Table 11 shows the phosphorous reductions observed in samples taken from the July 14, 2012 storm, post-WTR batch treatment.

Table 11: Dissolved P concentrations in untreated and WTR-treated samples at varying media: solution mass ratios. These data were obtained by performing batch experiments on a sample of Biomat effluent collected after a storm event on July 14, 2012. Method detection limit = 0.010 mg/L.

	Replicate 1 – Dissolved P concentration (mg/L)	Replicate 2 – Dissolved P concentration (mg/L)
Original sample	1.54	N/A
2.67 g WTR: 40 mL solution	0.010	<0.010
1.60 g WTR: 40 mL solution	0.015	0.022
1.33 g WTR: 40 mL solution	0.013	0.012

Given that batch treatment produced promising results for potential P and metals removal from Biomat effluent, a field-scale prototype was constructed to collect and treat Biomat effluent (Figure 7). Sampling occurred on 1/16/13, 1/30/13, and 2/26/13, to provide water quality data on the efficacy of this secondary treatment. During these three storms, phosphorous speciation was determined in inflow samples, Biomat outflow samples, and WTR-treated samples. Typical time-series results from discrete data are presented in Figures 35 and 36.

Figure 35 demonstrates the efficient removal of P by WTR treatment in a rainfall event on February 26, 2013. Concentrations of total P are reduced from 0.3-0.6 mg/L as Biomat effluent to <0.12 mg/L total P as WTR-treated effluent. Influent P concentrations, shown in the lighter time series, are on par with the WTR-effluent, at around 0.1 mg/L. Figure 35 therefore suggests that WTR-treated effluent is not

only greatly reduced in metals concentrations relative to influent, but also that nutrients are not significantly elevated due to secondary treatment.

Figure 36 shows the speciation data for Biomat effluent from discrete data samples taken on February 26, 2013. These data explain in part the efficient removal of P demonstrated in Figure 35. Soluble reactive P (SRP) accounts for the vast majority of total P in Biomat effluent. Very little organic P or particulate P was observed; concentrations of these two species were below 0.1 mg/L in all discrete samples, relative to SRP concentrations which were frequently 0.3-0.5 mg/L, as shown in Figure 36.

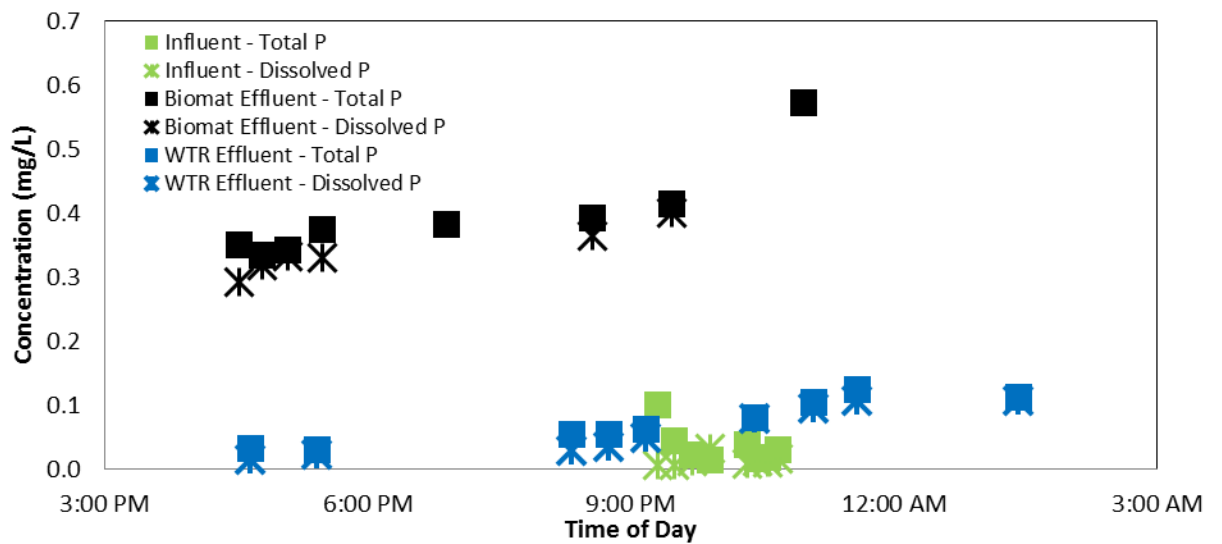


Figure 35: P concentrations in inflow, Biomat outflow, and WTR-treated outflow from a rainfall event sampled on 2/26/13.

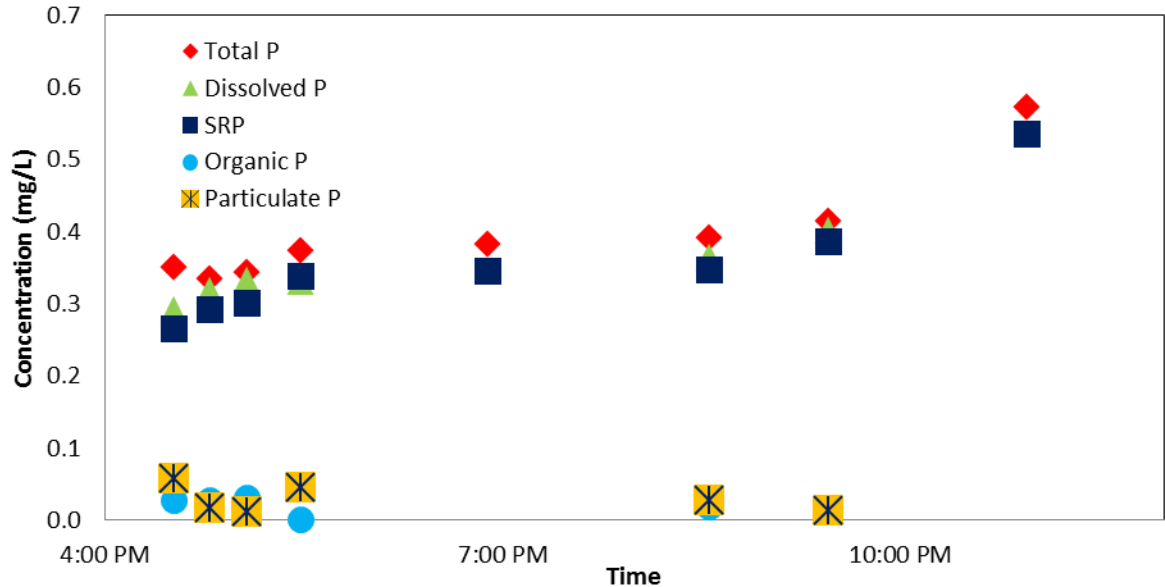


Figure 36: Forms of P present in Biomat effluent during the storm event sampled on 2/26/13.

Prevalence of SRP over organic P has been found in several previous compost studies. Running sequential extractions on 24 composts and manures, Sharpley and Moyer (2000) found that 63 to 92% of total P in manure came from SRP. The data in Figure 36 indicate a similar prevalence of SRP in water extractable P.

Soluble reactive phosphorous has been shown in previous studies (O'Neill and Davis, 2011b) to be more efficiently removed by WTR relative to organic phosphorous. Kim et al., (2013) pointed out that the majority of P in compost is likely to exist as SRP, and the data above confirm this finding, explaining the good removals observed at the field scale. The WTR treatment appears to alter solution speciation significantly, as shown in Figure 37. Nearly all SRP was removed by secondary treatment, and smaller removals of particulate P (likely attributable to sand filtration) and organic P are also visible. SRP was the overwhelming constituent of Biomat effluent total P, constituting 0.66 mg/L of 0.79 mg/L total P. However,

WTR/sand-treated samples have equal proportions of all three P species (SRP, dissolved organic P, and particulate P), each present at around 0.13 mg/L and each at lower concentrations than those present in Biomat effluent, where mean organic P was present at 0.07 mg/L and mean particulate P was present at 0.06 mg/L. The concentration of P in WTR/sand effluent is reduced to near pre-Biomat levels, around 0.05 mg/L, and specifically the predominance of SRP in Biomat effluent is negated by the effective treatment of SRP by the WTR/sand mixture.

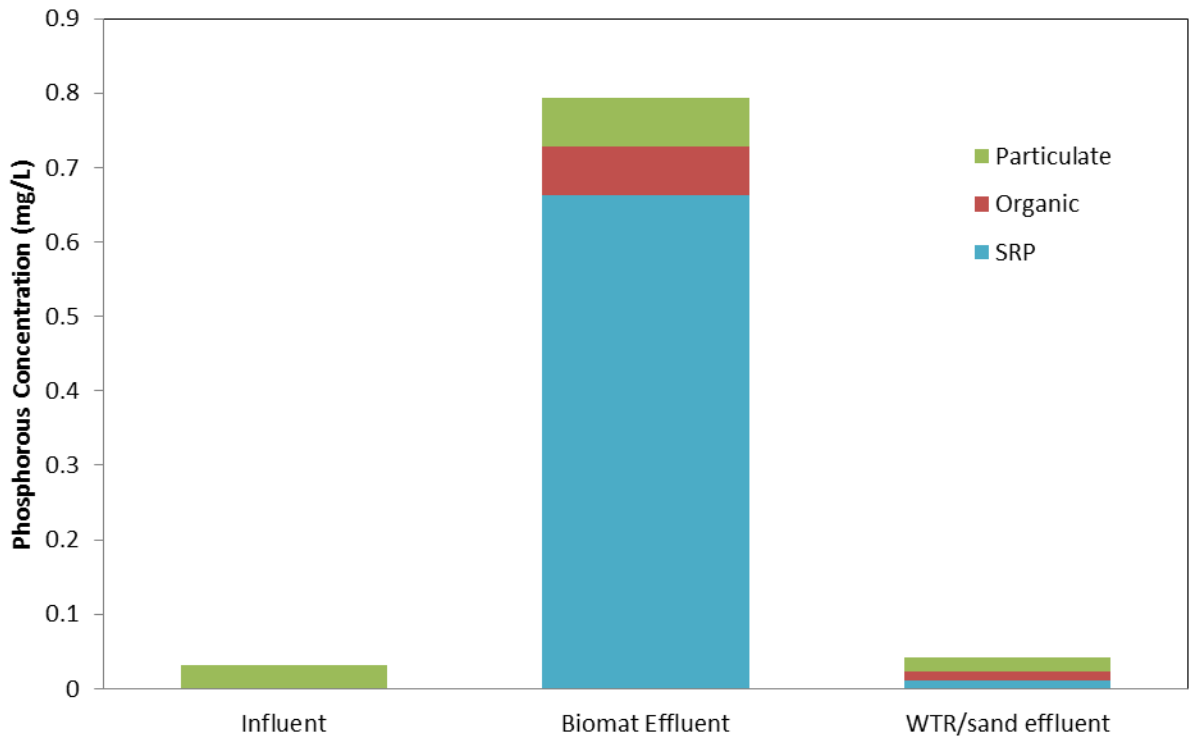


Figure 37: Phosphorous species concentrations in influent, Biomat effluent, and WTR-treated effluent in samples taken on January 30, 2013. The values shown are EMCs.

Table 12 summarizes the efficacy of WTR/sand treatment over the course of all 3 storms sampled at the wooden structure. These results indicate that the WTR/sand treatment was able to reduce phosphorous concentrations by over 90%



relative to Biomat effluent, to a level near influent levels and the USEPA Ecoregion XIV standard for P (31 µg/L). Furthermore, metals reductions by the WTR/sand treatment are also evident from Table 12. Mean effluent concentrations leaving the WTR/sand bucket were below regulatory levels with respect to all metals. Given that metals were removed to the point of regulatory compliance, and the potential issues caused by nutrient addition were addressed, treatment at the wooden structure was deemed satisfactory with regard to all water quality parameters and appears potentially useful in similar applications at other metals hotspots.

Table 12: Pollutant masses and flow-weighted mean concentration values observed during the 3 storms in which WTR/sand treatment was added after the Biomat to treat residual metals and leached nutrients in Biomat outflow. Standard deviations between the 3 storm event EMC values are listed below each mean concentration.

	<b>Pb</b>	<b>Diss. Pb</b>	<b>Cu</b>	<b>Diss. Cu</b>	<b>Zn</b>	<b>Diss. Zn</b>	<b>TP</b>	<b>DP</b>
<b>Mean conc. in (mg/L)</b>	2.5 +/-1.4	1.6 +/- 0.3	1.2 +/-0.3	0.7 +/-0.1	0.09 +/-0.03	0.06 +/-0.02	0.037 +/-0.03	0.003 +/-0.01
<b>Mean conc. out from Biomat (mg/L)</b>	0.039 +/- 0.012	0.022 +/-0.011	0.018 +/-0.005	0.014 +/-0.005	0.026 +/-0.023	0.017 +/- 0.015	0.63 +/-0.22	0.57 +/-0.21
<b>Mean conc. out from WTR (mg/L)</b>	0.011 +/- 0.004	0.004 +/-0.001	0.008 +/-0.004	0.006 +/-0.001	0.018 +/-0.018	0.020 +/- 0.004	0.056 +/-0.05	0.040 +/-0.05
<b>Mass in (mg)</b>	6380	4050	3060	1770	227	160	95.8	7.3
<b>Mass out from Biomat (mg)</b>	15.8	8.8	7.2	5.8	10.5	6.9	252	230
<b>Mass out from WTR (mg)</b>	4.6	1.8	3.3	2.4	7.3	7.9	22.4	16.1

#### Storms sampled at the swale site

18 storms were sampled at the swale site over a period of 10 months. A wide variety of storm depths and durations were included in these samples, which were taken in all seasons. The depth-duration distribution is shown in Figure 38 and Table

13. Table 5 was used to compare the sampled depth-duration distribution to Maryland's typical depth-duration distribution.

Sampled storms varied in duration from 12 minutes to 31 hours, and in depth from 0.08 cm to 3.51 cm. The warmest storm event was sampled on a day where the mean daily temperature was as 27.2 °C, and during the winter the coldest storm event sampled had a mean daily temperature of 0.2 °C. Table 13 shows that rainfall events at every depth category were sampled and every time category apart from 2-3 hr.-long storms was represented as well.

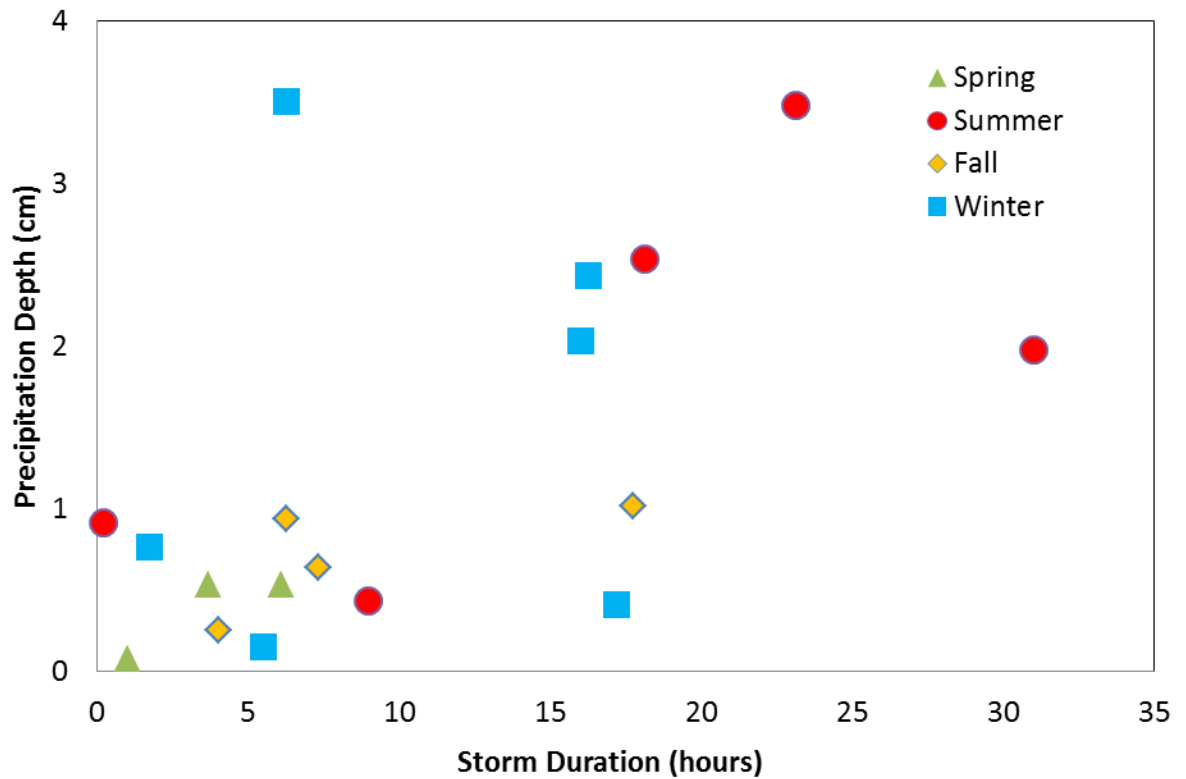


Figure 38: Depth-duration distribution of the 18 storms sampled at the swale site.

Table 13: Depth-duration distribution of the 18 storms sampled at the swale site. White/lighter boxes indicate higher frequencies, and darker boxes indicate lower frequencies.

Event	Rainfall Depth (cm)					Sum
	0.0254-0.254	0.255-0.635	0.636-1.27	1.28-2.54	> 2.54	
0-2 hr	0.06	0.00	0.11	0.00	0.00	0.167
2-3 hr	0.00	0.00	0.00	0.00	0.00	0.000
3-4 hr	0.00	0.06	0.00	0.00	0.00	0.056
4-7 hr	0.11	0.06	0.06	0.00	0.06	0.278
7-13 hr	0.00	0.11	0.00	0.00	0.00	0.111
13-24 hr	0.00	0.06	0.06	0.17	0.06	0.333
>24 hr	0.00	0.00	0.00	0.06	0.00	0.056
Sum	0.167	0.278	0.222	0.222	0.111	1

Given the sample size (n=18) and the depth-duration distribution covered at the swale site, the portfolio of storms sampled was accepted as sufficiently representative of Maryland’s typical rainfall distribution, as characterized by Kreeb (2003). Common storm depth/duration pairs were largely accounted for in the sampling distribution at the swale, and the data in Table 13 do not appear to be skewed towards larger or smaller storms than those typically observed in Maryland, nor towards longer or shorter storms.

#### Site Hydrology

As noted previously (Table 1), the hydraulic loading to the Biomat at the swale was significantly higher than that at the wooden structure. An increased ratio of drainage area: linear feet of treatment mat (Table 2) resulted in a linear ( $R^2=0.92$ )

rainfall-discharge relationship (Figure 39), in which water storage by the Biomat was negligible. Given that inflow volumes ranged from a minimum of 3 m<sup>3</sup> to upwards of 35 m<sup>3</sup>, the storage volume of the pores in the mat, which held 0.34 m<sup>3</sup> of pre-settled media, was discounted, and inflow volume was assumed to equal outflow volume.

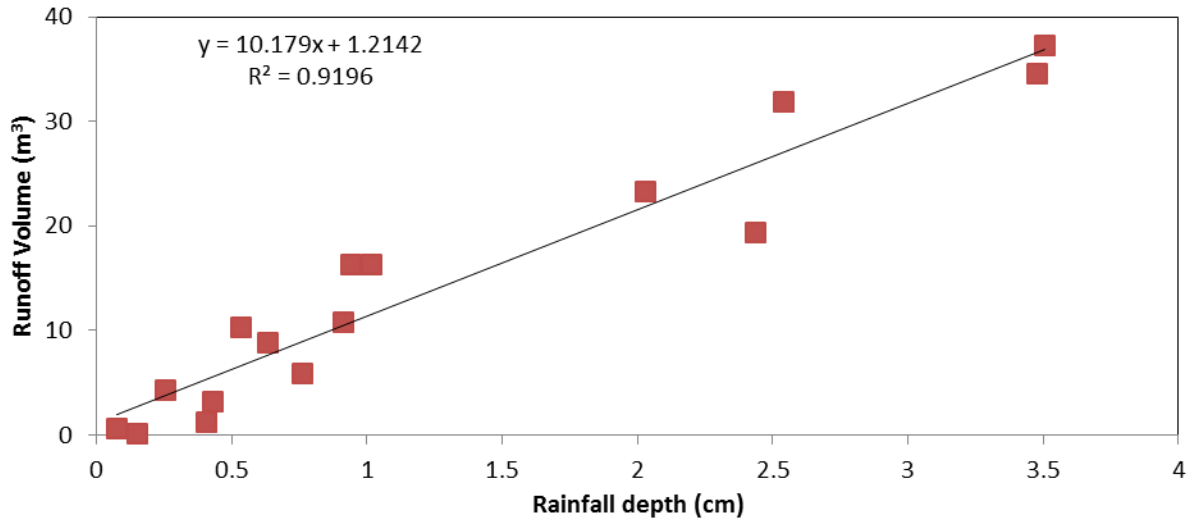


Figure 39: Rainfall-discharge relationship at the swale. Each point represents a data point measured at the swale during a single storm.

Figure 40 demonstrates that in storms with a rainfall depth above 2 cm, not all rainfall entering the swale passed through the weir while the Biomat was in place. In storms above 2 cm, it appears that a portion of influent water volume bypassed the Biomat, flowing over and out of the swale and not receiving treatment or passing through the effluent weir. Evidence of bypass is observable in Figure 40, in which hydrology data from the 18 storms in which the Biomat was in place for water quality monitoring are compared to hydrology data from 13 storms in which the Biomat had already been removed from the swale. In storms with total rainfall depth >2 cm,

greater flow volume was observed without the Biomat in place. This suggests that when the Biomat was in place, bypass did occur during larger storms.

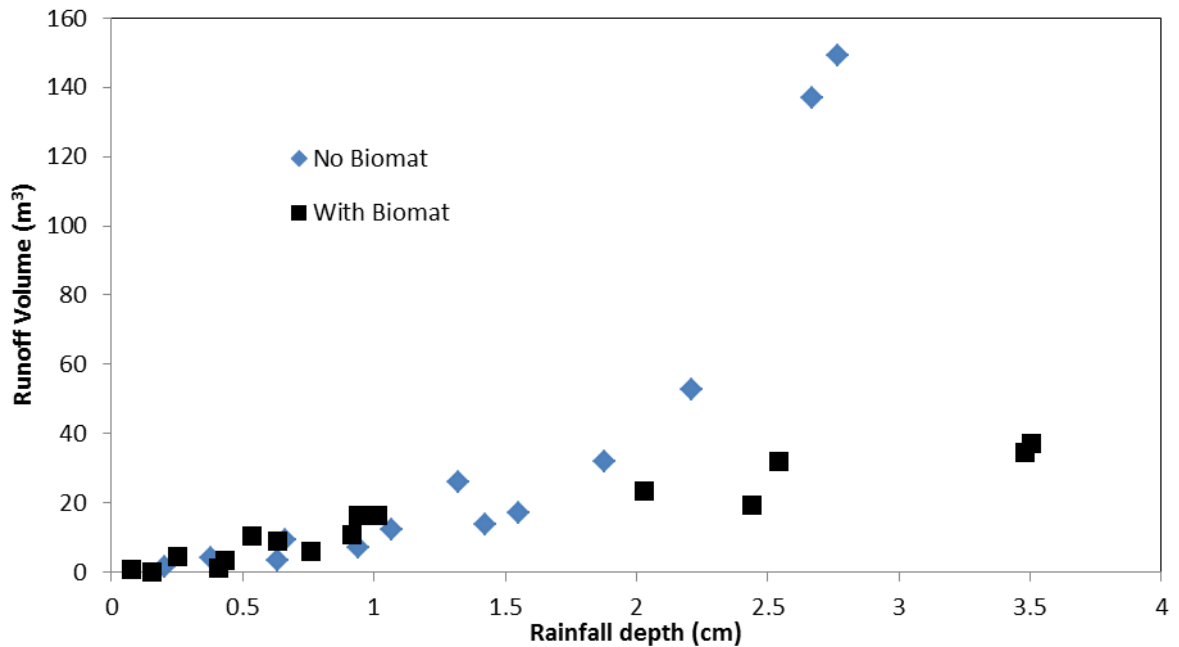


Figure 40: Rainfall-runoff relationship during large storms at the swale site with the Biomat in place (squares), and with no Biomat in place (diamonds).

#### Treatment efficacy at the swale

Biomat treatment efficacy at the swale was found to differ significantly from treatment efficacy at the wooden structure. This can be attributed to several key differences. Firstly, influent concentrations at the swale were consistently much lower than at the wooden structure. Pb, Cu, and Zn levels were often below regulatory limits as influent. The flow-weighted mean concentrations at the swale for total influent Pb, Cu, and Zn were 16 µg/L, 10 µg/L, and 135 µg/L, respectively. Secondly, influent pH at the swale (mean pH across all storms =7.6) was consistently higher relative to the wooden structure (mean pH across all storms =5.9), meaning that pH-

dependent treatment mechanisms for metals removal, including precipitation and pH-dependent adsorption, were not as likely to be effective as at the wooden structure. Figure 42, taken from Benjamin and Leckie (1981) shows adsorption edges for Pb, Cu, Zn, and Cd onto amorphous Fe hydroxides, which are present in the steel slag. These edges show that the pH difference effected by the mat at the wooden structure would effectively increase adsorption onto steel slag, but that no such removals would be observed at the swale pH conditions.

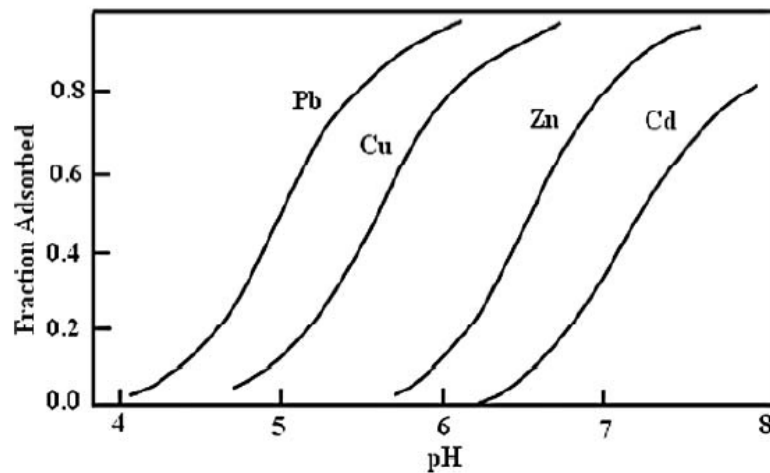


Figure 41: Adsorption curves for Pb, Cu, and Zn onto amorphous Fe hydroxides, from Benjamin and Leckie (1981).

Finally, the hydraulic loading at the swale was much higher than that at the wooden structure (Tables 1 and 2), resulting in lower treatment times. As shown in Figure 40, and due to high hydraulic loading, all storms sampled produced outflow at the swale site. As a result of these factors, the Biomat proved to be an ineffective means of removing trace metals from influent at the swale. Concentration decreases were small except in the case of Zn, with mean effluent concentrations of total metals across all storms being 11 µg/L Pb, 10 µg/L Cu, and 56 µg/L Zn.

The likelihood of regulatory compliance with the Pb, Cu, and Zn standards listed in Table 7 was assessed using probability plots, shown in Figure 42 and Figure 43. Figures 42 and 43 do not indicate significant changes in EMC for Pb, Cu, or Zn between influent and effluent. The fraction of storms in which metals EMC values met regulatory standards (in 100% of storms for acute Pb, in 75% of storms for acute Cu, and in 65% of storms for Zn) did not change significantly between inflow and outflow. Compliance with chronic Pb and Cu standards occurs in less than 10% of storms with respect to Pb, but in 62% of storms with regard to Cu.

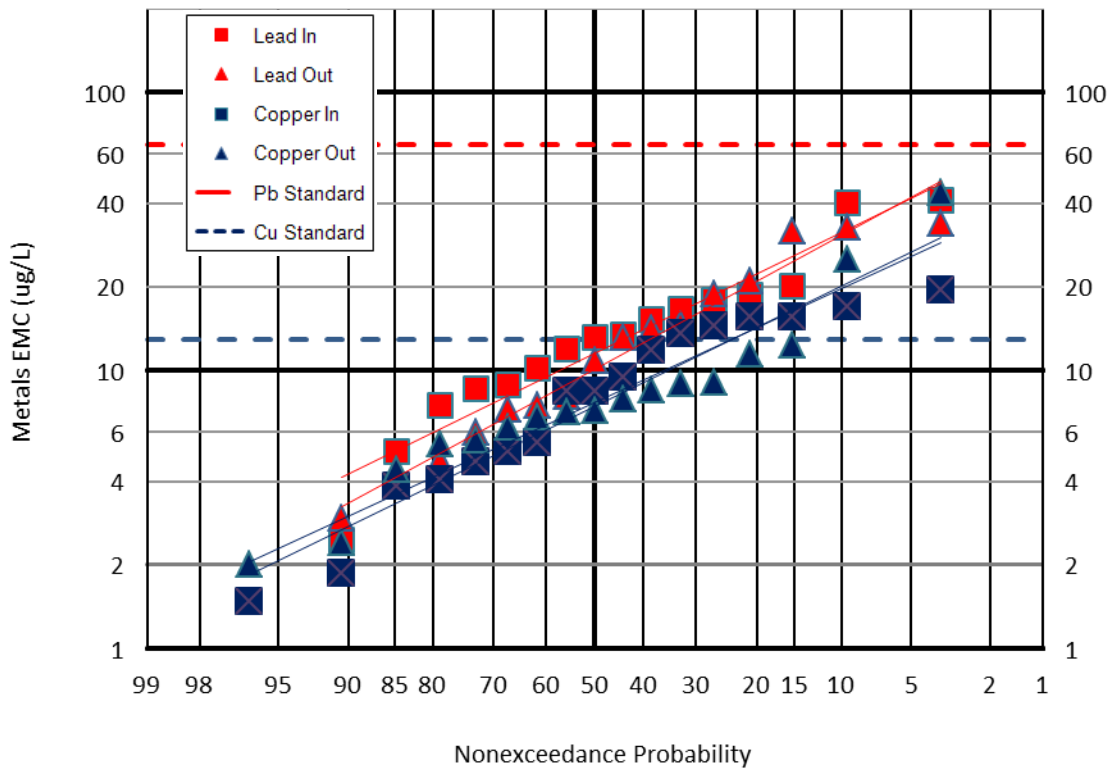


Figure 42: Probability plot for Pb and Cu concentrations at the swale site. Each data point represents an EMC value recorded in one of 18 storm events sampled

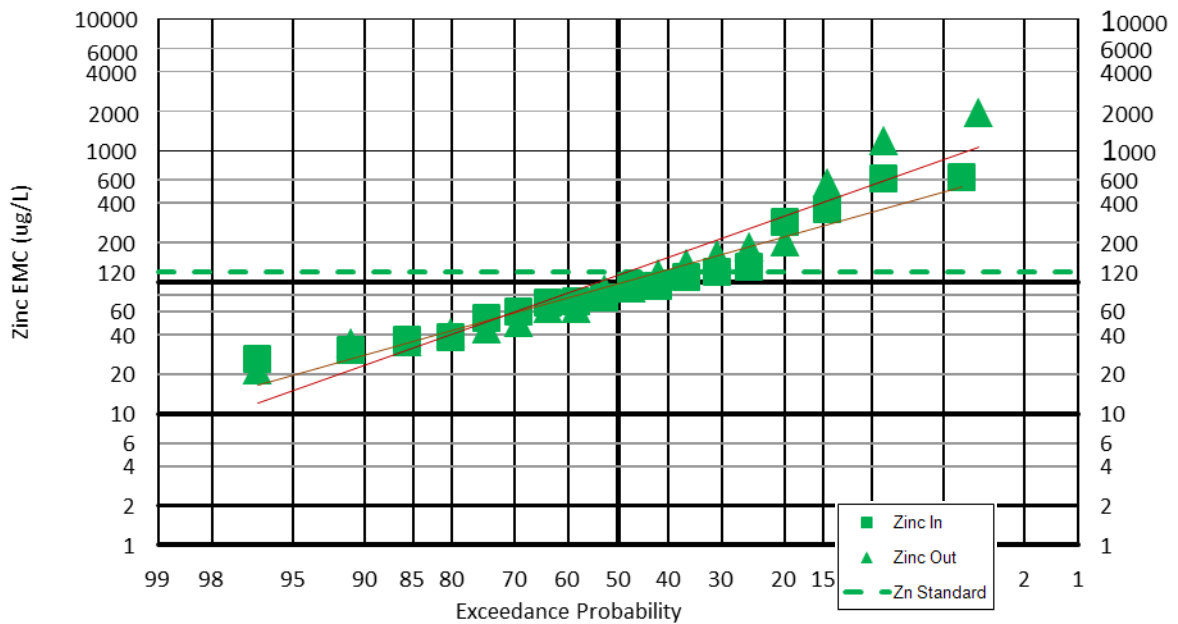


Figure 43 Probability plot for Zn concentrations at the swale site. Each data point represents an EMC value recorded in one of 18 storm events sampled.

Significant intra-storm variation was observed in the discrete data collected at the swale. Typically, slightly elevated concentrations of metals were observed during the first samples taken in each storm, similar to the behavior observed at the wooden structure. However, this behavior occurs to a much smaller extent at the swale. Figures 44 and 45 present discrete data taken on June 12, 2012 at the swale. The first sample is elevated in Pb and Cu relative to later samples, but by a very small amount (<5 µg/L). As previously mentioned, influent total Pb, Cu, and Zn concentrations were significantly lower at the swale site relative to roof runoff influent. Mean influent concentrations of total metals across all 18 storms were 16 µg/L Pb, 9 µg/L Cu, and 60 µg/L Zn. Mean effluent concentrations of total metals were 15 µg/L Pb, 10 µg/L Cu, and 52 µg/L Zn. Paired student's t-tests of equal variance were performed, comparing inflow concentrations to outflow concentrations for each



metal. Rejection probabilities ( $p=0.36$  for Pb,  $p=0.36$  for Cu, and  $p=0.11$  for Zn) were deemed too large to indicate a statistically significant change in EMC values from inflow to outflow for Pb, Cu, and Zn.

With concentrations of metals close to detection limits, noise in measurements of metals levels was a consistent issue at the swale. Effluent Pb EMCs, for example, varied from a maximum of  $33 \mu\text{g/L}$  during one storm to a minimum value of  $2.5 \mu\text{g/L}$ . The detection limit for Pb was  $2 \mu\text{g/L}$ , compared to  $5 \mu\text{g/L}$  Cu and  $40 \mu\text{g/L}$  Zn. Figures 44 and 45 show that metals concentrations were often below method detection limits, shown in dashed lines on the plots.

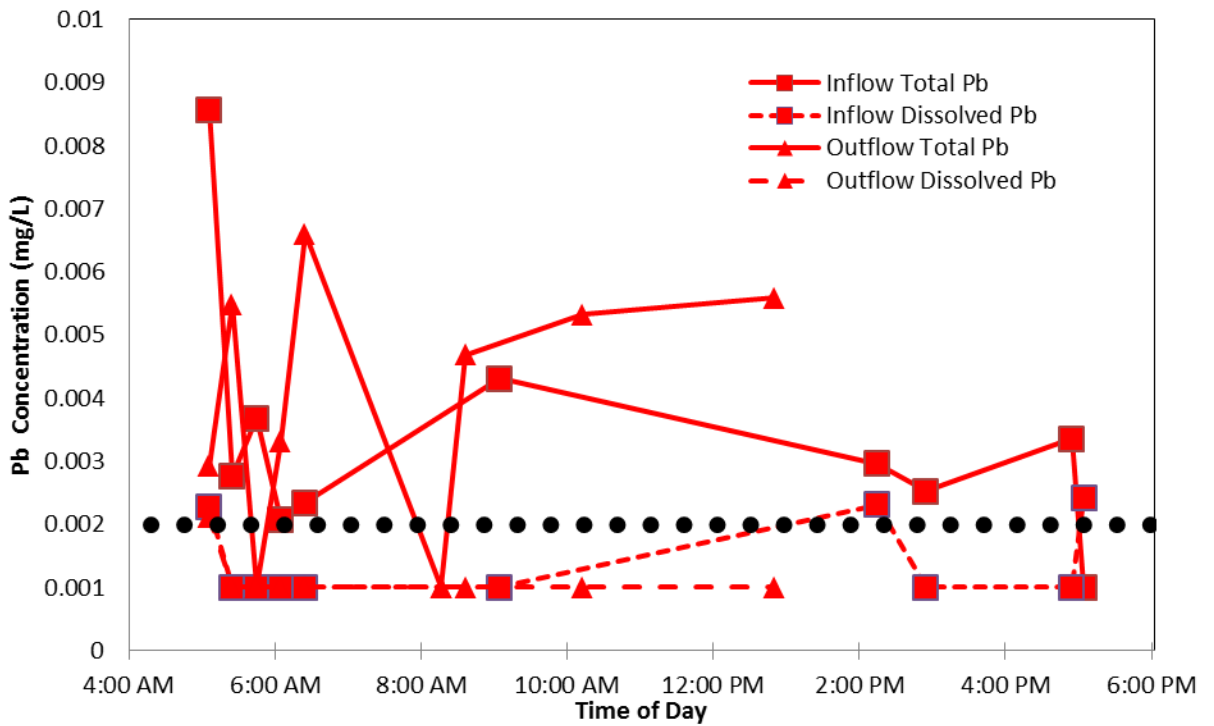


Figure 44: Dissolved and total Pb concentrations measured at the swale on June 12, 2012. The dashed line indicates the method detection limit.

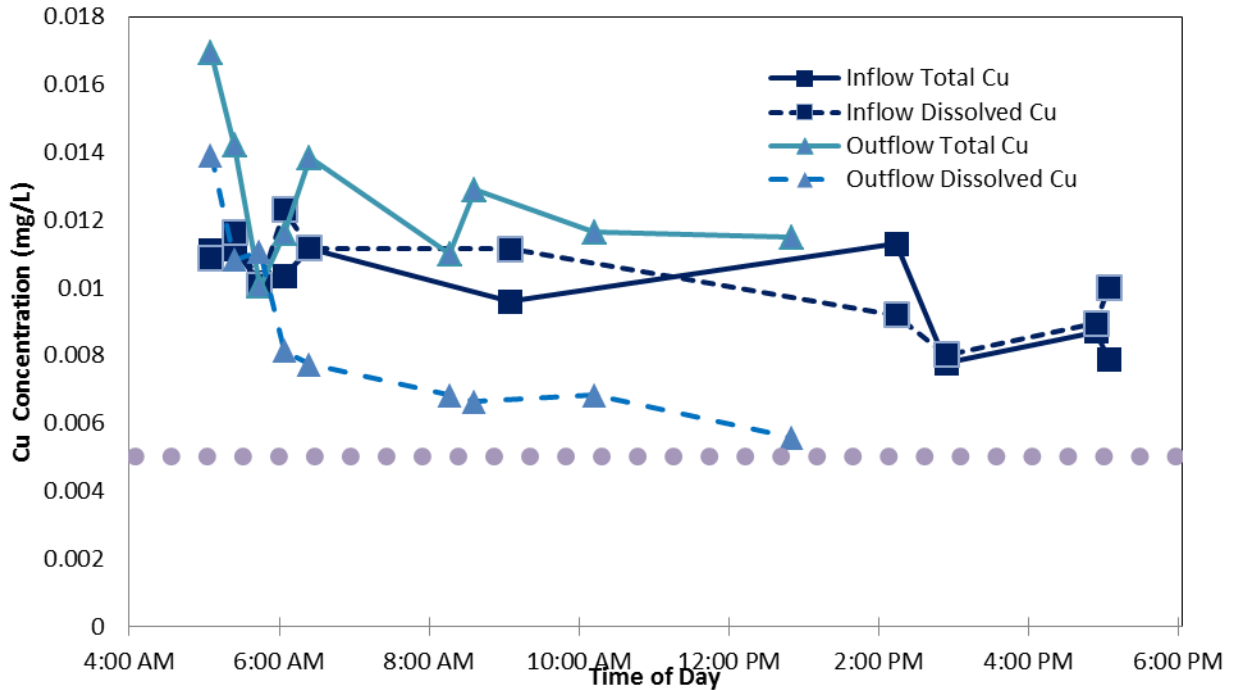


Figure 45: Dissolved and total Cu concentrations measured at the swale on June 12, 2012. The dashed line indicates the method detection limit.

Figures 46 and 47 present two pollutographs from discrete data collected on May 29, 2012. These data are comparable to the data in Figures 44 and 45, and underscore the trace metal concentrations that were typically observed at the swale. Concentrations in this storm were consistently below method detection limits, and at times dissolved concentrations appear up to 5  $\mu\text{g/L}$  higher than total metal concentrations, an irrational finding that is either attributable to experimental error or sensitivity limits of the method. Figure 46 does show some reduction in particulate Pb concentrations, but moreover Figures 46 and 47 show that concentrations at the swale often hovered around the lower limit of the detectable range.

Figures 44-47 also show that influent metals concentrations at the swale were lower than effluent metals concentrations at times. This indicates that at certain points the treatment media were leaching metals, either from native metals in/on the media,

or from sites on the media that had previously accumulated influent metals from solution. Equilibrium defines the state at which a removal rate is equal to a corresponding leaching rate. However, the kinetics of desorption and pollutant release are not as well understood as those of sorption and precipitation, and rate constants are path-dependent- (Stumm and Morgan, 1996). Even if Equation 10 adequately describes both treatments using the same constants (even though sieving the swale media likely decreased the specific surface area of the treatment media, and an increased hydraulic load likely reduced contact time at the swale), the model may be inadequate to describe leaching behavior where influent concentrations are below  $c^*$ . If recycled media is to be used for trace metals removal, the kinetics of metals release from recycled media (such as compost) is an area where further study may be required to optimize treatment.

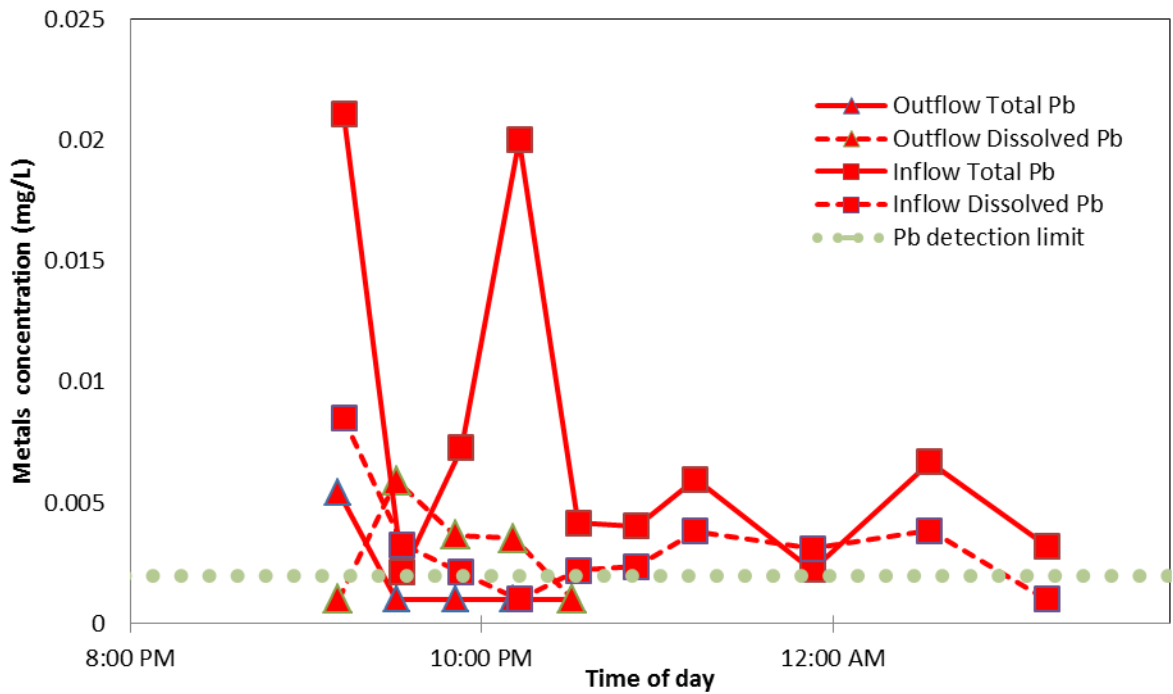


Figure 46: Dissolved and total Pb concentrations measured at the swale on May 29, 2012. The dashed line indicates the method detection limit.

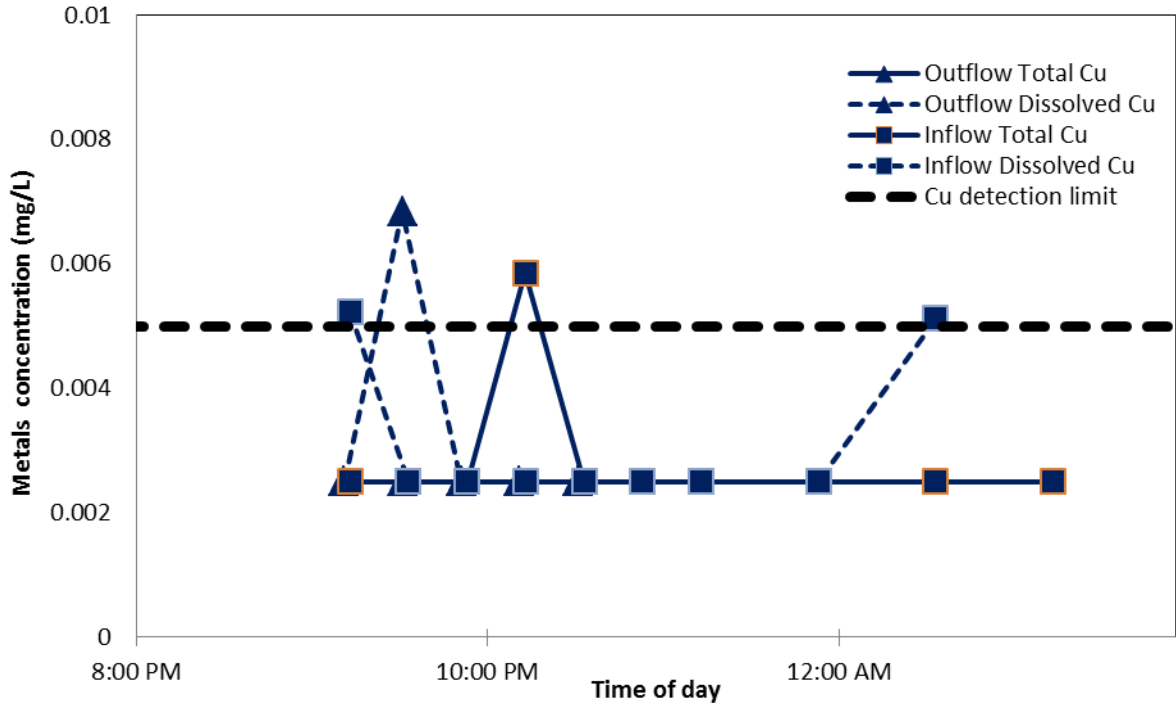


Figure 47: Dissolved and total Cu concentrations measured at the swale on May 29, 2012. The dashed line indicates the method detection limit.

Such low concentration ranges made correlation analysis comparing metals concentrations with other variables of interest (storm duration, pH, phosphorous concentration) difficult to draw useful conclusions from. Figure 48 correlates effluent pH with effluent dissolved metals. A pattern or correlation is not distinguishable, indicating that changes in effluent pH did not improve or worsen effluent dissolved metals pollution from the swale.

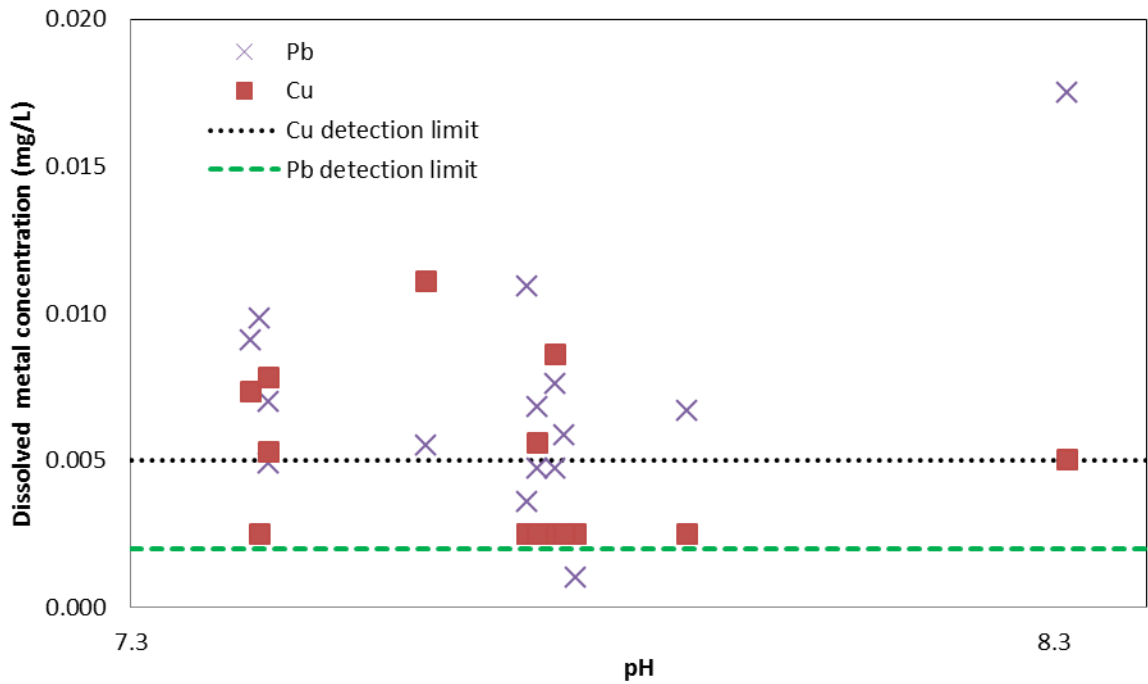


Figure 48: Effluent dissolved metals concentrations at the swale as a function of effluent pH value.

Discrete data were collected in a total of 5 storm events at the swale. As at the wooden structure, data were analyzed using pollutant duration curves, shown in Figures 49-51 and each based on 36 discrete inflow samples and 21 discrete outflow samples. Figure 49, the Pb pollutant duration curve, indicates that effluent dissolved Pb concentrations decrease below the method detection limit without appearing to asymptotically approach a steady-state level. It is possible that such a level still exists below the detection limit, or that insufficient data have been collected to determine the behavior of dissolved Pb in Biomat effluent at the swale.

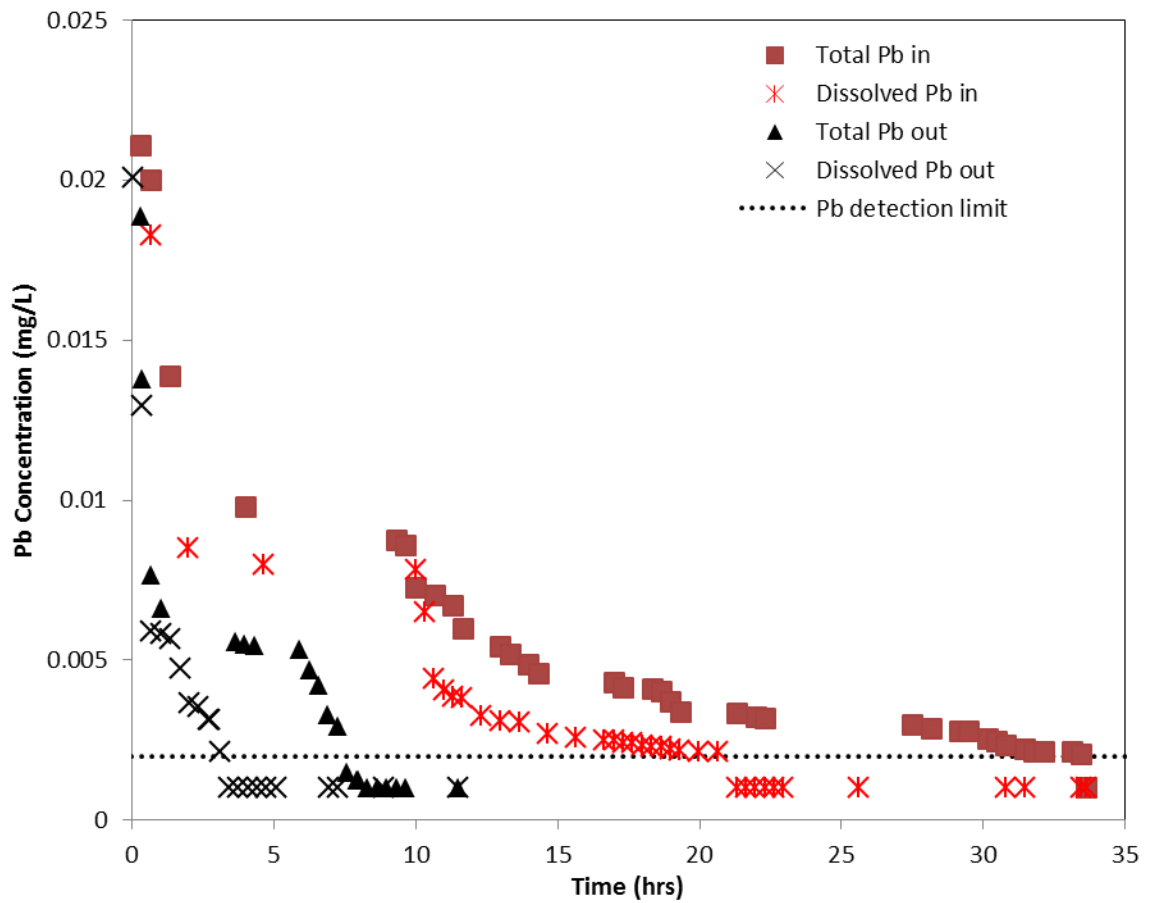


Figure 49: Pb Pollutant duration curve for swale data, showing both influent and effluent concentrations of total and dissolved Pb.

Figure 50 does appear to show equilibration of effluent dissolved Cu. Lower Cu concentrations approach 5  $\mu\text{g/L}$ , and in fact are below this threshold in a few cases. Nonetheless, effluent dissolved Cu does appear to approach a steady-state value: the dissolved Cu duration curve in Figure 50 shows a clear flattening behavior from  $t = 1.7$  hours to  $t = 9.8$  hours, a time span that encompasses 10 of 21 discrete data points in the figure. During this time period, concentrations were within a 3  $\mu\text{g/L}$  range, ranging from 5-8  $\mu\text{g/L}$ . Such a narrow expected concentration indicates that an

equilibrium relationship between the media and incoming stormwater is likely to predict Cu concentrations well.

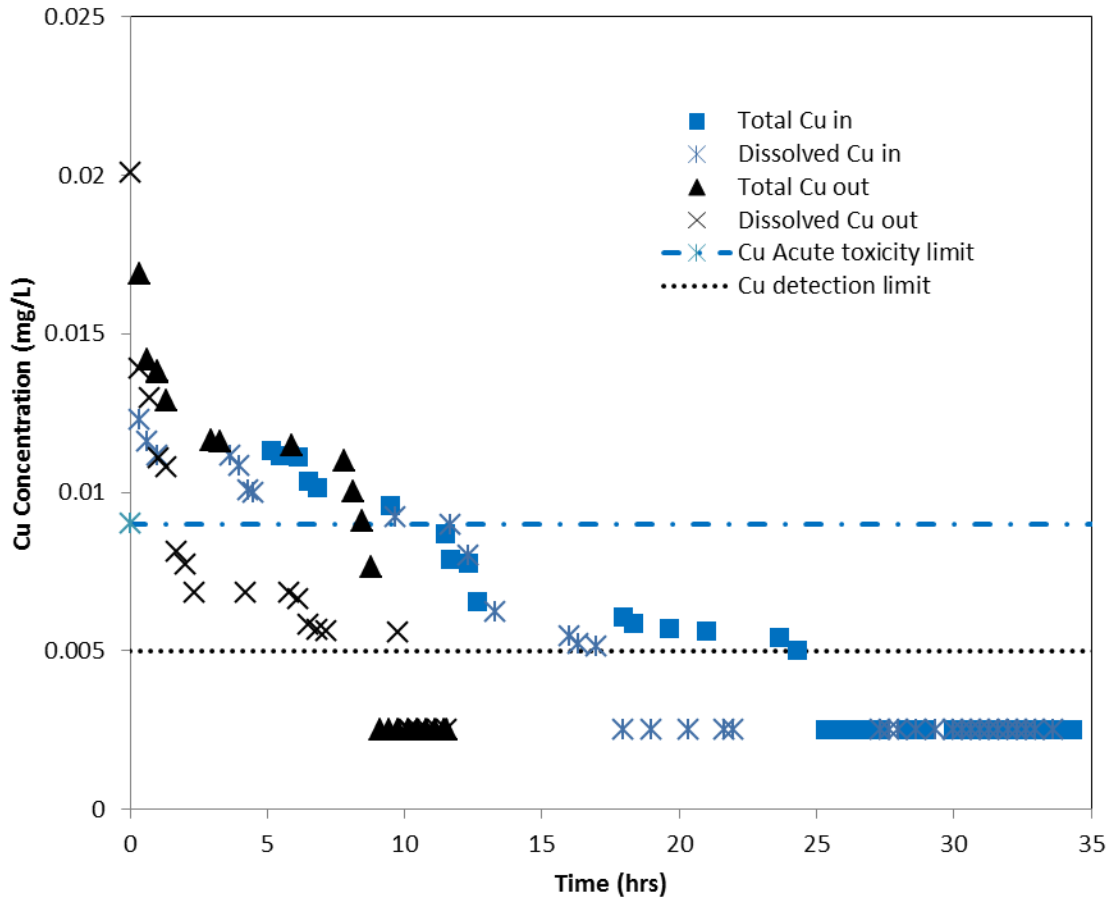


Figure 50: Cu pollutant duration curve for swale data, showing both influent and effluent concentrations of total and dissolved Cu.

Figure 51 indicates that Zn concentrations appear to approach equilibrium as well. From  $t = 1.7$  hours to  $t = 10$  hours, a time period comprising 11 of 21 discrete samples, Zn concentrations were between  $62 \mu\text{g/L}$  and  $75 \mu\text{g/L}$ . This small range of typical dissolved effluent Zn concentrations suggests that an equilibrium relationship describes Biomat treatment for Zn well. Several values for dissolved Zn do stand out

as extreme high values for both influent and effluent. These may be related to human error given that the dissolved concentrations were measured as higher than total.

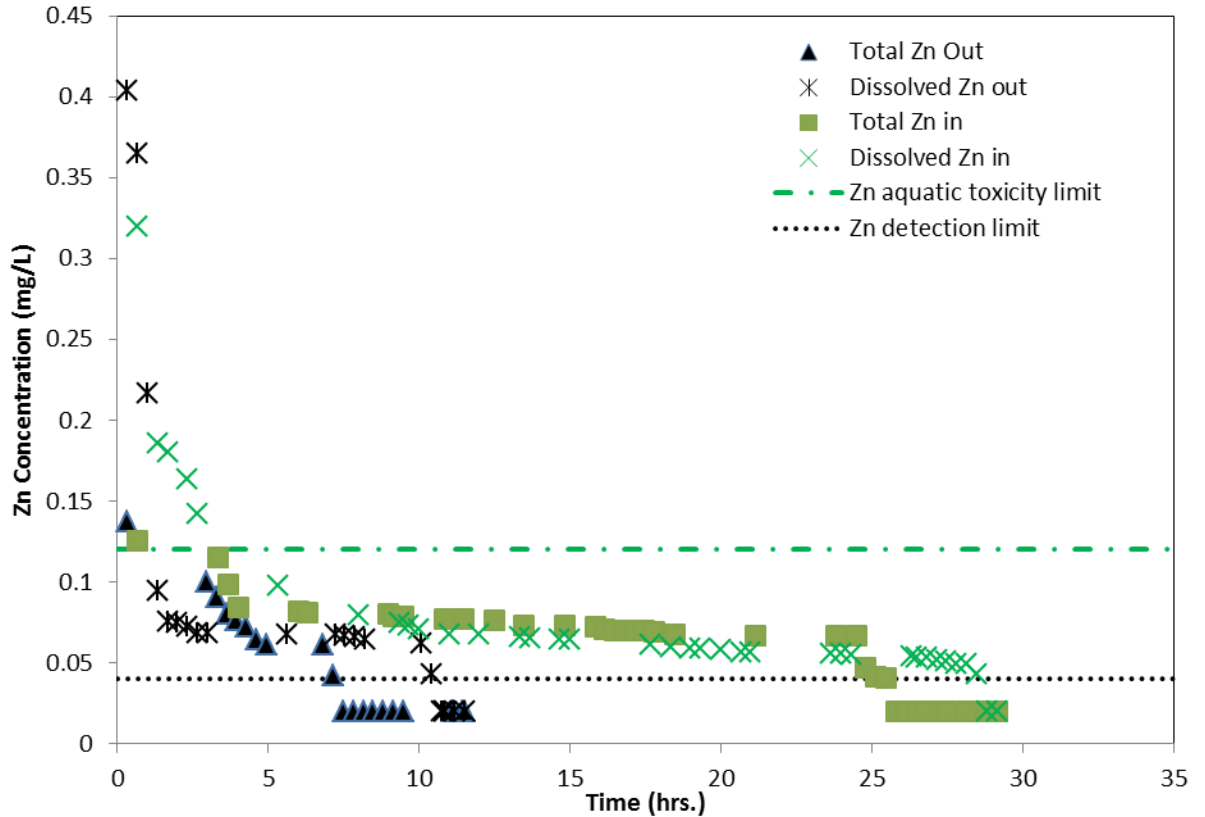


Figure 51: Zn pollutant duration curve for concentrations measured at the swale. Influent and effluent concentrations are both shown, in their total and dissolved forms.

#### Inter-site comparison of metals removal efficiencies

If dissolved-metals equilibrium exists between metals attached to the media and dissolved in stormwater, and if these equilibria are reached or at least approached, it is likely that effluent concentrations of each dissolved metal would be comparable at the two sites. This hypothesis was tested in Figures 52-54, which show pollutant duration curves for each metal with only dissolved effluent metals plotted. These figures overlay the effluent dissolved concentration data from Figures 49-51 on



Figures 21-23, normalizing the x-axis to account for the greater amount of data collected at the wooden structure. As in Figures 24 and 25, the uppermost portion of the data from the roof runoff data has been cut out to show steady-state data at the right of the figures more clearly.

The curves for dissolved effluent Pb at each site in Figure 52 show that Pb concentrations are  $<25 \mu\text{g/L}$  80% of the time at the roof runoff site, and nearly 100% of the time at the swale. The higher Pb concentrations in roof runoff effluent are explained by influent concentrations that are dramatically higher: mean inflow concentration of total Pb was  $2.5 \text{ mg/L}$  at the wooden structure, relative to  $16 \mu\text{g/L}$  mean influent total Pb at the swale. As shown in Equation 10, higher influent concentrations indicate that given the same media and environmental characteristics (e.g., temperature, pH) equilibration of dissolved metal in roof runoff with the treatment media will occur more slowly. Nonetheless, if Pb concentrations are approaching an equilibrium value, Figure 52 indicates that that value is below the method detection limit.

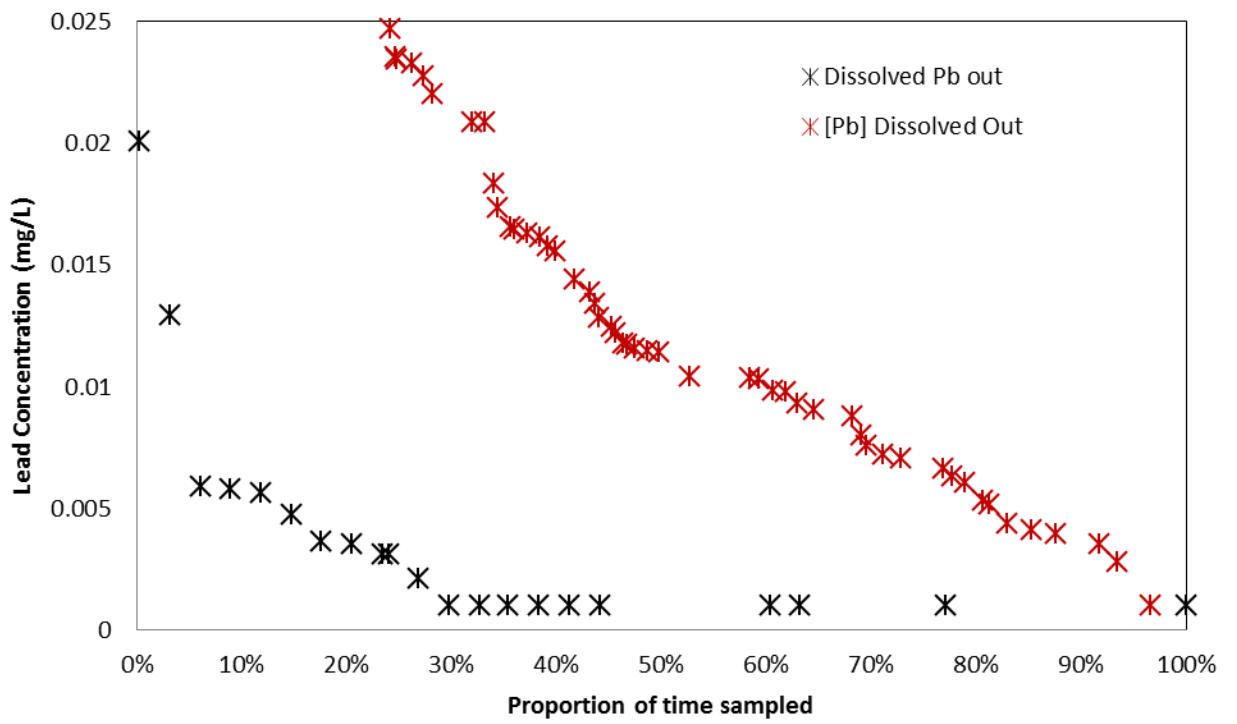


Figure 52: Pb dissolved pollutant duration curve showing effluent data from both sites.

Cu appears to behave differently from Pb, however. Figure 53 shows similar patterns for effluent dissolved Cu at each site. At the wooden structure, where influent Cu concentrations, like Pb, were greatly elevated, effluent Cu is also elevated compared to data from the swale effluent. However, the lower end of these data show the roof and swale effluent data converging near a concentration of 5 µg/L. While several data points are below the detection limit, the curves at each site show a clear flattening, or nearly asymptotic behavior.

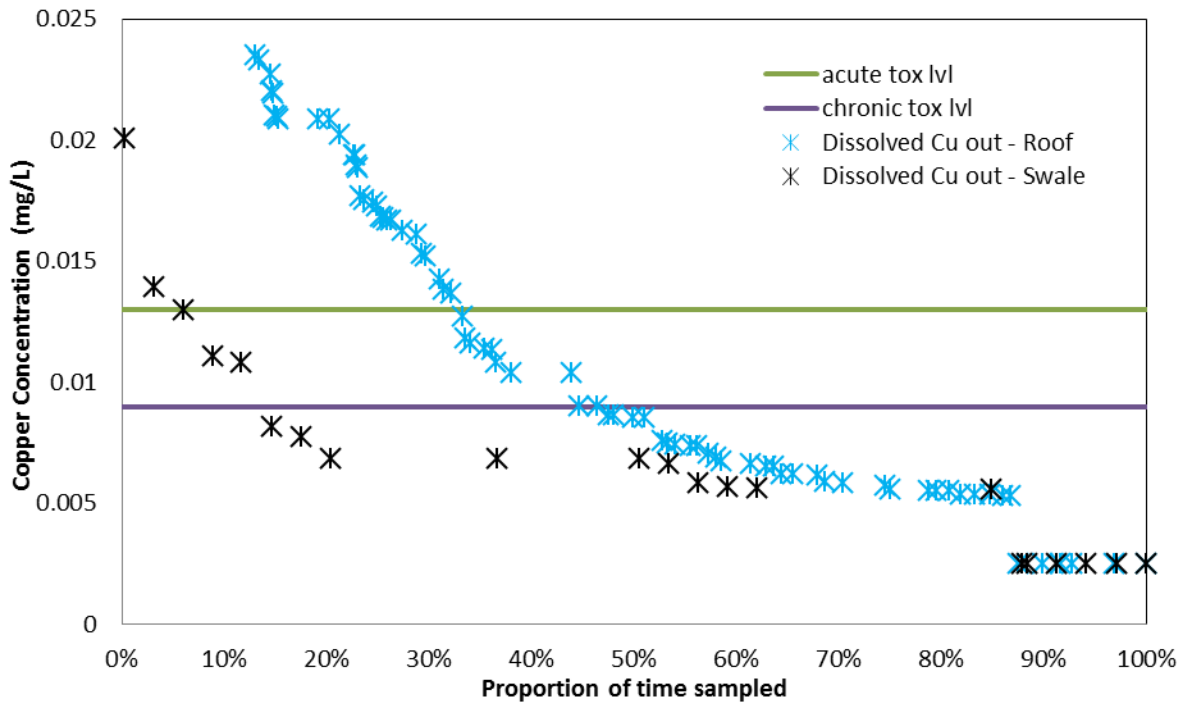


Figure 53: Cu dissolved pollutant duration curve showing effluent data from both sites.

As Figure 54 presents, Zn also appears to reach a steady-state concentration, although the concentration approached appears to differ at each site. One important difference that distinguished Zn from Pb and Cu is that influent concentrations of Zn at both sites were comparable. The overall mean concentration of influent dissolved

Zn at the swale was 97  $\mu\text{g/L}$ , relative to 75  $\mu\text{g/L}$  at the wooden structure. The swale data appear to reach steady-state slightly above 60  $\mu\text{g/L}$ , shown in Figure 54 as a flattening of the curve. The Zn data from the wooden structure appear to equilibrate at a lower level, somewhere right around the detection limit of 40  $\mu\text{g/L}$ . This is likely attributable to lower influent concentrations and to faster Zn removal rates at the wooden structure. Zn removal rates may be faster at the wooden structure due to the observed pH rise, (from roughly 5.5 to 7.5, on average), which did not occur at the swale, and the fact that compost in the Biomat there was not sieved to increase hydraulic conductivity. Referring to Equation 10, the smaller mean particle size of treatment media at the wooden structure would increase  $a$ , specific surface area, and increase  $t_c$ , contact time.

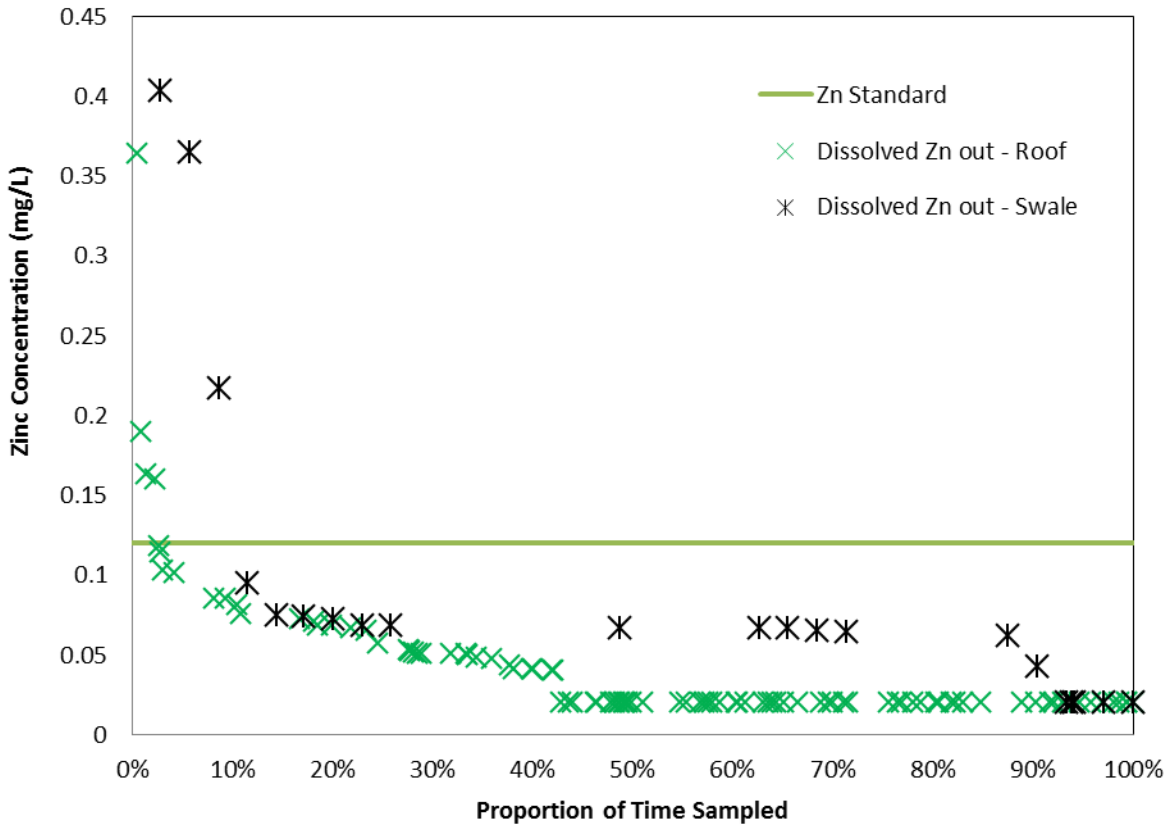


Figure 54: Zn dissolved pollutant duration curve showing effluent data from both sites.

The metals data from the swale indicate that percent concentration reductions and mass removals were much less at the swale relative to the wooden structure.

Table 14 shows the mass percent removals by metal at each site. These observations are predicted by an equilibrium model such as Equation 10. Firstly, the concentration gradient between influent and steady-state levels at the swale was shown to be much smaller. Treatment time and media specific surface area were both reduced at the swale as well; two factors which reduce the likelihood that complete equilibrium was reached in swale treatment. pH is not considered in Equation 10, specifically, but this variable also likely played a key role in determining the final equilibrium concentration at each site. Bench scale experiments by Kim et al. (2013) found that

the Biomat media were superior to other media mixtures at least in part because of the pH rise effected by this treatment. Given the close-to-detection limit concentrations at the swale, the effect of effluent pH variations on metals removal efficiency in field scale testing at the swale was difficult to assess.

Table 14: Percent concentration reductions for each metal by site.

	Pb	Cu	Zn
Wooden structure	98.7%	98.3%	36.1%
Swale	30.4%	-1.7%	-33.1%

#### Phosphorous leaching at the swale

Other changes in water quality parameters were observed, however, between influent and effluent. As at the wooden structure, phosphorous leaching was observed. Figure 55 presents a probability plot characterizing typical P concentrations based on EMC values measured at the swale.

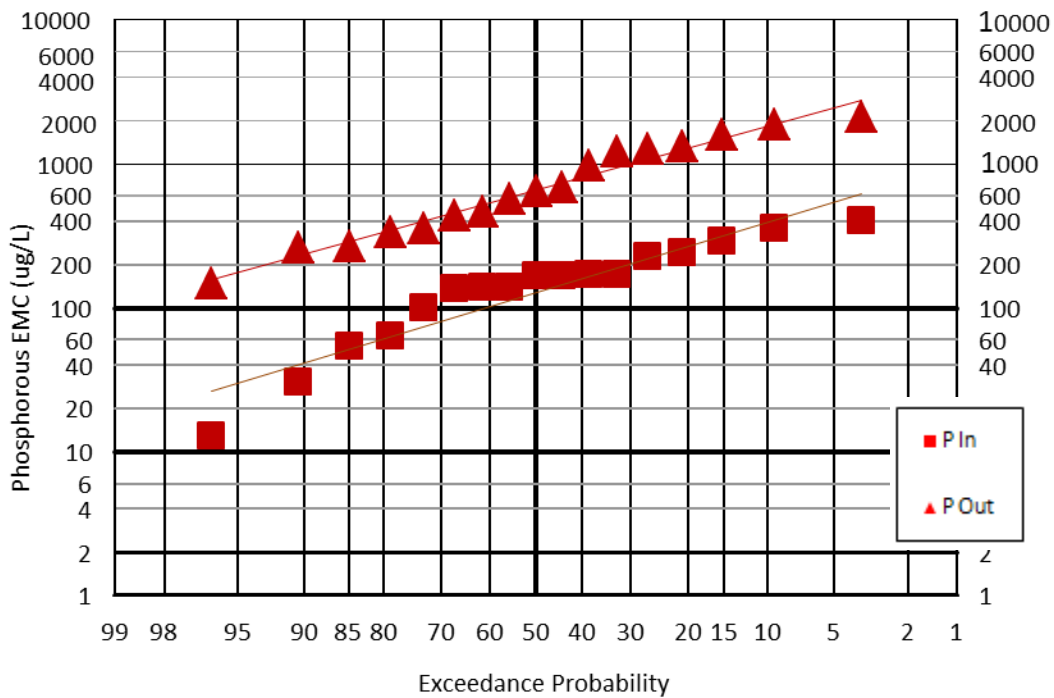


Figure 55: Exceedance plot characterizing P concentrations at the swale site.

Leaching of P is a clear issue at the swale as well as at the wooden structure. The mean concentration of total P across all measured storms was increased from 0.16 to 0.72 mg/L. Dissolved P increased as well, from 0.031 mg/L to 0.52 mg/L, indicating that leaching of particulate as well as dissolved phosphorous occurred. The fact that both dissolved and particulate phosphorous was leached to the effluent suggests that filtration by the Biomat at the swale was not as effective as filtration at the wooden structure. This interpretation is further supported by the higher TSS data observed at the swale; mean effluent TSS was 4.1 mg/L, compared to values regularly below the detection limit (1 mg/L) at the wooden structure. The increased hydraulic loading at the swale may have forced more particles through the geotextile and decreased the likelihood of particle attachment, which is dependent on treatment time

(Yao et al., 1971). Having sieved out and removed the finer compost particles to increase hydraulic conductivity may have also weakened the ability of the Biomat to filter out particulate matter from the influent and hold in small particles of the treatment media itself.

Sequential extractions performed on treatment media from the wooden structure

Three extractions were performed on media samples at each site. A  $\text{Sr}(\text{NO}_3)_2$  extraction (Madden, 1988) assessed the fraction of phyto-available Pb, Cu, and Zn held in the treatment mats. An acid ammonium oxalate extraction (McKeague and Day, 1966) was used in an attempt to measure chemically labile Pb, Cu, and Zn. Finally, an aqua regia digestion (McGrath and Cunliffe, 1985) removed all metals not bound in silicate crystals, a fraction which would not be increased or released during treatment. Control experiments were performed on virgin media from each mat. This extra media was reserved at the time that media were initially mixed, and the extraction data on these controls therefore represent background concentrations inherent to the treatment media. The background levels for Pb, Cu, and Zn are presented in Table 15. This table presents the data from three extractions which were carried out in triplicate on virgin Biomat media, conserved during initial media mixing at each site. The mean of these triplicate samples is presented in each cell of the table, with the standard deviation between the three replicate following in parentheses. Total background Pb, present at 12 mg/kg at the swale and 16 mg/kg at the wooden structure, was well within the normal range defined as any concentration below 50 mg/kg according to the American Association of Pediatrics, which also states that concentrations of up to 200 mg/kg Pb are frequently found in urban soils



(CDC, 2007). The USEPA has set a standard of 1200 mg/kg Pb as a threshold level in non-play areas for cleanup projects using federal funds (CDC, 2007). Cu and Zn concentrations in the virgin Biomat media were 10-13 mg/kg Cu and 50-58 mg/kg Zn. Relative to background levels of top-layer bioretention mulch, listed as 3.8 mg/kg Pb, 11 mg/kg Cu, and 28 mg/kg Zn, the levels in Table 15 are slightly elevated in Pb and Zn (Jones and Davis, 2013). However, metals in the virgin Biomat media are at or below typical background soil levels in Eastern Maryland, measured by Jones and Davis at 45 mg/kg Pb, 12 mg/kg Cu, and 63 mg/kg Zn.

Table 15: Metals background levels from control media extractions. The method detection limit for these measurements (performed on flame AAS) was 0.8 mg/kg. The mean of three replicates is shown in each cell, with the standard deviation among the three replicates shown in parentheses.

Pb	Sr(NO <sub>3</sub> ) <sub>2</sub>	Oxalate	Total
Swale Concentration (mg/kg)	<0.8	<0.8	12 (0.8)
Wooden Structure (mg/kg)	<0.8	1.1 (0.3)	16 (0.3)
Cu	Sr(NO <sub>3</sub> ) <sub>2</sub>	Oxalate	Total
Swale Concentration (mg/kg)	<0.8	2.2 (0.6)	10 (1)
Wooden Structure (mg/kg)	<0.8	3.0 (0.8)	13 (6)
Zn	Sr(NO <sub>3</sub> ) <sub>2</sub>	Oxalate	Total
Swale Concentration (mg/kg)	<0.8	30 (2)	58 (8)
Wooden Structure (mg/kg)	<0.8	34 (6)	50 (19)

## Lead

Tables 16 and 17 show the extraction results for Pb from the two rear Biomat cross-sections. Table 16 presents the data from samples in the side cross-section, and Table 17 presents the hotspot cross-section data. The Sr(NO<sub>3</sub>)<sub>2</sub> data from both cross-sections confirm what the water quality data from storm sampling shows: that Pb is minimally leachable from the Biomat by cation exchange. All concentrations of

Sr(NO<sub>3</sub>)<sub>2</sub>-extractable Pb are below 8 mg/kg, even in samples such as the lower inflow-facing corner where total metals concentrations are on the order of 1000 mg/kg. A clear spatial pattern within the cross-section is indistinguishable in the Sr(NO<sub>3</sub>)<sub>2</sub>-extractable Pb data, suggesting that variable flow patterns across the mat's width and height did not affect the degree to which Pb in the mat was released by cation exchange.

Lower areas of the Biomat received a greater volume of water during the treatment period. This is because storms of low intensity produced inflow at a slow rate, allowing water to penetrate the Biomat at ground-level before head built up. Additionally, the majority of metals removal from stormwater has been observed to occur at the top 3-12 cm of SCMs such as bioretention cells where first contact of water with media occurs (Jones and Davis, 2013). Water in the Biomat can be expected to flow more or less horizontally, and metals accumulation was therefore expected to occur predominantly at the layer of the mat facing the APHIS building, i.e., the part of the mat that first received influent.

Spatial patterns do emerge as expected in Tables 16 and 17 in the oxalate-extractable Pb data. The front-to-back decreasing Pb concentrations are most dramatically evidenced at Depth D in both cross-sections, where the Layer 1 sample has an oxalate-extractable Pb concentration of 125mg/kg at the side and 190 mg/kg at the hotspot, both an order of magnitude higher than further back strata such as Layer 3, where oxalate-extractable Pb was present at only 4 mg/kg at the side and 20 mg/kg at the hotspot. The fact that oxalate-extractable Pb concentrations are comparable in the A (190 +/- 31 mg/kg) and B (224 +/- 19 mg/kg) layers at Depth D in Table 17

suggests that the lower portion of Layer 1 may be saturated with respect to the oxalate-extractable fraction of Pb. As a whole, Pb appears strongly bound by the Biomat. Taking the average of all sample means presented in Table 16, the overall oxalate extractable Pb concentration was found to be 13 mg/kg out of 58 mg/kg mean total Pb at the side cross section. At the hotspot, the mean of all sample means presented in Table 17 was 50 mg/kg Pb, out of 671 mg/kg mean total Pb.

The total metals data support evidence from the oxalate extraction data that the strata of the mat closest to the APHIS wall remove the greatest portion of Pb. Over 75% of all Pb stored in the side cross section is present in the 1/5 of the mat closest to the APHIS building (Layer 1). The mean Pb concentration in this fraction of the mat was 210 mg/kg, relative to a mean concentration of 17 mg/kg total Pb across all samples in the further-back strata of the mat. Comparably, nearly 85% of all Pb stored in the hotspot cross section was found in Layer 1. The mean Pb concentration in Layer 1 at the hotspot was 2,840 mg/kg, relative to a mean concentration of 128 mg/kg total Pb across all samples in the further-back strata of the mat. Due to preferential flow to the lower portion of the mat, the individual sample 'Layer 1, Depth D' at each cross section was found to hold 59% of all Pb in each mat. Table 16 shows that Pb concentrations noticeable above background concentrations appear only in the 1<sup>st</sup> layer of the cross-section, suggesting that the media are not yet saturated in any section. Table 16 shows that Pb levels in samples at all depths from Layer 3 to Layer 5 range from 9 to 17 mg/kg. Interestingly, a majority of the media appears to remain relatively virgin, with total Pb levels close to the background concentration of 16 mg/kg in the layers furthest from the inflow. Table 17 however shows total Pb

concentrations an order of magnitude above background levels as far back as the Layer 3 at Depth D however, suggesting that the media is roughly half-saturated at this depth. At Depths A-C, in Layers 1-3, however, concentrations of Pb at the hotspot are all at or below 50 mg/kg. This is higher than the 16 mg/kg mean virgin media Pb concentration, but on par with the 45 mg/kg typical Pb concentration for Eastern MD soils as reported by Jones and Davis (2013).

Table 16: Pb concentrations in samples from the side cross-section of Biomat treatment media at the wooden structure. Data for each of the three sequential extractions are presented below. Because the cross-section was not perfectly rectangular, no sample could be taken at Layer 5, Depth A. The mean of three replicates is shown in each cell, with the standard deviation among the three replicates shown in parentheses.





	Layer 1	Layer 2	Layer 3	Layer 4	Layer 5	
Sr(NO <sub>3</sub> ) <sub>2</sub> Extractable Pb (mg/kg)	4.0 (1.9)	2.1 (1.4)	3.1 (1.6)	1.6 (0.9)		<b>Depth A</b>
Oxalate Extractable Pb (mg/kg)	17 (19)	11 (12)	10 (8)	7 (6)		
Total Pb (mg/kg)	17 (8)	10 (9)	15 (6)	11 (8)		
Sr(NO <sub>3</sub> ) <sub>2</sub> Extractable Pb (mg/kg)	1.8 (0.4)	1.7 (0.4)	1.3 (0.3)	1.3 (0.2)	1.4 (0.3)	<b>Depth B</b>
Oxalate Extractable Pb (mg/kg)	11 (4)	8 (2)	5 (2)	6 (4)	3 (2)	
Total Pb (mg/kg)	68 (24)	15 (8)	9 (8)	9 (8)	17 (6)	
Sr(NO <sub>3</sub> ) <sub>2</sub> Extractable Pb (mg/kg)	1.5 (0.4)	1.5 (0.1)	1.1 (0.3)	1.3 (0.6)	1.4 (0.4)	<b>Depth C</b>
Oxalate Extractable Pb (mg/kg)	9 (1)	4 (3)	2 (1)	2 (2)	2 (0)	
Total Pb (mg/kg)	114 (12)	17 (0)	12 (6)	10 (5)	14 (8)	
 Sr(NO <sub>3</sub> ) <sub>2</sub> Extractable Pb (mg/kg)	1.9 (0.6)	1.5 (0.6)	1.0 (0.5)	1.1 (0.4)	1.1 (0.5)	
Oxalate Extractable Pb (mg/kg)	125 (73)	20 (5)	4(2)	13 (14)	4 (2)	<b>Depth D</b>
Total Pb (mg/kg)	640 (271)	68 (19)	14 (5)	10 (5)	26 (19)	

Table 17: Pb concentrations in samples from the hotspot cross-section of Biomat treatment media at the wooden structure. Data for each of the three sequential extractions are presented below. The mean of three replicates is shown in each cell, with the standard deviation among the three replicates shown in parentheses.

	Layer 1	Layer 2	Layer 3	Layer 4	Layer 5	
Sr(NO <sub>3</sub> ) <sub>2</sub> Extractable Pb (mg/kg)	1.0 (0.7)	1.1 (0.5)	1.2 (0.7)	1.0 (0.6)	1.1 (0.2)	<b>Depth A</b>
Oxalate Extractable Pb (mg/kg)	72 (18)	10 (9)	6 (6)	4 (3)	4 (4)	
Total Pb (mg/kg)	582 (103)	45 (9)	23 (6)	13 (7)	23 (9)	
Sr(NO <sub>3</sub> ) <sub>2</sub> Extractable Pb (mg/kg)	1.9 (0.6)	0.8 (0.4)	1.3 (0.9)	0.6 (0.4)	1.1 (0.7)	<b>Depth B</b>
Oxalate Extractable Pb (mg/kg)	134 (24)	12 (2)	2 (2)	1 (2)	2 (2)	
Total Pb (mg/kg)	945 (129)	123 (18)	30 (5)	21 (2)	29 (4)	
Sr(NO <sub>3</sub> ) <sub>2</sub> Extractable Pb (mg/kg)	1.5 (0.1)	0.7 (0.5)	1.1 (0.7)	1.1 (0.6)	0.9 (0.4)	<b>Depth C</b>
Oxalate Extractable Pb (mg/kg)	292 (59)	21 (2)	4 (1)	2 (1)	1 (1)	
Total Pb (mg/kg)	1930(241)	193 (25)	50 (5)	34 (7)	33 (9)	
 Sr(NO <sub>3</sub> ) <sub>2</sub> Extractable Pb (mg/kg)	6.5 (3.2)	1.9 (1.3)	1.1 (0.8)	1.1 (1.1)	1.2 (0.7)	<b>Depth D</b> 
Oxalate Extractable Pb (mg/kg)	190 (31)	224 (15)	24 (7)	2 (1)	3 (2)	
Total Pb (mg/kg)	7920(1670)	1020(181)	342(261)	47 (11)	28 (4)	

## Copper

Tables 18 and 19 present Cu extraction data from the same two cross sections. Sr(NO<sub>3</sub>)<sub>2</sub>-extractable Cu was present at close-to-background levels throughout each cross section, with the average concentration of all samples at 1.3 mg/kg, just 0.5 mg/kg above the detection limit. To a small degree, more phytoavailable Cu appears

to be present at the lower influent-side samples in the hotspot cross-section, where extracted concentrations of Cu were as high as 7.3 mg/kg. The same spatial patterns are observable for the oxalate extractable and total Cu as were observed for Pb. One notable difference between the Pb and Cu data is that Cu appears to be much more oxalate-extractable relative to Pb. Oxalate-extractable Cu was present at 149 mg/kg as a mean concentration of all hotspot samples. The oxalate fraction therefore accounted for 83% of total Cu, which was present at a mean concentration of 179 mg/kg. At the side cross-section, 27.6 out of 28.4 mg/kg total Cu was oxalate-extractable on average. The results suggest that Cu was more predominantly bound to organic ligands on compost in the Biomat media that was readily broken down by the acid-ammonium oxalate extraction. In his extraction experiments on used Biomat media, Kim (2010) also found that Cu was much more oxalate-extractable relative to Pb. His results showed that oxalate-extractable Pb constituted 8-12% of total Pb, while oxalate-extractable Cu made up 65-88% of total Cu. By comparison, Pb may have been more predominantly bound to amorphous Fe and Mn on the steel slag in Biomat media.

Cu appears to have broken through Layer 1 only at the hotspot, and penetration of higher concentrations appears to be less severe relative to the Pb data. This is likely explained by the lower Cu concentrations observed at the APHIS building relative to Pb. During water quality testing, it was found that 22.2 g Pb and 6.8 g Cu were removed in all sampled storms, meaning that approximately 3.25 g Pb were removed for every gram of Cu removed. Averaging all samples at both cross-sections, the mean total Pb concentration was 364 mg/kg, compared to 104 mg/kg

mean total Cu. The corresponding ratio from the extraction data was therefore 3.23 g Pb for every gram of Cu removed. The closeness of these two equal but independently calculated ratios suggests that the extraction data are in good agreement with the water quality data.



Table 18: Cu concentrations in samples from the side cross-section of Biomat treatment media at the wooden structure. Data for each of the three sequential extractions are presented below. The method detection limit for these measurements (performed on flame AAS) was 0.8 mg/kg. Because the cross-section was not perfectly rectangular, no sample could be taken at Layer 5, Depth A. The mean of three replicates is shown in each cell, with the standard deviation among the three replicates shown in parentheses.

	Layer 1	Layer 2	Layer 3	Layer 4	Layer 5	
Depth A	Sr(NO <sub>3</sub> ) <sub>2</sub> Extractable Cu (mg/kg)	0.8 (0.5)	<0.8	<0.8	0.9 (0.4)	
	Oxalate Extractable Cu (mg/kg)	12 (3)	6 (4)	7 (2)	8 (3)	
	Total Cu (mg/kg)	10 (4)	10 (6)	9 (1)	12 (2)	
Depth B	Sr(NO <sub>3</sub> ) <sub>2</sub> Extractable Cu (mg/kg)	<0.8	<0.8	<0.8	<0.8	<0.8
	Oxalate Extractable Cu (mg/kg)	15 (3)	9 (2)	7 (2)	8 (4)	16 (5)
	Total Cu (mg/kg)	12 (4)	9 (2)	8 (4)	15 (13)	16 (3)
Depth C	Sr(NO <sub>3</sub> ) <sub>2</sub> Extractable Cu (mg/kg)	<0.8	<0.8	<0.8	<0.8	<0.8
	Oxalate Extractable Cu (mg/kg)	33 (6)	13 (4)	9 (4)	9 (4)	14 (5)
	Total Cu (mg/kg)	31 (8)	15 (3)	8 (2)	11 (7)	16 (4)
Depth D	Sr(NO <sub>3</sub> ) <sub>2</sub> Extractable Cu (mg/kg)	2.0 (0.3)	<0.8	<0.8	<0.8	<0.8
	Oxalate Extractable Cu (mg/kg)	302 (155)	59 (11)	9 (6)	8 (9)	8 (8)
	Total Cu (mg/kg)	282 (113)	44 (5)	9 (6)	7 (1)	15 (5)





Table 19: Cu concentrations in samples from the hotspot cross-section of Biomat treatment media at the wooden structure. Data for each of the three sequential extractions are presented below. The method detection limit for these measurements (performed on flame AAS) was 0.8 mg/kg. The mean of three replicates is shown in each cell, with the standard deviation among the three replicates shown in parentheses.

	Layer 1	Layer 2	Layer 3	Layer 4	Layer 5	
Sr(NO <sub>3</sub> ) <sub>2</sub> Extractable Cu (mg/kg)	1.5 (0.3)	<0.8	<0.8	<0.8	<0.8	<b>Depth A</b>
Oxalate Extractable Cu (mg/kg)	113 (25)	9 (4)	10 (4)	10 (5)	15 (6)	
Total Cu (mg/kg)	118 (25)	14 (3)	13 (4)	8 (3)	13 (8)	
Sr(NO <sub>3</sub> ) <sub>2</sub> Extractable Cu (mg/kg)	2.1 (0.4)	<0.8	<0.8	<0.8	<0.8	<b>Depth B</b>
Oxalate Extractable Cu (mg/kg)	237 (16)	28 (6)	5 (4)	8 (3)	11 (2)	
Total Cu (mg/kg)	230 (30)	27 (6)	11 (3)	9 (13)	10 (3)	
Sr(NO <sub>3</sub> ) <sub>2</sub> Extractable Cu (mg/kg)	3.0 (0)	<0.8	<0.8	<0.8	<0.8	<b>Depth C</b>
Oxalate Extractable Cu (mg/kg)	663 (68)	68 (19)	15 (2)	6 (3)	9 (7)	
Total Cu (mg/kg)	508 (78)	64 (1)	17 (3)	12 (3)	14 (5)	
 Sr(NO <sub>3</sub> ) <sub>2</sub> Extractable Cu (mg/kg)	7.3 (3.4)	3.6 (1.5)	0.6 (0.3)	<0.8	<0.8	<b>Depth D</b> 
Oxalate Extractable Cu (mg/kg)	1271(176)	391 (74)	72 (23)	19 (7)	10 (4)	
Total Cu (mg/kg)	2053(366)	301 (133)	141 (96)	17 (4)	10 (2)	

## Zinc

The Zn extraction data are presented in Tables 20 and 21. At an overall mean concentration of 76 mg/kg total Zn at the side and 70 mg/kg at the hotspot, increased flow appears not to have correlated with metals accumulation in the case of Zn. These average concentrations were each within one standard deviation of the mean total Zn

concentration in virgin material (58 mg/kg, +/- 19 mg/kg). Zn concentrations were observed to decrease by 37% on average during the water quality monitoring phase of research, but concentrations were so low that mass removals of Zn were estimated to be roughly one order of magnitude less than Pb and Cu removals (0.66 g Zn removed at the wooden structure, relative to 22.2 g Pb and 6.8 g Cu in sampled storms only). Two-sample student's t tests of unequal variance were performed comparing the triplicate virgin media measurements of total Zn to the raw total Zn data at each cross-section. At the side cross section, this test yielded a 0.12 rejection probability. At the hotspot, the rejection probability was 0.20. Both of these values were deemed too high ( $p > 10\%$ ) to reject the null hypothesis that both the fresh media and the used media at each cross-section belong to populations with the same mean total Zn concentration. Lower overall mass removals explain why significant accumulation of Zn did not occur.

Table 20: Zn concentrations in samples from the side cross-section of Biomat treatment media at the wooden structure. Data for each of the three sequential extractions are presented below. The method detection limit for these measurements (performed on flame AAS) was 0.8 mg/kg. Because the cross-section was not perfectly rectangular, no sample could be taken at Layer 5, Depth A. The mean of three replicates is shown in each cell, with the standard deviation among the three replicates shown in parentheses.





	Layer 1	Layer 2	Layer 3	Layer 4	Layer 5	
Sr(NO <sub>3</sub> ) <sub>2</sub> Extractable Zn (mg/kg)	<0.8 (0.2)	<0.8 (0.2)	<0.8(0.4)	0.8 (0.7)		<b>Depth A</b>
Oxalate Extractable Zn (mg/kg)	44 (8)	32 (4)	35 (6)	39 (9)		
Total Zn (mg/kg)	67 (3)	70 (10)	78 (12)	81 (7)		
Sr(NO <sub>3</sub> ) <sub>2</sub> Extractable Zn (mg/kg)	<0.8	<0.8	<0.8 (0.3)	<0.8	<0.8	<b>Depth B</b>
Oxalate Extractable Zn (mg/kg)	39 (5)	42 (7)	36 (5)	43 (7)	54 (11)	
Total Zn (mg/kg)	95 (47)	73 (10)	68 (10)	68 (18)	85 (14)	
Sr(NO <sub>3</sub> ) <sub>2</sub> Extractable Zn (mg/kg)	<0.8	<0.8	<0.8	<0.8	<0.8	<b>Depth C</b>
Oxalate Extractable Zn (mg/kg)	40 (9)	36 (8)	34 (5)	44 (2)	50 (8)	
Total Zn (mg/kg)	75 (19)	74 (12)	70 (9)	106 (54)	71 (7)	
 Sr(NO <sub>3</sub> ) <sub>2</sub> Extractable Zn (mg/kg)	<0.8	<0.8	<0.8	<0.8	<0.8	<b>Depth D</b> 
Oxalate Extractable Zn (mg/kg)	41 (11)	34 (6)	44 (6)	36 (7)	59 (7)	
Total Zn (mg/kg)	78 (3)	66 (14)	64 (13)	64 (3)	94 (9)	

Table 21: Zn concentrations in samples from the hotspot cross-section of Biomat treatment media at the wooden structure. Data for each of the three sequential extractions are

presented below. The method detection limit for these measurements (performed on flame AAS) was 0.8 mg/kg. The mean of three replicates is shown in each cell, with the standard deviation among the three replicates shown in parentheses.

	<b>Layer 1</b>	<b>Layer 2</b>	<b>Layer 3</b>	<b>Layer 4</b>	<b>Layer 5</b>	
Sr(NO <sub>3</sub> ) <sub>2</sub> Extractable Zn (mg/kg)	<0.8	<0.8	<0.8	<0.8	<0.8	<b>Depth A</b>
Oxalate Extractable Zn (mg/kg)	34 (0)	30 (3)	35 (2)	34 (4)	41 (7)	
Total Zn (mg/kg)	67 (18)	79 (28)	66 (5)	64 (14)	66 (16)	
Sr(NO <sub>3</sub> ) <sub>2</sub> Extractable Zn (mg/kg)	<0.8	<0.8	<0.8	<0.8	<0.8	<b>Depth B</b>
Oxalate Extractable Zn (mg/kg)	35 (5)	32 (4)	23 (0)	36 (4)	37 (11)	
Total Zn (mg/kg)	75 (5)	56 (5)	77 (25)	75 (3)	74 (8)	
Sr(NO <sub>3</sub> ) <sub>2</sub> Extractable Zn (mg/kg)	<0.8	<0.8	<0.8	<0.8	<0.8	<b>Depth C</b>
Oxalate Extractable Zn (mg/kg)	38 (3)	25 (7)	31 (3)	29 (8)	49 (13)	
Total Zn (mg/kg)	67 (28)	78 (16)	73 (19)	67 (9)	84 (8)	
 Sr(NO <sub>3</sub> ) <sub>2</sub> Extractable Zn (mg/kg)	4.0 (0.6)	<0.8	<0.8	<0.8	<0.8	<b>Depth D</b> 
Oxalate Extractable Zn (mg/kg)	38 (4)	33 (3)	35 (9)	34 (4)	37 (4)	
Total Zn (mg/kg)	67 (0)	76 (1)	70 (9)	58 (6)	63 (4)	

Mass balance of metals removed at the wooden structure

The data in Tables 16-21 indicate that significant amounts of Pb and Cu were transferred to the treatment media during the 19 months in which the Biomat served as a SCM. The water quality data from storm sampling indicate that this Pb and Cu was transferred during storms from the influent roof runoff to the Biomat media. The water quality data and extraction data were compared in order to estimate typical

concentrations of Pb and Cu in the Biomat media, and to help show the degree to which preferential flow may have accelerated penetration of high metals concentrations into the further back layers of the Biomat, as in shown at Depth D in Tables 16 and 18.

The mass of total Pb and Cu removed while the mat was in place was estimated from the water quality data and measured rainfall data at a nearby rain gauge (Wunderground site KMDLAURE5). During sampled storms, which had a total rainfall depth of 51.6 cm, 22 g Pb and 6.8 g Cu were removed by the Biomat. The Biomat at the wooden structure was treating water at the wooden structure from August 25, 2011 until March 11, 2013. During this period, a total of 152.6 cm of rain fell on-site. From these data, the Biomat at the wooden structure was estimated to have removed 65.7 g Pb and 20.1 g Cu. As described in the Methods and Materials chapter, the total volume of the Biomat during mixing was roughly measured as 530 L. Estimated overall bulk density of the mixed treatment media was  $0.73 \text{ g/cm}^3$  at the time of mixing, translating to roughly 386 kg media.

The extraction data showed the mean Pb concentration in treatment media at the swale to be 58 mg/kg at the side cross-section and 671 mg/kg at the hotspot. Accounting for a mean background concentration of 16 mg/kg, the concentration of Pb which was added a result of treatment was 42 mg/kg at the side cross-section and 655 mg/kg at the hotspot. If media across the entire length of the Biomat had Pb concentrations equal to those measured at the side-cross section, total Pb removed would only amount to 16.2 g. Therefore, areas such as the hotspot must more

accurately represent Pb (and Cu) concentrations at some points along the length of the Biomat.

In order to reconcile the water quality data with the extraction data, the Biomat was hypothetically separated into two sections, a preferential flow area and a non-preferential area. In the preferential flow area, media concentrations of metals were hypothesized to be equal to those measured at the hotspot cross-section. In the non-preferential area, the side cross-section extraction data were judged to accurately represent concentrations of metals in the media. Figure 56 shows the two distinct sections which were hypothesized to exist for the purpose of estimating which cross-section, the hotspot or the side, was more reflective of typical concentrations across the entire length of the Biomat. Given a total mat length of 6.7 m parallel to the APHIS building wall, the preferential flow area was estimated to occupy 21% of this space, or roughly 1.4 m. With these dimensions for each section, the total mass of Pb removed, 66 µg/L as estimated from the water quality data, is equal to the mass of Pb (65.9 g) accounted for by the extraction data.

The Cu data were used to validate this estimation. 18.1 g Cu were estimated to have been removed according the dimensional estimates based on extraction data, compared to the 20.1 g estimated from water quality and rainfall data. Given that these estimates were made to draw general conclusions from, this amount of error in the Cu estimate (just less than 10%) was considered acceptable. These dimensional estimations suggest that a large fraction of the Biomat media remained useful after breakthrough occurred at preferential flow points, and suggests that media may be

best deployed in raised or sunken beds, where selected areas of high flow could have media replaced more frequently with relative ease compared to a wrapped mat.

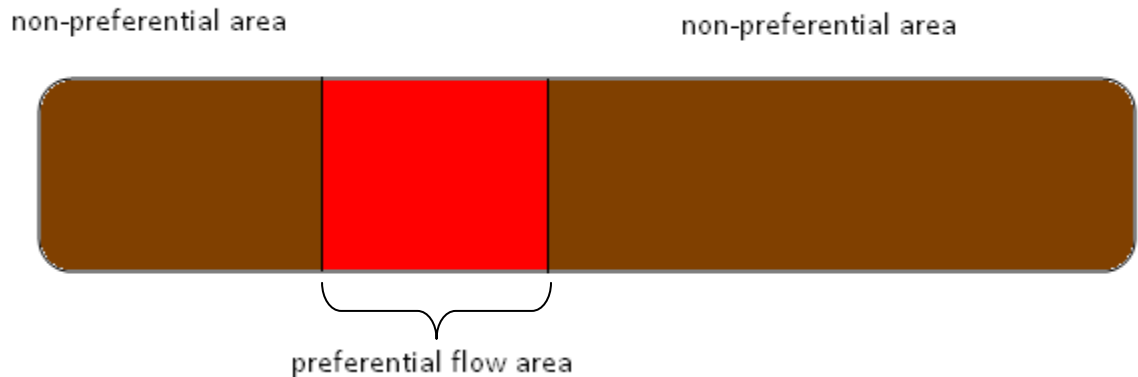


Figure 56: The two sections of the Biomat, used to estimate the typical concentrations of metals in the mat media

Sequential extractions performed on treatment media from the swale

The same extractions performed on the wooden structure media were also performed on media at the swale. Two cross-sections were taken from the swale Biomat, one in the middle of the mat and the other on the side, at the trapezoidal leg of the swale (Figures 17 and 18).

### **Lead**

Tables 22 and 23 show the Pb data from the side and middle cross-sections, respectively. The data in Table 22 from the  $\text{Sr}(\text{NO}_3)_2$  extraction show that Pb concentrations of  $\text{Sr}(\text{NO}_3)_2$ -extractable Pb in the treatment media remained at background levels even after treating stormwater at the swale for 18 months. Table 23 shows similarly low levels of  $\text{Sr}(\text{NO}_3)_2$ -extractable Pb at the middle cross-section. In

fact, concentrations of total Pb remained at similar levels relative to fresh media as well, indicating that no significant degree of metals removal occurred at the swale mat. This conclusion was drawn from a two-tailed, two-sample student's t test of unequal variance comparing the triplicate virgin media measurements of total Pb to the raw total Pb data at each cross-section. Rejection probabilities for these tests were 0.71 at the middle cross-section and 0.86 at the side cross-section, and the null hypothesis was therefore not rejected in either case. These observations are consistent with the water quality data obtained during storm monitoring, during which time concentration reductions of Pb were minimal, especially in comparison to the removals of Pb at the wooden structure.

As the data in Tables 15 and 16 confirm, Table 22 shows that only a small fraction of Pb was released by the acid ammonium oxalate extraction. Less than 7% of total Pb (as measured by the aqua regia digestion) was released. Concentrations of oxalate-extractable Pb remained below 1.5 mg/kg in all samples, at the side and middle cross sections. Table 23 shows that oxalate-extractable Pb constituted less than 5% of total Pb in the middle cross-section.



Table 22: Pb concentrations in samples from the side cross-section of Biomat treatment media at the swale. Data for each of the three sequential extractions are presented below. The method detection limit for these measurements (performed on furnace AAS) was 0.04 mg/kg. The mean of three replicates is shown in each cell, with the standard deviation among the three replicates shown in parentheses.

	<b>Layer 1</b>	<b>Layer 2</b>	<b>Layer 3</b>	<b>Layer 4</b>	
Sr(NO <sub>3</sub> ) <sub>2</sub> Extractable Pb (mg/kg)	0.2 (0.1)	0.2 (0.1)	0.5 (0.1)	0.1(0.05)	<b>Depth A</b>
Oxalate Extractable Pb (mg/kg)	1.1 (0.2)	0.9 (0.14)	0.8(0.1)	0.6(0.04)	
Total Pb (mg/kg)	16 (2.5)	14 (5.0)	11 (4.9)	12 (2.7)	
Sr(NO <sub>3</sub> ) <sub>2</sub> Extractable Pb (mg/kg)	0.2 (0.1)	0.2 (0.1)	0.2 (0.1)	0.2(0.05)	<b>Depth B</b>
Oxalate Extractable Pb (mg/kg)	0.9 (0.1)	0.7 (0.1)	1.2 (0.7)	0.7 (0.1)	
Total Pb (mg/kg)	14 (4.2)	13 (3.2)	10 (7.1)	12 (4.8)	
Sr(NO <sub>3</sub> ) <sub>2</sub> Extractable Pb (mg/kg)	0.3 (0.1)	0.4 (0.3)	0.5 (0.3)	0.2 (0.1)	<b>Depth C</b>
Oxalate Extractable Pb (mg/kg)	0.9 (0.04)	0.8 (0.1)	0.6(0.02)	0.7 (0.1)	
Total Pb (mg/kg)	12 (6.8)	12 (3.0)	10 (0.4)	9 (6.3)	








Table 23: Pb concentrations in samples from the middle cross-section of Biomat treatment media at the swale. Data for each of the three sequential extractions are presented below. The method detection limit for these measurements (performed on furnace AAS) was 0.04 mg/kg. The mean of three replicates is shown in each cell, with the standard deviation among the three replicates shown in parentheses.

	Layer 1	Layer 2	Layer 3	Layer 4	
Sr(NO <sub>3</sub> ) <sub>2</sub> Extractable Pb (mg/kg)	0.2 (0.3)	0.1 (0.02)	<0.04	0.1 (0.1)	<b>Depth A</b>
Oxalate Extractable Pb (mg/kg)	0.6 (0.1)	0.6 (0.05)	0.5 (0.1)	0.7 (0.1)	
Total Pb (mg/kg)	12 (2.5)	13 (4.5)	13 (2.8)	13 (3.7)	
Sr(NO <sub>3</sub> ) <sub>2</sub> Extractable Pb (mg/kg)	0.2 (0.2)	0.1 (0.1)	0.1 (0.2)	0.1 (0.05)	<b>Depth B</b>
Oxalate Extractable Pb (mg/kg)	0.5 (0.03)	0.5 (0.05)	0.4 (0.05)	0.6 (0.03)	
Total Pb (mg/kg)	9 (1.3)	11 (2.8)	13 (0.1)	11 (2.0)	
Sr(NO <sub>3</sub> ) <sub>2</sub> Extractable Pb (mg/kg)	0.1 (0.1)	0.1 (0.04)	0.0 (0.05)	0.1 (0.1)	<b>Depth C</b>
Oxalate Extractable Pb (mg/kg)	0.5 (0.04)	0.5 (0.03)	0.5 (0.1)	0.5 (0.05)	
Total Pb (mg/kg)	12 (2.0)	11 (0.5)	13 (3.2)	11 (0.6)	
 Sr(NO <sub>3</sub> ) <sub>2</sub> Extractable Pb (mg/kg)	0.1 (3.2)	0.1 (1.3)	0.1 (0.8)	0.1 (1.1)	
Oxalate Extractable Pb (mg/kg)	0.6 (0.1)	0.5 (0.04)	0.5 (0.05)	0.5 (0.05)	<b>Depth D</b>
Total Pb (mg/kg)	14 (2.8)	13 (2.5)	11 (4.7)	12 (2.5)	

## Copper

Tables 24 and 25 present the Cu data from each cross-section. Similar to Pb, these data indicate no spatial patterns of Cu accumulation. It was previously shown that total Cu concentrations were an order of magnitude higher in Layer 1 relative to other strata of the media in both cross-sections at the wooden structure. In

comparison, the mean total Cu concentrations in Layer 1 at each cross-section at the swale (12.5 mg/kg in the middle, 14.7 mg/kg in the side) were close to the corresponding mean total Cu concentration of all samples in each cross-section (12.6 mg/kg in the middle, 13.0 mg/kg on the side). Also, there does not appear to be any significant accumulation of Cu in data from any of the extractions. All  $\text{Sr}(\text{NO}_3)_2$  extractable Cu concentrations were below 0.2 mg/kg Cu at both cross-sections, compared to a concentration of <0.8 mg/kg Cu in the virgin media. The sample measurements at the swale were performed on furnace AAS, making the method detection limit much lower (0.04 mg/kg Cu) than the flame AAS method, which was used to test the virgin media and had a detection limit of 0.8 mg/kg Cu. In any case, however, all concentrations of  $\text{Sr}(\text{NO}_3)_2$  extractable Cu at both cross-sections and in the virgin media were found to be below 0.8 mg/kg. Overall, the data in Tables 24 and 25 indicate that less than 1% of total Cu was extracted by  $\text{Sr}(\text{NO}_3)_2$ . Cu was found again to be more oxalate-extractable than Pb. Oxalate-extractable Cu (at a mean concentration of 7 mg/kg, with a standard deviation of 1 mg/kg) constituted just greater than 50% of all metals at the side cross-section. Although mean total Cu concentrations were the roughly equal at the side and middle cross-sections (12.6 mg/kg in the middle vis-a-vis 13.0 mg/kg on the side), oxalate-extractable Cu at the middle cross-section constituted just 35% of the total, or 4 mg/kg on average, with a standard deviation of 0.5 mg/kg. However, a two-sided, two-sample t-test of equal variance comparing the raw Cu concentration data from the side cross-section with raw data from the middle cross-section produced a rejection probability of  $p=0.72$ , indicating that concentration differences between the two populations were not large

enough to be deemed significant. The similarity of Cu concentrations throughout each cross-section and between the two cross-sections further reinforces the water quality data which indicated that Cu was not significantly removed by the Biomat at the swale.

Table 24: Cu concentrations in samples from the side cross-section of Biomat treatment media at the swale. Data for each of the three sequential extractions are presented below. The method detection limit for these measurements (performed on furnace AAS) was 0.1 mg/kg. The mean of three replicates is shown in each cell, with the standard deviation among the three replicates shown in parentheses.

	<b>Layer 1</b>	<b>Layer 2</b>	<b>Layer 3</b>	<b>Layer 4</b>	
Sr(NO <sub>3</sub> ) <sub>2</sub> Extractable Cu (mg/kg)	0.2 (0.03)	<0.1	0.1(0.08)	0.1(0.02)	<b>Depth A</b>
Oxalate Extractable Cu (mg/kg)	8 (1.0)	7 (0.7)	7 (1.5)	8 (0.8)	
Total Cu (mg/kg)	15 (1)	19 (2)	11 (3)	14 (2)	
Sr(NO <sub>3</sub> ) <sub>2</sub> Extractable Cu (mg/kg)	<0.1	<0.1	<0.1	0.1(0.01)	<b>Depth B</b>
Oxalate Extractable Cu (mg/kg)	8 (0.8)	6 (0.7)	8 (1.4)	6 (0.3)	
Total Cu (mg/kg)	18 (7)	13 (2)	13 (4)	15 (7)	
Sr(NO <sub>3</sub> ) <sub>2</sub> Extractable Cu (mg/kg)	0.1 (0.05)	0.1 (0.1)	0.1(0.03)	0.1(0.04)	<b>Depth C</b>
Oxalate Extractable Cu (mg/kg)	7 (0.9)	6 (1.1)	6 (0.1)	5 (0.04)	
Total Cu (mg/kg)	11 (2)	10 (2)	10 (1)	8 (3)	








Table 25: Cu concentrations in samples from the middle cross-section of Biomat treatment media at the swale. Data for each of the three sequential extractions are presented below. The method detection limit for these measurements (performed on furnace AAS) was 0.1 mg/kg. The mean of three replicates is shown in each cell, with the standard deviation among the three replicates shown in parentheses.

	Layer 1	Layer 2	Layer 3	Layer 4	
Sr(NO <sub>3</sub> ) <sub>2</sub> Extractable Cu (mg/kg)	0.2 (0.03)	<0.1	<0.1	<0.1	<b>Depth A</b>
Oxalate Extractable Cu (mg/kg)	4 (0.6)	5 (0.7)	4 (0.4)	5 (1.0)	
Total Cu (mg/kg)	12 (1)	13 (3)	12 (4)	13 (2)	
Sr(NO <sub>3</sub> ) <sub>2</sub> Extractable Cu (mg/kg)	<0.1	<0.1	<0.1	<0.1	<b>Depth B</b>
Oxalate Extractable Cu (mg/kg)	4 (0.7)	4 (0.5)	5 (0.2)	4 (0.3)	
Total Cu (mg/kg)	10 (1)	11 (2)	12 (5)	12 (3)	
Sr(NO <sub>3</sub> ) <sub>2</sub> Extractable Cu (mg/kg)	<0.1	<0.1	<0.1	<0.1	<b>Depth C</b>
Oxalate Extractable Cu (mg/kg)	5 (0.8)	4 (0.6)	5 (0.9)	3 (0.5)	
Total Cu (mg/kg)	14 (4)	15 (9)	13 (2)	18 (18)	
 Sr(NO <sub>3</sub> ) <sub>2</sub> Extractable Cu (mg/kg)	<0.1	<0.1	<0.1	<0.1	<b>Depth D</b> 
Oxalate Extractable Cu (mg/kg)	5 (0.2)	4 (0.7)	5 (0.5)	4 (0.5)	
Total Cu (mg/kg)	14 (3)	11 (3)	10 (1)	10 (1)	

## Zinc

Tables 26 and 27 present the Zn data from the swale side and middle cross-sections, respectively. Mean concentrations of Zn at each cross-section were 63 mg/kg +/-14 mg/kg at the side and 57 mg/kg +/-11 mg/kg in the middle, both within one standard deviation of the mean background level, 50 mg/kg +/- 19 mg/kg. Mean

oxalate-extractable Zn constituted 65-70% of total Zn at both cross-sections. Like Pb and Cu, however, Zn was not highly  $\text{Sr}(\text{NO}_3)_2$  extractable. A mean of only 1% of total Zn was released at either cross-section in the strontium extractions. The lack of Zn accumulation relative to fresh media suggests that no significant amounts of Zn were removed by the Biomat. Two student's t-tests of equal variance were performed, one comparing the side cross-section raw total Zn data to total Zn concentrations in the triplicate virgin material samples ( $p=0.27$ ) and the second comparing raw total Zn data from the middle cross-section to virgin material total Zn concentrations ( $p=0.37$ ). Both tests did not allow for rejection of  $H_0$  at a 10% significance level, and accumulation of Zn at each cross-section was therefore deemed insignificant.

Table 26: Zn concentrations in samples from the side cross-section of Biomat treatment media at the swale. Data for each of the three sequential extractions are presented below. The method detection limit for these measurements (performed on flame AAS) was 0.8 mg/kg. The mean of three replicates is shown in each cell, with the standard deviation among the three replicates shown in parentheses.

	<b>Layer 1</b>	<b>Layer 2</b>	<b>Layer 3</b>	<b>Layer 4</b>	
Sr(NO <sub>3</sub> ) <sub>2</sub> Extractable Zn (mg/kg)	<0.8	<0.8	<0.8	<0.8	<b>Depth A</b>
Oxalate Extractable Zn (mg/kg)	51 (5)	44 (9)	44 (14)	43 (19)	
Total Zn (mg/kg)	80 (1)	88 (18)	58 (15)	65 (21)	
Sr(NO <sub>3</sub> ) <sub>2</sub> Extractable Zn (mg/kg)	<0.8	<0.8	0.8 (0.4)	<0.8	<b>Depth B</b>
Oxalate Extractable Zn (mg/kg)	54 (0.1)	38 (5)	41 (3)	36 (5)	
Total Zn (mg/kg)	83 (24)	58 (4)	57 (9)	67 (27)	
Sr(NO <sub>3</sub> ) <sub>2</sub> Extractable Zn (mg/kg)	<0.8	0.9 (0.5)	1.3 (0.5)	<0.8	<b>Depth C</b>
Oxalate Extractable Zn (mg/kg)	36 (13)	34 (6)	36 (10)	29 (13)	
Total Zn (mg/kg)	52 (15)	47 (5)	60 (22)	39 (18)	






Inflow
Outflow


Table 27: Zn concentrations in samples from the middle cross-section of Biomat treatment media at the swale. Data for each of the three sequential extractions are presented below. The method detection limit for these measurements (performed on flame AAS) was 0.8 mg/kg. The mean of three replicates is shown in each cell, with the standard deviation among the three replicates shown in parentheses.

	Layer 1	Layer 2	Layer 3	Layer 4	
Sr(NO <sub>3</sub> ) <sub>2</sub> Extractable Zn (mg/kg)	<0.8	<0.8	<0.8	<0.8	<b>Depth A</b>
Oxalate Extractable Zn (mg/kg)	31 (7)	42 (6)	36 (2)	45 (4)	
Total Zn (mg/kg)	60 (7)	58 (7)	56 (13)	60 (8)	
Sr(NO <sub>3</sub> ) <sub>2</sub> Extractable Zn (mg/kg)	0.9 (0.4)	<0.8	<0.8	<0.8	<b>Depth B</b>
Oxalate Extractable Zn (mg/kg)	41 (10)	52 (41)	42 (21)	29 (13)	
Total Zn (mg/kg)	50 (8)	54 (12)	57 (15)	59 (3)	
Sr(NO <sub>3</sub> ) <sub>2</sub> Extractable Zn (mg/kg)	<0.8	<0.8	<0.8	<0.8	<b>Depth C</b>
Oxalate Extractable Zn (mg/kg)	38 (2)	40 (7)	37 (5)	33 (7)	
Total Zn (mg/kg)	61 (10)	72 (41)	65 (16)	44 (7)	
 Sr(NO <sub>3</sub> ) <sub>2</sub> Extractable Zn (mg/kg)	0.8 (0.6)	<0.8	1.0 (0.3)	0.8 (0.4)	
Oxalate Extractable Zn (mg/kg)	62 (16)	37 (7)	45 (9)	40 (3)	<b>Depth D</b>
Total Zn (mg/kg)	72 (17)	48 (4)	48 (3)	54 (9)	

Comparison of extraction data from both sites

Comparing data from the two sites, obvious differences are visible in the extraction data from the wooden structure presented in Tables 16-21 vis-a-vis those from the swale presented in Tables 22-27. Higher concentrations of Pb and Cu were



observed at the wooden structure relative to the swale. Accumulation of Pb and Cu was also observable at lower, inflow-facing samples collected at the wooden structure, while no such spatial patterns were visible from the swale extraction data. Student's t-tests on mean concentrations of Pb at the side ( $p=0.86$ ) and middle ( $p=0.71$ ) cross-sections both indicated that Pb concentrations at these swale cross-sections did not vary significantly from the concentration of Pb in virgin material. It therefore appears that no Pb accumulation occurred at the swale. Cu concentrations were shown not to vary significantly between the side and middle cross-sections ( $p=0.72$ ) at the swale. Concentrations of  $\text{Sr}(\text{NO}_3)_2$ -extractable Pb, Cu, and Zn at each site were below 8 mg/kg in all individual samples, indicating a small but non-zero portion of metals which were easily dissolved off of the media by cation exchange. Oxalate data at the swale showed that Zn (64-71% extractable at the swale) was slightly more oxalate-extractable than Cu (35-53% extractable), and much more oxalate-extractable than Pb (4-7% extractable), based on the mean values of oxalate-extractable and total metals for each cross-section. Oxalate extractions on media samples from the wooden structure extracted 49-51% of total Zn, 83-97% of total Cu, and 8-23% of mean total Pb at each cross section. Based on these data, Pb appears to be the most strongly bound of all three metals. Kim (2010) similarly found a low proportion (9.6% of total Pb) of oxalate-extractable Pb in used Biomat media during bench-scale experiments. The work by Kim also indicates that oxalate-extractable Cu was found to account for 74% of total Cu, and that oxalate-extractable Zn comprised 77% of total Zn. Kim attributed the high Cu extractability to relatively larger formation of Cu complexes with organic ligands, including oxalate, relative to Pb and

Cu, as was found by Hsu and Lo (2000) and Zhou and Wong (2001). High Zn extractability was explained by the greater degree of pH dependent adsorption for Zn relative to Pb and Cu; an example of this was shown in Figure 42, taken from Benjamin and Leckie (1981). Jones and Davis (2013), in field-scale experiments on used bioretention soil media, found the order of oxalate-extractability to be  $Cu > Zn \approx Pb$ , based on 5-step sequential fractionation.

## Conclusions and Recommendations

Results from this study show that Biomat treatment at metals hotspots can reduce runoff concentrations of Pb, Cu, and Zn to levels near or below regulatory limits. At the wooden structure, overall mean pollutant concentrations were reduced from 2.68 mg/L Pb, 0.78 mg/L Cu, and 0.1 mg/L Zn as influent to 35 µg/L Pb, 13 µg/L Cu, and 66 µg/L Zn. The addition of WTR/sand treatment at the wooden structure reduced metals concentrations further, to levels consistently below regulatory limits: 11 µg/L Pb, 8 µg/L Cu, and 18 µg/L Zn as flow-weighted mean values from field-scale treatment during 3 storms.

Site-to-site comparisons of the water quality and extraction data demonstrate several important drivers of metals treatment. Firstly, pH increase appears to drive metals removals at the wooden structure. By elevating pH from the roof runoff influent level (between 5 and 6), a majority of the unbound Pb, Cu, and Zn was made susceptible to adsorption onto the amorphous Fe and Mn in the steel slag and/or onto the negatively-charged organic functional groups which serve as ligands in the compost. Past a certain pH, however, it appears likely that the increase in soluble organic matter reduces treatment efficiency (Figure 24-26). This threshold was found to exist around pH 7.5 in the case of the rear Biomat, but at the swale metals concentrations were too low to distinguish clear variations correlated with pH. Other researchers (Zhou and Haynes, 2010) have made similar observations regarding the effect of pH on the treatment efficacy of compost and biosolids. It appears that beyond a certain point of pH elevation, the release of metals attached to soluble

organic matter in compost outweighs the incremental increase in adsorption that occurs onto solid treatment media.

Secondly, it is evident that a concentration gradient drives metals removals in the Biomat media. Concentrations of Pb, Cu, and Zn are reduced at the wooden structure across a wide variety of influent concentrations, storm depths and durations, and temperatures. Despite this wide range of conditions, the standard deviations of dissolved effluent Pb and Cu EMCs over more than 20 storms was just 19  $\mu\text{g/L}$  and 15  $\mu\text{g/L}$  respectively (Table 8). After a first flush of particulate effluent metals, concentrations quickly stabilized to steady-state. At the wooden structure, these levels were estimated at 12  $\mu\text{g/L}$  Pb, 8  $\mu\text{g/L}$  Cu, and 66  $\mu\text{g/L}$  Zn. The steady-state level for these metals was shown to be described by an equilibrium model between the treatment media and dissolved metals in the Biomat (Equation 10). The water quality data and the model both suggest that concentrations of dissolved Pb and Cu in the Biomat cannot be reliably reduced below the steady-state value defined by the Biomat media treatment. This phenomenon is likely due to the small amount of impurities, which were shown to be relatively inert but still leachable at non-zero level (e.g., between 0.4 and 8 mg/kg extractable Pb) in the  $\text{Sr}(\text{NO}_3)_2$  extraction data (Tables 15-27). Nonetheless, Biomat treatment at the wooden structure was effective, and effluent concentrations were reduced from high levels of environmental concern (2.68 mg/L Pb and 0.78 mg/L Cu) in the influent to below typical urban runoff levels (0.036 mg/L Pb and 0.013 mg/L Cu) in the effluent.

First flush behaviors were observed at both the influent and the effluent. Such observations are likely due to the buildup of weakly-bound pollutants in both cases,

but the sources of these pollutants vary between the influent and the effluent. At the influent, it appears that continuous corrosion of Pb and Cu on the exterior surface of the APHIS building leads to a buildup of labile metals which are only released once rainwater begins to fall and dislodge and dissolve these metals. The influent first flush exhibited elevated concentrations of both dissolved and particulate metals as well as P in the rising limb of the rainfall hydrographs. The problem of acid rain accelerates this corrosion process during rainfall events by exposing solid Pb and Cu to concentrations of  $H^+$  capable of more rapidly dissolving  $PbO$ ,  $PbCO_3$ ,  $CuO$ , and  $CuCO_3$  into  $Pb^{2+}$  and  $Cu^{2+}$  than normal rainwater. The effluent first flush was observed for particulate metals, but this pattern did not extend to P, which built up over the storm until reaching a maximum, steady-state level. The fact that only metals and not nutrients were flushed at the beginning of outflow periods suggests that these metals were not bound strongly to the highly organic Biomat media. It is instead likely that the early flushing of metals occurred due to the buildup of untreated metals, which were left in the mat during small, non-outflow producing storms. Because no metals were released, treatment efficiency during these small storms was calculated at 100%, but in reality it is likely that a small fraction of metals left in the pore spaces of the mat remained unbound or bound to particles of highly broken down organic matter which continued to break down in the presence of residual moisture. It is likely that these metals were readily released as small particles at the beginning of the next storm. Some of these metals may have even been strongly bound or chelated to organic matter which was continuously breaking down in

between storm events, but could have been subsequently released in later storms nonetheless once the organic matter itself was mobilized.

P concentrations in Biomat effluent were elevated significantly relative to influent (overall mean effluent P concentration was 0.7 mg/L, relative to 0.05 mg/L as influent), and concentrations were observed to increase over the course of each storm. These observations suggest that the Biomat should not be used without secondary treatment in areas where nutrient addition is a water quality concern (e.g., areas with immediate drainage to rivers and streams in the Chesapeake Bay watershed). However, satisfactory P reduction was achieved with a secondary treatment of 50% sand, 50% water treatment residual. Over the 3 storms during which this secondary treatment was monitored, the concentration of total P was reduced from 0.6 mg/L to 0.06 mg/L, and the total mass of P released (22 mg) was significantly reduced relative to influent (96 mg). This secondary treatment also reduced metals concentrations to levels within regulatory limits, with mean levels of Pb, Cu, and Zn reduced to 11, 8, and 18 µg/L, respectively. Previous research (O'Neill and Davis, 2011a) has shown that, at typical stormwater concentrations of P, alum-based WTR effectively removes soluble reactive phosphorous, which was found to be the dominant species (comprising over 80%) of P in Biomat effluent.

Metals treatment at the swale site was not effective. Several factors contributed to this, including most importantly lower influent concentrations of Pb and Cu (on the order of 0.05 mg/L relative to 2.5 mg/L at the wooden structure), higher influent pH (7 at the swale, as opposed to 5.5 at the wooden structure), and lower treatment time due to higher hydraulic loading (Table 2). Concentration percent removal of Pb was

below 35% (Table 14; Figures 42 and 43), and Cu and Zn were net leached. The swale data suggest that the Biomat may not be an effective means of pre-treating typical urban stormwater.

The differences in treatment effectiveness at the swale and at the wooden structure underscore the importance of selecting BMPs on a case-by-case basis. What works at one site may not work at another. Similarly, percent removals cannot be expected to transfer from site to site and require the knowledge of site conditions, influent concentrations, and how the treatment works to be used as a legitimate measure of treatment effectiveness. Nonetheless, the excellent metals removals demonstrated at the wooden structure do suggest broader treatment applicability. In situations where high metals loadings must be reduced, and where influent pH is below neutral, the Biomat is a promising treatment technology for heavy metals removal. Such situations likely exist at galvanizing plants, copper-roofed buildings, galvanic-roofed buildings, and structures which make use of lead and/or copper flashing. As Table 8 shows, Pb and Cu mass loadings from comparable areas can be significant totals metals sources to local watersheds, and the Biomat can serve to reduce heavy metal loads at their source, before toxic effects occur in nearby aquatic environments.

#### *Recommendations for application at the APHIS site*

Given the water quality and extraction results, Biomat treatment appears to be an effective, inexpensive, and aesthetically attractive method of improving water quality at APHIS building 580. Given the severity of Pb and Cu pollution, treatment

should be implemented at the building as soon as is feasible. The two roofs in need of treatment at the APHIS building are surrounded by the red outlines in Figure 57.



Figure 57: The two roofs of environmental concern at the APHIS complex

Treatment media can be mixed on site and either placed directly next to the building, or wrapped in mats and placed at the foot of the two roofs, as shown in Figure 58. If bare media are used, plantings in the media could help prevent erosion and media loss in high flow events. Biomat treatment media, packed to a depth of at least 20 cm, could replace the gravel currently placed around the foot of the APHIS building and effectively treat metals on site for several years. Hardy, shallow-rooting plants that can survive occasional flooding would be best. Plants readily grew in the



Biomat media even at the hotspot (Figure 59), and the  $\text{Sr}(\text{NO}_3)_2$  extraction data confirm that phyto-toxic effects are not expected, even as metals accumulate to high levels in the media. Filter cloth-wrapped mats could be used just as easily. These would not necessarily require planting, although thin-stemmed plants could be seeded into the outer layers of the mat if desired.

The same media mixture of 70% sand, 25% compost, and 5% steel slag by mass is recommended for use at the APHIS building. If bulk density measurements cannot be made, media can be mixed by the volume ratio of 29 units compost: 14 units sand: 1 unit steel slag. Given the lab-scale results found by Kim et al. (2013), the use of plant and food waste based compost is preferable to manure based compost. Smartleaf compost from the Prince George's County Department of Public Works, for example, would be an affordable and well-suited option. On the sides of the building where the metal roofing tiles extend all the way to ground level, Biomat media can be placed as shown in Figure 52. On the halves of each roof draining towards the center of the complex, however, drainage interception becomes more complicated.



Figure 58: Proposed full-scale deployment for Biomat media at the APHIS building to treat direct roof runoff.






Figure 59: Plants growing across the length of the Biomat on March 11, 2013.

Phosphorous leaching concerns can easily be addressed with media directly abutting the APHIS building. As long as care is taken to ensure that water leaving the media does not drain directly into the nearby dry creek bed, but instead passes over grassed or landscaped areas, nutrient export onsite can be effectively minimized. Towards this end, converting the polypropylene-lined swale to a grass or bio-swale would slow water exiting the parking lot and allow for increased particulate phosphorous capture.

Maintenance will be necessary every 3 years, assuming a 20 cm mat depth. If loose media are used, replacement of all media should occur at this time. If a full mat is used, the mat could be rotated 90° counterclockwise to extend treatment lifetime by another 2-3 years. Table 28 uses the total Pb data from the hotspot at the rear mat to show how rotating 90° counterclockwise would place the saturated media in the less-used region of the mat, where only very high intensity storms would reach. The unspoiled media present in the Layer 3-5 strata at depths A-D, however, becomes the most used portion of the mat, thereby extending treatment lifetime.

Table 28: The cross-sectional variation of total Pb concentrations at the rear Biomat hotspot, as-is (a), and after 90° counterclockwise rotation (b)

(a)		1	2	3	4	5	
	Total Pb (mg/kg)	582 (103)	45 (9)	23 (6)	13 (7)	23 (9)	Depth A
	Total Pb (mg/kg)	945 (129)	123 (18)	30 (5)	21 (2)	29 (4)	Depth B
	Total Pb (mg/kg)	1930(241)	193 (25)	50 (5)	34 (7)	33 (9)	Depth C
	Total Pb (mg/kg)	7915(1665)	1022(181)	342(261)	47 (11)	28 (4)	Depth D
(b)		Depth D	Depth C	Depth B	Depth A		
	Total Pb (mg/kg)	7915(1665)	1930(241)	945(129)	592(103)	1	
	Total Pb (mg/kg)	1022(181)	193(25)	123(18)	45(9)	2	
	Total Pb (mg/kg)	342(261)	50(5)	30(5)	23(6)	3	
	Total Pb (mg/kg)	47(11)	34(7)	21(2)	13(7)	4	
	Total Pb (mg/kg)	28(4)	33(9)	29(4)	23(9)	5	

### Research Recommendations

The effectiveness of water treatment residual in several P treatment applications has been demonstrated (O'Neill and Davis, 2011a; Babatunde and Zhao, 2007; Codling et al., 2000). In other applications, however, WTR treatment has proven ineffective (Vacca and Wadzuk, EWRI 2013 presentation). The mechanisms which govern metals and nutrient removal by WTR must be studied further. Furthermore, processes for optimizing this waste media (e.g. drying, aging, and heating) are still just beginning to be explored and are little understood (Komlos et al., EWRI 2013 presentation). At the APHIS site, WTR treatment appears promising, but with water quality data from only 3 storms, no significant recommendations can be made. If nutrient reductions are desired on-site, further field-scale studies should be conducted into using a WTR-sand mixture as secondary full-scale treatment. If loose media are used for treatment, the WTR-sand mixture could be added as a bottom layer of media through which Biomat effluent could percolate. If mats are used, the WTR-sand mixture could form the bottom layer of the mat by adding this media mixture to the center of a filter-cloth strip. Pre-mixed Biomat media could then be added on top of the WTR/sand mixture before wrapping and sealing the filter cloth around the amassed media.

Biomat media also need to be studied at a wider variety of sites to fully understand the scope of applications where Biomat treatment will be successful. It is likely that the Biomat can reduce concentrations of Pb, Cu, and Zn at other buildings constructed with Pb, Cu, or Zn metallic roofing. Where Pb, Cu, and Zn are incorporated into non-metallic materials, however, this media may be less effective. It

is unknown, for instance, if Biomat media effectively remove Zn which has dissolved from vulcanized tires. Influent speciation and metals sources may prove to be an important variable controlling treatment effectiveness. Biomat treatment of other prevalent metallic pollutants, such as arsenic, iron, and selenium, is another topic worthy of further study. Finally, more long-term studies on Biomat media are also needed to develop maintenance and end-of-life guidelines that can be easily followed and implemented by property owners and environmental professionals.

## Appendix A- Water quality and flow data listed by rainfall event

Numbers in red in discrete samples indicate that a measurement was not taken. These numbers were filled out to facilitate computerized EMC calculation, and should not be mistaken for measured data points. Where data points were missed due to a lack of sample water or human error, (e.g. spilling a sample prior to measurement) missing data points were filled in by taking the mean value of the sample immediately prior and following. If the missed sample value was the first sample, then the value for the second sample was filled in as the first, solely for the sake of EMC calculation. Values in red were not used for discrete data analysis (e.g. pollution duration curves and/or pollutographs.)

September 23, 2011

SITE	Sample #	Time	Lead ppm	Zinc ppm	Copper ppm	TP mg/L	TSS mg/L	pH
WBI	1	10:16 AM	3.91	0.0575	1.08	0.06	3.6	5.88
WBI	2	10:36 AM	1.24	0.0197	0.364	0.05	0.5	5.08
WBI	3	10:56 AM	2.99	0.0218	0.882	0.03	3.9	4.75
WBI	4	11:16 AM	1.66	0.0537	0.477	0.03	2.3	5.50
WBI	5	11:36 AM	2.70	0.0334	0.724	0.04	0.5	5.37
WBI	6	11:56 AM	1.89	0.0211	0.328	0.04	0.5	5.60
WBI	7	12:16 PM	1.27	0.0224	0.128	0.04	2.1	5.69
WBI	8	12:36 PM	1.23	0.0180	0.121	0.03	3.1	5.62
WBI	9	12:56 PM	1.05	0.0105	0.128	0.04	4.9	5.49
WBI	11	2:56 PM	1.44	0.0353	0.177	0.04	4.6	5.61

SITE	Sample #	Time	Lead ppm	Zinc ppm	Copper ppm	TP mg/L	TSS mg/L	pH
WBO	1	10:18 AM	0.113	0.148	0.026	1.61	6.4	
WBO	2	10:38 AM	0.044	0.0294	0.0072	1.44	6.4	8.14
WBO	3	10:58 AM	0.035	0.0198	0.0040	1.53	6.4	8.23
WBO	4	11:18 AM	0.039	0.0254	0.0065	1.37	6.4	8.17
WBO	5	11:38 AM	0.045	0.0146	0.0054	1.39	3.45	8.09
WBO	6	11:58 AM	0.039	0.0242	0.0063	1.40	0.5	8.12
WBO	7	12:18 PM	0.027	0.0135	0.0062	2.00	4.9	7.97
WBO	8	12:38 PM	0.017	0.0442	0.0085	1.98	8	7.83
WBO	9	12:58 PM	0.028	0.0175	0.0061	1.79	4.5	7.67
WBO	10	1:58 PM	0.049	0.0132	0.011	1.81	0.5	7.59
WBO	11	2:58 PM	0.033	0.0301	0.0067	1.66	8.2	7.54
WBO	12	4:18 PM	0.037	0.0194	0.0077	1.76		7.50

wood in		
sample #	Time	flow(L)
1	9/23/11 10:16	16.28
2	9/23/11 10:36	8.14
3	9/23/11 10:56	8.14
4	9/23/11 11:16	40.71
5	9/23/11 11:36	32.56
6	9/23/11 11:56	219.80
7	9/23/11 12:16	431.48
8	9/23/11 12:36	89.55
9	9/23/11 12:56	138.40
11	9/23/11 14:56	586.16
		0
		0
		1571.22
		TOTAL FLOW (L)

wood out		
sample #	Time	flow(L)
1	9/23/11 10:18	0
2	9/23/11 10:38	0
3	9/23/11 10:58	0
4	9/23/11 11:18	0
5	9/23/11 11:38	0
6	9/23/11 11:58	1.84
7	9/23/11 12:18	45.02
8	9/23/11 12:38	23.75
9	9/23/11 12:58	13.49
10	9/23/11 13:58	0
11	9/23/11 14:58	3.08
12	9/23/11 16:18	0.06
		0
		87.24
		TOTAL FLOW (L)

October 12, 2012

SITE	Sample #	Time	Lead ppm	Diss. Lead ppm	Zinc ppm	Diss. Zinc ppm	Copper Ppm	Diss Cu ppm	TP mg/L	TSS mg/L	Turbidity NTU
WBI	1	3:47 PM	3.43	1.31	0.041	0.072	1.21	1.08	0.04	0.5	7.50
WBI	2	4:07 PM	2.97	2.49	0.059	0.017	0.94	0.86	0.06	0.5	7.98
WBI	3	4:27 PM	2.25	1.93	0.022	0.049	0.50	0.44	0.02	0.5	0.55
WBI	4	4:47 PM	2.23	2.19	0.039	0.020	0.56	0.57	0.01	0.5	0.75
WBI	5	5:07 PM	2.56	2.35	0.044	0.023	0.70	0.64	0.02	0.5	1.36

SITE	Sample #	Time	Lead ppm	Diss. Lead ppm	Zinc ppm	Diss. Zinc ppm	Copper Ppm	Diss Cu ppm	TP mg/L	TSS mg/L	Turbidity NTU
WBO	2	4:07 PM	0.16	0.14	0.24	0.036	0.070	0.094	0.46	0.5	
WBO	3	4:27 PM	0.18	0.18	0.040	0.014	0.061	0.094	0.46	1.2	10
WBO	4	4:47 PM	0.42	0.34	0.047	0.042	0.101	0.094	1.03	0.5	8.19
WBO	5	5:07 PM	0.23	0.14	0.041	0.051	0.046	0.038	1.63	0.5	16.3
WBO	6	5:27 PM	0.14	0.086	0.027	0.031	0.024	0.023	1.81		14.2

wood in		
sample #	time	flow(L)
1	10/12/11 15:47	24.42
2	10/12/11 16:07	65.13
3	10/12/11 16:27	81.41
4	10/12/11 16:47	16.28
5	10/12/11 17:07	16.28
		203.53
		TOTAL FLOW (L)

wood out		
sample #	time	flow(L)
2	10/12/11 16:07	0.012
3	10/12/11 16:27	4.73
4	10/12/11 16:47	0.18
5	10/12/11 17:07	0
6	10/12/11 17:27	0
		0
		4.92
		TOTAL FLOW (L)

December 22, 2011



SITE	Sample #	Time	Lead ppm	Diss. Lead ppm	Zinc ppm	Diss. Zinc ppm	Copper Ppm	Diss Cu ppm	TP mg/L	DP mg/L	TSS mg/L	pH
WBI	1	8:52 PM	7.14	5.10	0.060	0.047	2.59	2.22	0.21	0.00	3.2	5.92
WBI	2	9:12 PM	5.09	3.65	0.085	0.035	1.67	1.38	0.14	0	3.2	5.92
WBI	5	10:12 PM	3.50	2.20	0.035	0.023	0.71	0.54	0.07	0.00	3.2	5.92
WBI	6	10:52 PM	2.08	1.82	0.026	0.014	0.33	0.30	0.04	0.00	0.5	5.95
WBI	7	12:12 AM	1.90	1.82	0.025	0.027	0.36	0.35	0.02	0.00	0.5	6.01
WBI	8	1:12 AM	2.75	2.04	0.023	0.016	0.59	0.46	0.08	0.00	0.5	5.95
WBI	9	2:12 AM	3.47	1.61	0.023	0.022	0.58	0.39	0.19	0.01	5.1	5.85
WBI	12	5:52 AM	2.35	1.87	0.020	0.017	0.36	0.35	0.04	0.00	0.5	5.89

SITE	Sample #	Time	Lead ppm	Diss. Lead ppm	Zinc ppm	Diss. Zinc ppm	Copper Ppm	Diss Cu ppm	TP mg/L	DP mg/L	TSS mg/L	pH
WBO	3	9:42 PM	0.181	0.13	0.043	0.036	0.027	0.0167	0.29	0.29	0.5	7.40
WBO	4	10:02 PM	0.096	0.13	0.027	0.036	0.010	0.0167	0.91	0.84	0.5	7.97
WBO	5	10:22 PM	0.070	0.046	0.018	0.021	0.015	0.0113	1.03	1.00	0.5	8.03
WBO	6	11:02 PM	0.043	0.022	0.033	0.024	0.011	0.0069	1.08	1.12	0.5	7.95
WBO	7	11:42 PM	0.026	0.016	0.019	0.018	0.0074	0.0065	1.28	1.21	0.5	7.90
WBO	8	12:22 AM	0.027	0.017	0.026	0.020	0.0086	0.0053	1.24	1.27	0.5	7.52
WBO	9	1:22 AM	0.021	0.011	0.020	0.022	0.0055	0.0062	1.18	1.12	0.5	7.59
WBO	10	2:22 AM	0.018	0.0098	0.027	0.024	0.0046	0.0041	1.32	1.17	0.5	7.61
WBO	11	3:22 AM	0.026	0.016	0.025	0.014	0.0062	0.0076	1.35	1.25	0.5	7.56

wood in		
sample #	time	flow(L)
1	12/22/11 20:52	73.27
2	12/22/11 21:12	40.71
5	12/22/11 22:12	162.82
6	12/22/11 22:52	130.26
7	12/23/11 0:12	97.69
8	12/23/11 1:12	32.56
9	12/23/11 2:12	130.26
12	12/23/11 5:52	0

667.57  
TOTAL FLOW (L)

wood out		
sample #	time	flow(L)
3	12/22/11 21:42	0
4	12/22/11 22:02	0
5	12/22/11 22:22	6.28
6	12/22/11 23:02	32.72
7	12/22/11 23:42	22.56
8	12/23/11 0:22	17.93
9	12/23/11 1:22	7.30
10	12/23/11 2:22	3.20
11	12/23/11 3:22	13.63

0  
TOTAL FLOW (L)

January 11, 2012

SITE	Sample #	Time	Lead ppm	Diss. Lead ppm	Zinc ppm	Diss. Zinc ppm	Copper ppm	Diss Cu ppm	TP mg/L	TSS mg/L	pH
SI	Batch		0.0016	0.0022	0.076	0.11	0.0047	0.0059	0.14	52.3	7.52

SITE	Sample #	Time	Lead ppm	Diss. Lead ppm	Zinc ppm	Diss. Zinc ppm	Copper ppm	Diss Cu ppm	TP mg/L	TSS mg/L	pH
SO	Batch		0.0075	0.0047	0.063	0.13	0.0056	0.0038	0.27	34.8	7.76

SITE	Sample #	Time	Lead Ppm	Diss. Lead ppm	Zinc ppm	Diss. Zinc ppm	Copper ppm	Diss Cu ppm	TP mg/L	TSS mg/L	pH
WBI	3	8:02 PM	3.82	2	0.095	0.057	0.993	0.783	0.19	33.8	6.15
WBI	4	8:22 PM	2.91	2.33	0.082	0.070	0.894	0.886	0.06	12.5	6.10
WBI	7	10:42 PM	1.58	1.94	0.071	0.059	0.551	0.611	0.06	8.35	6.18
WBI	9	12:42 AM	2.24	1.94	0.081	0.059	0.615	0.611	0.06	8.35	6.18
WBI	10	1:42 AM	2.01	1.55	0.073	0.049	0.380	0.336	0.06	4.2	6.26
WBI	11	3:02 AM	1.86	1.90	0.074	0.073	0.349	0.350	0.01	0.5	6.19
WBI	16	9:42 AM	1.95	2.03	0.073	0.075	0.365	0.462	0.12	12.2	6.16

SITE	Sample #	Time	Lead ppm	Diss. Lead Ppm	Zinc ppm	Diss. Zinc ppm	Copper ppm	Diss Cu ppm	TP mg/L	TSS mg/L	pH
WBO	4	3:16 PM	0.420	0.021	0.110	0.085	0.136	0.0208	0.63	12.3	7.95
WBO	9	6:36 PM	0.050	0.021	0.072	0.085	0.013	0.0208	0.90	12.3	7.95
WBO	10	7:36 PM	0.032	0.016	0.056	0.101	0.0092	0.0163	1.24	11.8	8.04
WBO	11	8:36 PM	0.021	8.7E-05	0.066	0.051	0.0085	0.0872	1.21	10.5	7.85
WBO	12	9:56 PM	0.036	0.0018	0.064	0.053	0.0099	0.00180	1.39	2	7.78
WBO	15	12:36 AM	0.013	0.010	0.067	0.072	0.0081	0.0104	1.09	0.6	7.70
WBO	21	5:36 AM	0.023	0.023	0.067	0.081	0.0156	0.0227	0.93	0.5	7.59

swale in		
sample #	time	flow(L)
Batch		19415
		19415
		TOTAL FLOW (L)

swale out		
sample #	time	flow(L)
Batch		19415
		19415
		TOTAL FLOW (L)

wood in		
sample #	time	flow(L)
3	1/11/12 20:02	154.68
4	1/11/12 20:22	8.14
7	1/11/12 22:42	138.39
9	1/12/12 0:42	211.66

wood out		
sample #	Time	flow(L)
4	1/11/12 15:16	42.12
9	1/11/12 18:36	31.35
10	1/11/12 19:36	88.36
11	1/11/12	140.50

10	1/12/12 1:42	97.69
11	1/12/12 3:02	170.96
16	1/12/12 9:42	0
		781.54
		TOTAL FLOW (L)

12	20:36 1/11/12 21:56	230.22
15	1/12/12 0:36	776.42
21	1/12/12 5:36	813.26
		2122.23
		TOTAL FLOW (L)

January 17, 2012

SITE	Sample #	Time	Lead ppm	Diss. Lead ppm	Zinc ppm	Diss. Zinc ppm	Copper ppm	Diss Cu ppm	TP mg/L	DP mg/L	TSS mg/L	pH
SI	10	5:29 AM	0.007	0.0030	0.0771	0.0744	0.0057	0.0043	0.09	0.03	20.8	7.71
SI	11	6:49 AM	0.005	0.0024	0.0727	0.0658	0.0056	0.0044	0.06	0.03	6	7.73
SI	15	9:29 AM	0.01	0.0078	0.0666	0.0974	0.0054	0.0055	0.05	0.03	4.4	7.69
SI	21	2:49 PM	0.009	0.0011	0.0800	0.0795	0.0061	0.0037	0.06	0.02	9.3	7.77
SI	Grab		0.006	0.0053	0.0592	0.0643	0.0049	0.0049	0.03	0.03	2.9	7.80

SITE	Sample #	Time	Lead ppm	Diss. Lead ppm	Zinc ppm	Diss. Zinc ppm	Copper ppm	Diss Cu ppm	TP mg/L	DP mg/L	TSS mg/L	pH
SO	1	10:06 AM	0.019	0.0047	0.0906	0.0642	0.0091	0.0056	0.36	0.07	247.2	7.74
SO	Grab		0.015	0.0274	0.0642	0.0651	0.0108	0.0124	1.45	1.12		9.65

SITE	Sample #	Time	Lead ppm	Diss. Lead ppm	Zinc ppm	Diss. Zinc ppm	Copper ppm	Diss Cu ppm	TP mg/L	DP mg/L	TSS mg/L	pH
WBI	Batch	10:42 PM	3.193	2.251	0.0387	0.0572	0.983	0.909	0.13	0.11	14.6	6.25

swale in		
sample #	time	flow(L)
10	1/17/12 5:29	397
11	1/17/12 6:49	0
15	1/17/12 9:29	873
21	1/17/12 14:49	0
		1270
		TOTAL FLOW (L)

swale out		
sample #	time	flow(L)
1	1/17/12 10:06	1270.34
		0
Grab		0
		0
		1270.34
		TOTAL FLOW (L)

wood in

wood out

sample #	time	flow(L)
Batch		130.26
		130.26
		TOTAL FLOW (L)

sample #	time	flow(L)
No Outflow		3.40
		3.40
		TOTAL FLOW (L)

January 23, 2012

SITE	Sample #	Time	Lead ppm	Diss. Lead ppm	Zinc ppm	Diss. Zinc ppm	Copper ppm	Diss Cu ppm	TP mg/L	TSS mg/L	pH
SI	1	2:54 PM	0.0033	0.0065	0.0690	0.0425	0.0041	0.0038	0.03	7	7.11
SI	2	3:13 PM	0.0021	0.0014	0.0696	0.0509	0.0038	0.0027	0.03	1.2	6.96
SI	3	3:33 PM	0.0031	0.0022	0.0697	0.0520	0.0037	0.0033	0.03	0.8	7.04
SI	4	3:53 PM	0.0045	0.0025	0.0700	0.0532	0.0038	0.0034	0.04	1.5	7.09
SI	5	4:13 PM	0.0051	0.0026	0.0708	0.0545	0.0065	0.0027	0.03	0.8	7.06
SI	6	4:53 PM	0.013	0.0040	0.0769	0.0566	0.0035	0.0030	0.03	1.8	7.06
SI	7	5:33 PM	0.0048	0.0027	0.0672	0.0599	0.0038	0.0030	0.03	2.8	7.13
SI	8	6:13 PM	0.002	0.0021	0.0665	0.0579	0.0050	0.0031	0.03	0.5	7.13
SI	9	7:13 PM	0.0021	0.0024	0.0721	0.0674	0.0032	0.0044	0.03	2.7	7.24
SI	10	8:13 PM	0.002	0.0182	0.0761	0.0640	0.0036	0.0062	0.03	0.5	7.27
SI	11	9:13 PM	0.0041	0.0079	0.0728	0.0674	0.0046	0.0045	0.04	0.5	7.33
SI	Grab		0.0043	0.0045	0.0711	0.0711	0.0040	0.0051	0.03		

swale in		
sample #	time	flow(L)
1	1/23/12 14:54	55.8
2	1/23/12 15:13	0
3	1/23/12 15:33	0
4	1/23/12 15:53	0
5	1/23/12 16:13	0
6	1/23/12 16:53	21.9
7	1/23/12 17:33	0
8	1/23/12 18:13	0
9	1/23/12 19:13	0
10	1/23/12 20:13	0
11	1/23/12 21:13	0
		67.7
		TOTAL FLOW (L)

swale out		
sample #	time	flow(L)
No sample		67.73
		0
		0
		0
		0
		0
		0
		0
		0
		0
		0
		0
		67.73
		TOTAL FLOW (L)

January 27, 2012

SITE	Sample #	Time	Lead ppm	Diss. Lead ppm	Zinc ppm	Diss. Zinc ppm	Copper ppm	Diss Cu ppm	TP mg/L	DP mg/L	TSS mg/L	pH
SI	3	10:37 AM	0.0408	0.0036	0.129	0.091	0.0156	0.0061	0.36	0.05	120.7	7.15
SI	5	12:37 PM	0.0094	0.0077	0.100	0.099	0.0069	0.0046	0.22	0.04	60.1	7.90
SI	6	1:57 PM	0.0348	0.0024	0.096	0.087	0.0068	0.0047	0.20	0.04	37	8.08
SI	Grab		0.102	0.0033	0.087	0.165	0.0060	0.008	0.16	0.04	35.8	7.94

SITE	Sample #	Time	Lead ppm	Diss. Lead ppm	Zinc ppm	Diss. Zinc ppm	Copper ppm	Diss Cu Ppm	TP mg/L	DP mg/L	TSS mg/L	pH
SO	1	1/27/12 10:07 AM	0.0419	0.0065	0.260	0.0748	0.018	0.0045	0.16	0.09	341.3	8.05
SO	2	1/27/12 10:47 AM	0.0188	0.0380	0.0979	0.0867	0.091	0.006	0.66	0.46	55.4	8.58
SO	Grab		0.0134	0.0026	0.110	0.0896	0.011	0.007	1.49	1.19	79.2	9.37

SITE	Sample #	Time	Lead Ppm	Diss. Lead ppm	Zinc ppm	Diss. Zinc ppm	Copper ppm	Diss Cu ppm	TP mg/L	DP mg/L	TSS mg/L	pH
WBI	Batch		5.116	1.638	0.0879	0.147	0.84	0.432	0.10	0.03	13.6	6.06

SITE	Sample #	Time	Lead ppm	Diss. Lead ppm	Zinc ppm	Diss. Zinc ppm	Copper ppm	Diss Cu ppm	TP mg/L	DP mg/L	TSS mg/L	pH
WBO	Batch		0.1753	0.0259	0.0860	0.0823	0.0437	0.0232				7.93

swale in		
sample #	time	flow(L)
3	1/27/12 10:37 AM	5842
5	1/27/12 12:37 PM	0
6	1/27/12 1:57 PM	0
Grab		0
		5842
		TOTAL FLOW (L)

swale out		
sample #	Time	flow(L)
1	1/27/12 10:07	3796.95
2	1/27/12 10:47	2045.62
Grab		0
		0
		5842.57
		TOTAL FLOW (L)

wood in		
sample #	time	flow(L)
Batch		244.23
		244.23
		TOTAL FLOW (L)

wood out		
sample #	time	flow(L)
Batch		0.027
	0	0.03
		TOTAL FLOW (L)

February 16, 2012

SITE	Sample #	Time	Lead ppm	Diss. Lead Ppm	Zinc ppm	Diss. Zinc ppm	Copper ppm	Diss Cu ppm	TP mg/L	DP mg/L	TSS mg/L	pH
SI	7	6:43 PM	0.01	0.0439	0.0393	0.0365	0.0034	0.0022	0.08	0.03	16.6	7.90
SI	8	7:43 PM	0.013	0.0221	0.0368	0.0616	0.0021	0.0023	0.05	0.02	12.1	7.87
SI	9	8:43 PM	0.007	0.0081	0.0159	0.0355	0.0010	0.0014	0.04	0.04	4.9	7.66
SI	10	9:43 PM	0.009	0.0034	0.0400	0.0509	0.0020	0.0021	0.04	0.02	3.4	7.67
SI	11	10:43 PM	0.011	0.0356	0.0314	0.0970	0.00094	0.0016	0.04	0.02	5.6	7.64
SI	12	11:43 PM	0.006	0.0236	0.0242	0.0776	0.0016	0	0.03	0.02	0.4	7.60
SI	13	1:03 AM	0.011	0.0041	0.0269	0.0259	0.0001	0.0011	0.04	0.02	1.2	7.60
SI	14	2:23 AM	0.003	0.0114	0.0244	0.0563	0.0356	0.0055	0.04	0.02	1.2	7.62
SI	Grab pre		0.024		0.105	0.0234	0.0102		0.23	0.03		
SI	Grab post		0.003		0.0218	0.0353	0.0028		0.05	0.03		8.56

SITE	Sample #	Time	Lead ppm	Diss. Lead ppm	Zinc ppm	Diss. Zinc ppm	Copper ppm	Diss Cu ppm	TP mg/L	DP mg/L	TSS mg/L	pH
SO	Grab pre		.0168	0	0.0478	0.233	73.9	0	1.02	0.77	0	
SO	Grab post		.0106	0	0.0218	0.0351	6.04	0	1.15	0.71	0	9.78

SITE	Sample #	Time	Lead ppm	Diss. Lead ppm	Zinc ppm	Diss. Zinc ppm	Copper ppm	Diss Cu ppm	TP mg/L	DP mg/L	TSS mg/L	pH
WBI	Batch		6.99	1.76	0.0878	0.0543	1.826	0.667	0.09	0.01	0	5.87

SITE	Sample #	Time	Lead ppm	Diss. Lead ppm	Zinc ppm	Diss. Zinc ppm	Copper ppm	Diss Cu Ppm	TP mg/L	DP mg/L	TSS mg/L	pH
WBO	Batch		0.202	0.0251	0.0488	0.0383	0.0284	0.0092	0.67	0.63	9.6	7.87

swale in			swale out		
sample #	time	flow(L)	sample #	time	flow(L)
7	2/16/12 18:43	712.25	No sample		712.25
8	2/16/12 19:43	0			0
9	2/16/12 20:43	0			0
10	2/16/12 21:43	0			0
11	2/16/12 22:43	0			0
12	2/16/12 23:43	0			0
13	2/17/12 1:03	0			0
14	2/17/12 2:23	0			0
Grab pre		0			0
Grab post		0			0
		712.25			712.25
		TOTAL FLOW (L)			TOTAL FLOW (L)

wood in			wood out		
sample #	time	flow(L)	sample #	time	flow(L)
Batch		73.27	Batch		27.01
		73.27	0		27.01
		TOTAL FLOW (L)			TOTAL FLOW (L)

February 29, 2012

SITE	Sample #	Lead ppm	Diss. Lead Ppm	Zinc ppm	Diss. Zinc ppm	Copper ppm	Diss Cu ppm	TP mg/L	TSS mg/L	pH
SI	batch	0.018	0.0061	0.0257	0.0189	0.00187	0.0061	0.10	39.4	7.61

SITE	Sample #	Lead ppm	Diss. Lead Ppm	Zinc ppm	Diss. Zinc ppm	Copper ppm	Diss Cu ppm	TP mg/L	TSS mg/L	pH
SO	batch	0.032	0.0109	0.0411	0.0518	0.0024	0.0005	0.15	38.2	7.73

SITE	Sample #	Lead Ppm	Diss. Lead Ppm	Zinc ppm	Diss. Zinc ppm	Copper ppm	Diss Cu ppm	TP mg/L	TSS mg/L	pH
WBI	1	11.4	2.93	0.114	0.108	3.94	2.29	0.19	26.2	6.03
WBI	2	7.16	1.96	0.0689	0.0719	2.51	1.44	0.19	26.2	6.03
WBI	3	5.27	1.99	0.0420	0.0320	1.63	1.44	0.19	26.2	6.03
WBI	4	3.39	1.75	0.0352	0.0256	0.739	0.596	0.08	5.8	6.03
WBI	5	1.70	1.60	0.0287	0.0248	0.468	0.455	0.02	1.9	6.08
WBI	6	1.36	1.36	0.0205	0.0120	0.333	0.314	0.01	3.4	6.10
WBI	7	1.43	1.39	0.0237	0.0148	0.302	0.295	0.01	23.4	6.11
WBI	15	2.39	1.30	0.0266	0.0376	0.602	0.452	0.08	17	6.10
WBI	16	2.73	1.96	0	0.0273	0.839	0.744	0.06	17	6.20



SITE	Sample #	Time	Lead ppm	Diss. Lead ppm	Zinc ppm	Diss. Zinc ppm	Copper Ppm	Diss Cu ppm	TP mg/L	TSS mg/L	pH
WBO	3	10:39 AM	0.122	0.0316	0.0407	0.0329	0.0391	0.0086	0.93	2.2	7.83
WBO	4	11:19 AM	0.028	0.0157	0.0275	0.03	0.0107	0.0074	0.97	3.3	7.74
WBO	5	11:59 AM	0.076	0.0102	0.0311	0.0272	0.0087	0.0059	1.03	0.5	7.67
WBO	6	12:39 PM	0.023	0.0115	0.0279	0.0286	0.0068	0.0053	1.00	0.5	7.64
WBO	7	1:19 PM	0.017	0.0079	0.0337	0.0261	0.0056	0.0055	1.04	1.15	7.65
WBO	8	1:59 PM	0.017	0.0070	0.0296	0.0298	0.0054	0.0043	1.10	1.8	7.65
WBO	11	4:19 PM	0.025	0.0087	0.0256	0.0334	0.0078	0.0055	1.16	0.5	7.64
WBO	15	8:19 PM	0.024	0.0103	0.0340	0.0506	0.0069	0.0066	1.09	0.5	7.68
WBO	16	9:19 PM	0.017	0.0125	0.0293	0.0339	0.0056	0.0054	1.09	0.5	7.68
WBO	17	10:19 PM	0.016	0.0098	0.0463	0.0271	0.0062	0.0054	1.09	0.5	7.68
WBO	18	11:39 PM	0.019	0.0072	0.0632	0.0203	0.0046	0.0054	1.09	0.5	7.68
WBO	19	12:59 AM	0.016	0.0090	0.0490	0.0479	0.0060	0.0074	1.09	0.5	7.68

swale in		
sample #	time	flow(L)
Batch		37188
		37188
		TOTAL FLOW (L)

swale out		
sample #	time	flow(L)
batch		37188.11
		37188.11
		TOTAL FLOW (L)

wood in		
sample #	time	flow(L)
1	2/29/12 9:35	16.28
2	2/29/12 9:55	24.42
3	2/29/12 10:15	81.41
4	2/29/12 10:55	162.82
5	2/29/12 11:35	179.10
6	2/29/12 12:15	187.24
7	2/29/12 12:55	146.53
15	2/29/12 19:55	105.83
16	2/29/12 20:55	219.81
		0
		0
		0
		0
		0
		1123.47
		TOTAL FLOW (L)

wood out		
sample #	time	flow(L)
3	2/29/2012 10:39	6.31
4	2/29/2012 11:19	50.37
5	2/29/2012 11:59	81.72
6	2/29/2012 12:39	76.78
7	2/29/2012 13:19	39.06
8	2/29/2012 13:59	5.36
11	2/29/2012 16:19	4.55
15	2/29/2012 20:19	9.55
16	2/29/2012 21:19	10.39
17	2/29/2012 22:19	15.46
18	2/29/2012 23:39	6.06
19	3/1/2012 0:59	4.26
		0
		0
		309.89
		TOTAL FLOW (L)

March 2, 2012

SITE	Sample #	Time	Lead ppm	Diss. Lead ppm	Zinc ppm	Diss. Zinc ppm	Copper ppm	Diss Cu ppm	TP mg/L	DP mg/L	TSS mg/L	pH
SI	batch		0.0401	0.0048	0.108	0.121	0.0156	0.114	0.24	0.03	110.4	7.75

SITE	Sample #	Time	Lead Ppm	Diss. Lead Ppm	Zinc Ppm	Diss. Zinc Ppm	Copper Ppm	Diss Cu Ppm	TP mg/L	DP mg/L	TSS mg/L	pH
SO	batch		0.0147	0.0055	0.064	0.0813	0.0085	0.0111	0.26	0.03	95.69	7.62

swale in		
sample #	time	flow(L)
batch		23326
		23326
		<b>TOTAL FLOW (L)</b>

swale out		
sample #	time	flow(L)
batch		23326.49
		23326.49
		<b>TOTAL FLOW (L)</b>

April 18, 2012

SITE	Sample #	Time	Lead ppm	Diss. Lead ppm	Zinc ppm	Diss. Zinc ppm	Copper ppm	Diss Cu Ppm	TP mg/L	TSS mg/L	pH
WBI	1	4/18/12 1:59 PM	16.28	1.28	0.182	0.135	5.21	1.93	1.07	911.87	5.36
WBI	2	4/18/12 2:29 PM	10.27	1.57	0.175	0.140	3.92	1.99	0.48	640.07	5.28
WBI	3	4/18/12 2:59 PM	7.022	2.10	0.109	0.113	2.72	1.69	0.35	368.28	5.39
WBI	4	4/18/12 3:29 PM	6.824	2.03	0.127	0.089	2.71	1.66	0.18	258.46	5.19
WBI	5	4/18/12 3:59 PM	4.974	1.75	0.105	0.180	2.00	1.35	0.21	148.64	5.49
WBI	6	4/18/12 4:29 PM	5.16	1.75	0.108	0.180	2.15	1.35	0.05	148.64	5.12

wood in		
sample #	time	flow(L)
1	4/18/2012 13:59	32.56
2	4/18/2012 14:29	8.14
3	4/18/2012 14:59	24.42
4	4/18/2012 15:29	0
5	4/18/2012 15:59	0
6	4/18/2012 16:29	32.56
		97.69
		<b>TOTAL FLOW (L)</b>

wood out		
sample #	Time	flow(L)
		0
		0
		0
		0
		0
		0
	0	0.00
		<b>TOTAL FLOW (L)</b>

April 21, 2012

SITE	Sample #	Time	Lead ppm	Diss. Lead ppm	Zinc ppm	Diss. Zinc ppm	Copper ppm	Diss Cu ppm	TP mg/L	DP mg/L	TSS mg/L	pH
WBI	1	7:45 PM	11.65	3.55	0.078	0.055	3.39	1.83	0.75	0.05	211.4	5.65
WBI	2	8:15 PM	6.28	3.21	0.073	0.073	2.14	1.59	0.38	0.02	118.55	5.77
WBI	3	8:45 PM	4.306	2.62	0.065	0.062	1.82	1.43	0.21	0.01	25.7	5.74

wood in		
sample #	time	flow(L)
1	4/21/2012 19:45	40.71
2	4/21/2012 20:15	24.42
3	4/21/2012 20:45	16.28
		81.41
		TOTAL FLOW (L)

wood out		
sample #	time	flow(L)
		0
		0
		0
0		0.00
		TOTAL FLOW (L)

April 22, 2012

SITE	Sample #	Time	Lead ppm	Diss. Lead ppm	Zinc Ppm	Diss. Zinc ppm	Copper ppm	Diss Cu ppm	TP mg/L	DP mg/L	TSS mg/L	pH
WBI	19	11:05 AM	3.98	2.19	0.0592	0.0489	2.3	1.701	0.15	0.01	16.3	5.81
WBI	20	11:55 AM	2.74	1.81	0.0296	0.0324	1.605	1.335	0.06	0.01	16.3	5.92
WBI	21	2:25 PM	2.66	1.43	0.0246	0.0428	1.012	0.760	0.08	0.01	31.8	6.06
WBI	22	4:55 PM	2.32	1.37	0.0269	0.0222	0.825	0.638	0.04	0.04	26.6	6.03
WBI	23	7:25 PM	4.58	1.44	0.0264	0.1511	2.288	0.719	0.06	0.00	38.4	6.10
WBI	24	7:55 PM	3.70	1.37	0.0242	0.0649	1.848	0.771	0.03	0.01	13.8	6.07

wood in		
sample #	Time	flow(L)
19	4/22/2012 11:05	65.12
20	4/22/2012 11:55	113.97
21	4/22/2012 14:25	244.23
22	4/22/2012 16:55	203.52
23	4/22/2012 19:25	113.97
24	4/22/2012 19:55	293.07
		1033.91
		TOTAL FLOW (L)

April 25, 2012

SITE	Sample #	Lead ppm	Diss. Lead ppm	Zinc ppm	Diss. Zinc Ppm	Copper ppm	Diss Cu ppm	TP mg/L	DP mg/L	TSS mg/L	pH
WBI	batch	5.29	2.59	0.037	0.069	2.97	2.29	0.21	0.05	67.9	5.52

wood in		
sample #	time	flow(L)
batch		40.71
		40.71
		TOTAL FLOW (L)

wood out		
sample #	time	flow(L)
		0
0		0.00
		TOTAL FLOW (L)

May 22, 2012

SITE	Sample #	Time	Lead ppm	Diss. Lead ppm	Zinc ppm	Diss. Zinc ppm	Copper ppm	Diss Cu ppm	TP mg/L	DP mg/L	TSS mg/L	pH
SI	5	7:27 AM	0.0024	0.0044	0.0301	0.0320	0.0015	0.0024	0.01	0.01	15.82	7.40
SITE	Sample #	Time	Lead ppm	Diss. Lead ppm	Zinc ppm	Diss. Zinc ppm	Copper ppm	Diss Cu ppm	TP mg/L	DP mg/L	TSS mg/L	pH
SO	1	6:13 AM	0.0014	0.006	0.037	0.043	0.0038	0.0037	0.80	0.60	11.68	7.76
SO	2	6:33 AM	0.0076	0.0058	0.0305	0.0121	0.0038	0.0011	0.53	0.46	11.68	7.95
SO	3	6:53 AM	0.0042	0.0129	0.0314	0.01219	0.0032	0.0057	0.65	0.58	9.17	7.98
SO	4	6:55 AM	0.013	0.020	0.0194	0.0122	0.0036	0.0103	0.76	0.71	6.67	8.00
SO	5	7:15 AM	0.0012	0.0031	0.0107	0.0227	0	0.0035	0.61	0.46	6.67	8.00
SO	6	7:19 AM	0.0012	0.0031	0.0107	0.0227	0	0.0035	0.61	0.46	6.67	8.00
SITE	Sample #	Lead ppm	Diss. Lead ppm	Zinc Ppm	Diss. Zinc ppm	Copper ppm	Diss Cu ppm	TP mg/L	DP mg/L	TSS mg/L	pH	
WBI	Batch	3.42	2.03	0.047	0.069	2.12	1.62	0.53	0.21	49.82	6.28	

swale in		
sample #	Time	flow(L)
5	5/22/12 7:27	655.53
		0
		0
		0
		0
		0
		TOTAL FLOW (L)

swale out		
sample #	time	flow(L)
1	5/22/12 6:13	93.75
2	5/22/12 6:33	127.15
3	5/22/12 6:53	75.18
4	5/22/12 6:55	60.15
5	5/22/12 7:15	64.41
6	5/22/12 7:19	234.86
		TOTAL FLOW (L)

wood in		
sample #	time	flow(L)
Batch		24.42
		24.42
		TOTAL FLOW (L)

wood out		
sample #	time	flow(L)
		0
0		0.00
		TOTAL FLOW (L)

May 27, 2012

SITE	Sample #	Lead ppm	Diss. Lead ppm	Zinc ppm	Diss. Zinc ppm	Copper ppm	Diss Cu ppm	TP mg/L	DP mg/L	TSS mg/L	pH
WBI	Batch	4.77	3.61	0.067	0.194	1.66	1.34	0.13	0.06	25.8	6.25

wood in		
sample #	Time	flow(L)
batch		154.68
		154.68
		TOTAL FLOW (L)

wood out		
sample #	time	flow(L)
		0
0		0.00
		TOTAL FLOW (L)

May 29, 2012

SITE	Sample #	Time	Lead ppm	Diss. Lead Ppm	Zinc ppm	Diss. Zinc ppm	Copper ppm	Diss Cu ppm	TP mg/L	DP mg/L	TSS mg/L	pH
SI	1	9:13 PM	0.021	0.0085	0.0378	0.0381	0.0025	0.0052	0.15	0.04	42.1	7.48
SI	2	9:33 PM	0.002	0.0032	0.0464	0.0728	0.0025	0.0025	0.11	0.08	13	7.31
SI	3	9:53 PM	0.007	0.0021	0.0402	0.0586	0.0025	0.0025	0.09	0.08	13.2	7.26
SI	4	10:13 PM	0.02	0.001	0.0359	0.0495	0.0058	0.0025	1.11	0.09	9.1	7.16
SI	5	10:33 PM	0.004	0.0021	0.0413	0.0494	0.0025	0.0025	0.11	0.06	8.7	7.28
SI	6	10:53 PM	0.004	0.0023	0.0345	0.1799	0.0025	0.0025	0.10	0.05	7.2	7.18
SI	7	11:13 PM	0.006	0.0038	0.0371	0.142	0.0025	0.0025	0.10	0.08	10.4	7.39
SI	8	11:53 PM	0.002	0.0030	0.0320	0.18	0.0025	0.0025	0.11	0.07	3.1	7.15
SI	9	12:33 AM	0.007	0.0038	0.0300	0.319	0.0025	0.0051	0.09	0.06	5.5	7.16
SI	10	1:13 AM	0.003	0.001	0.0304	0.163	0.0025		0.10	0.06	7.1	7.18

SITE	Sample #	Time	Lead ppm	Diss. Lead Ppm	Zinc ppm	Diss. Zinc ppm	Copper ppm	Diss Cu ppm	TP mg/L	DP mg/L	TSS mg/L	pH
SO	2	9:11 PM	0.005	0.001	0.0422	0.216	0.0025	0.0025	0.44	0.24	21.6	7.23
SO	3	9:31 PM	0.001	0.0059	0.0302	0.0752	0.0025	0.0068	1.89	1.91	4	8.00
SO	4	9:51 PM	0.001	0.0036	0.033	0.364	0.0025	0.0025	2.49	2.41	5.4	7.81
SO	5	10:11 PM	0.001	0.0035	0.0367	0.403	0.0025	0.0025	2.67	2.38	4.3	7.85
SO	6	10:31 PM	0.001	0.001	0.0309	0.094	0.0025	0.0025	2.68	2.69	6.2	8.02

SITE	Sample #	Lead Ppm	Diss. Lead Ppm	Zinc ppm	Diss. Zn ppm	Copper ppm	Diss Cu ppm	TP mg/L	DP mg/L	TSS mg/L	pH
WBI	batch	5.39	4.24	0.050	0.042	1.54	1.31	0.08	0.05	4.3	5.78
swale in sample #		swale out									
	time	flow(L)		sample #	time	flow(L)					
	5/29/2012				5/29/2012						
1	21:13	7388.3		2	21:11	3449					
	5/29/2012				5/29/2012						
2	21:33	492.6		3	21:31	617					
	5/29/2012				5/29/2012						
3	21:53	985.3		4	21:51	567					
	5/29/2012				5/29/2012						
4	22:13	0		5	22:11	538					
	5/29/2012				5/29/2012						
5	22:33	0		6	22:31	5172					
	5/29/2012										
6	22:53	0					0				
	5/29/2012										
7	23:13	492.6					0				
	5/29/2012										
8	23:53	0					0				
	5/30/2012										
9	0:33	492.6					0				
	5/30/2012										
10	1:13	492.6					0				
		10345 TOTAL FLOW (L)				10345 TOTAL FLOW (L)					
wood in sample #		wood out									
	time	flow(L)		sample #	time	flow(L)					
	batch	170.962176				0					
		170.96 TOTAL FLOW (L)				0 TOTAL FLOW (L)					

June 12, 2012

SITE	Sample #	Time	Lead Ppm	Diss. Lead Ppm	Zinc Ppm	Diss. Zinc Ppm	Copper ppm	Diss Cu Ppm	TP mg/L	TSS mg/L	pH
SI	1	5:06 AM	0.009	0.0022	0.069	0.070	0.011	0.010	0.18	17.2	7.22
SI	2	5:25 AM	0.003	0.001	0.081	0.063	0.011	0.011	0.16	14.3	7.75
SI	3	5:45 AM	0.004	0.001	0.078	0.055	0.010	0.010	0.15	10	6.99
SI	4	6:05 AM	0.002	0.001	0.084	0.064	0.010	0.012	0.15	10.3	6.93
SI	5	6:25 AM	0.002	0.001	0.098	0.056	0.011	0.011	0.17	5.1	6.95
SI	10	9:05 AM	0.004	0.001	0.067	0.061	0.009	0.011	0.14	4.6	7.11
SI	16	2:15 PM	0.003	0.0023	0.11	0.055	0.011	0.009	0.09	1.8	7.18

SI	17	2:55 PM	0.003	0.001	0.12	0.058	0.007	0.008	0.09	5.3	7.20
SI	20	4:55 PM	0.003	0.001	0.081	0.054	0.008	0.008	0.08	0.9	7.41
SI	21	5:05 PM	0.001	0.0024	0.078	0.053	0.007	0.01	0.08	2.1	7.43

SITE	Sample #	Time	Lead ppm	Diss. Lead Ppm	Zinc Ppm	Diss. Zinc Ppm	Copper Ppm	Diss Cu Ppm	TP mg/L	TSS mg/L	pH
SO	1	5:06 AM	0.003	0.0021	0.137	0.072	0.016	0.013	1.49	30.2	7.88
SO	2	5:25 AM	0.005	0.001	0.080	0.074	0.014	0.010	2.30	5.9	8.04
SO	3	5:45 AM	0.001	0.001	0.076	0.066	0.010	0.011	2.09	16.7	7.79
SO	4	6:05 AM	0.003	0.001	0.064	0.068	0.011	0.008	2.27	5.3	7.97
SO	5	6:25 AM	0.007	0.001	0.072	0.065	0.013	0.007	2.42	5.5	8.32
SO	10	8:17 AM	0.001	0.001	0.061	0.061	0.010	0.006	2.29	5.6	7.80
SO	11	8:37 AM	0.005	0.001	0.061	0.068	0.012	0.006	2.29	5	7.90
SO	15	10:13 AM	0.005	0.001	0.023	0.067	0.011	0.006	2.33	2.1	7.95
SO	21	12:51 PM	0.006	0.001	0.10	0.067	0.011	0.005	2.12	4.2	7.96

SITE	Sample #	Time	Lead ppm	Diss. Lead Ppm	Zinc Ppm	Diss. Zinc ppm	Copper Ppm	Diss Cu Ppm	TP mg/L	TSS mg/L	pH
WBI	batch		6.70	4.65	0.081	0.0869	1.81	1.45	0.82	37.7	5.94

swale in		
sample #	time	flow(L)
1	6/12/2012 5:06	5087.15
2	6/12/2012 5:25	636
3	6/12/2012 5:45	0
4	6/12/2012 6:05	0
5	6/12/2012 6:25	0
10	6/12/2012 9:05	636
16	6/12/2012 14:15	4452.05
17	6/12/2012 14:55	1907.8
20	6/12/2012 16:55	0
21	6/12/2012 17:05	636
		13356
		TOTAL FLOW (L)

swale out		
sample #	Time	flow(L)
1	6/12/2012 5:06	902.25
2	6/12/2012 5:25	678.02
3	6/12/2012 5:45	717.02
4	6/12/2012 6:05	612.65
5	6/12/2012 6:25	1015.30
10	6/12/2012 8:17	560.12
11	6/12/2012 8:37	475.08
15	6/12/2012 10:13	696.91
21	6/12/2012 12:51	7698.78
		0
		13356.19
		TOTAL FLOW (L)

wood in		
sample #	time	flow(L)
Batch		170.96
		170.96
		TOTAL FLOW (L)

wood out		
sample #	time	flow(L)
		0
0		0.00
		TOTAL FLOW (L)

### June 22, 2012

SITE	Sample #	Time	Lead Ppm	Diss. Lead ppm	Zinc Ppm	Diss. Zinc ppm	Copper ppm	Diss Cu ppm	TP mg/L	DP mg/L	TSS mg/L	pH
WBI	1	8:13 PM	10.69	6.59	0.147	0.093	2.945	1.769	0.36	0.02	248.7	6.36
WBI	2	8:33 PM	9.87	2.88	0.097	0.060	2.078	0.608	0.18	0.02	84.3	6.26
WBI	3	2:53 AM	5.36	3.15	0.069	0.072	0.974	0.665	0.13	0.01	11.5	6.04
WBI	4	3:13 AM	4.2	3.56	0.025	0.098	0.606	0.584	0.05	0.02		6.05

SITE	Sample #	Time	Lead Ppm	Diss. Lead ppm	Zinc Ppm	Diss. Zinc ppm	Copper ppm	Diss Cu ppm	TP mg/L	DP mg/L	TSS mg/L	pH
WBO	5	6/23/12 3:08 AM	0.034	0.029	0.003	0.190	0.010	0.015	1.54	1.35	10.2	7.43
WBO	6	6/23/12 3:28 AM	0.023	0.017	0.019	0.023	0.014	0.0172	1.67	1.54	3.4	7.45
WBO	7	6/23/12 3:48 AM	0.018	0.011	0.021	0.075	0.011	0.0108	1.67	1.54	3.40	7.73

wood in		
sample #	time	flow(L)
1	6/22/2012 20:13	16.28
2	6/22/2012 20:33	65.12
3	6/23/2012 2:53	187.24
4	6/23/2012 3:13	65.12
		333.78
		TOTAL FLOW (L)

wood out		
sample #	time	flow(L)
5	6/23/2012 3:08	16.86
6	6/23/2012 3:28	5.85
7	6/23/2012 3:48	0.85
		0
		23.58
		TOTAL FLOW (L)



July 9, 2012

SITE	Sample #	Lead ppm	Diss. Lead ppm	Zinc Ppm	Diss. Zinc ppm	Copper ppm	Diss Cu ppm	TP mg/L	DP mg/L	TSS mg/L	pH
SI	Batch	0.01	0.005	0.053	0.037	0.008	0.0004	0.29	0.14	124.26	7.38
SO	batch	0.003	0.009	0.034	0.154	0.008	0.007	2.13	2.13	18.9	7.43

SITE	Sample #	Time	Lead ppm	Diss. Lead Ppm	Zinc Ppm	Diss. Zinc ppm	Copper ppm	Diss Cu ppm	TP mg/L	DP mg/L	TSS mg/L
WBI	1	7/9/12 2:19 AM	20.4	6.68	0.231	0.080	6.33	1.31	0.27	0.12	100.84
WBI	2	7/9/12 2:34 AM	10.6	7.25	0.103	0.001	3.40	2.60	0.16	0.03	100.84
WBI	3	7/9/12 2:49 AM	9.72	5.78	0.090	0.090	0.677	2.15	0.56	0.08	161.8
WBI	4	7/9/12 3:04 AM	7.09	4.87	0.058	0.050	2.31	1.70	0.06	0.02	39
WBI	5	7/9/12 3:19 AM	2.35	4.62	0.027	0.045	0.420	1.59	0.08	0.04	44
WBI	6	7/9/12 3:34 AM	6.13	4.53	0.047	0.053	2.16	1.66	0.03	0.05	33.15
WBI	7	7/9/12 3:49 AM	5.93	4.46	0.043	0.044	2.04	1.44	0.11	0.06	33.15
WBI	8	7/9/12 4:04 AM	6.26	3.88	0.061	0.043	2.23	1.56	0.09	0.04	33.15
WBI	9	7/9/12 7:04 AM	7.47	4.84	0.063	0.056	3.16	2.33	0.13	0.02	33.15
WBI	10	7/9/12 8:34 AM	4.56	4.01	0.036	0.056	1.85	1.78	0.07	0.02	22.3
WBI	11	7/9/12 8:49 AM	4.27	2.59	0.029	0.048	1.70	1.04	0.06	0.05	22.3

swale in		
sample #	time	flow(L)
batch		3206
		3206
		TOTAL FLOW (L)

swale out		
sample #	time	flow(L)
batch		3206.96
		3206.97
		TOTAL FLOW (L)

wood in		
sample #	time	flow(L)
1	7/9/2012 2:19	0
2	7/9/2012 2:34	16.28
3	7/9/2012 2:49	8.14
4	7/9/2012 3:04	16.28
5	7/9/2012 3:19	8.14
6	7/9/2012 3:34	8.14
7	7/9/2012 3:49	8.14
8	7/9/2012 4:04	8.14
9	7/9/2012 7:04	8.14
10	7/9/2012 8:34	32.56
11	7/9/2012 8:49	24.42
		138.40
		TOTAL FLOW (L)

wood out		
sample #	time	flow(L)
		0
		0
		0
		0
		0
		0
		0
		0
		0
		0
		0
		0
		0
0		0.00
		TOTAL FLOW (L)

### July 14, 2012

SITE	Sample #	Lead Ppm	Diss. Lead ppm	Zinc ppm	Diss. Zinc Ppm	Copper Ppm	Diss Cu ppm	TP mg/L	DP mg/L	TSS mg/L	pH
SI	batch	0.019	0.039	0.036	0.030	0.005	0.009	0.17	0.02	76.2	7.50

SITE	Sample #	Lead ppm	Diss. Lead ppm	Zinc ppm	Diss. Zinc Ppm	Copper ppm	Diss Cu ppm	TP mg/L	DP mg/L	TSS mg/L	pH
SO	Batch	0.008	0.0049	0.14	0.0578	0.005	0.005	1.22	1.10	9.09	7.45

swale in		
sample #	time	flow(L)
Batch		12481.21
		12481.21
		TOTAL FLOW (L)

swale out		
sample #	time	flow(L)
batch		10799.75
		10799.75
		TOTAL FLOW (L)

### July 19, 2012

SITE	Sample #	Lead ppm	Diss. Lead ppm	Zinc Ppm	Diss. Zinc ppm	Copper ppm	Diss Cu ppm	TP mg/L	TSS mg/L	pH
SI	Batch	0.012	0.011	0.059	0.059	0.011	0.009	0.17	103.6	7.52

SITE	Sample #	Lead ppm	Diss. Lead ppm	Zinc Ppm	Diss. Zinc ppm	Copper ppm	Diss Cu Ppm	TP mg/L	TSS mg/L	pH
SO	Batch	0.011	0.007	0.044	0.044	0.025	0.009	1.33	28.8	7.56

SITE	Sample #	Time	Lead Ppm	Diss. Lead ppm	Zinc Ppm	Diss. Zinc ppm	Copper ppm	Diss Cu Ppm	TP mg/L	DP mg/L	TSS mg/L	pH
WBI	1	8:32 PM	8.92	6.46	0.13	0.10	3.10	2.81	0.25	0.10	21.9	5.18
WBI	2	8:47 PM	5.53	5.85	0.070	0.17	1.07	1.17	0.05	0.03	21.9	5.12
WBI	3	9:02 PM	9.97	6.01	0.099	0.311	2.46	1.50	0.14	0.02	38.05	5.22
WBI	4	9:17 PM	7.79	7.84	0.071	0.099	1.65	1.48	0.10	0.01	54.2	5.25
WBI	5	9:32 PM	6.15	7.12	0.059	0.053	0.939	0.991	0.05	0.03	46.3	5.35
WBI	6	10:47 PM	5.18	5.66	0.071	0.068	1.28	1.28	0.06	0.01	38.4	5.24
WBI	7	11:02 PM	1.27	1.98	0.049	0.053	0.287	0.349	0.04	0.02	23.9	5.38
WBI	8	11:17 PM	1.86	1.75	0.046	0.071	0.341	0.299	0.01	0.02	9.4	5.59
WBI	9	11:32 PM	2.42	2.48	0.068	0.050	0.697	0.63	0.06	0.03	15.05	5.54
WBI	10	12:47 AM	2.8	3.45	0.059	0.051	0.784	0.867	0.08	0.02	20.7	5.48
WBI	11	1:02 AM	2.51	2.77	0.067	0.049	0.682	0.683	0.03	0.00	20.05	5.42
WBI	12	1:47 AM	3.15	2.77	0.063	0.049	0.817	0.683	0.03	0.01	19.4	5.35

SITE	Sample #	Time	Lead Ppm	Diss. Lead ppm	Zinc ppm	Diss. Zinc ppm	Copper ppm	Diss Cu ppm	TP mg/L	DP mg/L	TSS mg/L	pH
WBO	2	9:27 PM	0.073	0.068	0.034	0.16	0.032	0.026	1.11	1.00	16.1	7.29
WBO	3	10:49 PM	0.042	0.052	0.017	0.048	0.025	0.020	0.95	0.86	10.85	7.08
WBO	4	10:59 PM	0.031	0.040	0.023	0.050	0.028	0.021	0.75	0.69	5.6	7.25
WBO	5	11:02 PM	0.022	0.026	0.015	0.008	0.028	0.020	1.01	0.94	3.05	7.11
WBO	6	11:06 PM	0.018	0.029	0.033	0.036	0.023	0.021	1.12	1.11	0.5	7.16
WBO	7	11:12 PM	0.019	0.028	0.008	0.114	0.019	0.018	1.12	1.10	0.5	7.12
WBO	8	11:18 PM	0.017	0.29	0.01	0.037	0.019	0.049	1.05	0.98	0.5	7.16
WBO	9	11:26 PM	0.022	0.018	0.006	0.014	0.013	0.017	1.01	1.01	1.5	7.16
WBO	10	12:44 AM	0	0.041	0.005	0.014	0.016	0.019	0.98	0.89	2.5	7.02
WBO	11	1:52 AM	0	0.069	0.020	0.068	0.019	0.033	0.90	8.29	2.5	7.23

swale in		
sample #	time	flow(L)
batch		31795
		31795
		TOTAL FLOW (L)

swale out		
sample #	time	flow(L)
batch		31795.
		31795.95
		TOTAL FLOW (L)

wood in		
sample #	Time	flow(L)
1	7/19/2012 20:32	8.14
2	7/19/2012 20:47	81.41
3	7/19/2012 21:02	24.42
4	7/19/2012 21:17	89.55
5	7/19/2012 21:32	16.28
6	7/19/2012 22:47	162.82
7	7/19/2012 23:02	203.52
8	7/19/2012 23:17	16.28
9	7/19/2012 23:32	16.28
10	7/20/2012 0:47	73.26
11	7/20/2012 1:02	16.28
12	7/20/2012 1:47	105.83
		0
		0
		814.11
		TOTAL FLOW (L)

wood out		
sample #	time	flow(L)
2	7/19/2012 21:27	17.92
3	7/19/2012 22:49	3.59
4	7/19/2012 22:59	14.11
5	7/19/2012 23:02	10.50
6	7/19/2012 23:06	7.41
7	7/19/2012 23:12	11.73
8	7/19/2012 23:18	8.44
9	7/19/2012 23:26	15.53
10	7/20/2012 0:44	5.53
11	7/20/2012 1:52	10.55
		0
		0
		0
		0
		105.37
		TOTAL FLOW (L)

## July 22, 2012

SITE	Sample #	Time	Lead ppm	Diss. Lead ppm	Zinc ppm	Diss. Zinc Ppm	Copper ppm	Diss Cu ppm	TP mg/L	DP mg/L	TSS mg/L	pH
SI	batch		0.009	0.008	0.0920	0.25	0.0169	0.001	0.05	0.02	30.7	7.61

SITE	Sample #	Time	Lead ppm	Diss. Lead ppm	Zinc ppm	Diss. Zinc Ppm	Copper ppm	Diss Cu ppm	TP mg/L	DP mg/L	TSS mg/L	pH
SO	batch		0.006	0.005	0.049	0.015	0.007	0.001	0.98	0.98	3.5	7.77

SITE	Sample #	Time	Lead Ppm	Diss. Lead ppm	Zinc ppm	Diss. Zinc Ppm	Copper Ppm	Diss Cu ppm	TP mg/L	DP mg/L	TSS mg/L	pH
WBI	1	6:34 AM	2.01	1.48	0.700	0.476	0.700	0.499	0.02	0.00	7.3	5.91
WBI	2	9:04 AM	1.53	0.486	0.510	0.0463	0.510	0.421	0.01	0.00	5.3	5.84
WBI	3	9:52 AM	1.03	0.599	0.325	0.295	0.325	0.334	0.01	0.00	6.4	6.03

SITE	Sample #	Time	Lead ppm	Diss. Lead ppm	Zinc ppm	Diss. Zinc ppm	Copper ppm	Diss Cu Ppm	TP mg/L	DP mg/L	TSS mg/L	pH
WBO	1	9:18 AM	0.02	0.013	0.0184	0.163	0.0078	0.0073	0.67	0.63	0.5	7.23
WBO	2	9:44 AM	0.013	0.007	0.0150	0.364	0.0060	0.006	0.80	0.80	0.5	7.33

swale in				swale out			
sample #	time	flow(L)		sample #	Time	flow(L)	
Batch		34537		batch		34537	
		34537				34537	
		TOTAL FLOW (L)				TOTAL FLOW (L)	

wood in				wood out			
sample #	time	flow(L)		sample #	Time	flow(L)	
1	7/21/2012 6:34	284.93		1	7/21/2012 9:18	73.83	
2	7/21/2012 9:04	431.47		2	7/21/2012 9:44	54.88	
3	7/21/2012 9:52	398.91				0	
		1115.32		0		128.73	
		TOTAL FLOW (L)				TOTAL FLOW (L)	

September 17, 2012

SITE	Sample #	Time	Lead ppm	Diss. Lead ppm	Zinc ppm	Diss. Zinc ppm	Copper ppm	Diss Cu Ppm	TP mg/L	DP mg/L	TSS mg/L	pH
SI	batch		0.02	0.004	0.286	0.059	0.0135	0.004	0.23	0.07	55.10	

SITE	Sample #	Time	Lead ppm	Diss. Lead ppm	Zinc ppm	Diss. Zinc ppm	Copper ppm	Diss Cu Ppm	TP mg/L	DP mg/L	TSS mg/L	pH
SO	batch		0.005	0.003	0.161	0.034	0.0122	0.002	0.69	0.67	5.95	

SITE	Sample #	Time	Lead ppm	Diss. Lead ppm	Zinc Ppm	Diss. Zinc ppm	Copper ppm	Diss Cu Ppm	TP mg/L	DP mg/L	TSS mg/L	pH
WBI	1	3:52 PM	3.90	2.13	0.116	0.046	0.741	0.393	0.16	0.09	23.59	4.15
WBI	2	4:12 PM	2.65	1.49	0.122	0.048	0.265	0.243	0.04	0.07	0.5	5.36
WBI	3	4:32 PM	2.06	1.60	0.122	0.044	0.432	0.395	0.17	0.03	0.5	5.45

SITE	Sample #	Time	Lead ppm	Diss. Lead ppm	Zinc ppm	Diss. Zinc ppm	Copper ppm	Diss Cu ppm	TP mg/L	DP mg/L	TSS mg/L	pH
WBO	1	1:04 AM	0.184	0.144	0.050	0.033	0.110	0.083	1.29	1.16	3.82	6.97
WBO	2	1:23 AM	0.154	0.135	0.127	0.068	0.082	0.072	0.99	1.06	1.95	7.08
WBO	3	1:43 AM	0.133	0.124	0.042	0.030	0.066	0.059	1.00	0.97	1.22	7.13
WBO	4	2:03 AM	0.181	0.150	0.060	0.027	0.106	0.074	1.01	1.03	1.22	7.20
WBO	5	12:23 PM	0.098	0.078	0.263	0.051	0.057	0.048	0.92	0.89	1.22	7.20
WBO	6	12:43 PM	0.25	0.149	0.050	0.067	0.123	0.096	0.97	0.86	1.22	7.20
WBO	7	3:43 PM	0.173	0.115	0.048	0.040	0.089	0.067	0.96	0.89	0.5	7.27
WBO	8	4:03 PM	0.122	0.067	0.137	0.024	0.006	0.039	0.93	0.88	13.71	6.86
WBO	9	4:23 PM	0.082	0.051	0.032	0.051	0.030	0.026	0.90	0.88	2.17	6.94
WBO	10	4:43 PM	0.077	0.038	0.135	0.118	0.035	0.028	1.17	0.85	0.5	6.87
WBO	11	5:03 PM	0.086	0.051	0.138	0.024	0.035	0.028	0.87	0.80	0.5	6.87

swale in		
sample #	Time	flow(L)
batch		102649
		102649
		TOTAL FLOW (L)

swale out		
sample #	time	flow(L)
batch		102649
		102649
		TOTAL FLOW (L)

wood in		
sample #	Time	flow(L)
1	9/18/2012 15:52	464.04
2	9/18/2012 16:12	105.83
3	9/18/2012 16:32	65.12
		0
		0
		0
		0
		0
		0
		0
		0
		0
		635.00
		TOTAL FLOW (L)

wood out		
sample #	Time	flow(L)
1	9/18/2012 1:04	0.43
2	9/18/2012 1:23	9.17
3	9/18/2012 1:43	3.72
4	9/18/2012 2:03	0.56
5	9/18/2012 12:23	0
6	9/18/2012 12:43	0
7	9/18/2012 15:43	7.97
8	9/18/2012 16:03	23.44
9	9/18/2012 16:23	34.99
10	9/18/2012 16:43	19.39
11	9/18/2012 17:03	9.45
		0
		109.16
		TOTAL FLOW (L)

September 27, 2012

SITE	Sample #	Lead ppm	Diss. Lead ppm	Zinc ppm	Diss. Zinc ppm	Copper ppm	Diss Cu ppm	TP mg/L	DP mg/L	TSS mg/L	pH
SI	batch	0.007	0.0031	0.6171	0.053	0.008	0.003	0.17	0.10	27.53	7.68

SITE	Sample #	Lead ppm	Diss. Lead Ppm	Zinc ppm	Diss. Zinc Ppm	Copper Ppm	Diss Cu Ppm	TP mg/L	DP mg/L	TSS mg/L	pH
SO	Batch	0.007	0.0034	0.598	0.073	0.003	0.003	0.64	0.62	11.14	7.45

swale in		
sample #	time	flow(L)
Batch		17740
		17740
		TOTAL FLOW (L)

swale out		
sample #	Time	flow(L)
batch		17740
		17740
		TOTAL FLOW (L)

October 9, 2012

SITE	Sample #	Lead ppm	Diss. Lead ppm	Zinc ppm	Diss. Zinc ppm	Copper ppm	Diss Cu Ppm	TP mg/L	DP mg/L	TSS mg/L	pH
SI	Batch	0.013	0.006	0.354	0.348	0.014	0.007	0.17	0.07	20	7.26

SITE	Sample #	Lead ppm	Diss. Lead Ppm	Zinc Ppm	Diss. Zinc Ppm	Copper Ppm	Diss Cu Ppm	TP mg/L	DP mg/L	TSS mg/L	pH
SO	batch	0.021	0.0036	1.94	0.091	0.007	0.003	0.46	0.41	5.6	7.73

swale in		
sample #	time	flow(L)
batch		4302
		4302
		TOTAL FLOW (L)

swale out		
sample #	time	flow(L)
batch		4302
		4302
		TOTAL FLOW (L)

October 15, 2012

SITE	Sample #	Time	Lead ppm	Diss. Lead ppm	Zinc ppm	Diss. Zinc ppm	Copper ppm	Diss Cu ppm	TP mg/L	DP mg/L	TSS mg/L	pH
SI	Batch		0.015	0.005	0.118	0.080	0.019	0.005	0.41	0.12	174.6	7.65

SITE	Sample #	Time	Lead ppm	Diss. Lead ppm	Zinc ppm	Diss. Zinc ppm	Copper ppm	Diss Cu ppm	TP mg/L	DP mg/L	TSS mg/L	pH
SO	batch		0.014	0.006	0.185	0.068	0.0071	0.004	0.44	0.36	34.21	7.74

SITE	Sample #	Time	Lead ppm	Diss. Lead ppm	Zinc ppm	Diss. Zinc ppm	Copper ppm	Diss Cu ppm	TP mg/L	DP mg/L	TSS mg/L	pH
WBI	1	3:28 PM	2.45	1.21	0.347	0.042	0.923	0.493	0.09	0.04	16.5	5.84
WBI	2	5:42 PM	1.87	0.72	0.347	0.052	0.521	0.423	0.05	0.03	7.8	6.09

SITE	Sample #	Time	Lead ppm	Diss. Lead ppm	Zinc ppm	Diss. Zinc ppm	Copper ppm	Diss Cu ppm	TP mg/L	DP mg/L	TSS mg/L	pH
WBB	1	3:26 PM	0.062	0.026	0.044	0.038	0.032	0.016	0.87	0.82	4.4	7.88
WBB	2	3:45 PM	0.023	0.023	0.044	0.036	0.017	0.016	0.86	0.84	9.8	7.90
WBB	3	5:45 PM	0.029	0.024	0.049	0.031	0.019	0.014	0.91	0.89	15.2	7.78
WBB	4	6:05 PM	0.018	0.012	0.039	0.031	0.013	0.011	0.85	0.84	2.3	7.94

swale in		
sample #	time	flow(L)
batch		16287
		16287
		TOTAL FLOW (L)

swale out		
sample #	Time	flow(L)
batch		16286
		16286
		TOTAL FLOW (L)

wood in		
sample #	Time	flow(L)
1	10/15/2012 15:28	113.97
2	10/15/2012 17:42	187.24
		0
		0
		301.22
		TOTAL FLOW (L)

biomat out		
sample #	time	flow(L)
1	10/15/2012 15:26	1.43
2	10/15/2012 15:45	2.31
3	10/15/2012 17:45	8.61
4	10/15/2012 18:05	7.01
		0
		19.38
		TOTAL FLOW (L)

October 19, 2012

SITE	Sample #	Lead ppm	Diss. Lead ppm	Zinc ppm	Diss. Zinc ppm	Copper ppm	Diss Cu ppm	TP mg/L	DP mg/L	TSS mg/L	pH
SI	batch	0.013	0.003	0.628	0.036	0.009	0.002	0.14	0.05	72.2	6.87

SITE	Sample #	Lead ppm	Diss. Lead ppm	Zinc ppm	Diss. Zinc ppm	Copper ppm	Diss Cu ppm	TP mg/L	DP mg/L	TSS mg/L	pH
SO	batch	0.007	0.009	0.575	0.024	0.006	0.004	0.57	0.56	29.3	7.44



swale in		
sample #	time	flow(L)
batch		16286
		16286
		TOTAL FLOW (L)

swale out		
sample #	time	flow(L)
batch		16286
		16286
		TOTAL FLOW (L)

SITE	Sample #	Time	Lead ppm	Diss. Lead ppm	Zinc ppm	Diss. Zinc ppm	Copper ppm	Diss Cu ppm	TP mg/L	DP mg/L	pH
WBI	1	5:20 AM	3.01	0.71	0.100	0.138	1.404	0.581	0.05	0.03	7.69
WBI	2	6:04 AM	3.03	0.60	0.090	0.087	1.133	0.470	0.04	0.03	7.47
WBI	3	6:49 AM	1.97	0.92	0.092	0.076	0.632	0.414	0.02	0.01	7.47
WBI	5	8:19 AM	1.49	0.93	0.089	0.114	0.460	0.340	0.01	0.01	7.40
WBI	8	1:34 PM	1.58	0.89	0.103	0.078	0.474	0.255	0.02	0.02	7.35
WBI	11	3:49 PM	1.38	0.94	0.096	0.089	0.366	0.296	0.00	0.01	7.88
WBI	14	6:04 PM	2.13	1.03	0.099	0.085	0.511	0.293	0.03	0.02	7.54
WBI	18	9:04 PM	0.98	0.86	0.094	0.088	0.172	0.150	0.00	0.02	6.45

SITE	Sample #	Time	Lead ppm	Diss. Lead ppm	Zinc ppm	Diss. Zinc Ppm	Copper ppm	Diss Cu ppm	TP mg/L	DP mg/L	pH
WBO	1	11:39 PM	0.111	0.009	0.439	0.057	0.030	0.008	0.98	0.83	8.25
WBO	3	1:38 AM	0.023	0.005	0.417	0.017	0.021	0.007	1.10	0.96	7.81
WBO	4	2:38 AM	0.031	0.004	0.451	0.028	0.029	0.009	0.90	0.75	7.36
WBO	6	4:39 AM	0.055	0.003	0.037	0.037	0.017	0.006	0.76	0.68	7.36
WBO	8	6:38 AM	0.034	0.002	0.032	0.041	0.014	0.005	0.74	0.64	7.62
WBO	9	7:38 AM	0.032	0.004	0.447	0.026	0.019	0.004	0.66	0.57	7.62
WBO	12	10:38 AM	0.032	0.006	0.037	0.017	0.011	0.005	0.48	0.41	7.60
WBO	16	2:38 PM	0.029	0.003	0.045	0.024	0.010	0.002	0.49	0.42	7.76

wood in		
sample #	Time	flow(L)
1	10/29/2012 5:20	407
2	10/29/2012 6:04	146
3	10/29/2012 6:49	187
5	10/29/2012 8:19	67
8	10/29/2012 13:34	757
11	10/29/2012 15:49	439
14	10/29/2012 18:04	651
18	10/29/2012 21:04	1742
		5006
		TOTAL FLOW (L)

wood out		
sample #	time	flow(L)
1	10/28/2012 23:39	1
3	10/29/2012 1:38	2
4	10/29/2012 2:38	1
6	10/29/2012 4:39	28
8	10/29/2012 6:38	101
9	10/29/2012 7:38	203
12	10/29/2012 10:38	384
16	10/29/2012 14:38	1377
		0
		2101
		TOTAL FLOW (L)

### January 16, 2013

SITE	Sample #	Time	Lead ppm	Diss. Lead ppm	Zinc ppm	Diss. Zinc ppm	Copper ppm	Diss Cu ppm	TP mg/L	DP mg/L	TSS mg/L	pH
WO	7	9:06 PM	0.006	0.002	0.044	0.011	0.010	0.008	0.02	0.02	6.2	7.54
WO	8	9:26 PM	0.006	0.002	0.014		0.013	0.007	0.04	0.04	0.5	7.54
WO	9	9:46 PM	0.01	0.007	0.017	0.010	0.014	0.011	0.06	0.06	0.7	7.43
WO	11	10:26 PM	0.01	0.008	0.017	0.007	0.015	0.009	0.10	0.08	0.5	7.48
WO	13	11:06 PM	0.009	0.003	0.015	0.045	0.015	0.007	0.10	0.09	0.5	7.51
WO	16	12:06 AM	0.008	0.010	0.017	0.032	0.011	0.007	0.14	0.10	0.5	7.30
WO	17	12:26 AM	0.01	0.006	0.014	0.020	0.012	0.007	0.13	0.12	0.5	7.48
WO	21	1:46 AM	0.023	0.005	0.012	0.010	0.014	0.005	0.14	0.13	0.5	7.58

SITE	Sample #	Time	Lead ppm	Diss. Lead ppm	Zinc ppm	Diss. Zinc ppm	Copper ppm	Diss Cu ppm	TP mg/L	DP mg/L	TSS mg/L	pH
WBI	3	9:59 PM	2.80	0.77	0.074	0.031	1.078	0.747	0.01	0.00	5.6	6.03
WBI	6	10:39 PM	1.53	1.22	0.051	0.029	0.693	0.631	0.01	0.00	5.6	6.03
WBI	7	10:49 PM	1.48	1.24	0.065	0.053	0.617	0.608	0.01	0.00	0.5	5.83
WBI	8	10:59 PM	1.27	1.22	0.045	0.046	0.614	0.603	0.01	0.00	0.5	5.96
WBI	9	11:09 PM	1.33	1.23	0.051	0.048	0.644	0.655	0.01	0.00	0.5	5.61
WBI	10	11:19 PM	1.08	1.06	0.05	0.044	0.652	0.660	0.01	0.00	1	5.77
WBI	15	12:39 AM	1.42	1.24	0.063	0.097	0.734	0.743	0.01	0.00	1.5	5.92
WBI	21	1:39 AM	1.64	1.24	0.056	0.044	0.802	0.750	0.01	0.00	1.5	5.92

SITE	Sample #	Time	ResinPhos mg/L	Seph Pb	Seph Cu	Seph Zn
WO	7	9:06 PM	0.01	0	0.0064	0.021
WO	8	9:26 PM	0.01	0	0.0065	0.015
WO	9	9:46 PM	0.01	0.01	0.009	0.03
WO	11	10:26 PM	0.02	0	0.0094	0.021
WO	13	11:06 PM	0.01	0	0.007	0.041
WO	16	12:06 AM	0.02	0.01	0.007	0.023
WO	17	12:26 AM	0.02	0.01	0.0062	0.032
WO	21	1:46 AM	0.02	0.01	0.0071	0.021

SITE	Sample #	Time	ResinPhos mg/L	Seph Pb	Seph Cu	Seph Zn
WBI	3	9:59 PM	0			
WBI	6	10:39 PM	0	1.11	0.62	0.118
WBI	7	10:49 PM	0	1.16	0.60	0.076
WBI	8	10:59 PM	0	1.09	0.60	0.096
WBI	9	11:09 PM	0	1.15	0.67	0.071
WBI	10	11:19 PM	0	0.97	0.69	0.072
WBI	15	12:39 AM	0	1.16	0.72	0.064
WBI	21	1:39 AM	0	1.1	0.74	0.053

SITE	Sample #	Time	ResinPhos mg/L	Seph Pb	Seph Cu	Seph Zn
WBO	4	10:20 PM	0.04	0.04	0.009	0.015
WBO	5	10:44 PM	0.04	0.02	0.008	0.025
WBO	6	11:18 PM	0.04	0.01	0.007	0.014
WBO	7	12:04 AM	0.04	0.02	0.007	0.040
WBO	9	1:22 AM	0.04	0.01	0.010	0.010
WBO	10	1:55 AM	0.04	0.02	0.007	0.083
WBO	11	2:36 AM	0.04	0.01	0.006	0.027
WBO	12	3:15 AM	0.04	0.02	0.007	

WTR out		
sample #	Time	flow(L)
7	1/15/2013 21:06	0.431
8	1/15/2013 21:26	0.376
9	1/15/2013 21:46	1.27
11	1/15/2013 22:26	6.26
13	1/15/2013 23:06	6.72
16	1/16/2013 0:06	3.60
17	1/16/2013 0:26	5.87
21	1/16/2013 1:46	28.14
		52.7 TOTAL FLOW (L)

wood in		
sample #	time	flow(L)
3	1/15/2013 21:59	65.1
6	1/15/2013 22:39	32.5
7	1/15/2013 22:49	8.14
8	1/15/2013 22:59	16.2
9	1/15/2013 23:09	8.14
10	1/15/2013 23:19	56.9
15	1/16/2013 0:39	65.1
21	1/16/2013 1:39	341.9
		594.3 TOTAL FLOW (L)

biomat out		
sample #	time	flow(L)
4	1/15/2013 22:20	6.44
5	1/15/2013 22:44	4.67
6	1/15/2013 23:18	4.15
7	1/16/2013 0:04	7.45
9	1/16/2013 1:22	7.06
10	1/16/2013 1:55	3.65
11	1/16/2013 2:36	5.31
12	1/16/2013 3:15	13.92
		0 52.7 TOTAL FLOW (L)

### January 30, 2013

SITE	Sample #	Time	Lead ppm	Diss. Lead ppm	Zinc ppm	Diss. Zinc ppm	Copper Ppm	Diss Cu Ppm	TP mg/L	DP mg/L	TSS mg/L	pH
WTRO	1	9:46 PM	0.020	0.011	0.055	0.056	0.007	0.007	0.06	0.03	3.3	7.56
WTRO	2	10:11 PM	0.009	0.003	0.028	0.031	0.006	0.005	0.04	0.02	0.5	7.51

SITE	Sample #	Time	Lead Ppm	Diss. Lead ppm	Zinc ppm	Diss. Zinc ppm	Copper Ppm	Diss Cu Ppm	TP mg/L	DP mg/L	TSS mg/L	pH
WBI	1	9:37 PM	4.41	1.31	0.072	0.041	1.89	0.47	0.02	0.01	25.4	5.55
WBI	2	9:52 PM	1.76	1.54	0.124	0.092	0.822	0.43	0.02	0.00	0.5	5.48
WBI	3	10:07 PM	2.43	1.58	0.062	0.052	1.25	0.67	0.01	0.00	0.5	5.45
WBI	4	10:22 PM	2.59	1.55	0.136	0.039	1.61	0.75	0.04	0.00	11.8	5.56
WBI	5	10:37 PM	2.48	2.07	0.069	0.047	1.45	0.63	0.07	0.00	6.15	5.59
WBI	8	2:22 AM	2.51	1.69	0.133	0.045	1.17	0.63	0.05	0.00	0.5	5.54
WBI	10	2:52 AM	1.88	1.73	0.122	0.046	1.13	0.60	0.02	0.02	0.5	5.57
WBI	11	3:07 AM	1.71	1.47	0.121	0.125	1.09	0.61	0.02	0.02	1.2	5.61

SITE	Sample #	Time	Lead ppm	Diss. Lead ppm	Zinc ppm	Diss. Zinc ppm	Copper ppm	Diss Cu Ppm	TP mg/L	DP mg/L	TSS mg/L	pH
WBO	1	9:39 PM	0.132	0.044	0.133	0.040	0.033	0.022	0.60	0.20	8.4	7.56
WBO	2	9:44 PM	0.084	0.076	0.108	0.029	0.027	0.023	0.46	0.42	4.7	7.50
WBO	3	9:48 PM	0.067	0.030	0.047	0.052	0.022	0.019	0.98	0.52	1.4	7.52
WBO	4	9:53 PM	0.075	0.026	0.112	0.041	0.027	0.018	0.91	0.60	0.5	7.65
WBO	6	10:01 PM	0.045	0.023	0.131	0.03	0.023	0.016	0.96	0.69	0.5	7.70
WBO	8	10:13 PM	0.056	0.025	0.048	0.034	0.019	0.017	0.89	0.79	0.5	7.73
WBO	11	10:28 PM	0.044	0.026	0.028	0.027	0.019	0.015	0.78	0.77	0.5	7.67
WBO	15	11:00 PM	0.033	0.023	0.033	0.027	0.018	0.017	0.77	0.77	0.5	7.62

SITE	Sample #	Time	Seph P mg/L	SRP mg/L	SRP+Seph mg/L	Organic P mg/L	Seph Pb	Seph Cu	Seph Zn
WTRO	1	9:46 PM	0.004	0.011	0.015	0.019	0.025	0.008	0.11
WTRO	2	10:11 PM	0.006	0.010	0.017	0.011	0.028	0.009	0.06

SITE	Sample #	Time	Seph P mg/L	SRP mg/L	SRP+Seph mg/L	Organic P mg/L	Seph Pb	Seph Cu	Seph Zn
WBI	1	9:37 PM	0	0	0	0.0075	0.47	0.21	0.078
WBI	2	9:52 PM	0	0	0	0	1.50	0.44	0.198
WBI	3	10:07 PM	0	0	0	0.0013	1.57	0.60	0.06
WBI	4	10:22 PM	0	0	0	0.0006	1.50	0.77	0.13
WBI	5	10:37 PM	0	0	0	0.0036	1.59	0.70	0.070
WBI	8	2:22 AM	0	0	0	0.0027	0.33	0.15	0.037
WBI	10	2:52 AM	0	0	0	0.0186	1.65	0.64	0.068
WBI	11	3:07 AM	0	0	0	0.0186	1.35	0.60	0.11

SITE	Sample #	Time	Seph P mg/L	SRP mg/L	SRP+Seph mg/L	Organic P mg/L	Seph Pb	Seph Cu	Seph Zn
WBO	1	9:39 PM	0.024	0.181	0.205	0.0203	0.0355	0.016	0.054
WBO	2	9:44 PM	0.038	0.301	0.340	0.119	0.0546	0.017	0.046
WBO	3	9:48 PM	0.057	0.424	0.482	0.0940	0.0321	0.009	0.089
WBO	4	9:53 PM	0.080	0.489	0.570	0.105	0.0138	0.006	0.114
WBO	6	10:01 PM	0.085	0.638	0.724	0.0541	0.0192	0.007	0.104
WBO	8	10:13 PM	0.101	0.726	0.827	0.0606	0.0085	0.007	0.060
WBO	11	10:28 PM	0.096	0.710	0.807	0.0551	0.0330	0.010	0.060
WBO	15	11:00 PM	0.081	0.700	0.782	0.0656	0.0288	0.0096	0.182

wood WTR			wood in			wood out biomat		
sample #	Time	flow(L)	sample #	time	flow(L)	sample #	time	flow(L)
1	1/30/13 21:46	27.72	1	1/30/13 21:37	73.59	1	1/30/2013 21:39	6.75
2	1/30/13 22:11	203.97	2	1/30/13 21:52	114.46	2	1/30/2013 21:44	4.09
		0	3	1/30/13 22:07	91.91	3	1/30/2013 21:48	7.06
		0	4	1/30/13 22:22	96.79	4	1/30/2013 21:53	7.15
		0	5	1/30/13 22:37	431.15	6	1/30/2013 22:01	9.98
		0	8	1/31/13 2:22	219.88	8	1/30/2013 22:13	12.02
		0	10	1/31/13 2:52	162.73	11	1/30/2013 22:28	17.65
		0	11	1/31/13 3:07	381.32	15	1/30/2013 23:00	166.96
		231.70			1571.88	0		231.70
		TOTAL FLOW (L)			TOTAL FLOW (L)			TOTAL FLOW (L)

February 26, 2013

SITE	Sample #	Time	Lead ppm	Diss. Lead ppm	Zinc ppm	Diss. Zinc ppm	Copper ppm	Diss Cu Ppm	TP mg/L	DP mg/L	TSS mg/L	pH
WTRO	4	2/26/13 4:40 PM	0.0100	0.010	0.015	0.009	0.010	0.005	0.03	0.02	0.5	7.42
WTRO	5	2/26/13 5:25 PM	0.0129	0.008	0.019	0.038	0.006	0.002	0.03	0.02	0.5	7.48
WTRO	6	2/26/13 8:20 PM	0.010		0.022		0.006	0.006	0.05	0.03	0.5	7.44
WTRO	7	2/26/13 8:45 PM	0.006	0.003	0.021	0.023	0.007	0.004	0.05	0.04	0.5	7.41
WTRO	8	2/26/13 9:10 PM	0.008	0.011	0.018	0.022	0.008	0.005	0.06	0.05	0.5	7.43
WTRO	11	2/26/13 10:25 PM	0.006	0.002	0.022	0.026	0.010	0.004	0.08	0.08	0.5	7.44
WTRO	13	2/26/13 11:05 PM	0.007	0.007	0.028	0.014	0.009	0.005	0.10	0.09	0.5	7.44
WTRO	15	2/26/13 11:35 PM	0.023	0.011	0.027		0.011	0.005	0.12	0.11	0.5	7.42
WTRO	21	2/27/13 1:25 AM	0.013	0.006	0.018	0.013	0.008	0.006	0.11	0.11	0.5	7.38

SITE	Sample #	Time	Lead ppm	Diss. Lead Ppm	Zinc ppm	Diss. Zinc ppm	Copper ppm	Diss Cu Ppm	TP mg/L	DP mg/L	TSS mg/L	pH
WBI	1	9:18 PM	5.64	1.99	0.063	0.051	1.55	0.97	0.10	0.01	7.2	5.23
WBI	2	9:30 PM	4.42	1.1	0.102	0.04	2.22	0.70	0.04	0.01	0.5	5.44
WBI	3	9:42 PM	1.92	1.14	0.088	0.062	0.969	0.68	0.02	0.01	0.5	5.68
WBI	4	9:54 PM	1.92	1	0.104	0.044	0.985	0.79	0.02	0.03		5.72
WBI	7	10:20 PM	2.38	1.08	0.045	0.065	1.10	0.75	0.04	0.01	0.5	5.77
WBI	8	10:27 PM	1.64	1.09	0.094	0.057	0.94	0.70	0.02	0.01	3.1	5.71
WBI	9	10:34 PM	1.68	1.01	0.047	0.054	0.941	0.73	0.02	0.01		5.72
WBI	10	10:41 PM	2.10	0.89	0.050	0.067	1.09	0.70	0.03	0.02		5.77

SITE	Sample #	Time	Lead Ppm	Diss. Lead Ppm	Zinc Ppm	Diss. Zinc Ppm	Copper Ppm	Diss Cu Ppm	TP mg/L	DP mg/L	TSS mg/L	pH
WBO	2	2/26/13 4:32 PM	0.066	0.031	0.032	0.020	0.030	0.020	0.35	0.29	0.5	7.67
WBO	3	2/26/13 4:48 PM	0.057	0.028	0.004	0.102	0.024	0.011	0.33	0.32	0.5	7.68
WBO	4	2/26/13 5:05 PM	0.047	0.012	0.045	0.012	0.022	0.013	0.34	0.33	0.5	7.77
WBO	6	2/26/13 5:29 PM	0.069	0.011	0.043	0.014	0.015	0.008	0.37	0.33	0.5	7.75
WBO	8	2/26/13 6:54 PM	0.021	0.014	0.049	0.043	0.012	0.008	0.38		0.5	7.71
WBO	10	2/26/13 8:34 PM	0.025	0.025	0.003	0.065	0.013	0.010	0.39	0.36	0.5	7.67
WBO	12	2/26/13 9:28 PM	0.027	0.013	0.064	0.014	0.012	0.006	0.41	0.40	0.5	7.58
WBO	16	2/26/13 10:58 PM	0.029	0.029	0.071	0.070	0.012	0.011	0.57		0.5	7.52

SITE	Sample #	Time	SRP mg/L	A-25 Phos mg/L	Organic P mg/L	Part. P mg/L	anionic P	Seph. Pb mg/L	Seph Cu mg/L	Seph Zn mg/L
WTRO	4	#####	0.00	0.01	0.01	0.02	0.01	0.0047	0	0.047
WTRO	5	#####	0.01		0.01	0.01	#N/A	0.012	0	0.038
WTRO	6	#####	0.01	0.02	0.02	0.03	0.00	0.025	0.01	0.031
WTRO	7	#####	0.03		0.01	0.02	#N/A	0.008	0	0.045
WTRO	8	#####	0.04	0.02	0.01	0.01	0.03	0.008	0	
WTRO	11	#####	0.07	0.03	0.01	0.00	0.04	0.005	0	0.022
WTRO	13	#####	0.08	0.02	0.01	0.01	0.08	0.006	0	
WTRO	15	#####	0.10	0.02	0.01	0.02	0.09	0.009	0	
WTRO	21	#####	0.10		0.01	0.01	#N/A	0.005	0	

SITE	Sample #	Time	SRP	A-25 Phos	Organic P	Part. P	anionic P	Seph. Pb	Seph Cu	Seph Zn
			mg/L	mg/L	mg/L	mg/L	mg/L	mg/L	mg/L	mg/L
WBI	1	9:18 PM				0.09	#N/A			
WBI	2	9:30 PM	0.00	0.01	0.00	0.04	-0.01	1.16	0.77	0.339
WBI	3	9:42 PM	0.01	0.01	0.00	0.01	0.00	1.19	0.73	0.071
WBI	4	9:54 PM	0.00	0.01	0.03	0.00	0.03	1.18	0.85	0.054
WBI	7	10:20 PM	0.00		0.01	0.03	#N/A	1.25	0.84	0.086
WBI	8	10:27 PM	0.00	0.01	0.01	0.00	0.00	1.10	0.76	0.087
WBI	9	10:34 PM	0.01	0.01	0.00	0.01	0.00	1.05	0.76	0.065
WBI	10	10:41 PM				0.01	#N/A			

SITE	Sample #	Time	SRP	A-25 Phos	Organic P	Part. P	anionic P	Seph. Pb	Seph Cu	Seph Zn
			mg/L	mg/L	mg/L	mg/L	mg/L	mg/L	mg/L	mg/L
WBO	2	#####	0.26	0.04	0.03	0.06	0.25	0.017	0.01	0.032
WBO	3	#####	0.29	0.05	0.03	0.02	0.27	0.041	0.01	0.054
WBO	4	#####	0.30		0.03	0.01	#N/A	0.009	0	0.021
WBO	6	#####	0.34		0.00	0.04	#N/A	0.011	0	
WBO	8	#####	0.35	0.06			#N/A	0.015	0	
WBO	10	#####	0.35	0.07	0.02	0.03	0.30	0.012	0	0.013
WBO	12	#####	0.39	0.05	0.02	0.01	0.35	0.011	0	
WBO	16	#####	0.54	0.07			#N/A	0.015	0	0.065

wtr out sample #	time	flow(L)
	2/26/2013	
4	16:40	28.92
	2/26/2013	
5	17:25	27.34
	2/26/2013	
6	20:20	13.56
	2/26/2013	
7	20:45	3.03
	2/26/2013	
8	21:10	17.97
	2/26/2013	
11	22:25	16.59
	2/26/2013	
13	23:05	6.24
	2/26/2013	
15	23:35	4.87
	2/27/2013	
21	1:25	0
		118.56
		TOTAL FLOW (L)

wood in sample #	time	flow(L)
	2/26/2013	
1	21:18	244.2
	2/26/2013	
2	21:30	24.42
	2/26/2013	
3	21:42	24.42
	2/26/2013	
4	21:54	16.28
	2/26/2013	
7	22:20	16.28
	2/26/2013	
8	22:27	16.28
	2/26/2013	
9	22:34	0
	2/26/2013	
10	22:41	81.41
		0
		423.33
		TOTAL FLOW (L)

wood out sample #	time	flow(L)
	2/26/2013	
2	16:32	13.7
	2/26/2013	
3	16:48	10.8
	2/26/2013	
4	17:05	11.9
	2/26/2013	
6	17:29	15.0
	2/26/2013	
8	18:54	6.76
	2/26/2013	
10	20:34	15.4
	2/26/2013	
12	21:28	23.7
	2/26/2013	
16	22:58	20.9
		0
		118.56
		TOTAL FLOW (L)



## Appendix B – Raw Data from Extraction Experiments

### Sr(NO<sub>3</sub>)<sub>2</sub> Extraction Data, Rear Side Cross-section

	mg metal/ kg media				mg metal/ kg media				mg metal/ kg media			
	Pb 1	Pb 2	Pb 3	St dev	Cu 1	Cu 2	Cu 3	St dev	Zn 1	Zn 2	Zn 3	St dev
1AS	6.16	3.14	2.64	1.90	0.4	1.348	0.632	0.5	0.4	0.74	0.4	0.2
2AS	3.76	1.34	1.32	1.40	0.4	0.4	0.4	0.0	0.80	0.4	0.4	0.2
3AS	2.84	1.62	4.82	1.61	0.4	0.4	0.4	0.0	1.07	0.4	0.4	0.4
4AS	2.64	1.08	1.08	0.90	1.03	0.4	1.12	0.4	1.54	0.4	0.4	0.7
5AS	0	0	0	0.00	0	0	0	0.0	0	0	0	0.0
1BS	1.96	1.3	2.08	0.42	0.4	0.068	0	0.2	0.4	0.4	0.4	0.0
2BS	2.12	1.86	1.26	0.44	0.4	0.178	0	0.2	0.4	0.4	0.4	0.0
3BS	1.46	0.9	1.58	0.36	0.4	0.4	0.4	0.0	0.4	0.4	0.83	0.3
4BS	1.54	1.08	1.4	0.24	0.4	0.4	0.4	0.0	0.4	0.4	0.4	0.0
5BS	1.5	1.62	1.12	0.26	0.4	0.4	0.4	0.0	0.4	0.4	0.4	0.0
1CS	1.16	1.44	1.9	0.37	0.4	0.4	0.4	0.0	0.4	0.4	0.4	0.0
2CS	1.46	1.68	1.46	0.13	0.4	0.4	0.4	0.0	0.4	0.4	0.4	0.0
3CS	0.74	1.24	1.22	0.28	0.4	0.4	0.4	0.0	0.4	0.4	0.4	0.0
4CS	0.78	1.12	1.94	0.60	0.4	0.4	0.4	0.0	0.4	0.4	0.4	0.0
5CS	1.18	1.86	1.12	0.41	0.4	0.4	0.4	0.0	0.4	0.4	0.4	0.0
1DS	1.56	2.66	1.56	0.64	1.70	2.22	2.08	0.3	0.4	0.4	0.4	0.0
2DS	0.92	1.5	2.08	0.58	0.4	0.4	0.4	0.0	0.4	0.4	0.4	0.0
3DS	0.36	1.16	1.36	0.53	0.4	0.4	0.4	0.0	0.4	0.4	0.4	0.0
4DS	0.66	1.2	1.54	0.44	0.4	0.4	0.4	0.0	0.4	0.4	0.4	0.0
5DS	0.6	1.46	1.28	0.45	0.4	0.4	0.4	0.0	0.4	0.4	0.4	0.0

Sr(NO<sub>3</sub>)<sub>2</sub> Extraction Data, Rear Middle Cross-section

	mg metal/ kg media				mg metal/ kg media				mg metal/ kg media			
	Pb 1	Pb 2	Pb 3	St dev	Cu 1	Cu 2	Cu 3	St dev	Zn 1	Zn 2	Zn 3	St dev
1AH	1.74	0.4	1	0.671	1.79	1.17	1.40	0.3	0.4	0.4	0.4	0.0
2AH	0.4	1.12	1.38	0.508	0.4	0.4	0.4	0.0	0.4	0.4	0.4	0.0
3AH	0.4	1.88	1.04	0.742	0.4	0.4	0.4	0.0	0.4	0.4	0.4	0.0
4AH	0.4	1.12	1.52	0.568	0.4	0.4	0.4	0.0	0.4	0.4	0.4	0.0
5AH	0.8	1.12	1.34	0.272	0.4	0.4	0.4	0.0	0.4	0.4	0.4	0.0
1BH	1.4	2.56	1.62	0.616	2.30	1.62	2.26	0.4	0.4	0.4	0.4	0.0
2BH	0.4	0.86	1.1	0.356	0.4	0.4	0.4	0.0	0.4	0.4	0.4	0.0
3BH	0.4	1.58	2.06	0.854	0.4	0.4	0.4	0.0	0.4	0.4	0.4	0.0
4BH	0.4	0.4	1.1	0.404	0.4	0.4	0.4	0.0	0.4	0.4	0.4	0.0
5BH	0.4	1.68	1.34	0.663	0.4	0.4	0.4	0.0	0.4	0.4	0.4	0.0
1CH	1.6	1.48	1.4	0.101	3.31	2.34	3.28	0.6	0.4	0.4	0.4	0.0
2CH	0.4	0.4	1.28	0.508	0.4	0.4	0.4	0.0	0.4	0.4	0.4	0.0
3CH	0.4	0.96	1.82	0.715	0.4	0.4	0.4	0.0	0.4	0.4	0.4	0.0
4CH	0.4	1.18	1.6	0.609	0.4	0.4	0.4	0.0	0.4	0.4	0.4	0.0
5CH	0.4	0.92	1.24	0.424	0.4	0.4	0.4	0.0	0.4	0.4	0.4	0.0
1DH	6.72	3.1	9.56	3.23	7.60	3.80	10.54	3.4	3.70	3.60	4.74	0.6
2DH	0.4	2.46	2.86	1.32	4.25	1.83	4.60	1.5	0.4	0.4	0.4	0.0
3DH	0.4	2.06	0.92	0.849	0.99	0.4	0.4	0.3	0.4	0.4	0.4	0.0
4DH	0.4	2.36	0.4	1.13	0.4	0.4	0.4	0.0	0.4	0.4	0.4	0.0
5DH	0.4	1.78	1.32	0.703	0.4	0.4	0.4	0.0	0.4	0.4	0.4	0.0

Ammonium oxalate extraction – Rear side cross section

	Mg/kg				Mg/kg				Mg/kg			
	Pb 1	Pb 2	Pb 3	% RSD	Cu 1	Cu 2	Cu 3	% RSD	Zn 1	Zn 2	Zn 3	% RSD
1AS	7.16	4	39.1	19	11.3	15.5	9.23	3	36.4	52.7	42.7	8
2AS	4.96	3.12	24.5	12	2.65	10.2	6.25	4	30.3	37.1	29.1	4
3AS	5.48	4.64	19.2	8	5.42	9.82	6.64	2	30.0	33.8	42.1	6
4AS	4.16	3.88	13.6	6	4	9.94	9.12	3	29.8	38.5	48.0	9
5AS	0	0	0	0	0	0	0		0	0	0	
1BS	6.6	11.2	14.6	4	13.2	17.6	12.8	3	38.6	34.7	44.1	5
2BS	7.64	5.76	10.1	2	6.85	9.24	10.3	2	49.2	35	42.3	7
3BS	5.72	2.6	5.52	2	4.04	8.34	7.48	2	30.4	38.4	39.1	5
4BS	6.24	1.8	9.2	4	4.14	7.95	12.2	4	50.0	35.4	42.9	7
5BS	4.12	1.52	4.4	2	11.0	15.9	20.5	5	55.1	42.3	63.8	11
1CS	8.12	8.8	9.44	1	32.9	26.9	38.5	6	42.2	29.2	47.6	9
2CS	1.6	2.48	8	3	10.8	11.0	18.4	4	29.6	34.8	44.4	8
3CS	2	1.4	3.76	1	5.49	7.41	13.7	4	37.8	27.8	35.9	5
4CS	1	0.76	5	2	4.78	9.25	11.9	4	43.0	46.5	41.8	2
5CS	1.2	2.04	1.4	0	7.87	15.7	17.9	5	57	51.6	41.0	8
1DS	60.7	204	109	73	163	470	273	155	49.9	28.5	43.0	11
2DS	19.6	15.4	24.8	5	46.5	67.0	63.2	11	27.8	35.8	39.4	6
3DS	2.4	2.8	5.68	2	10.0	15.18	2.29	6	38.5	50.4	43.6	6
4DS	4.4	29.0	4.28	14	6.33	18.3	0.696	9	34.6	44	29.6	7
5DS	5.44	1.8	4	2	8.66	15.8	0.688	8	64.3	61.8	50.3	7

### Ammonium oxalate extraction – Rear hotspot cross-section

	mg/kg			% RSD	mg/kg			% RSD	mg/kg			% RSD
	Pb 1	Pb 2	Pb 3		Cu 1	Cu 2	Cu 3		Zn 1	Zn 2	Zn 3	
1AH	64	93	58	18	112	139	89	25		33.9		#DIV/0!
2AH	6	20	4	9	12	10	6	4	32.8	28.3	28.0	3
3AH	6	12	0	6	12	13	6	4	32.7	37.5	35.9	2
4AH	1	6	5	3	9	16	5	5	38.7	32.5	31.3	4
5AH	2	8	0	4	20	16	8	6	43.1	46.3	33.7	7
1BH	110	134	159	24	224	254	233	16	32.8	40.7	32.3	5
2BH	11	14	12	2	35	23	26	6	28.8	31.8	36.2	4
3BH	0	4	1	2	1	8	7	4		23.6	23.2	0
4BH	0	3	0	2	7	11	6	3	35.0	33.3	40.8	4
5BH	0	0	4	2	10	14	10	2	28.3	48.7	33	11
1CH	299	346	230	59	662	732	595	68	35.6	41.2	37.6	3
2CH	24	20	20	2	83	74	47	19	32.9	21.9	21.4	7
3CH	6	4	3	1	16	15	12	2	29.0	29.9	33.7	3
4CH	1	3	2	1	9	2	6	3	37.7	26.2	23.3	8
5CH	3	0	1	1	14	1	11	7	56.3	34.4	57.0	13
1DH	190	221	158	31	1360	1069	1384	176	40.2		35.2	4
2DH	216	241	214	15	429	438	305	74	33.5	30.3	36.0	3
3DH	25	31	16	7	86	84	45	23	41.7	39.6	24.7	9
4DH	1	1	3	1	26	17	12	7	37.9	30.6	33.3	4
5DH	2	2	5	2	15	7	10	4	41.4	37.3	33.6	4

Aqua Regia Extraction – Rear side cross-section

	mg/kg					mg/kg					mg/kg			
	Pb 1	Pb 2	Pb 3	St dev		Cu 1	Cu 2	Cu 3	St dev		Zn 1	Zn 2	Zn 3	St dev
1AS	25.4	14.9	9.9	8	12.86	5.87	11.24	4	64.7	66.07	70.65	3		
2AS	20.4	5.4	4.4	9	14.91	3.92	10.06	6	73.68	58.64	77.54	10		
3AS	20.8	9.4	13.4	6	9.08	8.47	9.81	1	65.16	89.2	80.93	12		
4AS	20.2	4.2	8.5	8	11.57	14.19	11.56	2	80.32	88.86	74.33	7		
5AS				#DIV/0!				#DIV/0!				#DIV/0!		
1BS	88.1	74.2	40.6	24	16.11	13.39	7.78	4	85.92	145.4	52.3	47		
2BS	23.6	11	9.1	8	9.33	6.94	11.73	2	63.7	70.11	83.72	10		
3BS	17.7	2.7	5.2	8	11.64	4.45	8.58	4	73.93	55.99	74.3	10		
4BS	17.2	5.8	2.6	8	7.91	7.14	29.73	13	55.58	81.13		18		
5BS	23.7	15.2	11.7	6	12.25	17.5	17.74	3	71.25	99.05	84.09	14		
1CS	100.1	117	123.8	12	21.7	32.64	37.19	8	54.81	92.22	79.28	19		
2CS		17.6	17.1	0		13.48	17.08	3		82.63	65.12	12		
3CS	18.7	10.7	7	6	5.79	8.72	8.94	2	64.53	80.49	66.17	9		
4CS	14.7	5.7	10.3	5	5.93	7.92	18.75	7	70.25	79.3	168.5	54		
5CS	22	15	5.6	8	19.78	15.12	12.39	4	70.67	63.73	78.38	7		
1DS	547.1	428.3	945.8	271	270.5	175.5	400.5	113	74.47	80.57	79.53	3		
2DS	77.8	79.1	46.4	19	42.74	49.61	40.19	5	53.47	64.58	81.42	14		
3DS	18.9	10.5	11.4	5	4.43	7.62	15.76	6	49.68	66.19	75.4	13		
4DS	16.1	5.1	8.1	6	7.19	5.69	8.66	1	67.95	63.64	61.79	3		
5DS	20.3	47.5	10.4	19	12.59	11.52	21.39	5	98.44	83.48	100.3	9		

### Aqua Regia Extraction – Rear hotspot cross-section

	Pb 1	Pb 2	Pb 3	St dev	Cu 1	Cu 2	Cu 3	St dev	Zn 1	Zn 2	Zn 3	St dev
1AH	469.7	671.6	603.7	103	89	135	131	25	47.76	82.12	71.96	18
2AH	35.7	47.9	52.2	9	13	12	18	3	51.33	77.58	107.5	28
3AH	17.3	22.7	28.5	6	16	14	8	4	72.37	63.03	63.64	5
4AH	10.6	8.3	20.8	7	8	5	12	3	57.35	54.07	80.17	14
5AH	29.7	13.2	26.1	9	22	5	13	8	66.11	49.43	82.32	16
1BH	988.6	799.8	1046	129	227	201	261	30	69.59	78.54	76.02	5
2BH	120.3	142.7	106.1	18	28	32	21	6	51.3	61.06	55.23	5
3BH	25.4	35.1	29.8	5	14	8	12	3	70.35	54.98	104.2	25
4BH	18.7	20.4	22.7	2	12	9	6	3	76.77	71.82	75.11	3
5BH	23.8	31.2	30.6	4	12	11	6	3	64.65	79.78	77.05	8
1CH	2112	1657	2020	241	544	418	560	78	37.31	69.41	93.2	28
2CH	211.7	202	164.7	25	63	65	63	1	62.88	76	94.67	16
3CH	54.5	50.9	45	5	20	17	13	3	62.45	60.81	94.58	19
4CH	26	38	38.5	7	10	11	15	3	57.34	69.58	74.82	9
5CH	26.9	43.5	28.2	9	16	18	8	5	92.22	79.72	78.67	8
1DH	6387	9690	7668	1665	1935	1761	2464	366	66.77			#DIV/0!
2DH	1176	1067	822	181	324	158	421	133	74.86	76.12	77.2	1
3DH	214.6	170	642.1	261	89	82	251	96	77.01	59.69	72.55	9
4DH	43.9	59	38.6	11	18	20	13	4	58.24	64.3	52.65	6
5DH	23.7	28.4	31.7	4	12	8	9	2	65.85	58.43	63.8	4

Sr(NO<sub>3</sub>)<sub>2</sub> Extraction data – Swale side cross-section

	mg/kg			St. dev.	mg/kg			St. dev.	mg/kg			St. dev.
	Pb 1	Pb 2	Pb 3		Cu 1	Cu 2	Cu 3		Zn 1	Zn 2	Zn 3	
1AS	0.238	0.139	0.145	0.1	0.132	0.194	0.158	0.0	0.4	0.4	0.4	0.0
2AS	0.364	0.182	0.181	0.1	0.05	0.05	0.05	0.0	0.4	0.4	0.4	0.0
3AS	0.450	0.578	0.471	0.1	0.05	0.208	0.126	0.1	0.4	0.4	0.4	0.0
4AS	0.072	0.165	0.131	0.0	0.100	0.137	0.135	0.0	0.4	0.832	0.4	0.2
1BS	0.255	0.192	0.102	0.1	0.05	0.05	0.05	0.0	0.4	0.4	0.4	0.0
2BS	0.267	0.224	0.156	0.1	0.05	0.109	0.05	0.0	0.4	0.4	0.4	0.0
3BS	0.244	0.130	0.161	0.1	0.05	0.05	0.05	0.0	1.15	0.823	0.4	0.4
4BS	0.288	0.235	0.191	0.0	0.124	0.102	0.10	0.0	0.4	0.4	0.4	0.0
1CS	0.150	0.346	0.388	0.1	0.05	0.155	0.10	0.1	0.4	0.80	0.4	0.2
2CS	0.793	0.238	0.171	0.3	0.05	0.23	0.05	0.1	1.18	1.25	0.4	0.5
3CS	0.752	0.622	0.239	0.3	0.05	0.05	0.103	0.0	1.21	1.77	0.85	0.5
4CS	0.265	0.052	0.195	0.1	0.114	0.05	0.108	0.0	0.4	0.4	0.4	0.0

Sr(NO<sub>3</sub>)<sub>2</sub> Extraction data – Swale middle cross-section

	mg/kg				St. dev.	mg/kg				St. dev.	mg/kg				St. dev.
	Pb 1	Pb 2	Pb 3	St. dev.		Cu 1	Cu 2	Cu 3	St. dev.		Zn 1	Zn 2	Zn 3	St. dev.	
1AM	0.0	0.0	0.5	0.3	0.2416	0.17	0.21	0.0	0.4	0.4	0.4	0.0			
2AM	0.1	0.0	0.1	0.0	0.05	0.05	0.15	0.1	0.4	0.4	0.4	0.0			
3AM	0.0	0.0	0.0	0.0	0.05	0.05	0.05	0.0	0.4	0.4	0.4	0.0			
4AM	0.2	0.1	0.0	0.1	0.05	0.05	0.11	0.0	0.4	0.4	0.4	0.0			
1BM	0.0	0.4	0.1	0.2	0.05	0.05	0.10	0.0	0.4	1.13	1.02	0.4			
2BM	0.1	0.0	0.1	0.1	0.05	0.05	0.11	0.0	0.4	0.4	0.4	0.0			
3BM	0.0	0.0	0.3	0.2	0.05	0.05	0.05	0.0	0.4	0.4	0.4	0.0			
4BM	0.1	0.1	0.0	0.0	0.05	0.05	0.05	0.0	0.4	0.80	0.4	0.2			
1CM	0.2	0.0	0.0	0.1	0.05	0.12	0.05	0.0	0.4	0.83	0.4	0.3			
2CM	0.1	0.1	0.1	0.0	0.05	0.05	0.05	0.0	0.8694	0.86	0.4	0.3			
3CM	0.0	0.0	0.1	0.0	0.05	0.05	0.05	0.0	0.4	0.4	0.4	0.0			
4CM	0.1	0.3	0.0	0.1	0.05	0.05	0.05	0.0	0.4	1.00	0.4	0.3			
1DM	0.0	0.2	0.0	0.1	0.05	0.11	0.05	0.0	0.4	1.51	0.4	0.6			
2DM	0.0	0.0	0.2	0.1	0.05	0.05	0.05	0.0	0.4	1.23	0.4	0.5			
3DM	0.0	0.2	0.0	0.1	0.05	0.05	0.05	0.0	0.81	1.30	0.85	0.3			
4DM	0.0	0.0	0.3	0.2	0.05	0.05	0.05	0.0	1.12	0.89	0.4	0.4			

Ammonium oxalate extraction data – swale side cross-section

	mg/kg				mg/kg				mg/kg			
	Pb 1	Pb 2	Pb 3	St. Dev.	Cu 1	Cu 2	Cu 3	St. Dev.	Zn 1	Zn 2	Zn 3	St. Dev.
1AS	1.17	1.29	0.94	0.2	8.75	9.20	7.21	1.0	51.1	56.3	46.8	5
2AS	0.891	0.965	0.701	0.1	7.45	7.83	6.45	0.7	54.2	38.1	40.6	9
3AS	0.725	0.822	0.766	0.0	6.05	8.45	5.71	1.5	58.1	44.2	29.6	14
4AS	0.676	0.606	0.59	0.0	9.20	8.64	7.54	0.8	58.9	47.6	22.4	19
1BS	0.930	0.952	0.82	0.1	7.79	7	8.55	0.8	53.9	54		0
2BS	0.784	0.683	0.625	0.1	6.8	5.42	6.10	0.7	41.4	40.2	31.8	5
3BS	0.7	0.810	1.96	0.7	7.03	6.52	9.1	1.4	39.66	45.1	39.0	3
4BS	0.741	0.754	0.628	0.1	6.31	5.81	6.2	0.3	39.7	36.6	30.1	5
1CS	0.891	0.964	0.888	0.0	7.2	7.60	5.85	0.9	45.0	42.8	20.8	13
2CS	0.80	0.821	0.672	0.1	5.69	7.51	5.6	1.1	41.6	30.4	31.4	6
3CS	0.647	0.651	0.607	0.0	5.96	6.16	6.23	0.1	47.9	29.3	31.9	10
4CS	0.709	0.729	0.606	0.1	5.03	5.10	5.12	0.0	44.1	22.7	21.3	13

Ammonium oxalate extraction data – swale middle cross-section

	mg/kg			St. Dev.	mg/kg			St. Dev.	mg/kg			St. Dev.
	Pb 1	Pb 2	Pb 3		Cu 1	Cu 2	Cu 3		Zn 1	Zn 2	Zn 3	
1AM	0.551	0.568	0.790	0.1	3.847	3.72	4.84	0.6	23.7	36.4	33.9	7
2AM	0.512	0.569	0.607	0.0	4.86	5.08	3.83	0.7	48.4	39.1	36.9	6
3AM	0.593	0.455	0.528	0.1	4.28	4.05	3.46	0.4	37.3	33.7	35.7	2
4AM	0.776	0.612	0.731	0.1	5.81	5.15	3.93	1.0	44.7	48.0	40.9	4
1BM	0.503	0.502	0.562	0.0	4.68	4.99	3.68	0.7	52.6	35.4	35.0	10
2BM	0.459	0.460	0.543	0.0	3.33	4.19	4.05	0.5	98.6	25.2	32	41
3BM	0.437	0.405	0.503	0.0	4.51	4.91	4.55	0.2	66.1	25.1	34.9	21
4BM	0.552	0.609	0.584	0.0	4.43	4.2	3.89	0.3	44.8	21.1	22.0	13
1CM	0.538	0.47	0.478	0.0	5.13	3.96	5.42	0.8	39.4	35.9	39.0	2
2CM	0.520	0.546	0.486	0.0	4.29	3.81	5.09	0.6	43.2	32.1	45.9	7
3CM	0.447	0.3632	0.614	0.1	4.86	3.54	5.28	0.9	42.6	33.4	35.6	5
4CM	0.444	0.538	0.482	0.0	3.64	3.89	2.93	0.5	41.6	28.2	30.0	7
1DM	0.581	0.634	0.709	0.1	5.21	5.52	5.48	0.2	79.8	52.0	53.0	16
2DM	0.514	0.557	0.476	0.0	3.92	4.11	5.22	0.7	44.4	36.9	30.0	7
3DM	0.58	0.503	0.498	0.0	4.24	5.19	5.02	0.5	44.4	35.8	53.6	9
4DM	0.489	0.582	0.526	0.0	4.41	3.76	4.8	0.5	40.4	37.0	42.0	3



Aqua Regia extraction data – swale side cross-section

	mg/kg			St. dev.	mg/kg			St. dev.	mg/kg			St. dev.
	Pb 1	Pb 2	Pb 3		Cu 1	Cu 2	Cu 3		Zn 1	Zn 2	Zn 3	
1AS	13.5	15.4	18.5	2.5	15.8	14.9	13.6	1	81.8	79.0	80.0	1
2AS	8.2	18	14.5	5.0	17.2	20.8	17.6	2	80.4	108	74.9	18
3AS	15.5	5.8	11.2	4.9	13.6	8.05	12.6	3	67.3	41.3	65.5	15
4AS	8.8	14.2	12.4	2.7	11.1	15.8	13.9	2	50.6	89.4	55.3	21
1BS	9.3	14.5	17.7	4.2	13.1	26.4	15.4	7	68.1	110	71.1	24
2BS	9.7	16.1	13	3.2	11.0	15.5	13.0	2	58.4	53.6	61.3	4
3BS	4.5	17.9	7.1	7.1	9.71	17.0	10.7	4	46.0	60.9	62.6	9
4BS	11.9	7.6	17.2	4.8	22.3	8.98	12.9	7	97.7	47.8	56.2	27
1CS	4.3	17.8	12.7	6.8	9.24	13.1	9.5	2	40.5	68.5	47.5	15
2CS	8.9	14.9	12.4	3.0	8.59	12.6	8.79	2	42.2	52.3	47.0	5
3CS	10.1		9.6	0.4	9.24	9.24	10.1	1	44.1		75.0	22
4CS	2.2	14.4	11.3	6.3	5.45	10.6	8.33	3	19.3	53.5	44.0	18

Aqua Regia extraction data – swale middle cross-section

	mg/kg				St. dev.	mg/kg				St. dev.	mg/kg				St. dev.
	Pb 1	Pb 2	Pb 3	St. dev.		Cu 1	Cu 2	Cu 3	St. dev.		Zn 1	Zn 2	Zn 3	St. dev.	
1AM	8.8	12.7	13.5	2.5	11.8	11.3	13.5	1	54.5	56.9	67.8	7			
2AM	17.7	12.5	8.7	4.5	16.3	11.2	11.4	3	65.2	57.2	51.4	7			
3AM	16.3	11.1	11.8	2.8	13.0	14.9	7.8	4	57.0	68.0	42.3	13			
4AM	9.6	13	17	3.7	11.2	15.6	12.6	2	56.3	53.9	68.2	8			
1BM	7.9	9	10.4	1.3	10.3	9.4	11.1	1	45.1	45.4	59.2	8			
2BM	9.3	14.5	10.3	2.8	8.54	9.97	13.3	2	46.0	49.3	67.5	12			
3BM	13.2	13.2	13.3	0.1	6.95	16.0	12.6	5	40.5	62.8	68.0	15			
4BM	10.7	9.4	13.3	2.0	10.9	10.2	15.9	3	59.3	55.7	62.1	3			
1CM	10.5	14.5	12.2	2.0	10.4	18.0	14.4	4	53.3	57	72.6	10			
2CM	11.4	11.7	10.7	0.5	7.04	24.8	11.7	9	37.6	117	59.4	41			
3CM	11.9	17	11.1	3.2	14.1	14.7	10.8	2	49.6	81.3	62.7	16			
4CM	10.5	11.6	11.5	0.6	38.7	6.8	9.8	18	41.0	38.0	51.7	7			
1DM	14.5	17.2	11.7	2.8	12.5	17.5	12.7	3	58.9	90.8	64.8	17			
2DM	11.1	11.8	15.8	2.5	8.87	10.7	14.0	3	44.8	51.2		4			
3DM	15.8	6.5	11.1	4.7	9.78	8.76	10.3	1	47.6	44.4	50.4	3			
4DM	14.6	12.7	9.6	2.5	8.55	10.6	11.2	1	43.8	60.9	55.9	9			

## Appendix C – Material specifications of the roof tiles at APHIS Building #580

### SECTION 07610 SHEET METAL ROOFING AND SIDING

#### PART 1 -GENERAL

##### 1.01 SUMMARY

###### A. Section Includes:

1. Lead-coated copper with sealed joints for sloped roof and for wall surfaces.
2. Lead-coated copper with soldered joints for flat roof canopy and bay window.
3. Lead-coated copper louvers

###### B. Related Sections:

1. Section 06100 -Plywood Roof Sheathing.

##### 1.02 SUBMITTALS

###### A. Submit in accordance with Section 01300, unless otherwise indicated.

###### B. Product Options Brand Name or Equal:

1. Comply with Section 01630, unless otherwise indicated.

###### C. Quality Control Submittals:

###### 1. Statement of qualifications.

- a. Manufacturer's/Installer's Qualifications: Submit on letterhead statement qualifications including list of successful projects giving name of project, location, dates of participation, and name and telephone number of owner's representative who will verify information given.

###### D. Shop Drawings: Indicate dimensions, description of materials and finishes, general construction, specific modifications, component connections, anchorage methods, hardware, and installation procedures, plus the following specific requirements.

1. Indicate on shop drawings, material profile, jointing pattern, jointing details, fastening methods, and installation details.

E. Roofing Samples: One 24 inch by 24 inch sample of metal roofing with typical seam condition and with specified material and finish.

### 1.03 QUALITY ASSURANCE

A. Installer's Qualifications: Demonstrate successful completion of five (5) projects of similar type and scope using products/systems similar in complexity to those required for this Project.

B. Mock-Up: Prepare mock-up of lead-coated copper roof at radius edge for Contracting Officer's review and to establish requirements for workmanship.

1. Correct areas, modify method of application/installation, or adjust configuration as directed by Contracting Officer to comply with specified requirements.
2. Maintain mock-up, and mock-up accessibility, so as to serve as a standard of quality for this Section.

USDA GERMPLASM LAB. 07610 -1 01/26/93 7667-901

1. Mock-up shall consist of the following:

a. Minimum 4 ft. by 4 ft. section of radius portion of lead-coated copper roof, so as to indicate transition from vertical to sloped roof, and using same materials and methods to be used in the actual installation, including plywood substrate and anchoring devices. Structure under the plywood may be any SUBstantial material but must conform to radius required. Erect on ground level adjacent to brick mock up panels as directed by the Contracting Officer.

C. Pre-installation Conference: Contractor, installer, Contracting Officer, manufacturer's representative, and representatives of other affected trades shall meet at Site to review mock-up, and to confirm procedures, acceptance of substrate surfaces, and coordination with other trades.

1. Schedule meeting at least 1 week before start of installation.

1.04 DELIVERY, STORAGE, AND HANDLING

A. Packing and Shipping: Deliver materials so as to prevent damage.

B. Storage and Protection: Store materials so as to prevent damage to materials.

PART 2 -PRODUCTS

2.01 MATERIALS

A. Lead-Coated Copper: ASTM B370, cold-rolled temper, 20 oz. per sq. ft. weight sheet copper; lead-coated complying with ASTM B101, Type 1, Class A, coated both sides with lead weighing 6 to 7-1/2 lbs. per 100 sq. ft. for each side.

2.02 ACCESSORIES

A. Solder: 60 -40 tin/lead solder (ASTM B32).

B. Flux: Rosin, muriatic acid neutralized with zinc or an approved soldering paste.

C. Fastening and Anchoring Devices: Hard copper, brass or bronze.

1. Nails: Flat head, wire-slating type, not less than 12 gauge and 3.4 inch long.

2. Screws: Round heads with lead washers.

3. Expansion shields: Lead sleeves and washers.

D. Sealant:ASTM C920, one-component silicone based, movement capability plus or minus 50 percent. Transparent and copper compatible.

- E. Metal Accessories: Provide sheet metal clips, straps, anchoring devices, and similar accessory units as required for installation of Work, matching material being installed, size and gauge required for performance.
- F. Underlayment: Asphalt saturated roofing felt conforming to ASTM *D226* or *D2178*, No. 30.
- G. Slip Sheet: Rosin sized building paper.

USDA GERMPLASM LAB. 07610 -2 01/26/93 7667-901

## 2.03 FABRICATION

- A. Form sections true to shape, accurate in size, square, and free from distortion or defects.
- B. Fabricate cleats of same material as sheet, interlockable with sheet.
- C. Form pieces of 18 inch by 24 inch squares.

## 2.04 LOUVER FABRICATION

- A. Formed lead-coated copper louver 4" deep, 20 ounce copper, blade pitch 45 degrees, soldered construction with continuous drainable blades. Design to provide not more than 8.29 square feet of free area for a 4'-0" wide by 41'-0" high area.
- B. Insect screen: fourteen by eighteen mesh in folded frame.
- C. Blank off panel: Mfgr. standard insulated panel, close all unused louver

## area. PART 3 -EXECUTION

### 3.01 EXAMINATION

- A. Verification of Conditions: Examine areas and conditions under which Work is to be performed and identify conditions detrimental to proper or timely completion.
  - 1. Do not proceed until unsatisfactory conditions have been corrected.
  - 2. Inspect roof deck and wall sheathing to verify surface is clean and smooth, free of depressions, waves, or projections.
  - 3. Verify openings, curbs, pipes, sleeves, ducts, or vents are solidly set, cant strips and reglets are in place, and nailHng strips located.
  - 4. Beginning of installation means acceptance of existing conditions.

### 3.02 PREPARATION

- A. Field measure site conditions prior to fabricating work.
- B. Install starter and edge strips, and cleats before starting installation.
- C. Install surface mounted reglets true to lines and levels. Seal top of reglets with sealant.
- D. Protect elements surrounding work of this Section from damage or disfigurement.

### 3.03 GENERAL

- A. Apply underlayment in single layer laid perpendicular to slope; weather lap edges 2 inches and nail in place. Minimize nail quantity.
- B. Apply slip sheet in one layer, laid loose.
- C. Cleat and seam all joints.
- D. Use sealant joints of work not required to be soldered.

END OF SECTION

## Appendix D – Filter cloth specifications

# N035

## Polypropylene NonWoven Fabric

N035 is a polypropylene, needle punched nonwoven geotextile for use in drainage and separation applications. It has been stabilized to resist degradation due to ultraviolet exposure and is resistant to commonly encountered mildew,

insects and soil chemicals, and is non-biodegradable.

Property Test Method Min Avg.

Roll Values

Grab Tensile Strength<sup>1</sup> ASTM D4632 90 Lbs

Grab Tensile Elongation ASTM D4632 50%

CBR Puncture ASTM D6241 250 Lbs

Trapezoid Tear Strength ASTM D4533 40 Lbs

Apparent Opening Size (AOS) ASTM D4751 50 US Sieve

Permittivity (sec<sup>-1</sup>) ASTM D4491 2.2 sec<sup>-1</sup>

Flow Rate ASTM D4491 150 gpm/ft<sup>2</sup>

UV Resistance after 500 hrs. ASTM D4355 70%

*Values quoted above are the result of multiple tests conducted at an independent testing facility.*

*N035 meets or exceeds values listed.*

*<sup>1</sup>Values apply to both machine and cross-machine directions*

Packaging

Roll Width 12.5 ft 15 ft

Roll Length 360 ft 360 ft

Roll Area 500 sy 600 yd<sup>2</sup>

## Technical Data Sheet

# N035

2831 Cardwell Road □ Richmond, VA 23234

800-448-3636 □ [www.acfenvironmental.com](http://www.acfenvironmental.com)

10/18/2011



## Bibliography

American Public Health Association (APHA); American Water Works Association; Water Environment Federation. 1998. "Standard Methods for the Examination of Water and Wastewater", 19th ed.; Washington, D.C.

Babatunde, A.O., and Zhao, Y.Q. 2007. [Constructive Approaches Toward Water Treatment Works Sludge Management: An International Review of Beneficial Reuses. Critical Reviews in Environmental Science and Technology](#), 37(2):129-164.

Benjamin, M. M., and Leckie, J. O. 1981. Multiple-site adsorption of Cd, Cu, Zn, and Pb on amorphous iron oxyhydroxides. *Journal of Colloid Interface Science*, 79, 209–221.

Berndtsson, J.C. 2010. Green roof performance towards management of runoff water quantity and quality: A review. *Ecological Engineering*, 36(4):351-360.

Boller, M. 1997. Tracking heavy metals reveals sustainability deficits of urban drainage systems, *Wat Sci Tech*, 35(9):77-87.

Bradl, H.B. 2004. Adsorption of heavy metals ions on soils and soil constituents. *J. Colloid Interf. Sci.*, 277:1-18.

Centers for Disease Control (CDC). Lead toxicity – what are the US standards for lead levels? <<http://www.atsdr.cdc.gov/csem/csem.asp?csem=7&po=8>>, accessed 2013.

Chang-Chien, S.W., Wang, M.C., Huang, C.C., and Sessaiah, K., 2007. Characterization of humic substances derived from swine manure-based compost and correlation of their characteristics with reactivities with heavy metals.

Chu, W. 1999. Lead metal removal by recycled alum sludge. *Water Res.*, 33:3019–3025.

Codling, E.E., R.L. Chaney, C.L. Mulchi. 2000. Use of aluminum- and iron-rich residues to immobilize phosphorus in poultry litter and litter-amended soils. *J. Environ. Qual.*, 29:1924-1931.

Davis, A.P. 2007. Field performance of bioretention. *Environmental Engineering Science*. 24(8): 1048-1064.

Davis, A.P., M. Shokouhian, and S. Ni. 2001. Loading estimates of lead, copper, cadmium, and zinc in urban runoff from specific sources. *Chemosphere*, 44(5): 997-1009.

- Drizo, A., Forget, C., Chapuis, R.P., and Comeau, Y. 2006. Phosphorus removal by electric arc furnace steel slag and serpentinite. *Water Research*, 40(8):1547-1554.
- Erickson, A.J., Gulliver, J.S., and Weiss, P.T. 2007. Enhanced sand filtration for storm water phosphorous removal. *Journal of Environmental Engineering*, 133(5):485-497.
- Evans, L.J. 1989. Chemistry of metal retention by soils. *Environmental Science and Technology*, 23(9):1046-1056.
- Gibert, O., J. de Pablo, J. L. Cortina, and C. Ayora. 2005. Municipal compost-based mixture for acid mine drainage bioremediation: Metal retention mechanisms. *Appl. Geochem.*, 20:1648-1657.
- Glanville et al. 2003. *Impacts of Compost Blankets on Erosion Control, Revegetation, and Water Quality at Highway Construction Sites in Iowa*, T. Glanville, T. Richard, and R. Persyn, Agricultural and Biosystems Engineering Department, Iowa State University of Science and Technology, Ames, Iowa.
- Gupta, K. and Saul, A.J. 1996. Specific relationships for the first flush load in combined sewer flows. *Water Research*, 30(5):1244-1252.
- Hewitt, C.N., and Rashed, M.B. 1991. The deposition of selected pollutants adjacent to a major rural highway. *Atmospheric Environment*, 25(5-6):979-983.
- Irving, H., and Williams, J.P. 1948. Order of stability of metal complexes. *Nature*, 162(4123):746-747.
- Jang, A. Y. Seo, and P.L. Bishop. 2005. The removal of heavy metals in urban runoff by sorption on mulch. *Environ. Pollut.*, 133:117-127.
- Jensen, D.L., Ledin, A., and Christensen, T.H. 1999. Speciation of heavy metals in landfill-leachate polluted groundwater. *Wat. Res.* 33(11):2642-2650.
- Jones, P.S., and Davis, A.P. 2013. Spatial accumulation and strength of affiliation of heavy metals in bioretention media. *J. Environ. Eng.* 139:479-487.
- Karlen, C., Wallinder, I.O., Heijerick, D., and Leygraf, C. 2002. Runoff rates, chemical speciation and bioavailability of copper released from naturally patinated copper. *Environmental pollution*. 120: 691-700.
- Kim, H. (2010). "Use of organic by-product amended compost/manure to sequester metals and phosphorous from diffuse source pollution". PhD Dissertation, Univ. of Maryland, College Park, MD.

Kim, H., Davis, A.P., and Chaney, R.L. (2013). Treatment of heavy metals in runoff using industrial byproducts: column studies. Under Review.

Kreeb, L. B. (2003). "Hydrologic efficiency and design sensitivity of bioretention facilities." Honors Research Thesis, Univ. of Maryland, College Park, MD.

Lee, C. E., Yang, W. F., and Chiou, S. S. 2006. Utilization of water clarifier sludge for copper removal in a liquid fluidized-bed reactor. *Journal of Hazardous Materials*, B129:58–63.

Li, H., and Davis, A.P. 2009. Water quality improvement through reductions of pollutant loads using bioretention. *J. Environ. Eng.* 135(8):567-576.

Loeppert, R.H., and W.P. Inskeep. 1996. Iron. 639–664. In D.L. Sparks (ed.) "Methods of soil analysis" Part 3. SSSA Book Ser. no. 5. SSSA, Madison, WI.

Madden, M.S. 1988. "Adapting the Sr(NO<sub>3</sub>)<sub>2</sub> methods for determining available cations to a routine soil procedure". MS thesis. University of Wisconsin. Madison, WI.

Madrid, L. 1999. Metal retention and mobility as influenced by some organic residues added to soils: A case study. In: Selim, H. M., and Iskandar, I. K. (eds.). *Fate and transport of heavy metals in the Vadose Zone*. Boca Raton, Fla.: Lewis Publ., 201–223.

Mason, Y., Amman, A.A., Ulrich, A., and Sigg, L. 1999. Behavior of heavy metals, nutrients, and major components during roof runoff infiltration. *Environ. Sci. Technol.* 33,1588-1597.

McGrath, S.P., and C.H. Cunliffe. 1985. Simplified Method for the Extraction of the Metals Fe, Zn, Cu, Ni, Cd, Pb, Cr, Co and Mn from Soils and Sewage Sludges. *J. Sci. Food Agric.*, 36:794-798.

McKeague, J.A., and Day, J.H. 1966. Dithionite and oxalate extractable Fe and Al as aids in differentiating various classes of soils. *Canadian Journal of Soil Science*, 46(1): 13-22.

Nieboer, E. and Richardson, D.H.S. 1980. The replacement of the nondescript term 'heavy metals' by a biologically and chemically significant classification of metal ions. *Environmental pollution*, 1(1): 3-26.

O'Neill, S. and Davis, A. 2012. Water treatment residual as a bioretention amendment for phosphorus. I: evaluation studies. *J. Environ. Eng.* 138(SI):318–327.

- O'Neill, S. and Davis, A. 2012. "Water treatment residual as a bioretention amendment for phosphorus. II: long-term column studies." *J. Environ. Eng.* 138(SI):328–336.
- Okochi, N.C., McMartin, D.W. 2011. Laboratory investigations of stormwater remediation via slag: Effects of metals on phosphorus removal. *Journal of Hazardous Materials*, 187(1–3):250-257.
- Seelsaen, N., R. McLaughlan, S. Moore, and R.M. Stuetz. 2007. Influence of compost characteristics on heavy metal sorption from synthetic stormwater. *Wat Sci Technol*, 55(4):219-226.
- Sharpley, A. and Moyer, B. 2000. Phosphorous forms in manure and compost and their release during simulated rainfall. *Journal of Environmental Quality*. 29(5):1462-1469.
- Sibbesen, E. and Sharpley, A. (1997). Setting and justifying upper critical limits for phosphorous in soils. 151-176. In: Tunney, H., Carton, O.T., Brookes, P.C., and Johnston, A.E. (eds.) Phosphorous loss from soil to water. CAB International.
- Stumm, W. and Morgan, J.J. 1981. *Aquatic chemistry: chemical equilibria and rates in natural waters*. 3<sup>rd</sup> Edition, John Wiley & Sons.
- United States Environmental Protection Agency (USEPA). National summary of impaired waters and TMDL information. 2013.  
[http://iaspub.epa.gov/waters10/attains\\_nation\\_cy.control?p\\_report\\_type=T](http://iaspub.epa.gov/waters10/attains_nation_cy.control?p_report_type=T).  
 Accessed 2013.
- Weather Underground. Weather history for KMDLAURE5\ . 2013.  
<http://www.wunderground.com/weatherstation/WXDailyHistory.asp?ID=KMDLAURE5>> accessed 2013.
- Yao, K., Habibian, M.T., and O'Melia, C.R. 1971. Water and waste water filtration: concepts and application. *Environmental Science & Technology*. 5(11):1105-1112.
- Zhou, Y., and Haynes, R. 2010. Sorption of Heavy Metals by Inorganic and Organic Components of Solid Wastes: Significance to Use of Wastes as Low-Cost Adsorbents and Immobilizing Agents, *Critical Reviews in Environmental Science and Technology*, 40(11):909-977.
- Zhou, Y.F., Haynes, R.J., and Naidu, R. 2011. Use of inorganic wastes for in situ immobilization of Pb and Zn in a contaminated alkaline soil. *Environ. Sci. Pollut. Res.* 19:1260-1270.